

Dissertation zur Erlangung des Doktorgrades  
der Fakultät für Chemie und Pharmazie  
der Ludwig-Maximilians-Universität München

**Biomimetic Screening of Class B G protein-Coupled Receptors:  
Design of Tailored Ligands for the  
Corticotropin-Releasing-Hormone Receptor**

**Christian Serge Marie Devigny**

aus

Chevreuse, Frankreich

2012

## Erklärung

Diese Dissertation wurde im Sinne von § 7 der Promotionsordnung vom 28. November 2011 von Herr Prof. C. Turck betreut von der Fakultät für Chemie und Pharmazie vertreten.

## Eidesstattliche Versicherung

Diese Dissertation wurde eigenständig und ohne unerlaubte Hilfe erarbeitet.

München, den 20.02.2012

.....  
Christian Devigny

Dissertation eingereicht am 20.02.2012

1. Gutachter: Prof. Dr. C. W. Turck
2. Gutachter: Prof. Dr. R. Beckmann

**Mündliche Prüfung am 12.07.2012**

# Table of Contents

<b>Abbreviations</b> .....	<b>7</b>
<b>Abstract</b> .....	<b>11</b>
<b>Zusammenfassung</b> .....	<b>13</b>
<b>1 Introduction</b> .....	<b>15</b>
1.1 Stress and the hypothalamic-pituitary-adrenal axis.....	15
1.2 Implication of the HPA axis in psychiatric disorders.....	17
1.3 The CRH receptor and its ligands.....	19
1.3.1 The CRHR: structure, localization and function.....	19
1.3.2 CRH and CRH-like peptides.....	20
1.3.3 Peptide ligands binding mechanism.....	22
1.3.4 G protein-coupled receptor-dependent signaling cascades.....	24
1.4 CRHR <sub>1</sub> antagonists.....	26
1.4.1 Peptide antagonists.....	26
1.4.2 CRHR <sub>1</sub> non-peptide ligands.....	27
<b>2 Objective of the study</b> .....	<b>31</b>
<b>3 Results and discussion</b> .....	<b>33</b>
3.1 Peptide-peptide conjugates as CRH mimics.....	33
3.1.1 Choice of a ligation technique for the synthesis of biomimetic probes.....	33
3.1.2 Synthesis and characterization of CRHR <sub>1</sub> -ECD1 high affinity probes.....	35
3.1.3 Synthesis of a “clicked” biomimetic probe: proof of concept.....	39
3.1.4 Urocortin1 <sup>1-15</sup> C- and N-terminal truncation: characterization of a minimal CRHR <sub>1</sub> stimulation sequence.....	42
3.1.5 Alternative ligation method: the hydrazone bioconjugation of a UCN <sup>4-15</sup> biomimetic probe.....	45
3.1.6 Role of the ethylene glycol connector between the two ligands binding domains.....	49
3.2 Urocortin1 <sup>4-15</sup> biomimetic screening.....	54
3.2.1 Synthesis and potency evaluation of a Urocortin1 <sup>4-15</sup> peptide conjugate library.....	54
3.2.2 Purification of exemplary conjugates: validation of the crude biomimetic screening....	60
3.2.3 Synthesis and evaluation of optimized UCN <sup>4-15</sup> peptide probes.....	63
3.2.4 Pharmacological characterization of a CRHR <sub>1</sub> -TMD specific probe.....	72

3.2.5	Synthesis and evaluation of a peptide amide library.....	81
3.2.6	Structure-Activity-Relationship at [Phe <sup>11</sup> ]UCN <sup>4-15</sup> .....	84
3.2.7	Summary of the UCN biomimetic screening.....	86
3.3	Biomimetic screening of a synthetic CRHR <sub>1</sub> modulator: astressin .....	88
3.3.1	Evaluation of astressin conjugates: rationale and proof of concept .....	89
3.3.2	Astressin <sup>1-14</sup> truncations: characterization of a minimal inhibition sequence .....	91
3.3.3	Role of the Astressin <sup>1-11</sup> conjugate middle domain.....	93
3.3.4	Astressin <sup>1-11</sup> stimulation biomimetic screening .....	96
3.3.5	Astressin <sup>1-11</sup> inhibition biomimetic screening .....	100
3.3.6	Evaluation of multisubstituted Astressin <sup>1-11</sup> biomimetic probes .....	104
3.3.7	Summary of the astressin biomimetic screening.....	111
3.4	Synthesis and characterization of nonpeptide CRHR <sub>1</sub> antagonists .....	113
<b>4</b>	<b>Conclusion.....</b>	<b>117</b>
<b>5</b>	<b>Material and methods .....</b>	<b>119</b>
5.1	Chemical methods .....	119
5.1.1	Nuclear Magnetic Resonance .....	119
5.1.2	Mass Spectrometry .....	119
5.1.3	Liquid chromatography-mass spectrometry.....	119
5.1.4	High-performance liquid chromatography .....	119
5.1.5	Flash chromatography .....	120
5.1.6	Thin layer chromatography.....	120
5.1.7	Chemicals .....	121
5.1.8	Solvents.....	126
5.1.9	Others materials .....	127
5.2	Synthetic methods .....	128
5.2.1	Synthesis of azide-functionalized spacers .....	128
5.2.2	Synthesis of HNA and SFB modification reagents.....	135
5.2.3	Solid phase synthesis of peptides .....	137
5.2.4	The bioconjugation of peptide fragments .....	154
5.2.5	Synthesis of nonpeptide CRHR <sub>1</sub> antagonists.....	166
5.3	cAMP cell-based assays .....	172
5.3.1	Stimulation assay typical protocol .....	173
5.3.2	Inhibition assay standard protocol .....	173
5.4	Data analysis .....	176

**References ..... 177**

**Acknowledgments ..... 187**

**Curriculum Vitae ..... 189**



## Abbreviations

3D	three dimensional
AA	amino acid
AC	adenylyl cyclase
AcOEt	ethyl acetate
ACTH	adrenocorticotropin
AST	astressin
AVP	arginine vasopressin
BAL	backbone amide linker
Boc	<i>tert</i> -butyloxycarbonyl
cAMP	cyclic adenosine monophosphate
CNS	central nervous system
CPM	counts per minute
CRE	cAMP response element
CREB	cAMP response element-binding
CRH	corticotropin-releasing hormone
CRH-BP	CRH binding protein
CRHR	CRH receptor
CSF	cerebrospinal fluid
CuCAAC	copper-catalyzed azide-alkyne cycloaddition
DAG	diacylglycerol
DCM	dichloromethane
DEG	diethylene glycol
DIEA	diisopropylethylamine
DMF	dimethylformamide
DMSO	dimethyl sulfoxide
DST	dexamethasone suppression test
EC <sub>50</sub>	half maximal effective concentration
ECD	extracellular domain
eq.	equivalent
$E_{max}$	maximal potency
$E_{min}$	minimal potency
ERK	extracellular signal-regulated kinase
ESI	electrospray ionisation

Fmoc	Fluorenylmethyloxycarbonyl
FRET	fluorescence resonance energy transfer
GDP	guanosine diphosphate
GLP1	glucagon-like peptide-1
GLP1R	glucagon-like peptide receptor
GPCR	G protein-coupled receptor
GR	glucocorticoid receptor
GRK	G protein-coupled receptor kinase
GTP	guanosine triphosphate
HATU	<i>O</i> -(7-azabenzotriazol-1-yl)- <i>N,N,N',N'</i> -tetramethyluronium hexafluorophosphate
HBA	hydrogen bond-accepting atom
HBTU	<i>O</i> -(benzotriazol-1-yl)- <i>N,N,N',N'</i> -tetramethyluronium hexafluorophosphate
HEK293	human embryonic kidney 293 cells
HNA	hydrazinonicotinic acid
HOBt	1-hydroxybenzotriazole
HPA	hypothalamic-pituitary-adrenocortical
HTRF	homogenous time-resolved fluorescence
ICD	intracellular domain
IP3	inositol 1,4,5-trisphosphate
MAPK	mitogen-activated protein kinase
MEG	monoethylene glycol
MS	mass spectrometry
MTS	medium-throughput screening
NBD	4-(7-nitro)benzofurazanyl
NMM	<i>N</i> -methylmorpholine
NMP	<i>N</i> -methyl-2-pyrrolidone
NMR	nuclear magnetic resonance
PEG	polyethylene glycol
PEG <sup>4</sup>	tetraethylene glycol
PEG <sup>5</sup>	pentaethylene glycol
PKA	protein kinase A
PKC	protein kinase C



---

PLC	phospholipase C
POMC	propiomelanocortin
PTH	parathyroid hormone
PTHR	parathyroid hormone receptor
PVN	hypothalamic paraventricular nucleus
PyBop	benzotriazol-1-yl-oxytripyrrolidinophosphonium hexafluorophosphate
SAR	structure-activity-relationship
s.e.m.	standard error of the mean
SFB	4-formylbenzoate
SPPS	solid phase peptide synthesis
SVG	sauvagine
TBTA	tris[(1-benzyl-1 <i>H</i> -1,2,3-triazol-4-yl)methyl]amine
TEG	triethylene glycol
TFA	trifluoroacetic acid
TIS	triisopropylsilane
TLC	thin layer chromatography
TMD	transmembrane domain
UCN	urocortin
UV	ultraviolet
WHO	World Health Organization
WT	wild type

Please note that all units are indicated as defined by the International System of units (SI) or are SI derived units with the respective prefixes and are therefore not considered in the list of abbreviations.



## Abstract

Dysregulation of the hypothalamic-pituitary-adrenal (HPA) axis is a hallmark of complex and multifactorial psychiatric diseases such as anxiety and mood disorders. The 41-amino acid neuropeptide Corticotropin Releasing Hormone (CRH) is a major regulator of the mammalian stress response. Upon stressful stimuli, it binds to the Corticotropin Releasing Hormone Receptor 1 (CRHR<sub>1</sub>), a typical member of the class B GPCRs and a potential novel target for the therapeutic intervention in major depressive disorder. A precise understanding of the peptide-receptor interactions is an essential prerequisite towards the development of efficient CRHR<sub>1</sub> specific antagonists. To chemically probe the molecular interaction of CRH with its cognate receptor, a high-throughput conjugation approach which mimics the natural activation mechanism for class B GPCRs was developed. Acetylene-tagged peptide libraries were synthesized and conjugated to high-affinity azide-modified carrier peptides using copper-catalyzed dipolar cycloaddition. The resulting conjugates reconstitute potent ligands and were tested in situ for modulation of the CRHR<sub>1</sub> activity in a cell-based assay. This approach allows to (i) define the sequence motifs which are required for receptor activation or inhibition, (ii) identify the critical functional groups and investigate structure-activity-relationships, and (iii) develop novel optimized, highly potent peptide probes which are specific for the transmembrane domain of the receptor. The membrane recruitment by a high-affinity carrier peptide enhances the potency of tethered peptides and allows the initial testing of weak fragments that otherwise would be inactive. The biomimetic screening led to the discovery of transtressin, a highly modified and potent CRHR<sub>1</sub> transmembrane domain-specific optimized agonist ( $EC_{50} = 4$  nM). Beyond its intrinsic agonistic activity, transtressin is an essential tool for the pharmacological characterization of CRHR<sub>1</sub> antagonists in competition assays (*Devigny et al.* 2011; *Sakmar* 2011).



## Zusammenfassung

Die Fehlregulation der Hypothalamus-Hypophysen-Nebennierenrinde-Achse ist ein Kennzeichen psychiatrischer Erkrankungen wie Angststörungen und Depressionen. Das 41-Aminosäuren-lange Neuropeptid Corticotropin-freisetzende Hormon (CRH) ist ein wichtiger Regulator der Stressantwort in Säugetieren. Nach einem Stressstimulus bindet das Hormon an den Corticotropin-freisetzendes Hormon Rezeptor Typ 1 (CRHR<sub>1</sub>), einem typischen Vertreter der Klasse B G-Proteingekoppelten Rezeptoren (GPCR) und einem potenziellen neuen pharmakologischen Zielprotein für die Therapie depressiver Störungen. Ein genaues Verständnis der Peptid-Rezeptor-Interaktion ist eine essenzielle Voraussetzung für die Entwicklung spezifischer und effizienter CRHR<sub>1</sub>-Antagonisten.

Um die molekulare Interaktion zwischen CRH und seinem zugehörigen Rezeptor chemisch zu charakterisieren, wurde eine Hochdurchsatz-Konjugationsstrategie entwickelt, welche den natürlichen Aktivierungsmechanismus für Klasse B GPCRs nachahmt. Peptidbibliotheken wurden mit Acetylen-Markierungen synthetisiert und mit hochaffinen Azid-modifizierten Trägerpeptiden durch Kupfer-katalysierte, 1,3-dipolare Cycloaddition konjugiert. Die entstandenen Konjugate stellen potente Liganden dar und wurden in situ in Zell-basierten Assays für die Modulation der CRHR<sub>1</sub> Aktivität getestet. Dieses Verfahren ermöglicht (i) das minimal Sequenzmotiv, welche für die Rezeptoraktivierung oder -inhibition notwendig ist, zu definieren, (ii) die wesentlichen funktionellen Gruppen zu identifizieren und systematisch die Struktur-Aktivität-Beziehung zu untersuchen und (iii) neue, optimierte, hoch-potente Peptide zu entwickeln, welche spezifisch für die Transmembrandomäne des Rezeptors sind. Die Rekrutierung über hochaffine Trägerpeptide verstärken die Potenz von gebundenen Peptiden und erlaubt dadurch ein initiales Testen von schwach bindenden Fragmenten, die sonst inaktiv wären. Unsere biomimetische Untersuchung führte zur Entdeckung von „Transtressin“, einem modifizierten und hoch-potenten, Transmembrandomän-spezifischen CRHR<sub>1</sub>-Agonisten (EC<sub>50</sub> = 4 nM).

Neben seiner intrinsischen Aktivität als Agonist fand Transtressin als pharmakologisches Hilfsmittel in Konkurrenzverfahren für die Charakterisierung von peptidischen und nicht-peptidischen CRHR<sub>1</sub>-Antagonisten Verwendung. Dabei führte die biomimetische Untersuchung des peptidischen Antagonisten Astressin zu neuen und überraschend potenten, verkürzten Peptidagonisten. Zudem wurde ein neuer Syntheseweg für nicht-peptidische CRHR<sub>1</sub>-Antagonisten etabliert. Dabei wurden Pyrazolotriazin-Derivate wie DMP696 im Grammaßstab synthetisiert, und in Tierexperimente zur Charakterisierung von Stressverhalten eingesetzt.



# 1 Introduction

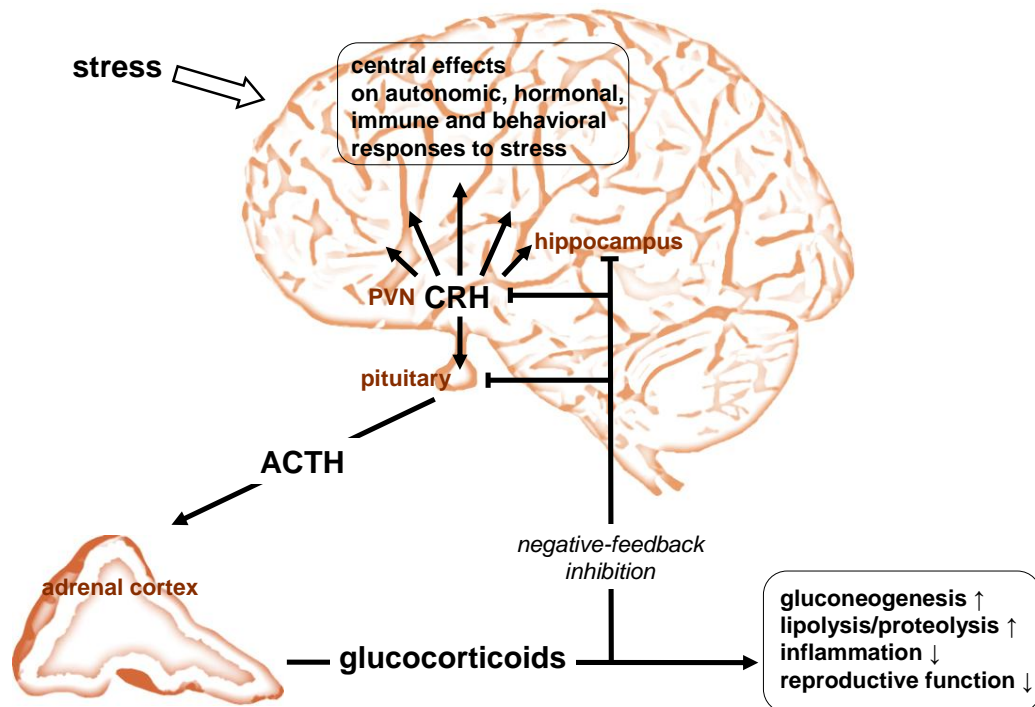
## 1.1 Stress and the hypothalamic-pituitary-adrenal axis

Stress is defined as “conditions where an environmental demand exceeds the natural regulatory capacity of an organism” (*Koolhaas et al. 2011*). First described by the pioneering endocrinologist Hans Selye, the so-called “general adaptation syndrome” constitutes an essential mechanism for the survival of all organisms (*SELYE 1951*). Different stressors, internal or external stimuli, activate the stress system and lead to major biochemical, functional and behavioral changes. The behavioral and physical responses include enhanced vigilance and cognition, analgesia, activation of the cardiovascular system and suppression of vegetative functions such as appetite, sex drive and sleep (*Chrousos 1998; Tsigos and Chrousos 2002*).

The neuroendocrine response to stress is mediated by the hypothalamic-pituitary-adrenal (HPA) axis (Figure 1). The key regulator of the HPA axis is the corticotropin-releasing-hormone (CRH), a 41 amino-acid neuropeptide discovered in 1981. CRH coordinates the neuroendocrine, autonomic, immune and behavioral responses to stress constituting an “acute defense of homeostasis” (*Vale et al. 1981; Vale et al. 1983*). Upon stressful stimuli, increased CRH secretions are released from the hypothalamic paraventricular nucleus (PVN) into the median eminence. CRH subsequently enters the hypothalamic-pituitary portal system and binds the corticotropin-releasing-hormone receptor type 1 (CRHR<sub>1</sub>). The activation of the CRHR<sub>1</sub>-dependent signaling cascades causes the processing of proopiomelanocortin (POMC) into adrenocorticotrophic hormone (ACTH) and its release in the bloodstream. ACTH in turn stimulates the secretion of glucocorticoids by the cortex of adrenal glands. Glucocorticoids, such as cortisol, regulate a variety of important metabolic, immunologic and homeostatic functions. Glucocorticoids levels in the blood are regulated by a negative feedback mechanism that in turn, downregulates the HPA axis activity (*Dallman et al. 1987*). In addition, the arginine vasopressin neuropeptide (AVP) plays an important role in modulating ACTH responsiveness in stressful conditions. Major evidences show that AVP and CRH acts synergistically to potentiate the release of ACTH (*DeBold et al. 1984; Young et al. 2007*).

CRH is also a neuromodulator that regulates the neuronal activity. Expression of the CRH system in extrahypothalamic regions mediate the behavioral response to stress (*DeSouza 1985; Koob 1999*). The expression of the CRH system in forebrain glutamatergic and  $\gamma$ -aminobutyric acid containing neurons as well as in midbrain dopaminergic neurons was recently shown to control the emotional response to stress (*Refojo et al. 2011*). CRH has been shown to modulate various behavioral

attributes including learning and memory, food intake, anxiety, arousal, startle and fear responses, general motor activity and sexual behavior (Bale et al. 2000; Hauger et al. 2006; Radulovic et al. 1999).



**Scheme illustrating the activation, the effects and the negative-feedback inhibition of the HPA axis (courtesy of H. Kronsbein).** Upon stress, CRH release from the hypothalamic PVN to the pituitary is increased. In turn, the pituitary releases more ACTH. ACTH stimulates the production and the release of glucocorticoids. Within this cascade, CRH has profound effects on autonomic, hormonal, immune and behavioural responses to stress. Amongst others, glucocorticoids activate gluconeogenesis, lipolysis and proteolysis and diminish inflammation and reproductive function. Additionally, glucocorticoids exert a negative feedback mechanism on the pituitary and on structures of the CNS like the PVN in the hypothalamus and the hippocampus.



## 1.2 Implication of the HPA axis in psychiatric disorders

Several clinical and preclinical findings demonstrate the central role of CRH in a variety of psychiatric disorders such as depression and anxiety. Persistent enhancement of stress reactivity leads to dysregulation of the HPA axis and increased CRH levels (*Raadsheer et al.* 1994). Environmental factors but also genetic factors contribute to the development of these HPA system abnormalities (*Hauger et al.* 2006). Exposure to stress early in life was shown to produce long-term sensitization of CRH-mediated stress responses and increases the risk of developing anxiety and depressive disorders (*Carpenter et al.* 2004; *Essex et al.* 2002). Increased CRH concentrations lead to elevated ACTH and glucocorticoid levels, thus causing hypercortisolemia (*Gold et al.* 1988; *Nemeroff* 1996). In contrast, reduced CRH secretions lead to hypoactivation of the stress system and an enhanced negative feedback mechanism (*Juruena et al.* 2004). CRH plays an important role in the mediation of emotional processes such as fear, anxiety and panic. Hence, a dysregulation of the HPA axis is involved in the pathology of several neuropsychiatric disorders (Table 1) (*Tsigos and Chrousos* 2002). In predisposed humans, chronic stress or continuous exposure to stress may trigger the symptoms of depression and anxiety.

Increased HPA axis activity	Decreased HPA axis activity	Disrupted HPA axis activity
Severe chronic disease		
Melancholic depression	Atypical depression	Cushing syndrome
Anorexia nervosa	Seasonal depression	Glucocorticoid deficiency
Obsessive–compulsive disorder	Chronic fatigue syndrome	Glucocorticoid resistance
	Fibromyalgia	
Panic disorder	Hypothyroidism	
Chronic excessive exercise	Adrenal suppression	
Malnutrition	Post glucocorticoid therapy	
Diabetes mellitus	Post stress	
	Nicotine withdrawal	
	Postpartum	
Hyperthyroidism	Menopause	
Central obesity	Rheumatoid arthritis	
Childhood sexual abuse		
Pregnancy		

**Table 1. Disorders associated with disturbed HPA axis function** (*Tsigos and Chrousos* 2002).

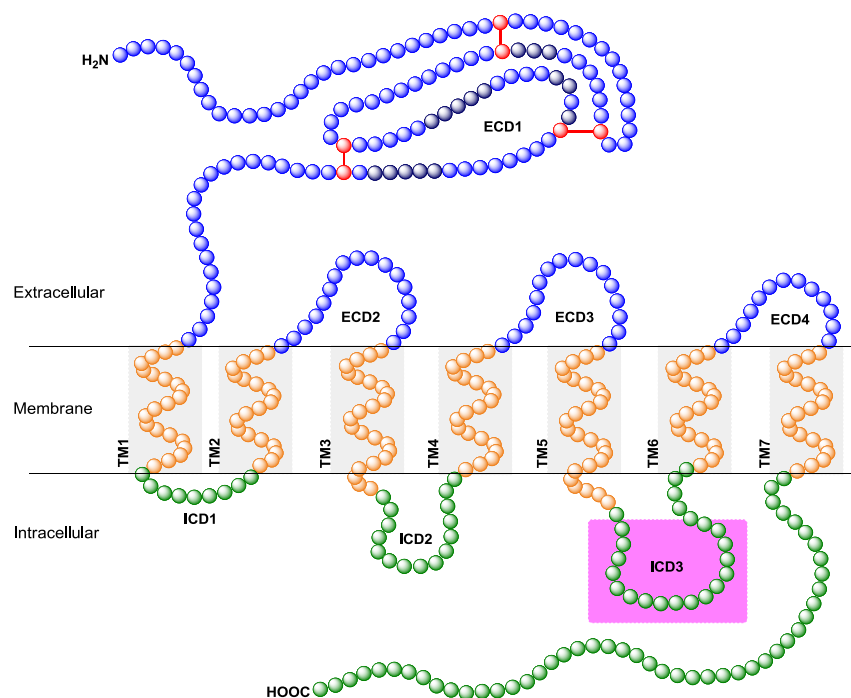
Mood and anxiety disorders have a high prevalence in the general population of industrialized countries. Recently, the World Health Organization (WHO) estimated the 12-month prevalence of mood disorders to 3.6 % in Germany and 9.6 % in the United States. The evaluated 12-month prevalence of anxiety disorders ranges to 6.2 % in Germany and to 18.2 % in the United States (*Demyttenaere et al. 2004*). According to the WHO, depression will become the second cause of disability in 2020. Neuropsychiatric disorders lead to a tremendous loss of life quality and have a considerable impact on the economy.

Common and characteristic symptoms of depression and anxiety disorders are insomnia, reduced sex drive, loss of appetite, weight loss, constipation and psychomotor changes among others. The important neuroendocrine findings among depressive patients are elevated levels of CRH in the cerebrospinal fluid (CSF) as well as hypercortisolemia (*Holsboer 2000; Nemeroff et al. 1984*). Additionally, an unrestrained CRH release in the context of impaired glucocorticoid receptor (GR) function has been proposed to have an impact on the development and course of major depression (*Holsboer 1999*). In the standard dexamethasone suppression test (DST), patients with various affective disorders display elevated cortisol levels suggesting an impaired feedback mechanism through the GRs. Although pronounced HPA axis alterations are commonly found in patients suffering from depressive disorders, HPA abnormal functions are also found in other neuropsychiatric disorders such as e.g. acute mania, anxiety and schizophrenia. Altogether, a number of clinical and preclinical studies have characterized the crucial role of the CRH system and HPA dysregulation in the etiology of stress-related disorders such as depression and anxiety. In view of these data, the CRH system has been suggested as a novel and promising target for the treatment of stress-related disorders.

## 1.3 The CRH receptor and its ligands

### 1.3.1 The CRHR: structure, localization and function

The corticotropin-releasing-hormone receptors (CRHRs) are G protein-coupled receptors (GPCRs), which are widely distributed throughout the body (Civelli 2005). GPCRs constitute a superfamily of proteins whose function is to transduce a chemical signal across the cell membrane. All GPCRs possess seven highly conserved transmembrane helices and interact with a heterotrimeric G protein that subsequently triggers signal transduction pathways. Because of their integral role in cell signaling, GPCRs are important in understanding and treating a variety of diseases. GPCRs are prime drug targets and it is estimated that greater than 40 % of all modern marketed drugs target GPCRs (Moro *et al.* 2005).



**Figure 2. Diagram of the human CRHR<sub>1</sub>:** extracellular domain (ECD), transmembrane domain (TMD), and intracellular domain (ICD). The peptide binding site (ECD1) is highlighted in dark blue. The G protein binding site is highlighted in pink (ICD3).

The CRH receptor (CRHR) is a GPCR belonging to the class B or secretin family (Figure 2) (Bale and Vale 2004; Dautzenberg and Hauger 2002; Hoare *et al.* 2003; Hoare 2005). Three subtypes of CRHRs have been identified. The human CRHR<sub>1</sub> and CRHR<sub>2</sub> consist of 415 and 411 amino acids respectively, sharing 70 % of amino acid sequence homology and are coded by separate genes (Grammatopoulos and Chrousos 2002; Liaw *et al.* 1997). The structure of the CRH receptors consists of a large N-

terminus (ECD1) and three loops in the extracellular domain (ECDs), seven hydrophobic transmembrane  $\alpha$ -helices constituting the transmembrane domain (TMD), and the C-terminus as well as three loops in the intracellular domain (ICDs). The ECD loops region is the initial region for ligand binding and possesses the greatest variation between the receptor subtypes (*Grammatopoulos and Chrousos 2002*). The N-terminus regions (ECD1) share only 40 % sequence identity between CRHR<sub>1</sub> and CRHR<sub>2</sub>. However, the TMD and ICD regions are highly conserved and share more than 80 % homology. The third IC loop (IC3) is found to be strictly identical between all CRH receptors and interacts with the G protein (*Bale and Vale 2004; Dautzenberg and Hauger 2002*). Interestingly, the receptors subtypes differ in their tissue distribution and pharmacology, suggesting different physiological functions. CRHR<sub>1</sub> is mainly expressed in the central nervous system (e.g., pituitary gland, cerebral cortex, sensory relay nuclei and cerebellum), whereas CRHR<sub>2</sub> expression is limited to peripheral organs and to specific brain regions (*Chalmers et al. 1995; Van et al. 2000*). CRHR<sub>1</sub> is the primary receptor involved in the response to stress, thus the CRH/CRHR<sub>1</sub> system constitute the key regulator of the HPA axis. In addition to CRHRs, class B GPCRs include important drug targets such as the calcitonin, the glucagon-like peptide (GLP1R) and parathyroid hormone receptors (PTHR).

### **1.3.2 CRH and CRH-like peptides**

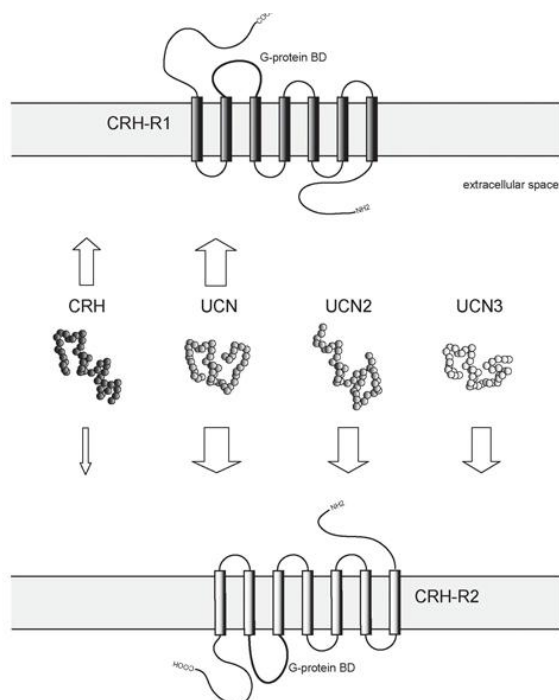
The Corticotrophin-Releasing-Hormone (CRH) is a 41 amino acid polypeptide that was isolated and characterized in 1981 (Table 2) (*Vale et al. 1981*). The CRH peptides from different species show a remarkable degree of sequence homology. Among mammalian CRH peptides, human, rat, mouse and pig CRH homologues are strictly identical (*Hauger et al. 2006*). Besides CRH as regulator of the HPA axis, closely related peptides (CRH-like peptides) have been identified. In mammals, the CRH family comprises three distinct CRH-like peptides: urocortin 1 (UCN), urocortin 2 (UCN2) and urocortin 3 (UCN3) (*Hsu and Hsueh 2001; Vaughan et al. 1995*). In addition to endogenous CRH and CRH-like peptides, a variety of synthetic peptides have been reported (e.g., stressin1-A, astressin 2B and cortagine). CRH and CRH-like peptides expressing neurons are widely distributed throughout the body. In the mammalian CNS, a very high density of CRH-expressing neurons is present in the PVN of the hypothalamus. These neurons are primary responsible for mediating and regulating the stress response. CRH-containing neurons are also found in the central nucleus of the amygdala and hindbrain regions as well as in the periphery (*Bale and Vale 2004; Swanson et al. 1983*). Beyond the multiple brain functions, the presence of CRH-expressing neurons in the pancreas, stomach, intestine and lymphocytes suggests a possible role of CRH in digestion and immune functions. Similarly, UCN, UCN2, and UCN3 peptides are widely expressed within the brain and the periphery.

Both CRH and UCN have high affinities for the CRH-binding protein (CRH-BP) whereas neither UCN2 nor UCN3 bind to this protein (Dautzenberg and Hauger 2002).

Peptide	Amino acid sequence			CRHR <sub>1</sub> CRHR <sub>2</sub>	
	N-terminal domain	Central domain	C-terminal domain	K <sub>i</sub> (nM)	K <sub>i</sub> (nM)
<b>Endogenous agonists</b>					
hCRH	S E E P P I S L D L T F H L L R E V L E M A R A E Q L A Q Q A H S N R K L M E I I N H <sub>2</sub>			1.5	42
hUCN	D N P S L S I D L T F H L L R T L L E L A R T Q S Q R E R A E Q N R I I F D S V N H <sub>2</sub>			0.4	0.3
hUCN2	I V L S L D V P I G L L Q I L L E Q A R A R A A R E Q A T T N A R I L A R V N H <sub>2</sub>			>100	1.7
hUCN3	T K F T L S L D V P T N I M N L L F N I A K A K N L R A Q A A N A H L M A Q I N H <sub>2</sub>			>100	22
<b>Synthetic antagonists</b>					
α-helical CRH <sup>9-41</sup>		D L T F H L L R E M L E M A K A E Q E A E Q A A T N R L L L E E A N H <sub>2</sub>		19	1.1
Astressin		f H L L R E V L E X A R A E Q L A Q E A H K N R K L X E I I N H <sub>2</sub>		0.7	0.6
Yamada			A c E A E K N R K L X D I I N H <sub>2</sub>	5.5	n.d.

**Table 2. Sequence and homology of peptide agonists and antagonists with affinities at the CRH<sub>1</sub> and CRH<sub>2</sub> receptors (Grigoriadis 2005; Yamada et al. 2004). X = cyclohexyl alanine; f = D-phenylalanine; EAEK = lactam bridge.**

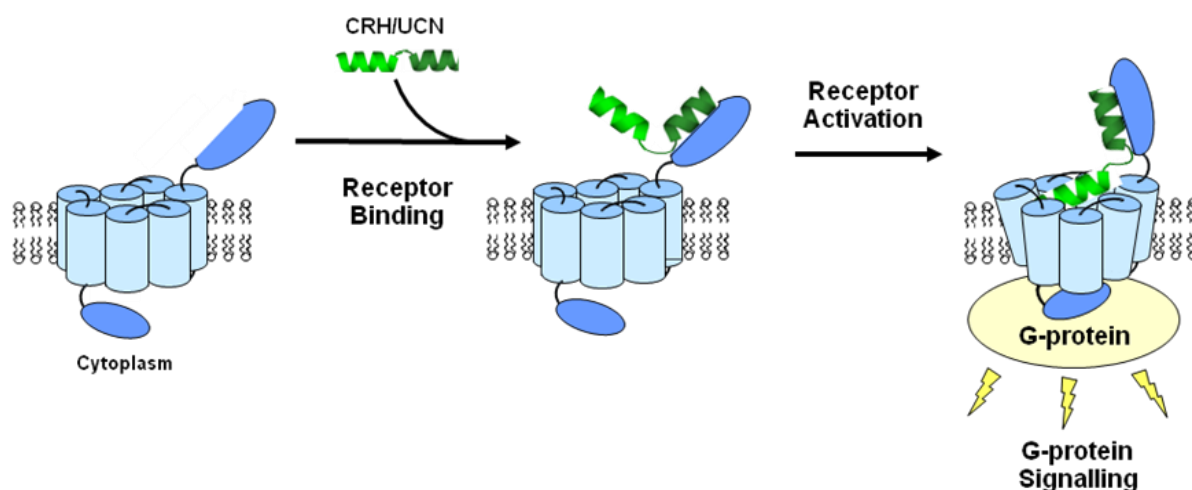
The CRHR<sub>1</sub> and CRHR<sub>2</sub> have been shown to bind the CRH and CRH-like peptides with different affinities. CRH is selective for CRHR<sub>1</sub> and possess a tenfold higher affinity for CRHR<sub>1</sub> than for CRHR<sub>2</sub>. UCN has equal binding affinities for both receptors subtypes (Perrin et al. 1995). In contrast, UCN2 and UCN3 are the CRHR<sub>2</sub>-selective natural peptides. Synthetic CRH analogues such as α-helical CRH9-41 and stressin have been shown to bind both CRHR<sub>1</sub> and CRHR<sub>2</sub> (Figure 4 and Table 2).



**Figure 3. Mammalian family members of CRH-related neuropeptides and their receptors.** Arrows represent ligand-receptor interactions. The thickness of arrows reflects the relative binding affinities of the peptide ligands for the receptor subtypes (Deussing and Wurst 2005)

### 1.3.3 Peptide ligands binding mechanism

Peptide ligands bind and activate class B GPCRs in a two step general mechanism, called the “two-domain” model (Figure 4). In this low-resolution model, the C-terminal segment of the peptide ligand binds the ECD1 of the CRHR with high-affinity, mainly via hydrophobic interactions. Formation of this complex orients the ligand and the receptor, enabling receptor activation and intracellular signalling through interaction between the serpentine segment of the receptor and the N-terminal segment of the ligand. Although complex and multiple receptor-ligand contact are present, this simplified two-step activation model provides a useful conceptual and analytical framework to evaluate the properties of peptide ligands (Hoare 2005).

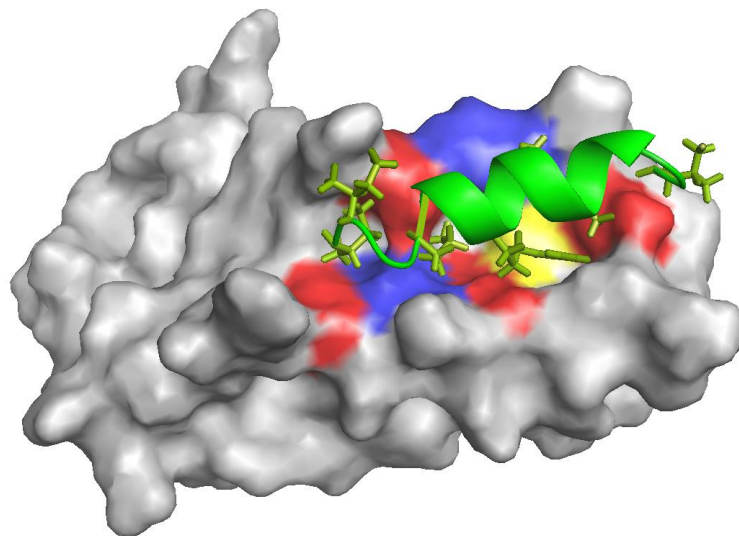


**Figure 4.** The “two-domain” mechanism of peptide ligands binding to class B GPCRs. The peptide hormone carboxyl-terminal portion first binds the CRHR<sub>1</sub>-ECD1 with high-affinity. A second interaction then occurs between the CRHR<sub>1</sub> juxtamembrane domain and peptide hormone amino-terminal portion that induces a structural rearrangement leading to G protein activation.

Although the exact spatial arrangement between the ECD1- and J-domains is presently unclear, many studies support the two-domain model for CRHR<sub>1</sub> stimulation. In particular, the ECD1- and J-domain peptide interactions have been shown to be functionally independent. The CRH and CRH-related peptides (e.g., UCN, UCN2, UCN3) can be segmented into three functional parts. The N-terminal segment (residues 1-16) is believed to be important for agonist binding and receptor activation. The middle segment (residues 17-31) contains the CRH-BP binding site and is assumed to control the structural conformation of the peptide hormone, while the C-terminal segment (residues 32-41) is crucial for ECD1 receptor binding (Mazur *et al.* 2004). The 3D structure of these peptides is not fully established but it is believed that the central region is  $\alpha$ -helical, and that both terminal ends

are relatively unstructured. However there are strong evidences that the C-terminus of the peptide form another  $\alpha$ -helix when bound to the receptor (*Hoare 2005*).

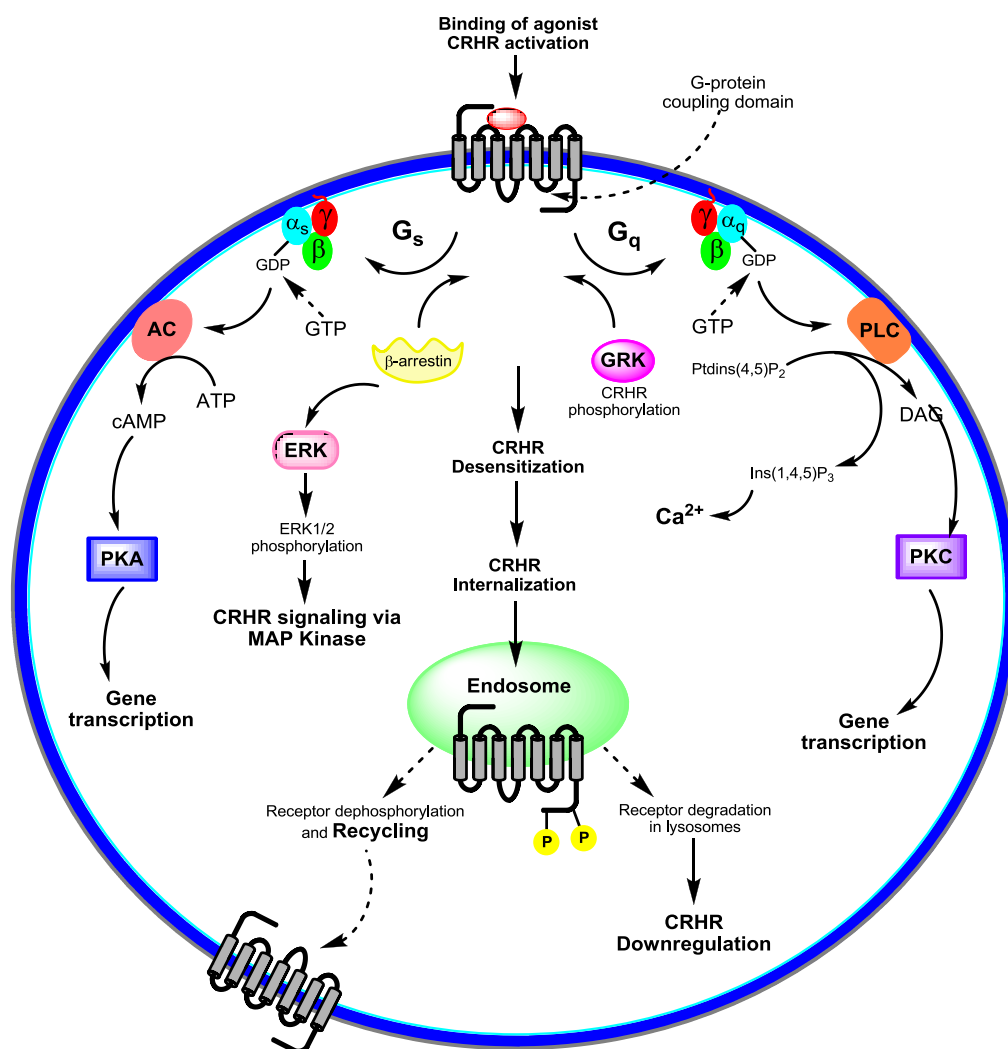
Recently, a considerable insight into the ligand binding mechanisms of class B GPCRs has been gained from several reports of ECD-peptide complex structures determined by NMR and X-ray methods (*Grace et al. 2007; Grace et al. 2010; Pioszak et al. 2008*). The NMR solution structure of astressin (a peptide antagonist analogue based on human CRH, table 2) bound to the mouse CRHR<sub>2</sub>-ECD1 showed that the ECD1 consists of two antiparallel  $\beta$ -sheets, each with two  $\beta$ -strands that are held together by three conserved disulfide bonds. The astressin 27-41 amino acid fragment forms an  $\alpha$ -helix that interacts with a hydrophobic surface of the ECD1 at the interface of three loops regions. Similar 3D NMR and cocrystal structures of the CRHR<sub>1</sub>-ECD1 in complex with the peptide antagonist  $\alpha$ -helical CRH<sup>9-41</sup> or CRH were recently disclosed (*Grace et al. 2010; Pioszak et al. 2008*). Interestingly, these studies show that complex formation between a peptide ligand and the CRHR<sub>1</sub>-ECD1 promotes the ligands helical conformation, thereby enhancing the ligands affinity.



**Figure 5. NMR structure of the peptide antagonist astressin bound to the CRHR<sub>2</sub>-ECD1** (*Grace et al. 2007*). Shown are hydrophobic interactions (red), hydrogen bonds (blue) and salt bridges (yellow).

### 1.3.4 G protein-coupled receptor-dependent signaling cascades

The CRH receptors are members of the class B subfamily of GPCRs and activate different G protein and signaling cascades upon ligand binding. In most tissues, stimulation of both CRHR<sub>1</sub> and CRHR<sub>2</sub> by CRH or CRH-like peptides leads to guanine nucleotide stimulatory protein (G<sub>s</sub>) signaling and activates the adenylyl cyclase protein kinase (AC-PKA) pathway (Aguilera *et al.* 1983; Olinas *et al.* 1995). Upon ligand binding, an allosteric change occurs within the CRH receptor that increases its affinity for G<sub>s</sub>, triggering activation and dissociation of the G protein heterotrimers in its G<sub>α</sub> and G<sub>βγ</sub> subunits. Similarly, the coupling of G<sub>s</sub> to the intracellular loop of the CRHR<sub>1</sub> (CRHR<sub>1</sub>-IC3) produces a ~1300-fold increase in the receptor affinity for CRH.



**Figure 6. Major intracellular pathways for signal transduction by CRH receptors.** Upon CRH binding to CRHR<sub>1</sub>, signaling pathways both in the cytoplasm and in the nucleus are initiated. ACTH synthesis and release are induced by the activation of PKA and PKC as well as the MAP kinase cascade.



The dissociated  $G_{\alpha}$  and  $G_{\beta\gamma}$  subunits then interact with a variety of effector molecules. In particular, the released  $G_{\alpha_s}$  subunit triggers the activation of adenylyl cyclase (AC) inducing an increase of cyclic adenosine monophosphate (cAMP) levels. In turn, cAMP binds and regulates the activity of the protein kinase A (PKA). Among others, the PKA activates the cAMP responsive element binding protein (CREB), which in turn binds the cAMP response element (CRE). This cascade of biochemical events ultimately stimulates gene transcription and leads to the synthesis of ACTH from the POMC precursor molecule (Figure 6). The AC-PKA pathway, which regulates stress and anxiety responses, is the dominant signaling pathway in endogenous and recombinant cell lines.

Both  $CRHR_1$  and  $CRHR_2$  have been shown to couple to  $G_q$  and signal via the phospholipase C-protein kinase C pathway (PLC-PKC). Activation of PLC promotes the formation of inositol (1,4,5)-triphosphate (IP3) and diacylglycerol (DAG), leading to increased intracellular  $Ca^{2+}$  levels and activation of protein kinase C (PKC) isoforms. CRHRs can also signal *via* the ERK-mitogen-activated protein kinase (MAPK) pathway. In addition,  $\beta$ -arrestin recruitment terminates G protein activation, inhibits further downstream signaling and induces desensitization and internalization. A potential mechanism of stress adaptation has been associated with G protein-coupled receptor kinases (GRKs) and  $\beta$ -arrestin-recruitment when exposed to increased levels of CRH (*Dautzenberg et al. 2001*). Upon excessive agonist binding, GRKs are recruited to the intracellular domain of the CRH receptor and phosphorylates specific residues, enhancing the receptors affinity for  $\beta$ -arrestin.  $\beta$ -arrestin-bound receptor is G protein uncoupled and therefore downstream signaling is inhibited. CRHRs have also been shown to signal via a variety of other pathways such as the Akt/protein kinase B-PI-3 kinase pathway, the NOS-guanylyl cyclase pathway and the caspase pro-apoptotic pathway (*Hauger et al. 2006*).

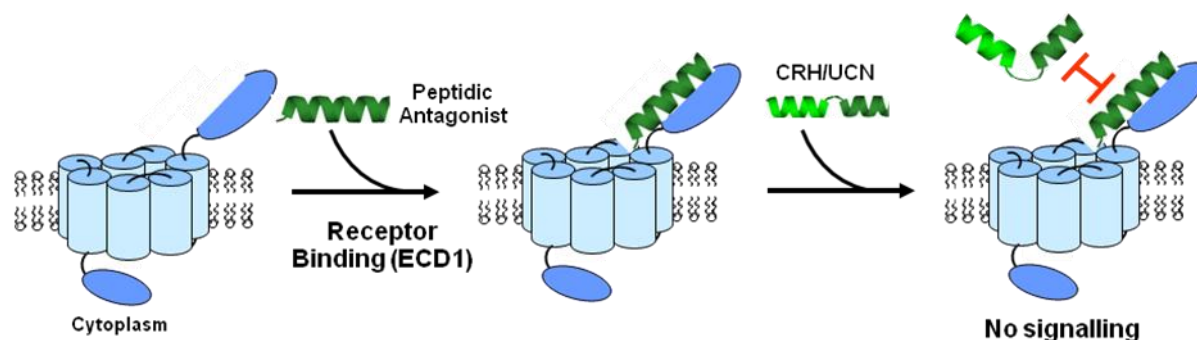
## 1.4 CRHR<sub>1</sub> antagonists

Tricyclic antidepressants, selective reuptake inhibitors and monoamine oxidase inhibitors are the common drugs used for the treatment of psychiatric disorders such as depression and anxiety. All three drug classes act by modulating the concentration of neurotransmitter (e.g., serotonin, noradrenalin and dopamine, respectively) in the synaptic cleft (Nestler *et al.* 2002). Although the effectiveness of antidepressants is significant for patients with severe forms of depression, it is minimal for those with mild or moderate forms of the disease (Kirsch 2009; Kirsch 2010). It is estimated that greater than 40 % of the patients treated with an antidepressant do not show any response (Baghai *et al.* 2006; Ruhe *et al.* 2006). Moreover, the mechanisms of action of antidepressants are not fully understood. Lack of efficacy and severe side effects have pointed out the need of drugs based on alternative biochemical mechanisms. The CRH/CRHR<sub>1</sub> system is a target of choice for the therapeutic intervention in stress-related disorders.

### 1.4.1 Peptide antagonists

Structure-activity-relationship (SAR), mutant, chimeric and substitution studies of the endogenous peptide ligands have led to the development of highly potent CRHR<sub>1</sub> peptide antagonists. In particular, N-terminal truncation of the first twelve amino acids of CRH abolishes agonistic activity and led to the development of astressin (cyclo(30-33)-[D-Phe<sup>12</sup>, Nle<sup>21,38</sup>, Glu<sup>30</sup>, Lys<sup>33</sup>]r/h CRH<sup>12-41</sup>) (Gulyas *et al.* 1995). Recently, Yamada *et al.* described a twelve amino acid long peptide antagonist based on the C-terminus of CRH, indicating that this short C-terminal sequence is enough for binding the extracellular domain of the CRHR<sub>1</sub> (CRHR<sub>1</sub>-ECD1) (Yamada *et al.* 2004). Peptide antagonists such as astressin are highly alpha-helical and often use an intramolecular lactam bridge to constrain the peptide conformation (Table 2).

Peptide antagonists bind with high-affinity to the extracellular domain of the receptor and blocks binding of an agonist and subsequent signal transduction (Rivier *et al.* 2002). This mechanism of inhibition supports the two domain model hypothesis for the activation of class B GPCRs. In general, the C-terminal segment of a CRHR<sub>1</sub> peptidic ligand determines the binding affinity, while the N-terminal segment governs the potency of the agonist. Lacking the N-terminus responsible for CRHR<sub>1</sub> activation, peptide antagonists effectively block the endogenous ligand from binding the CRHR<sub>1</sub>-ECD1 by competition (Figure 7).



**Figure 7. Mechanism of the CRHR<sub>1</sub> peptidic antagonism.** Peptide antagonists such as astressin bind the CRHR<sub>1</sub>-ECD1 with high-affinity, an interaction which blocks the endogenous peptide agonist from binding by competition.

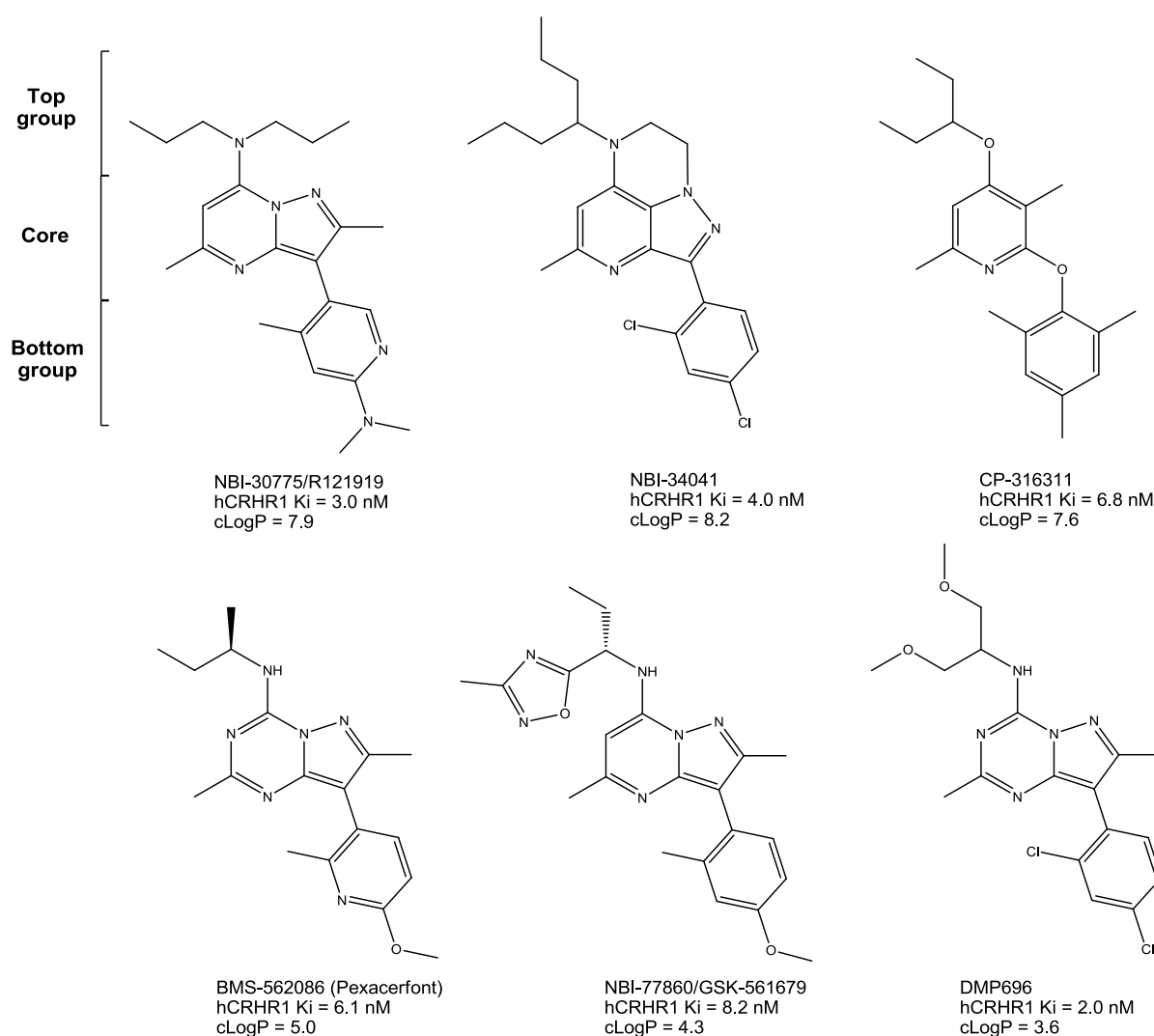
### 1.4.2 CRHR<sub>1</sub> non-peptide ligands

Small molecule, orally active, brain-penetrating CRHR<sub>1</sub> antagonists represent a promising and novel class of drugs for therapeutic use in the treatment of anxiety, depression and other stress-related disorders (*Holsboer and Ising 2008; Ising and Holsboer 2007; Kehne and De 2002; Stahl and Wise 2008*). First reports of small molecule CRHR<sub>1</sub> antagonists date to 1996 (*Chen et al. 1997b; Schulz et al. 1996b*). Since then, hundreds of small molecules with high and selective CRHR<sub>1</sub> affinity have been identified; however none have made it onto the pharmaceutical market. The pharmacology and properties of the most well-studied CRHR<sub>1</sub> nonpeptide antagonists were recently reviewed (*Chen 2006; Tellew and Luo 2008; Zorrilla and Koob 2010*). All small molecule CRHR<sub>1</sub> antagonists share several common pharmacophoric features (Figure 8).

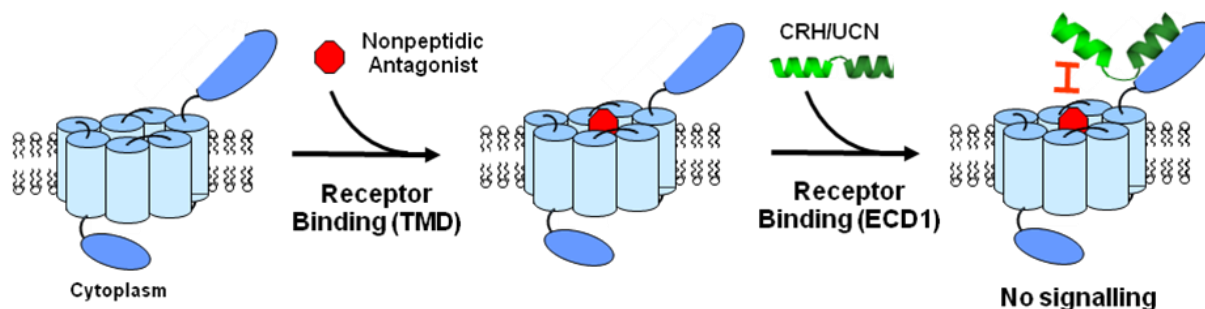
A five- or six-membered nitrogen heterocyclic core bears a key hydrogen bond-accepting nitrogen atom (HBA). A pendant aryl group (bottom aryl) is attached to the core at the position adjacent to the HBA via a one atom spacer, which is frequently part of a fused ring. The bottom aryl group is typically 2,4-disubstituted or 2,4,6-trisubstituted, with methyl, chloro, and methoxy groups common at both the ortho and para positions. The ortho substituent enforces an orthogonal orientation between the bottom aryl and the core ring. The HBA-containing core heterocycles bears a small lipophilic group, which is typically methyl for six-membered rings and ethyl for five-membered rings. Finally, a “top-group”, often a lipophilic alkylamino or branched alkyl group, is appended to the core heterocycles (*Tellew and Luo 2008*).

The molecular details of the nonpeptide ligand interaction with CRHR<sub>1</sub> are not well characterized at present. However, evidences indicate that nonpeptide antagonists bind an allosteric site in the J-domain of the CRHR<sub>1</sub> exclusively (*Hoare 2005; Hoare et al. 2006*). The nonpeptide ligands bind a

J-domain fragment with the same affinity as the whole receptor; moreover mutations within the J-domain (H199V and M276I) affect the binding of nonpeptide ligands but not peptide interaction. A functional model for the nonpeptide antagonism at the CRHR<sub>1</sub> was proposed: the nonpeptide antagonist binds the J-domain, producing a conformational change that blocks the peptide agonist binding site on the J-domain (Figure 9). Because the peptide can no longer bind the J-domain, it is not able to induce receptor activation (Hoare 2005; Hoare et al. 2008). Recently, computer-based approaches have given a more precise insight into the binding mechanism of small molecules antagonists of class B GPCRs (Bhattacharya et al. 2010; de et al. 2011).



**Figure 8. Notable CRHR<sub>1</sub> antagonists reported to have reached clinical trials.**



**Figure 9. Mechanism of the nonpeptidic CRHR<sub>1</sub> antagonism.** Nonpeptide CRHR<sub>1</sub> antagonists bind an allosteric binding site within the receptor TMD. It induces a conformational change that hinders the peptide agonist to bind its orthosteric binding site and trigger G protein signalling.

Early CRHR<sub>1</sub> nonpeptide antagonists were very potent *in vitro* and demonstrated efficacy in animal models (Chen *et al.* 1997a; Schulz *et al.* 1996a). However, they were highly lipophilic (cLogP > 7) and poorly water-soluble. Clinical development of such compounds, especially as CNS drugs, has been hindered because of unattractive pharmacokinetics, extensive tissue accumulation and long elimination half-lives. Recently, efforts have been focused on adding drug-like properties to these molecules and turn it into suitable CNS drugs (Chen 2006).

Although limited clinical results and data are currently available, a number of CRHR<sub>1</sub> antagonists have been reported to have entered clinical trials for depression and anxiety related disorders (Kehne and Cain 2010) (Figure 8). Notably, NBI-30775/R121919 demonstrated efficacy in treating patients with depression in a small open-label phase IIa clinical trial, although further development was discontinued due to hepatotoxicity issues (Kunzel *et al.* 2003; Zobel *et al.* 2000). In a placebo-controlled clinical study with NBI-34041, improved resistance to psychological stress was observed (Ising *et al.* 2007). However, in a double-blind, placebo-controlled clinical trial for the treatment of major depressive disorder, CP-316311 was declared not efficacious (Binneman *et al.* 2008; Chen *et al.* 2008a). Likewise, pexacerfont (BMS-562086) was also declared not efficacious in generalized anxiety disorder (Coric *et al.* 2010). In a recent press release dated 9/14/10, Neurocrine Biosciences Inc. ([www.neurocrine.com](http://www.neurocrine.com)) announced top-line efficacy and safety results from a Phase II, double-blind, placebo-controlled clinical trial with CRHR<sub>1</sub> antagonist NBI-77860/GSK561679 in patients with major depressive disorder.

While the clinical results to date have been disappointing, a complete evaluation requires consideration of a number of factors, including the potential need to target clinical subpopulations with demonstrated CRHR<sub>1</sub> hyperactivation in stress response pathways (*Kehne and Cain 2010*). Additional compounds have been reported to enter clinical trials (*Chen et al. 2008b; Gilligan et al. 2009b; Tellew et al. 2010*), the results of these trials and clinical studies may further define the role of CRH antagonism for the treatment of human illnesses.

## 2 Objective of the study

The CRH/CRHR<sub>1</sub> system orchestrates the neuroendocrine and behavioral responses to stress has attracted major interest as a potential novel target for the therapeutic intervention in psychiatric disorders (*Holsboer and Ising 2008; Ising et al. 2007; Zobel et al. 2000*). Generally, transmembrane receptors of the class B GPCR subtype have a huge clinical potential to ameliorate numerous of diseases of high severity and prevalence. Nonetheless, the development of drugs targeting these receptors has been hampered by the difficulty to identify tractable leads as well as by a limited biochemical understanding. Moreover, the molecular determinants involved in the recognition of CRH peptide ligands and in the modulation of the CRHR<sub>1</sub> signaling cascade are not well characterized at present. Therefore, a more precise understanding of the involved interaction mechanisms is an essential prerequisite towards the development of more efficient CRHR<sub>1</sub>-specific modulators.

The aim of this study was the development of tools to pharmacologically address class B GPCRs in tractable and relevant biological systems. In particular, we aimed to address the following questions:

- a) How do peptide ligands bind and activate the CRHR<sub>1</sub> and class B GPCRs? In particular, what are the specific ligands domains involved in receptor binding and modulation?
- b) What are the role and contribution of individual amino acid residues of the peptide ligands for CRHR<sub>1</sub> binding and modulation?
- c) Can the structure-activity-relationship analysis of the CRHR<sub>1</sub> ligands give an insight into the activation mechanism of class B GPCRs?
- d) Can the structure-activity-relationship informations be used for the design of novel and tailored CRHRs ligands, agonists or antagonists?





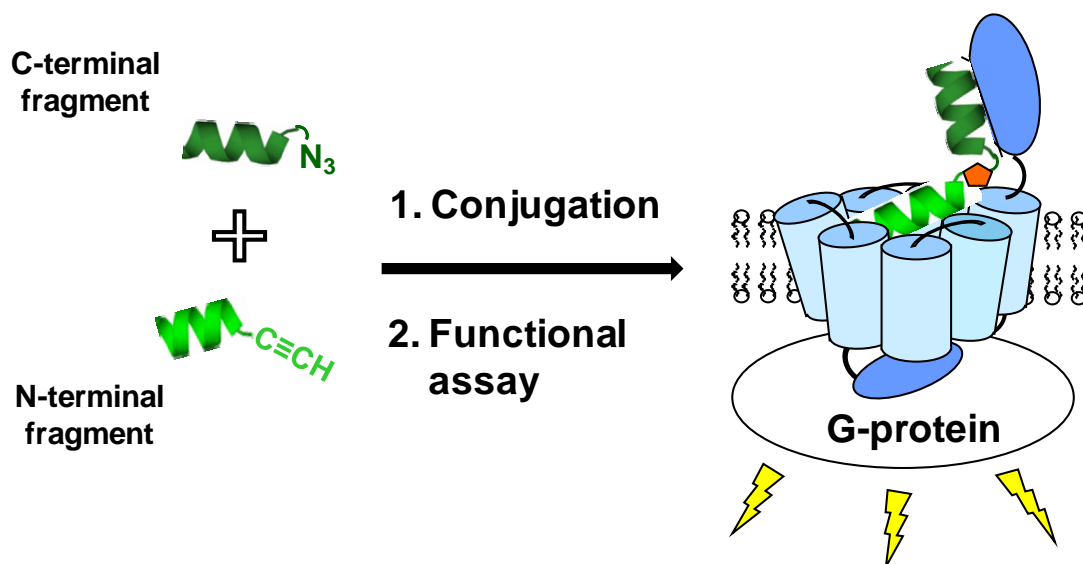
## 3 Results and discussion

### 3.1 Peptide-peptide conjugates as CRH mimics

Several structure-activity-relationship studies have investigated the amino acid sequence of CRHR peptide ligands. In particular, Beyermann et al. have successfully shown the existence of two segregated receptor binding sites in the sequence of CRHRs ligands (Beyermann et al. 2000). CRHR<sub>1</sub> peptide ligands bind and activate their cognate class B GPCR thanks to a low resolution “two domain” mechanism. Stepwise, the C-terminal part of the hormone binds the CRHR<sub>1</sub> extracellular domain (CRHR<sub>1</sub>-ECD1) with high-affinity, an interaction that directs the N-terminal part of the hormone to interact with the CRHR<sub>1</sub> transmembrane domain (CRHR<sub>1</sub>-TMD) leading to G-protein signaling. In particular, the middle domain of the CRH hormone, which connects the two functional sites of the peptide hormone, was successfully replaced by a helical “connector”, thereby reconstituting a potent peptide agonist (Beyermann et al. 2000). Based on this work, we developed a peptide-peptide conjugation strategy to chemically probe the molecular interactions of CRH-like peptide ligands with their cognate receptor. We propose that the coupling of a CRHR<sub>1</sub>-ECD1 specific C-terminal peptide with an N-terminal peptidic fragment could produce high potency agonists.

#### 3.1.1 Choice of a ligation technique for the synthesis of biomimetic probes

The conjugation consists in the linking of two biomolecules to form a hybrid, the bioconjugate, which retains the properties of each individual component. The coupling of two peptide fragments logically begins with the choice of a suitable ligation chemistry. Many criteria have to be fulfilled to produce an adapted conjugation technique: in optimal conditions, the conjugation method should be fast and quantitative, highly selective and insensitive to the chemical environment. Moreover the functional groups required for the conjugation reaction should be mildly and easily incorporated, preferentially during solid phase peptide synthesis (SPPS). Finally, the conjugation reaction should provide a robust and stable linkage that remains neutral toward ligand binding to its target receptor. For its versatility and broad applicability, we chose the Copper-Catalyzed Azide-Alkyne Cycloaddition (CuCAAC) as a starting point for our study. This 1,3-dipolar cycloaddition has such a large scope that it has been defined as “the cream of the crop” of “click” chemistry by K. Barry Sharpless himself (Kolb et al. 2001). Lately, the CuCAAC was extensively applied to small molecules for drug discovery purposes but to our knowledge, only few examples of peptide-peptide CuCAAC-mediated conjugations have been reported.



**Figure 10. Biomimetic probe principle for the investigation of Class B GPCR-ligand interaction.**

An alkyne-tagged peptide (light green) is conjugated to a constant peptide fragment (dark green) that has high-affinity for the extracellular domain of the class B GPCR. The peptide-peptide conjugate is tested for modulation of the GPCR transmembrane domain activity in a cell-based functional assay.

The CuCAAC is quantitative, robust and insensitive, thereby fulfilling most of our chemical requirements. Importantly, the 1,2,3-triazole linkage obtained is known to be insensitive and stable in most pH conditions. The copper(I) catalyzed variant of the CuCAAC afford exclusively 1,2,3-triazoles as 1,4-regioisomers (*Toroe et al.* 2002). Moreover, the conjugation can be performed under a wide variety of conditions and with almost any source of solvated Cu(I). For the reconstitution of CRH-like peptide hormone mimics, the CuCAAC is better suited than the commonly used native chemical or Staudinger ligations, which require N-terminal cysteine residues and detrimentally produce native amide bonds. Many arguments making us believe that the CuCAAC can be successfully applied to the reconstitution of CRH hormone mimics (Figure 10). As an alternative conjugation technique, we chose to apply and investigate the hydrazone bioconjugation of peptides. The hydrazone ligation occurs spontaneously and does not require additives such as oxidant or metal, making it attractive for the testing of crude peptide conjugates *in vitro* and *in vivo*.

### 3.1.2 Synthesis and characterization of CRHR<sub>1</sub>-ECD1 high affinity probes

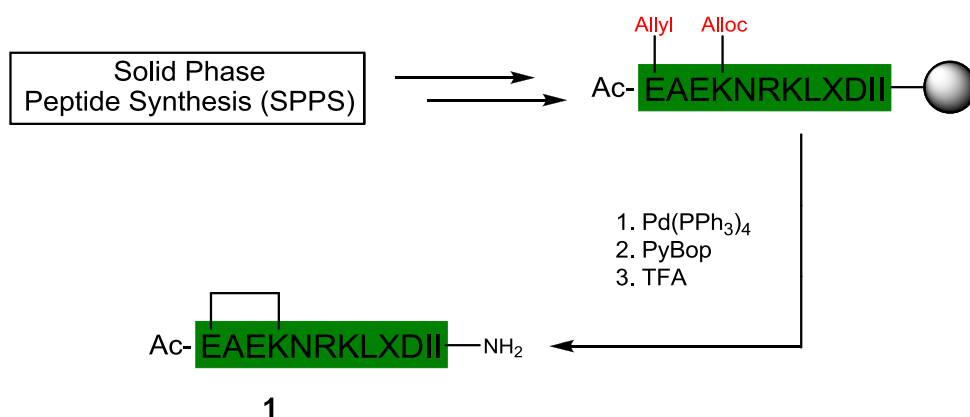
The peptides **1-3** were designed as CRHR<sub>1</sub>-ECD1 high-affinity peptide carriers based on known optimized C-terminal CRH analogs (Yamada *et al.* 2004) and were synthesized using standard Fmoc-SPPS (Figure 11). The high-affinity carrier peptides **1-3** share common and specific structural features: all three possess an intramolecular lactam bridge. This conformational constrain is well characterized and has been shown to stabilize the peptide's helical conformation thus enhancing its affinity for the CRHR<sub>1</sub>-ECD1 (Gulyas *et al.* 1995; Hernandez *et al.* 1993; Koerber *et al.* 1998; Miranda *et al.* 1994; Rivier *et al.* 1998b). Similarly, recent structure-activity-relationship studies have identified the cyclohexyl-alanine (X) substitution to be greatly potency enhancing (Yamada *et al.* 2004). This led to the synthesis of N-terminally acetylated peptide **1** (Figure 11a). Peptide **1** was designed as a high-affinity CRHR<sub>1</sub>-ECD1 peptide antagonist and was successfully used for the pharmacological characterization of the CRHR<sub>1</sub>-ECD1 (Gordon *et al.* 2010).

Peptides **2** and **3** were designed for the use in CuCAAC and hydrazone ligation reactions, respectively. Peptide **2** bears a fluorescent tag (NBD, 4-(7-nitro)benzofurazanyl) for quantification and analytical purposes (Figure 11b). The fluorophore was selectively introduced on the side chain of lysine<sup>8</sup> during SPPS. This residue was shown to point out of the CRHR<sub>1</sub>-ECD1 binding cavity, thus it does not contribute to the binding of the peptide to the CRHR<sub>1</sub> (Grace *et al.* 2007). An azide-functionalized polyethylene glycol spacer was introduced at the N-terminus of the high-affinity peptide sequence for use in CuCAAC conjugation reactions. Moreover, the flexibility of this spacer allows optimal positioning of the ligands binding domains towards the receptors ECD1 and TMD (Beyermann *et al.* 2000). The synthesis of the spacer was straightforward and achieved in four steps with an overall 51 % yield (Figure 12a). Gratifyingly, the triethylene glycol spacer greatly improved the solubility of the high-affinity peptide **2** in aqueous solvents, thereby facilitating chromatographic purification.

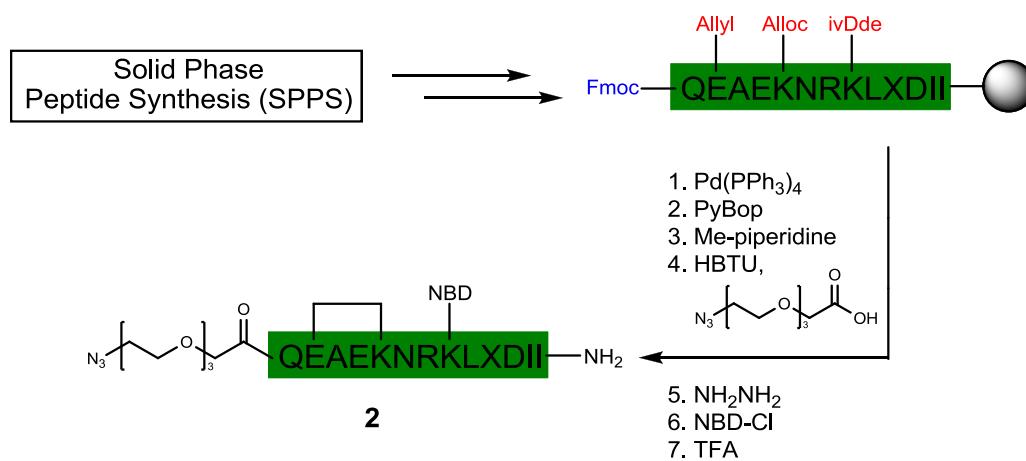
Similarly, peptide **3** was designed for hydrazone ligations (Figure 11c). We synthesized a Boc-protected hydrazinonicotinic acid (HNA, Figure 12b) which was coupled to the peptides N-terminus during SPPS (Abrams *et al.* 1990). In contrast with peptide **2**, peptide **3** was not fluorescently tagged as the aryl-hydrazone conjugation product was shown to yield a constitutive chromophore.

The affinity of peptides **1-3** for the CRHR<sub>1</sub>-ECD1 was tested in a radioactive competition assay using I<sup>125</sup>(Tyr<sup>0</sup>)-sauvagine as a tracer (Figure 13 and Table 3).

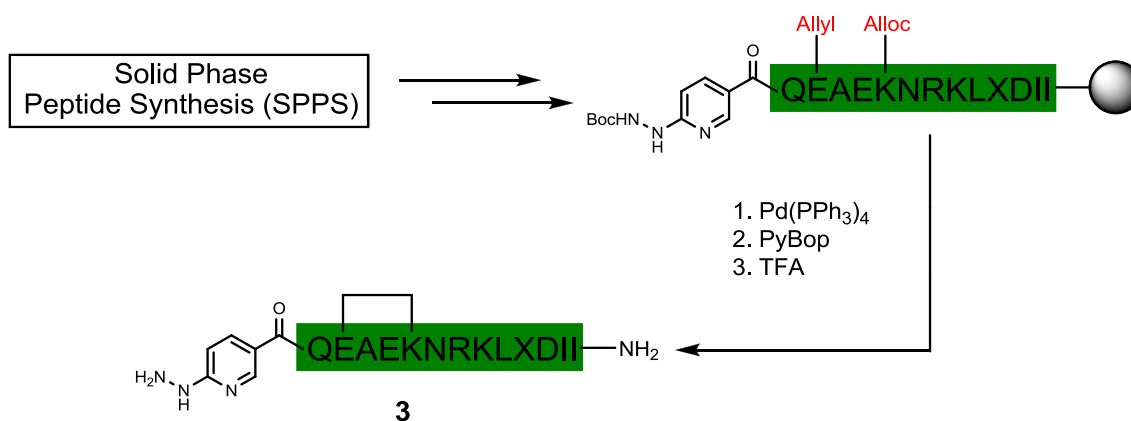
a)



b)

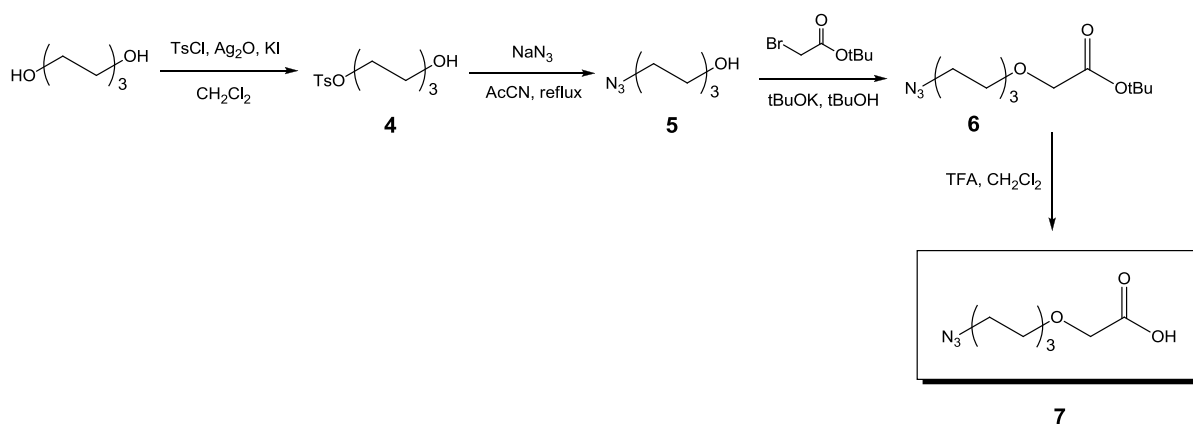


c)

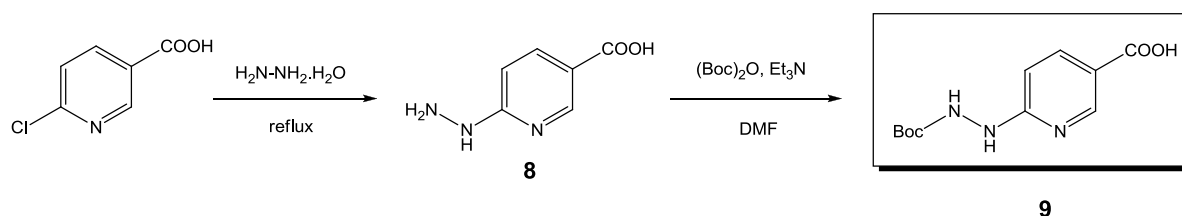


**Figure 11. SPPS scheme for the synthesis of high-affinity peptide carriers.** a) SPPS of the N-terminally acetylated peptide **1**. b) SPPS of the N-terminally azide-functionalized carrier **2**. c) SPPS of the N-terminally hydrazine-functionalized carrier **3**. X = cyclohexyl alanine; EAEK = lactam bridge, NBD = 4-(7-nitro)benzofurazanyl.

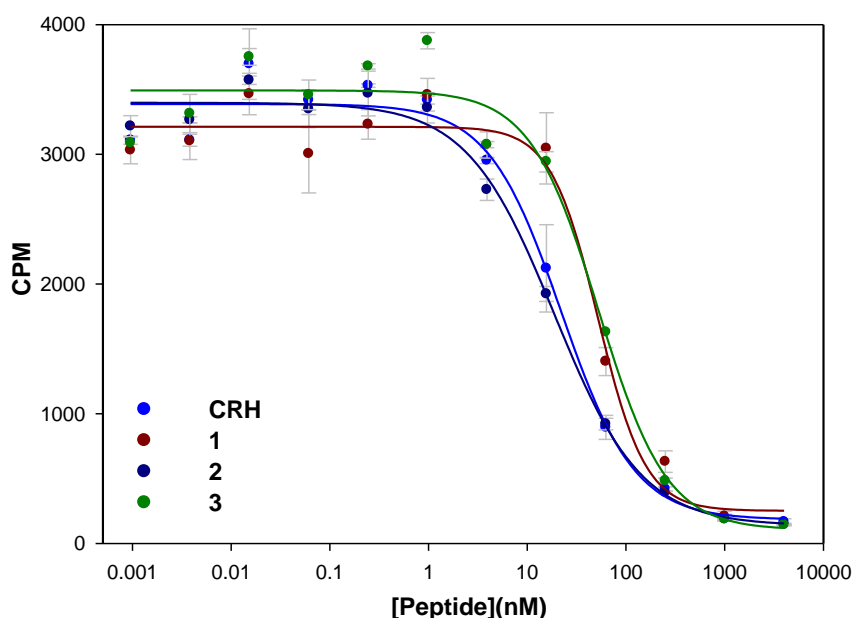
a)



b)



**Figure 12. Synthesis of functionalized modification reagents.** a) Synthesis of the triethylene glycol based azide-functionalized spacer **7**. b) Synthesis the Boc-protected hydrazinonicotinic acid **9**.



**Figure 13. Binding of CRHR<sub>1</sub>-ECD1 high-affinity peptide probes 1-3.** Radioactive competition assay using  $^{125}\text{I}(\text{Tyr}^0)$ -sauvagine and membrane preparations from HEK293 cells stably overexpressing CRHR<sub>1</sub>.

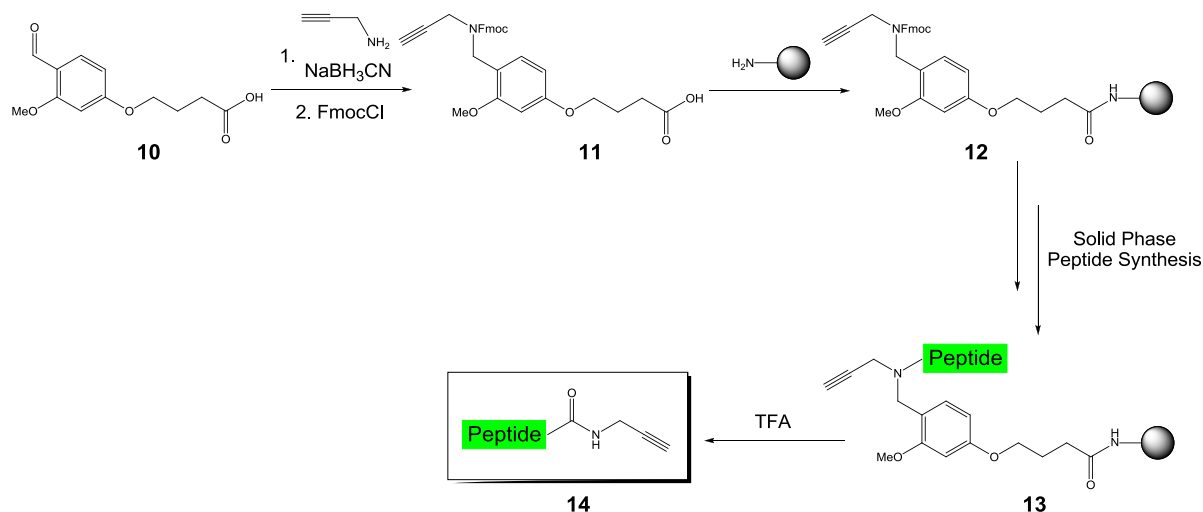
		IC <sub>50</sub> [nM] (s.e.m.)
●	CRH	22.1 ± 4.5
●	1	52.2 ± 8.3
●	2	18.8 ± 2.8
●	3	52.6 ± 13.3

**Table 3. Characterization of CRHR<sub>1</sub>-ECD high-affinity peptide probes.**

Gratifyingly, we observed that peptide carriers **1-3** retain high-affinity for the CRHR<sub>1</sub>-ECD1 and show affinities similar to the endogenous hormone CRH (Figure 13 and Table 3). The azide-functionalized peptide **2**, which bears the N-terminal spacer showed the highest affinity for the CRHR<sub>1</sub>-ECD1. This proves that the presence of a highly flexible spacer and the NBD fluorescent tag do not disturb or influence the binding to the CRHR<sub>1</sub>-ECD1. Peptides **1** and **3** showed slightly weaker affinities than peptide **2**. This might be due to the presence and binding contributions of the acetyl or HNA N-terminal functional groups respectively. Although the affinities of the carriers **2** and **3** were two-fold lower than that of the endogenous ligand CRH, the peptides **1-3** were considered as efficient CRHR<sub>1</sub>-ECD1 high-affinity probes and were used for further investigations.

### 3.1.3 Synthesis of a “clicked” biomimetic probe: proof of concept

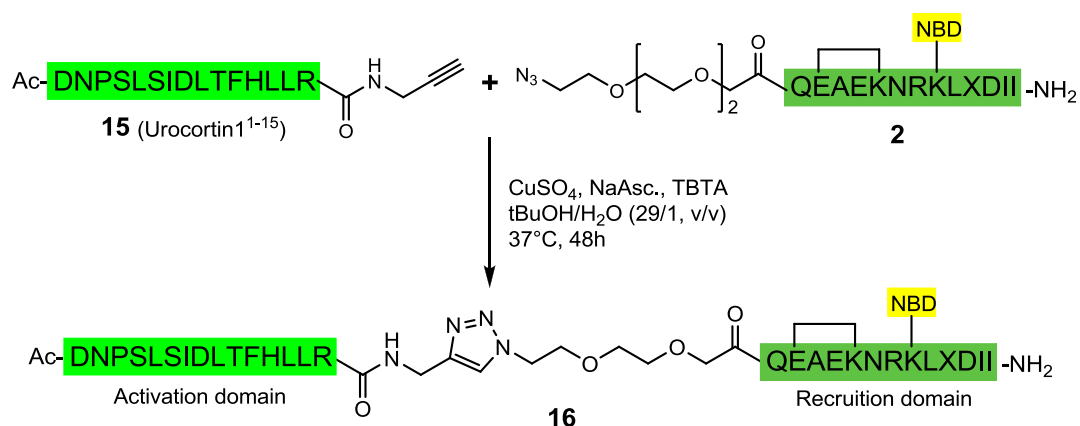
The synthesis of C-terminally modified peptides was achieved by using the Backbone Amide Linker (BAL) approach whereby the growing peptide is anchored through a backbone nitrogen (Figure 14). The synthesis of the required 4-(3-methoxy-4-([(9H-fluoren-9-ylmethoxycarbonyl)(prop-2-ynyl)-amino]methyl)(1)phenoxy)butanoic acid linker **11** (FMPB) was achieved by reductive amination using propargylamine and sodium cyanoborohydride, followed by fluorenylmethyloxycarbonyl (Fmoc) protection of the resulting secondary amine. The synthesis of the FMPB linker **11** was first optimized, and then performed in a “one-pot” reaction. This building block was then attached to a poly-(ethylene glycol)-polystyrene (PEG-PS) support and used to assemble peptides by standard Fmoc solid-phase chemistry. The final cleavage from the resin yield the C-terminally modified peptide **14** (Devigny *et al.* 2011).



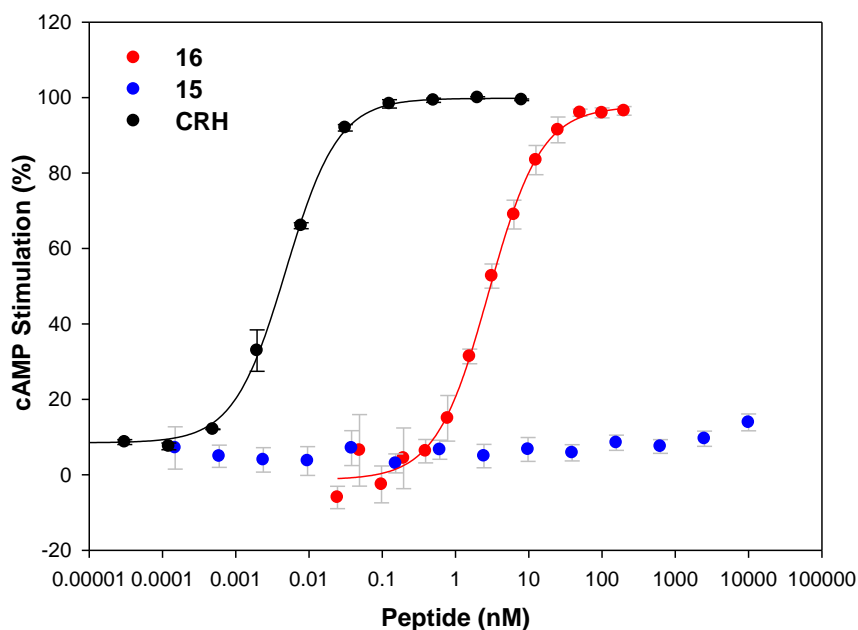
**Figure 14. BAL strategy for the synthesis of C-terminally propargylated peptides.** Briefly, the synthesis of the FMPB linker **11** was performed in a “one-pot” reaction. The linker **11** was then attached to a PEG-PS solid support yielding resin **12** that was used for SPPS. Cleavage of the peptide from the resin afford the desired N-terminally propargylated peptide **14**.

In the next step, we investigated if the coupling of an N-terminal “activation” fragment with peptide **2** could reconstitute a CRH-like hormone mimic. The endogenous peptide agonist Urocortin1 (UCN) was chosen as a starting point for the investigation of ligand-CRHR<sub>1</sub> interactions. UCN is closely related to the CRH hormone and a highly potent nonselective CRHR<sub>1</sub> and CRHR<sub>2</sub> agonist (see Introduction, figure 3 and table 2). Based on several structure-activity-relationship (SAR) studies of the full length CRH peptide hormone, we chose to first investigate whether the fragment 1-15 of the UCN hormone could provide the required amino acid residue sequence that leads to CRHR<sub>1</sub> activation (Beyermann *et al.* 2000; Kornreich *et al.* 1992).

a)



b)



**Figure 15. Stimulation of CRHR<sub>1</sub> by a peptide conjugate.** a) Synthesis of the activation segment **15** (light green) using BAL resin **12** and “click” conjugation with membrane recruitment segment **2** that is derived from CRHR<sub>1</sub> ligands (dark green). X = cyclohexyl alanine; EAEK = lactam bridge; NBD = 4-(7-nitro)benzofurazanyl. b) Stimulation of cAMP production in HEK293 cells stably over-expressing CRHR<sub>1</sub> by the C-terminally propargylated peptide **15** (blue), peptide conjugate **16** (red) and CRH (black).

For this purpose, the N-terminal fragment peptide **15**, corresponding to the fragment (1-15) of UCN, was synthesized using the BAL strategy in order to introduce the alkyne moiety at the peptide



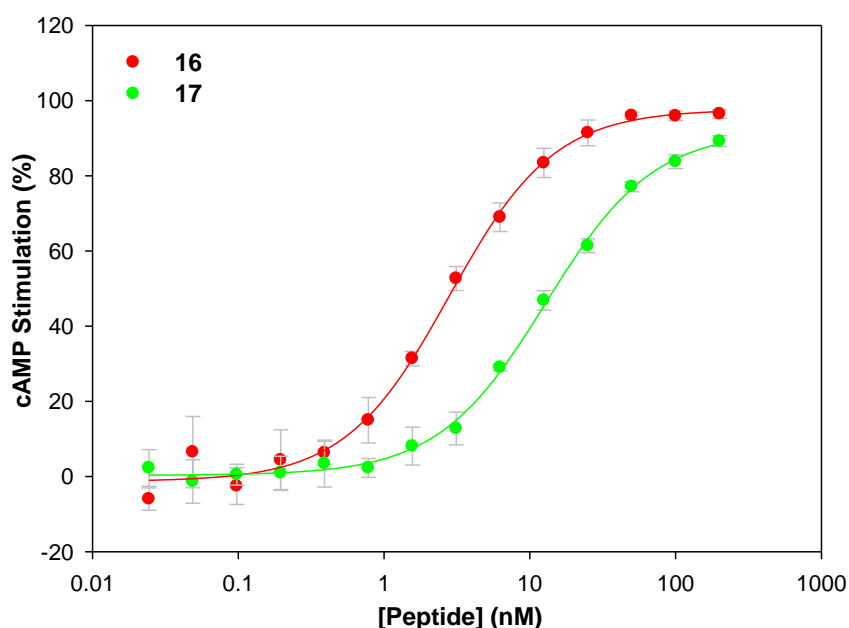
C-terminus (Figure 15a). After HPLC purification, the peptide **15** was conjugated to the high-affinity peptide **2** by CuCAAC. The specific reaction conditions required for the CuCAAC were investigated by Francisco Perez-Balderas during his post-doctoral work in our laboratory. Notable features of the reaction conditions are: tert-butanol, a solvent in which the peptides are readily well-soluble; a six-fold excess of the C-terminally propargylated peptide counterpart; a large excess of copper sulfate and a sufficient reaction time. The obtained conjugate **16** was purified by HPLC, quantified by fluorescence, and tested for CRHR<sub>1</sub> stimulation in a cell-based cAMP assay (Figure 15b).

The isolated peptide fragment **15** did not show any activity at the CRHR<sub>1</sub> by itself up to a concentration of 10 μM in the cellular cAMP stimulation assay. The conjugation of peptide **15** with peptide carrier **2** by CuCAAC, however, reconstituted a full agonist with a potency of  $2.82 \pm 0.23$  nM (Figure 15b and Table 4). Although the potency of conjugate **16** was much weaker than the CRH full hormone, it was a full agonist in the low nanomolar range thus proving that the fifteen UCN N-terminal residues contain a sequence motif sufficient to induce CRHR<sub>1</sub> full-stimulation. This experiment established the peptide-peptide conjugation methodology as a fast and efficient alternative to the synthesis of full length peptide hormones. Importantly, the conjugation to the high-affinity carrier **2** dramatically enhanced the detection limits for very weak agonists such as fragment **15**, which would have been inactive otherwise.

### 3.1.4 Urocortin1<sup>1-15</sup> C- and N-terminal truncation: characterization of a minimal CRHR<sub>1</sub> stimulation sequence

Having proven that a “clicked” conjugate can act as high potency agonist, we went on to determine the minimal N-terminal peptide sequence that is necessary to fully activate the CRHR<sub>1</sub>. Bidirectionally truncated derivatives of peptide **15** were synthesized using the BAL strategy. As previously described, the purified truncated peptides were coupled to peptide **2** by CuCAAC. Interestingly, after the reactions were shaken for two days, the presence of a fine yellow-colored precipitate was observed. The precipitate was easily isolated by centrifugation and analyzed. Gratifyingly, HPLC and mass spectrometry analysis identified the precipitate as the conjugation product while unreacted counterparts stayed in solution (Figure 17). Peptide conjugates **17-22** were thus isolated as precipitates and further purified by HPLC. After fluorescence quantification, the obtained conjugates were tested for CRHR<sub>1</sub> stimulation in a cell-based cAMP assay (Figure 16 and Table 4).

a)



b)

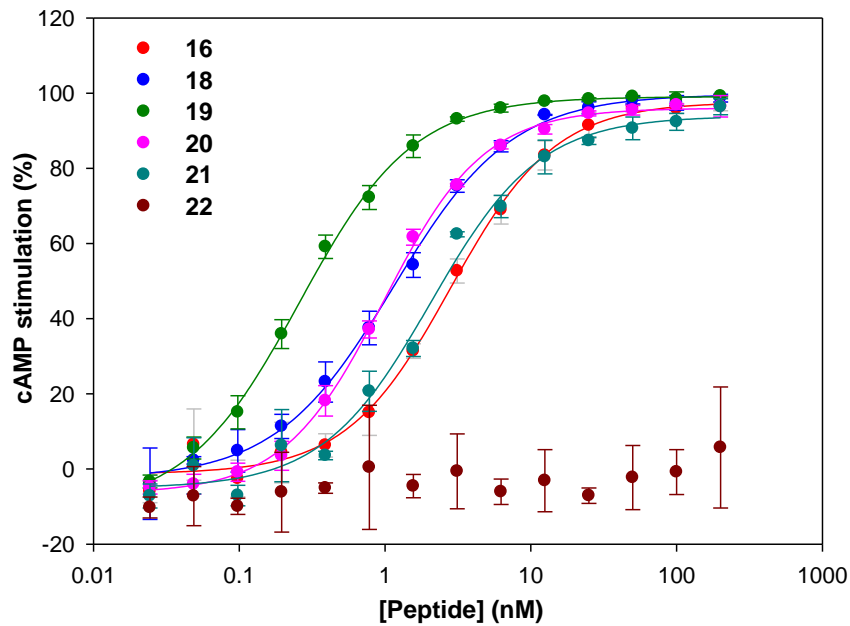


Figure 16. cAMP stimulation curves corresponding to the truncated peptide conjugates listed in Table 4. a) Curves of the C-terminally truncated conjugates. b) Curves of the N-terminally truncated conjugates.

			Peptide sequence R = carrier 2	EC <sub>50</sub> [nM] (s.e.m.)
●	CRH	-	-	0.0048±0.0002
●	16	Ac-UCN <sup>1-15</sup>	Ac-DNPSLSIDLTFHLLR-R	2.82±0.23
●	17	Ac-UCN <sup>1-14</sup>	Ac-DNPSLSIDLTFHLL-R	12.88±0.75
●	18	Ac-UCN <sup>2-15</sup>	Ac-NPSLSIDLTFHLLR-R	1.14±0.06
●	19	Ac-UCN <sup>3-15</sup>	Ac-PSLSIDLTFHLLR-R	0.26±0.01
●	20	Ac-UCN <sup>4-15</sup>	Ac-SLSIDLTFHLLR-R	0.98±0.03
●	21	Ac-UCN <sup>5-15</sup>	Ac-LSIDLTFHLLR-R	2.07±0.24
●	22	Ac-UCN <sup>6-15</sup>	Ac-SIDLTFHLLR-R	Inactive

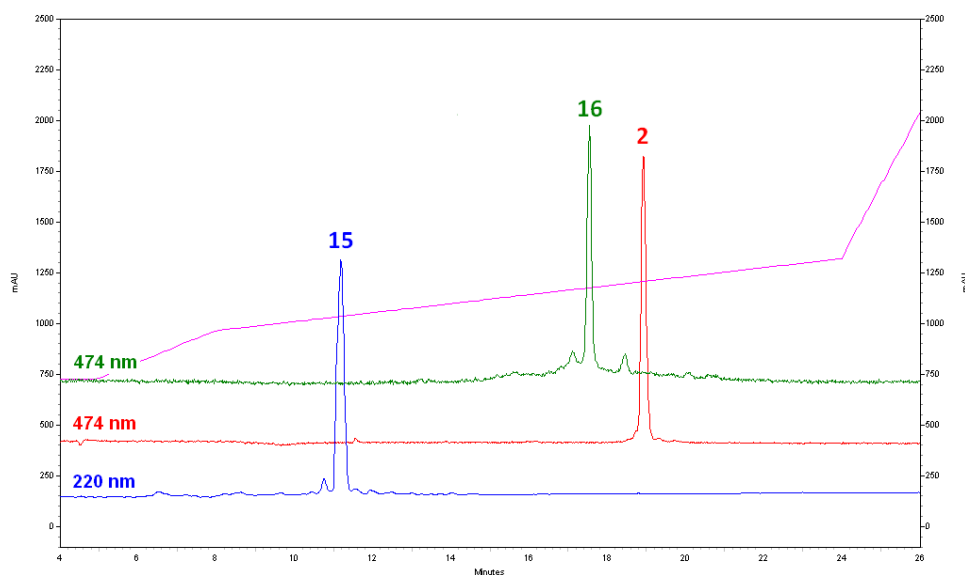
Table 4. Characterization of truncated analogs of the human UCN<sup>1-15</sup> N-terminal fragment.

a)



$\text{CuSO}_4$       +      -

b)



**Figure 17. Cycloaddition and workup of an exemplary conjugate.** a) Fluorescence visualization (Excitation: 480 nm) of the conjugation mixture after centrifugation in the presence (left reaction tube) or absence (right reaction tube) of  $\text{CuSO}_4$ . b) HPLC trace of an exemplary CuCAAC conjugation reaction, N-terminally propargylated peptide **15** (blue trace) was coupled to the high-affinity peptide carrier **2** (red trace) yielding peptide conjugate **16** (green trace) as a precipitate.

We observed that the C-terminal deletion of  $\text{Arg}^{15}$  led to a five-fold decrease in potency (Figure 16a and Table 4), indicating that  $\text{Arg}^{15}$  seem to be important for activation. Surprisingly, the N-terminal truncation of the  $\text{UCN}^{1-15}$  fragment initially increased potency. Truncation beyond  $\text{Leu}^5$ , however, completely abrogated the stimulating potency of the conjugates (Figure 16b and Table 4). Although the  $\text{UCN}^{3-15}$  conjugate **19** was the most potent of all conjugates, we considered that the

UCN<sup>4-15</sup> sequence motif presented a better balance between size and potency. With a potency of  $0.98 \pm 0.03$  nM, the conjugate **20** established the 12 amino acid UCN<sup>4-15</sup> sequence motif as a minimized activation fragment. This minimized template was used as a starting point for the further SAR investigation of individual amino acid residues, the UCN<sup>4-15</sup> native sequence of conjugate **20** being used as a potency control.

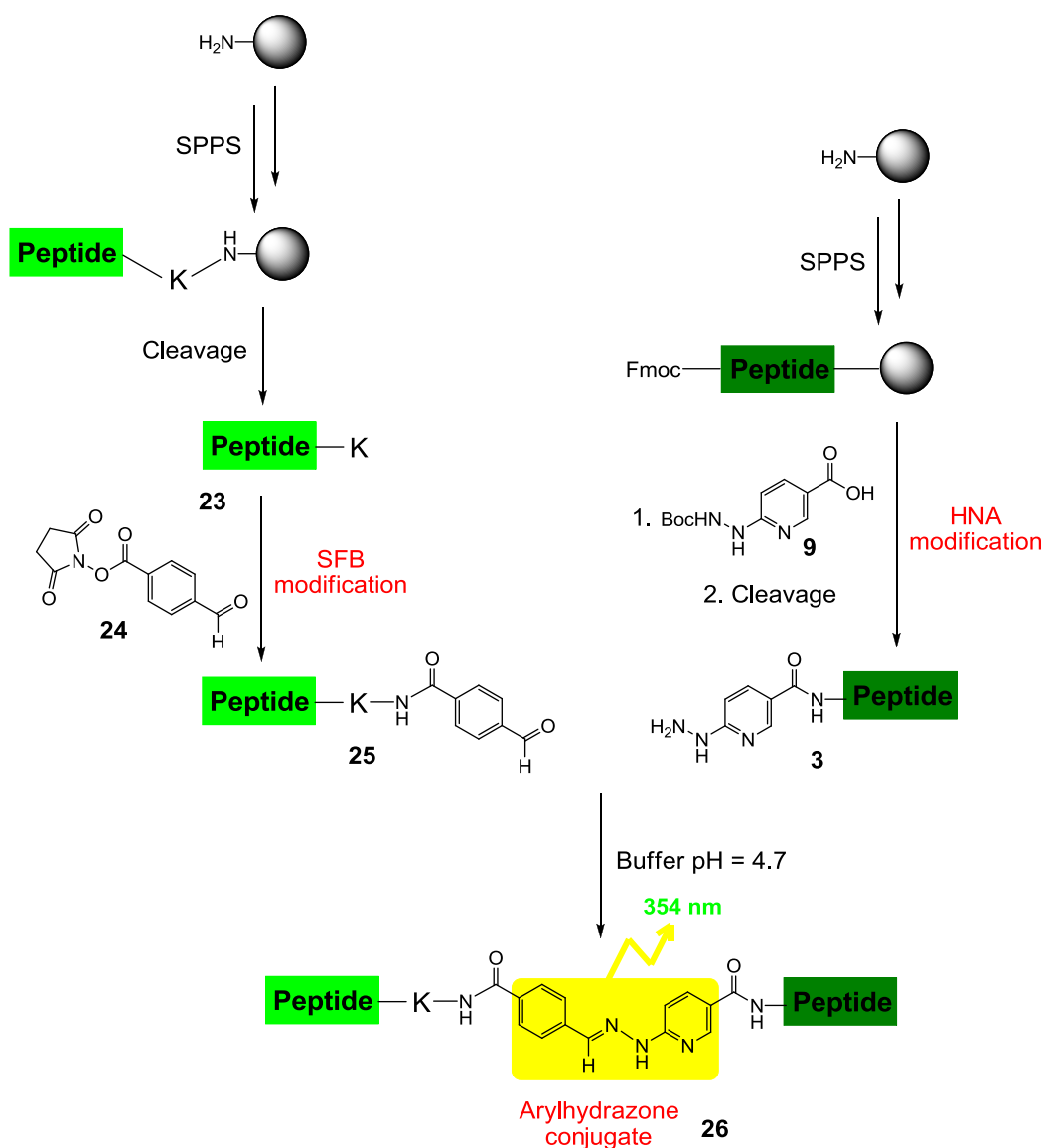
Based on our observations that peptide conjugates precipitated out of solution, a fast and efficient procedure for the work-up of peptide conjugates was established: after the reaction was shaken for two days at 37 °C, the mixture was cooled to room temperature and centrifugated (Figure 17a). The supernatant containing the soluble unreacted counterparts as well as conjugation reagents was removed; the isolated precipitate was then further washed with tert-butanol. Finally, the precipitate was dried and subsequently dissolved in DMSO. This easy procedure allowed us to quantitatively isolate the truncated conjugates **16-22** with acceptable crude purities (Figure 17b). In the following, this workup procedure was systematically used for the isolation of CuCAAC-coupled crude conjugates.

### 3.1.5 Alternative ligation method: the hydrazone bioconjugation of a UCN<sup>4-15</sup> biomimetic probe

The UCN<sup>4-15</sup> minimized activation template was used to test the suitability of the hydrazone bioconjugation as an alternative ligation method to the CuCAAC. The ligation chemistry is based on the reaction of an aromatic hydrazine with an aromatic aldehyde, yielding a stable bis-arylhydrazone conjugate bond (Figure 18). The aromatic hydrazine is based on 6-hydrazino-nicotinic acid (HNA) and is incorporated on the peptide N-terminus during SPPS using its N-Boc protected derivative **9** (Figure 11c and Figure 12b). The aromatic aldehyde is incorporated on the desired biomolecule in solution on a lysine side chain using the succinimidyl 4-formylbenzoate **24** (SFB, Figure 18). Simple addition of a HNA-modified peptide to a SFB-modified peptide in a mildly acidic buffer, i.e., pH 5.0-6.0, yields spontaneously the desired conjugate. Another useful feature of the bis-arylhydrazone ligation is that it forms a characteristic chromophore which absorbs at 354 nm. This unique property allows following of the conjugation reaction as well as easy UV quantification of the products.

For the hydrazone ligation, we synthesized, modified and purified peptide **27** (Figure 19a). In particular, peptide **27** incorporates several structural features: first, the N-terminus contains the UCN<sup>4-15</sup> CRHR<sub>1</sub> minimized CRHR<sub>1</sub> activation motif; it includes a triethylene glycol (TEG) moiety that was introduced directly on the UCN<sup>4-15</sup> C-terminus, and that plays the role of “connector” between the CRHR<sub>1</sub>-ECD1 recruitment segment (peptide **3**) and activation segment (UCN<sup>4-15</sup>). Finally, a lysine

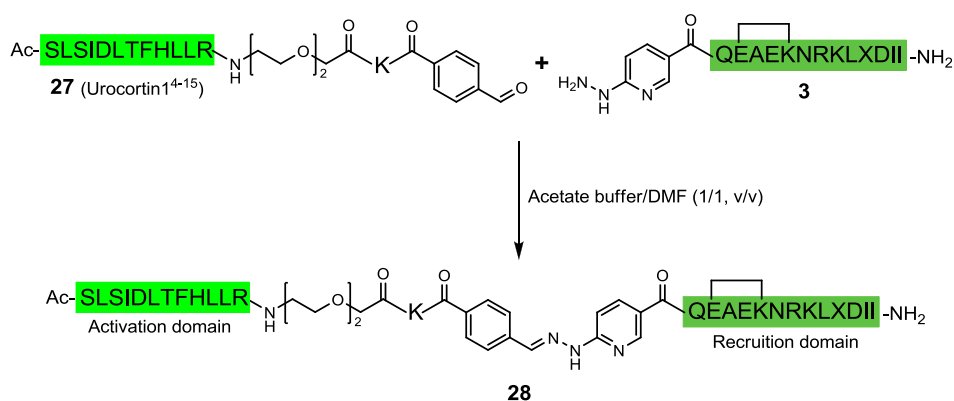
residue is coupled to the C-terminus of the TEG spacer. This residue is subsequently used to selectively introduce the SFB modification reagent and thus plays a crucial role in the whole synthetic sequence, but not for the potency of the conjugate. Notably, the TEG spacer ensures that the lysine residue does not disturb the interaction of the UCN<sup>4-15</sup> activation motif with the CRHR<sub>1</sub>-TMD.



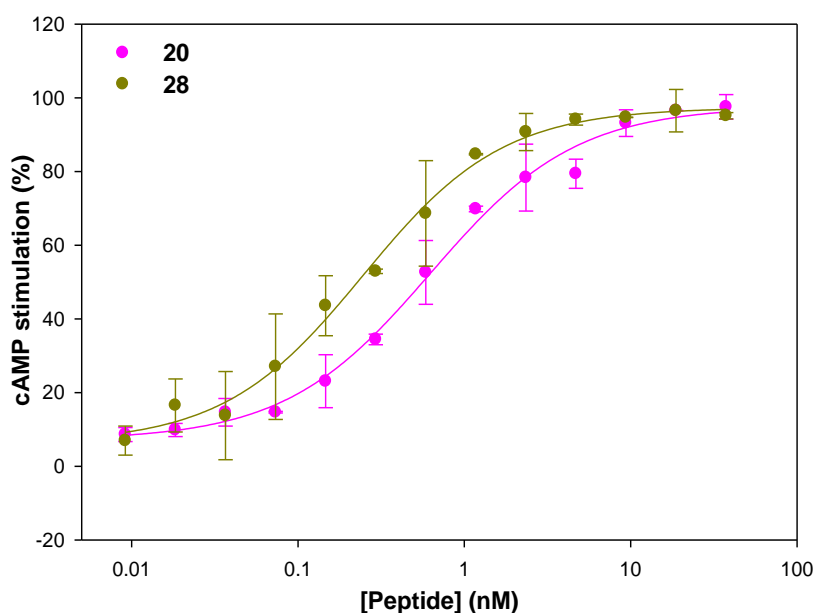
**Figure 18. Reaction scheme used for the incorporation of modification reagents and hydrazone bioconjugation of peptide fragments.** The peptide N-terminal fragment is synthesized by SPPS (left). Upon cleavage from the solid support, a C-terminal lysine residue is modified with the SFB reagent **24**. The peptide C-terminal fragment is synthesized by SPPS (right). The N-terminus of the peptide is modified with the HNA reagent during SPPS and upon cleavage from the solid support; the hydrazine-functionalized peptide **3** is obtained. SFB and HNA modified peptides are mixed in conjugation buffer to afford the arylhydrazone conjugate **26**.

Peptide **27** was coupled to the high-affinity peptide carrier **3** by hydrazone ligation (Figure 19a). The conjugate **28** was purified by HPLC, quantified by UV absorption spectroscopy, and tested for CRHR<sub>1</sub> stimulation in cAMP assay (Figure 19b and Table 5).

a)



b)

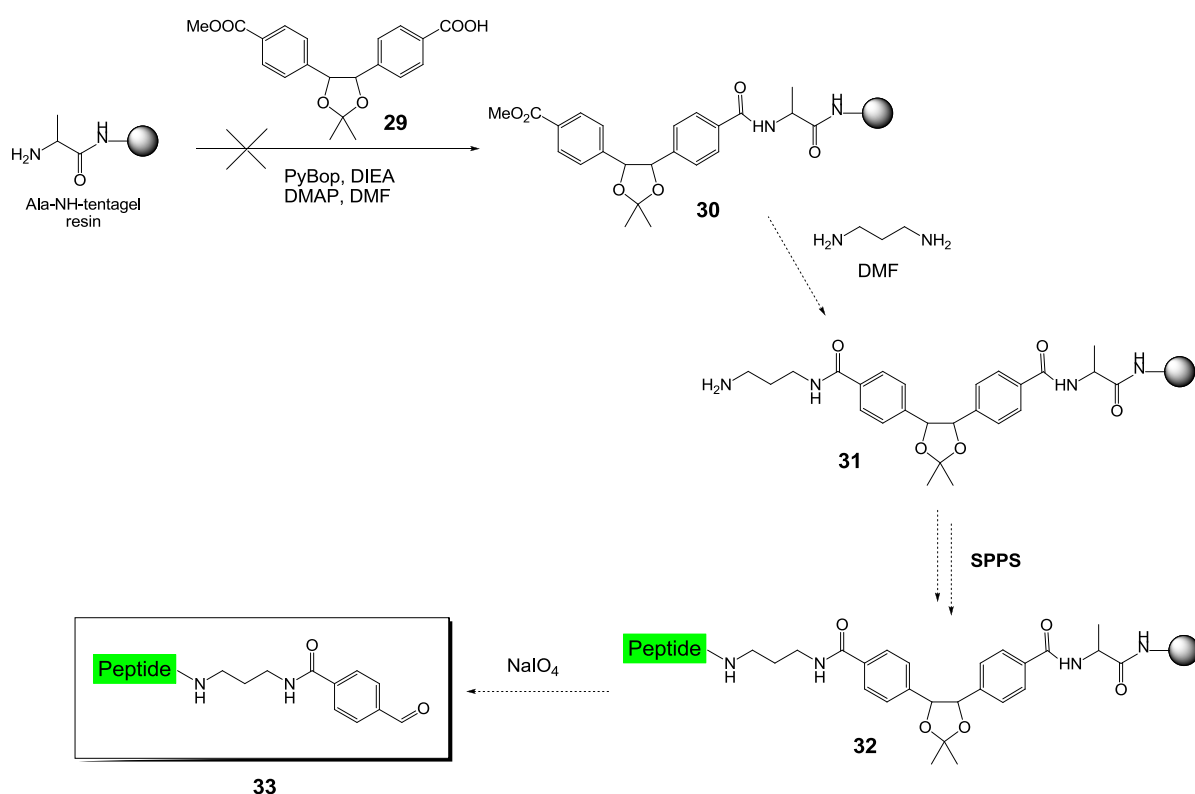


**Figure 19. Stimulation of CRHR<sub>1</sub> by a hydrazone-coupled peptide conjugate.** a) Synthesis of the activation segment **27** (light green) and hydrazone conjugation with membrane recruitment segment **3** (dark green). X = cyclohexyl alanine; EAEK = lactam bridge. b) Stimulation of cAMP production in HEK293 cells stably over-expressing CRHR<sub>1</sub> by peptide conjugates **20** and **28**.

		Peptide carrier	EC <sub>50</sub> [nM] (s.e.m.)
●	20	2	0.63±0.08
●	28	3	0.25±0.03

**Table 5.** Characterization of “clicked” and hydrazone coupled peptide analogs of the N-terminal fragment of human UCN<sup>4-15</sup>.

The hydrazone ligation of the UCN<sup>4-15</sup> activation motif with the high-affinity peptide carrier **3** reconstituted a full agonist with a potency  $0.25 \pm 0.03$  nM. Although the hydrazone conjugate **28** was slightly more potent than its “clicked” counterpart **20**, it does not seem that the linkage plays any role in CRHR<sub>1</sub> binding. This observation is again, in full agreement with the two-domain model of activation for Class B GPCRs. Thereby, the hydrazone ligation is a fast and efficient method for the synthesis of CRH hormone mimics. Advantageously, the hydrazone ligation does not require additives such as metal or oxidant, thus decreasing the risk for contaminations in the testing of crude conjugates.



**Figure 20.** A novel linker for the synthesis of C-terminally formylbenzoate modified peptides.



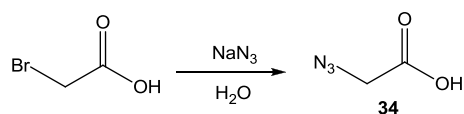
The hydrazinonicotinic acid (HNA) moiety is easily incorporated at the N-terminus of the peptide carrier during SPPS; the 4-formylbenzoate (SFB) modification, however, requires an additional synthetic step which includes the HPLC purification of the peptide intermediates and products. This is a major limitation for the application of the method to a broader context, such as the synthesis of libraries of peptides. To overcome this problem, we designed a novel linker for the synthesis of C-terminally formylbenzoate-modified peptides (Figure 20). The approach is based on the work of Dubs et al. (Dubs et al. 2007) and shall provide a readily SFB-modified peptide upon cleavage from the solid support. The linker **29** was successfully synthesized under my supervision by Stephanie Finsterbusch during her Master's degree practical work in our laboratory. Despite many trials, the coupling of linker **29** to a solid support could not be achieved due to its poor solubility in the solvents used for SPPS (e.g., CH<sub>2</sub>Cl<sub>2</sub>, DMF, and NMP).

Although the hydrazone ligation method is advantageous in terms of reaction conditions, the lack of suitable linker chemistry for the direct synthesis of C-terminally formylbenzoate-modified peptides was detrimental towards the synthesis of conjugates in higher throughput. In contrast, the synthesis of C-terminally propargylated peptides using the BAL linker strategy is straightforward. Moreover, the easy isolation and purification of the "clicked" conjugates by precipitation makes the CuCAAC methodology applicable in a medium-throughput-screening (MTS) fashion. Given that both ligation methods afford CRHR<sub>1</sub> agonists with similar potencies, we chose to continue our investigations by using the CuCAAC conjugation.

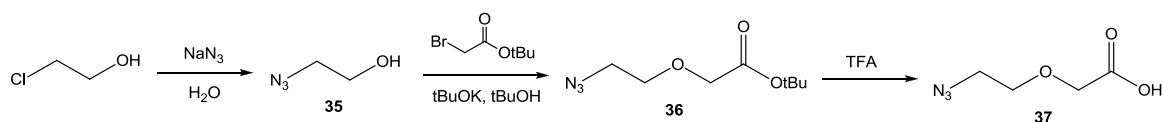
### **3.1.6 Role of the ethylene glycol connector between the two ligands binding domains**

Our conjugation methodology uses two segregated receptor binding sites at the N- and C-termini of UCN to reconstitute a full hormone mimic. The UCN hormone "middle" domain was successfully replaced by a TEG spacer that was introduced at the N-terminus of high-affinity carrier **2** during SPPS. However, the length of this functionalized ethylene glycol chain might play an important role for the final potency of the conjugates. We thus decided to investigate whether an optimal spacer length could afford conjugates with optimized potencies. In other words, the PEG spacer could be used as a molecular "ruler" to determine the optimal distance between the two CRHR<sub>1</sub> binding sites within the conjugate. For this purpose, we synthesized a series of azide-functionalized spacers with increasing ethylene glycol lengths (Figure 21).

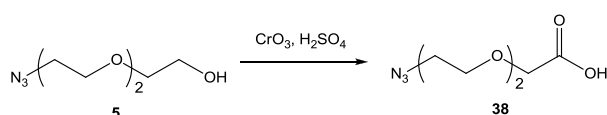
a)



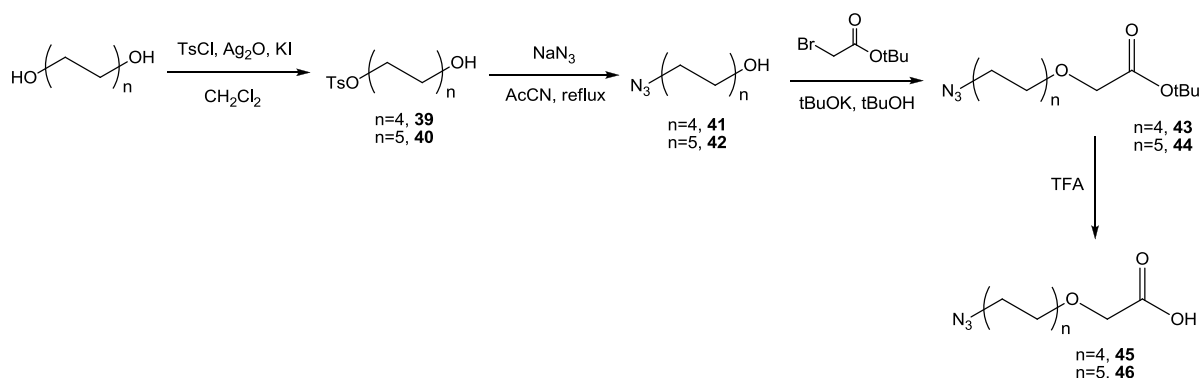
b)



c)



d)

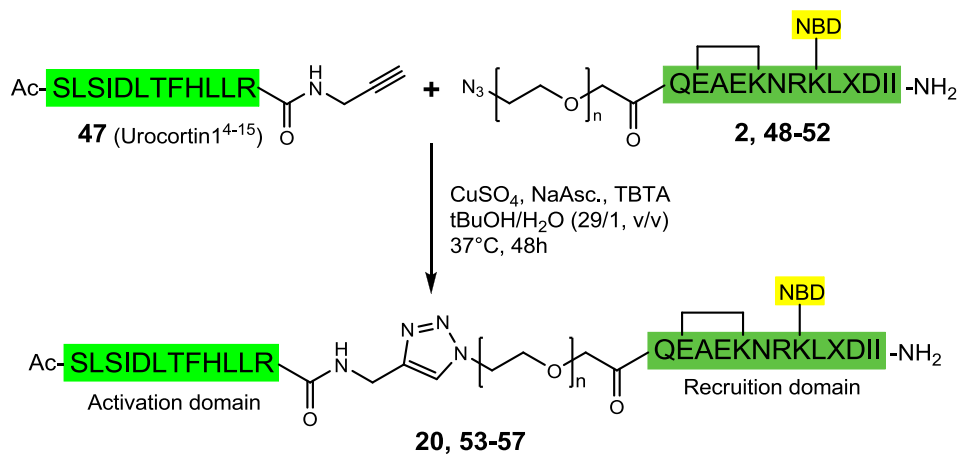


**Figure 21. Overview of the synthesis routes used for the azide spacers used in the study.**

The synthesis of azide **34** ( $n = 0$ ) was straightforward and performed as described (*Bouzide and Sauve* 2002). Azides **37**, **45** and **46** ( $n = 1, 4$  and  $5$  respectively) were obtained in few steps as previously described (Figure 12a and 21). The synthesis of azide **38** ( $n = 2$ ), for which the tosylated derivative easily cyclizes to form a six-membered ring, was achieved by Jones oxidation of azide **5**. Thereby, the ethylene glycol chain of the spacer varies in length between “short” (no ethylene glycol moiety,  $n = 0$  in compound **34**) and “long” ( $n = 5$  in compound **46**). The azide-PEG spacers were subsequently introduced on the CRHR<sub>1</sub>-ECD1 high-affinity carrier N-terminus during SPSS. Additionally, the carriers were tagged with the NBD fluorophore for quantification purposes. After cleavage and HPLC purification, we obtained the complementary high-affinity peptide carriers with N-terminal PEG lengths **48-52** ( $n = 0 \rightarrow n = 5$ ). These carriers were coupled to the minimized

activation motif UCN<sup>4-15</sup> by CuCAAC (Figure 22a). After HPLC purification and fluorescence quantification, the conjugates were tested for CRHR<sub>1</sub> stimulation in cAMP assay (Figure 22b and Table 6).

a)



b)

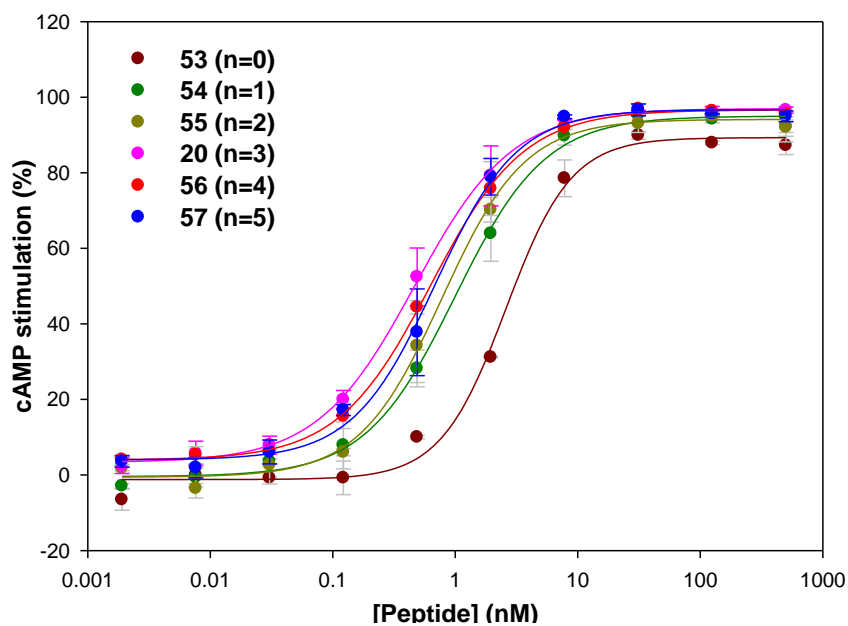


Figure 22. Stimulation of CRHR<sub>1</sub> by “clicked” UCN<sup>4-15</sup> peptide conjugates listed in Table 6.

		N-term.	Peptide carrier n =	EC <sub>50</sub> [nM] (s.e.m.)
●	53	Ac-UCN <sup>4-15</sup>	0	2.59±0.28
●	54	Ac-UCN <sup>4-15</sup>	1	1.00±0.08
●	55	Ac-UCN <sup>4-15</sup>	2	0.78±0.06
●	20	Ac-UCN <sup>4-15</sup>	3	0.47±0.02
●	56	Ac-UCN <sup>4-15</sup>	4	0.63±0.02
●	57	Ac-UCN <sup>4-15</sup>	5	0.68±0.06

**Table 6. Characterization of clicked UCN<sup>4-15</sup> conjugates.**

Surprisingly, the peptide conjugates **20** and **53-57** show high and similar potencies for stimulation of CRHR<sub>1</sub> (Figure 22b and Table 6). The TEG conjugate **20** (n = 3) was the most potent (pink curve, 0.47 ± 0.02 nM) while the conjugate **53** bearing the shortest linker (n = 0) was the weakest (dark red curve, 2.59 ± 0.28 nM). Gratifyingly, the spacer length which provided the most potent agonist (peptide **20**, n = 3) corresponds to the high-affinity carrier **2**.

The replacement of the middle portion (16-27) of UCN by ethylene glycol spacers of various lengths reconstituted full low nanomolar agonists which exhibited similar biopotencies, thus confirming that the amino acid residues of the middle portion (16-27) of UCN are individually not essential for activation (Table 6). This is consistent with the results of Beyermann et al. (*Beyermann et al.* 2000). The length of the spacers between the two receptor binding sites had only a little effect on receptor activation. This shows that an appropriate distance between both C-terminal and N-terminal binding sites in UCN, although advantageous (e.g., for conjugate **20**), is not essential for receptor binding and activation. As suggested by Beyermann et al., the relative orientation of the two binding sites rather than the maintenance of a distinct distance between them seems to be essential for a high potency. Moreover, these results also suggest a remarkable flexibility of the receptor domains toward ligand binding. Importantly, a helical connector between the two ligand binding sites may contribute to confer an optimized conformation and orientation of the ligands; however, the high potencies of the UCN<sup>4-15</sup> conjugates listed in Table 6 indicate that a helical middle domain is not essential for receptor binding and activation. The ten-fold difference in potency between conjugates and full length hormones also indicates that the UCN middle portion (16-27)

may not only influence the conformation of the ligand, but provide important additional receptor-ligand interactions.

Taken together, these results allow us to propose a three-step “low resolution” mechanism for the binding events of our UCN<sup>4-15</sup> “clicked” conjugates. The peptide carrier **2** first binds the CRHR<sub>1</sub>-ECD1 with high-affinity. The UCN<sup>4-15</sup> N-terminal portion of the conjugate then freely rotates around the ethylene glycol spacer to adopt an optimized orientation for binding the CRHR<sub>1</sub>-TMD. At the same time, both the flexibilities of the receptor’s domains and the ethylene glycol spacer help the N-terminal segment of the ligand to adjust its position for binding. Finally, the UCN<sup>4-15</sup> N-terminal segment binds the CRHR<sub>1</sub>-TMD, an event which activates the receptor and triggers G protein signaling. The limited flexibility conferred by the “short” spacer in conjugate **53** may explain its lower potency compared to the others UCN<sup>4-15</sup> conjugates. Hereby, we established the triethylene glycol (n = 3) spacer of conjugate **20** as offering optimized flexibility and distance between the two ligands binding sites.

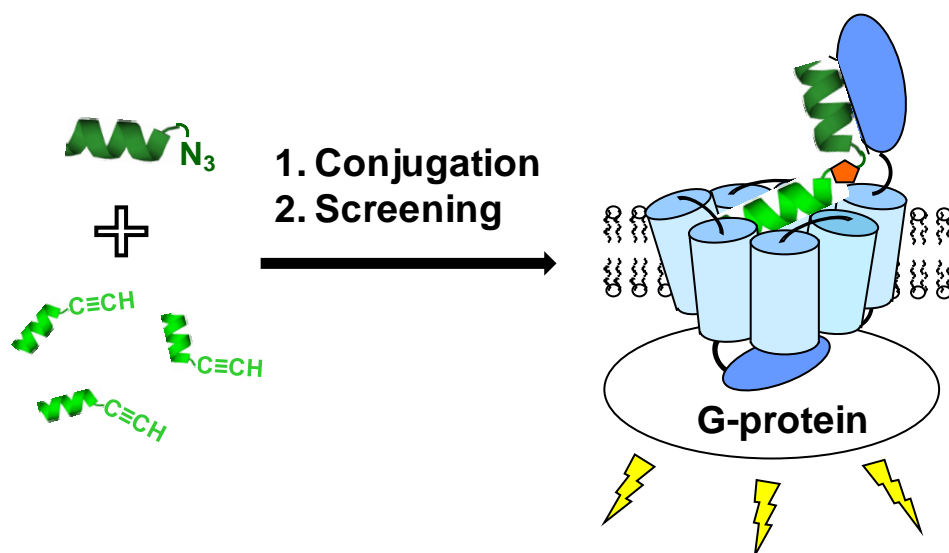
## 3.2 Urocortin1<sup>4-15</sup> biomimetic screening

The use of CuCAAC “clicked” conjugates allowed us to characterize the 12 amino acid minimal template required for the full CRHR<sub>1</sub> activation. To explore the contribution of individual residues to CRHR<sub>1</sub> stimulation in more detail, we engaged on a medium throughput screening (MTS) of peptide-peptide conjugates.

### 3.2.1 Synthesis and potency evaluation of a Urocortin1<sup>4-15</sup> peptide conjugate library

Based on the previously characterized minimal activation template UCN<sup>4-15</sup>, a library of 96 C-terminally propargylated peptidic fragments containing a series of single amino acid substitutions was synthesized (Table 7). Conveniently, the synthesis of this peptide library was achieved using the BAL strategy in the FlexChem<sup>®</sup> parallel synthesis system (see Methods). Standard SPPS was performed in a 96 deep-well plate allowing the fast and parallel synthesis of the 96 C-terminally propargylated activation fragments. Each position of the UCN<sup>4-15</sup> peptide sequence was systematically changed to alanine, aminoisobutyric acid (Aib), the corresponding D-amino acid, as well as five structurally related natural or unnatural amino acids. Thereby, the systematic amino acid replacements shall provide a complete SAR and activity profile of the UCN<sup>4-15</sup> activation segment (*Devigny et al.* 2011).

After SPPS, the propargylated peptides were cleaved from the solid support and the cleavage mixture was collected in a 96-deep-well plate. All 96-propargylated peptides were dried and weighted, then redissolved in a mixture of acetonitrile/water (50/50, v/v). At this point, we performed a first analysis round in order to estimate the quality of our library synthesis. HPLC and mass spectrometry analysis were performed for all 96-propargylated peptides. The estimation of the library quality is important because such parallel SPPS requires training and needs to be optimized. In addition, the FlexChem<sup>®</sup> system often leaks or breaks down, threatening the growing peptides of contamination. The crude UCN<sup>4-15</sup> analogs were then coupled via their C-terminal alkyne group to the purified high-affinity carrier **2** by CuCAAC (Figure 23).



**Figure 23. Biomimetic screening principle for the investigation of Class B GPCR ligand interactions.**

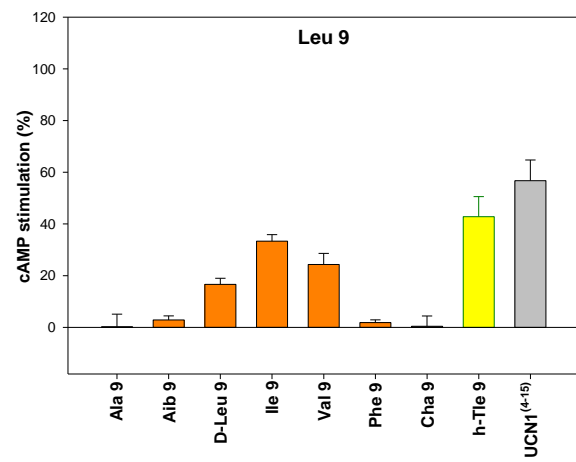
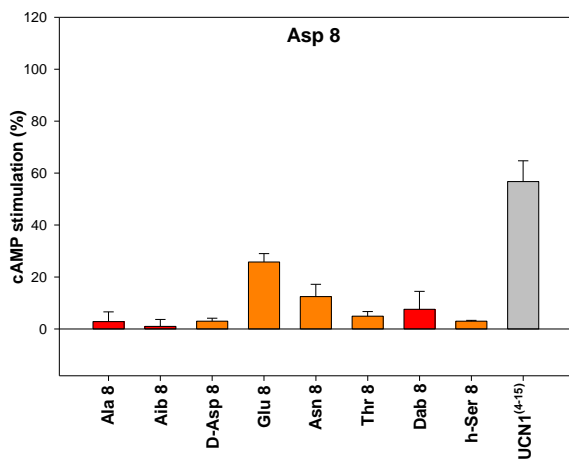
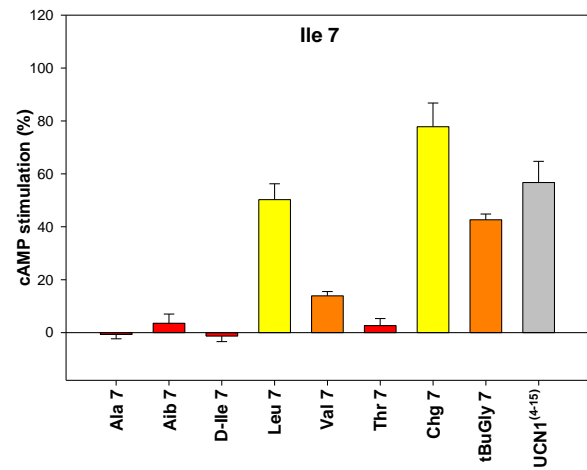
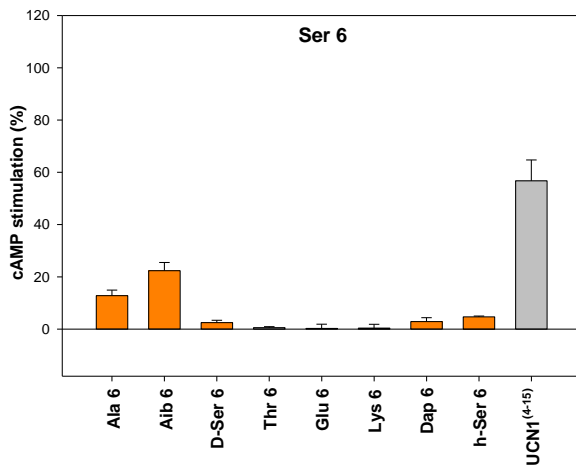
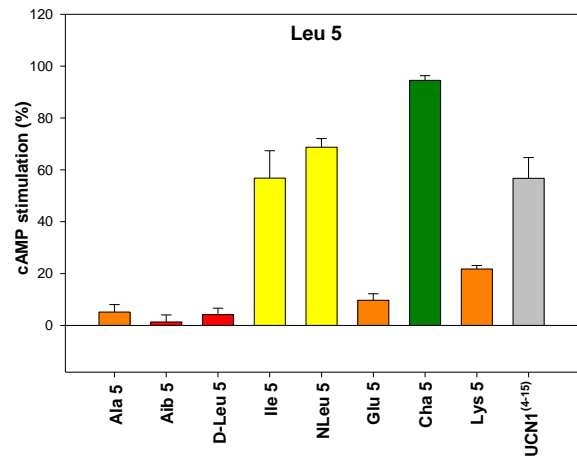
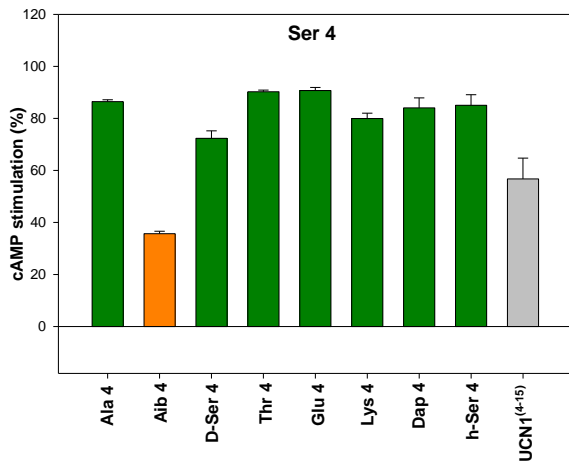
A library of alkyne-tagged peptides (light green) is conjugated to a constant peptide fragment (dark green) that has high-affinity for the extracellular domain of the class B GPCR. These conjugates are probed for modulation of the GPCR transmembrane domain.

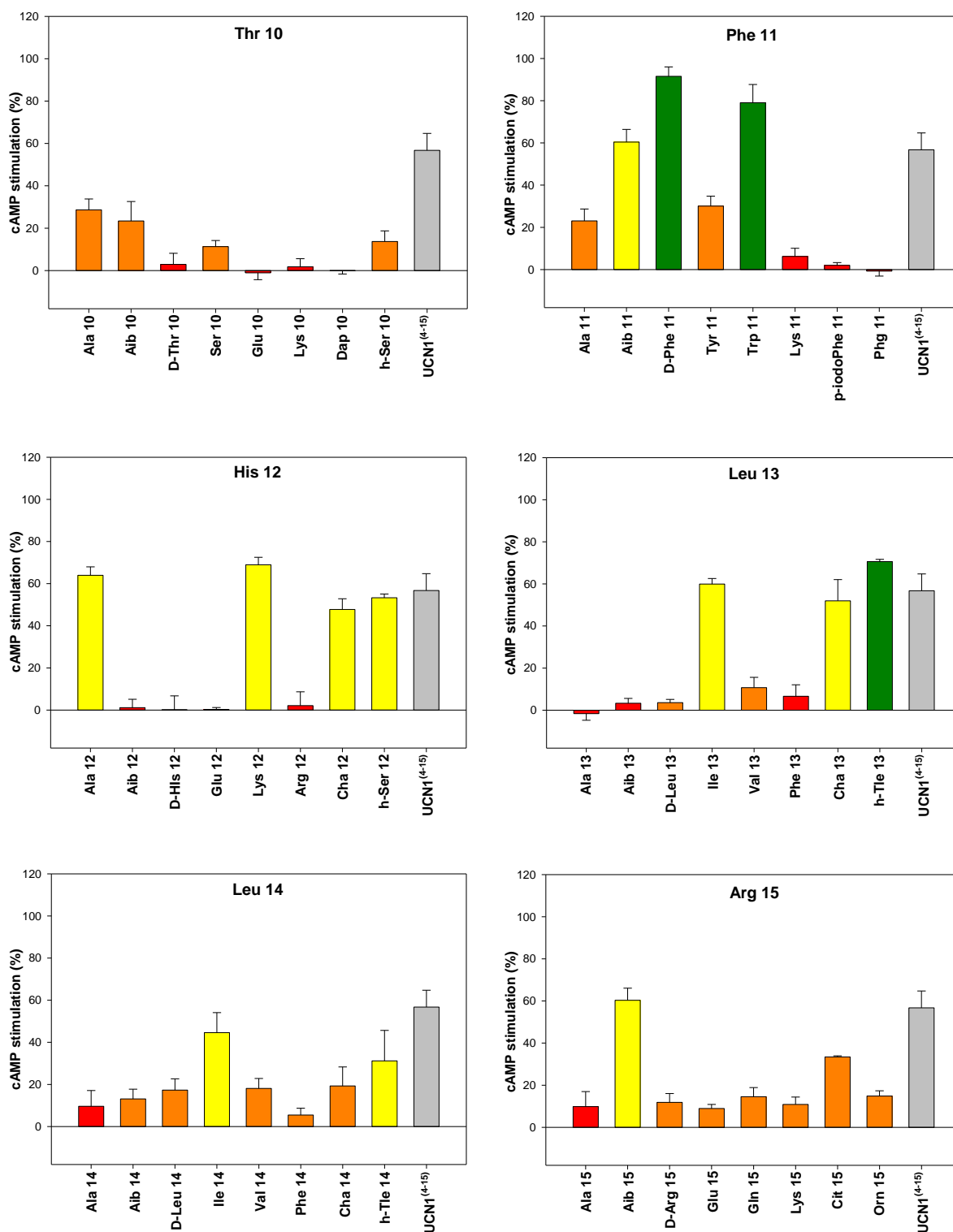
Gratifyingly, the peptide-peptide conjugates were routinely found to be much less soluble than their precursors allowing simple precipitation for their purification as previously described. The easy isolation of conjugates is a crucial feature of the biomimetic screening approach. Indeed, the systematic isolation or purification of individual conjugates is typically the rate limiting step in a medium throughput synthesis and can be extremely laborious. HPLC analysis showed complete conversion of the carrier peptide **2** for all the 96 conjugation reactions. The integration of the HPLC traces showed acceptable purities ( $\geq 65\%$ ) for most crude conjugates (89 out of 96). At this stage we decided to test these crude peptide-peptide conjugates directly in a cellular assay without any further purification. This was possible as any residual reaction components (e.g.,  $Cu^+$ , t-butanol, or any remaining unconjugated peptide fragment) were minimal and were found not to disturb the cellular assay. The activities of the conjugates were compared with the purified conjugate **20** at 2 nM (Figure 24 and Table 7).

Ser <sup>4</sup>	Leu <sup>5</sup>	Ser <sup>6</sup>	Ile <sup>7</sup>	Asp <sup>8</sup>	Leu <sup>9</sup>	Thr <sup>10</sup>	Phe <sup>11</sup>	His <sup>12</sup>	Leu <sup>13</sup>	Leu <sup>14</sup>	Arg <sup>15</sup>
Ala	Ala	Ala	Ala <sup>(a)</sup>	Ala	Ala	Ala	Ala	Ala	Ala	Ala	Ala
Aib	Aib	Aib	Aib	Aib	Aib	Aib	Aib	Aib	Aib	Aib	Aib
D-Ser	D-Leu	D-Ser	D-Ile	D-Asp <sup>(a)</sup>	D-Leu	D-Thr	D-Phe <sup>(a)</sup>	D-His	D-Leu	D-Leu	D-Arg
Thr <sup>(a)</sup>	Ile	Thr	Leu	Asn	Ile	Ser	Tyr <sup>(a)</sup>	Arg	Ile	Ile	Gln
Glu	Glu	Glu	Val <sup>(a)</sup>	Glu	Val	Glu	Trp	Glu	Val <sup>(a)</sup>	Val	Glu
Lys	Lys	Lys	Thr <sup>(a)</sup>	Thr	Phe	Lys	Lys	Lys	Phe	Phe	Lys
Dap	Cha <sup>(a)</sup>	Dap	Chg <sup>(a)</sup>	Dab	Cha	Dap	pI-Phe	Cha	Cha <sup>(a)</sup>	Cha	Cit
h-Ser	Nle	h-Ser	tBuGly	h-Ser	tBuAla <sup>(a)</sup>	h-Ser	PhGly <sup>(a)</sup>	h-Ser <sup>(a)</sup>	tBuAla	tBuAla	Orn

**Table 7. Summary of single-point substitutions of the UCN<sup>4-15</sup> sequence.** Crude peptide-peptide conjugates carrying the indicated amino acid modification were assayed at 2 nM for cAMP stimulation of HEK293 cells stably overexpressing CRHR<sub>1</sub>. Inactive sequences are indicated in red, minimal activity is indicated in orange, equal activity compared to the purified UCN<sup>4-15</sup> conjugate **20** is indicated in yellow and activity-enhancing substitutions are highlighted green. <sup>(a)</sup> These conjugates were additionally HPLC purified and retested for activity (see section 3.2.2). Aib =  $\alpha$ -aminoisobutyric acid; Cha = 3-cyclohexyl-L-alanine; Chg = L- $\alpha$ -cyclohexylglycine; Cit = L-citrulline; Dap = L-2,3-diaminopropionic acid; Dab = L-2,4-diaminobutyric acid; h-Ser = homoserine; Nle = norleucine; Orn = ornithine; PhGly = L- $\alpha$ -phenylglycine; pI-Phe = para-iodo phenylalanine; tBuAla =  $\beta$ -*tert*-butyl-L-alanine; tBuGly = L- $\alpha$ -*tert*-butylglycine.







**Figure 24. Positional MTS of a crude UCN<sup>4-15</sup> peptide conjugate library at 2nM.** Inactive sequences are indicated in red, minimal activity is indicated in orange, equal activity compared to the original UCN<sup>4-15</sup> conjugate **20** is indicated in yellow, and activity-enhancing substitutions are highlighted in green. The difference of potencies between crude conjugates from the library and peptide **20** was estimated using a student's t-test.

The biomimetic screening of the peptide conjugate library resulted in 70 conjugates where the stimulatory activity for CRHR<sub>1</sub> was reduced or completely abolished (Figure 24 and Table 7). For 15 of these peptide conjugates, the CRHR<sub>1</sub> stimulation was not found to be significantly different compared to the wild-type sequence of UCN<sup>4-15</sup>. However, an enhanced CRHR<sub>1</sub> stimulation was observed for 11 peptide conjugate analogs. Analysis of the activities for the single amino acid substitution analogs allows several conclusions about the structure-activity-relationship of CRHR<sub>1</sub> agonists (*Devigny et al.* 2011).

First, replacement of Arg<sup>15</sup> led to a substantial loss of potency. Consistently with the truncation study, the hydrogen bonding pattern of Arg<sup>15</sup> seems to contribute importantly to CRHR<sub>1</sub> stimulation. Replacement of Leu<sup>5,9,13,14</sup> residues by similar aliphatic residues such Ile was quite well tolerated. Interestingly, the replacement of these residues by the unnatural amino acids such as Cha and tBuAla provided conjugates with similar or enhanced potencies. These sterically hindering side chains of Cha and tBuAla might constrain the whole N-terminal activation segment in an advantageous conformation to bind the CRHR<sub>1</sub>-TMD. Such substitutions might also optimize the hydrophobic interactions between the peptide ligand and the receptor. A similar structure-activity-relationship was observed at Ile<sup>7</sup> that could be advantageously replaced by Leu or bulky Chg residues. Generally, it seems that positions 5, 7, 9, 13, and 14 tolerate conservative aliphatic substitutions which can partially enhance potency.

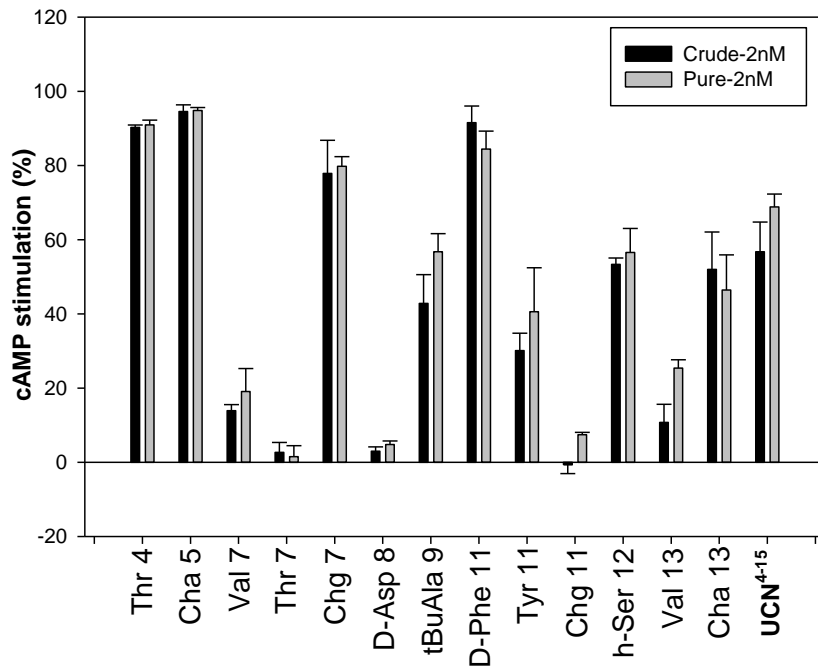
Replacement of His<sup>12</sup> was well tolerated and it seems that this residue contribute comparatively less to the interaction with the CRHR<sub>1</sub> receptor. An L- to D-Phe substitution at position 11 substantially improved the activity of the peptide conjugate. Interestingly, this substitution is also present in the high-affinity CRHR<sub>1</sub> peptide antagonist astressin (*Gulyas et al.* 1995). The replacement of Phe<sup>11</sup> by Trp also provided an analogue with improved potency. Replacement of polar residues Ser<sup>6</sup>, Asp<sup>8</sup>, and Thr<sup>10</sup> abolished activity. Consistent with our truncation study (section 3.1.4) and with prior studies on full length CRH (*Beyermann et al.* 1996; *Kornreich et al.* 1992), the side chains of these three residues seem to be essential for CRHR<sub>1</sub> activation. Ser<sup>4</sup> could be advantageously substituted for several amino acids. The potency of the Ala<sup>4</sup> conjugate indicates that the Ser<sup>4</sup> side chain does not play an important role for CRHR<sub>1</sub> activation. Again, this is consistent with our N-terminal truncation study in which UCN<sup>5-15</sup> conjugate **21** showed significant activity (Table 4). Interestingly, the Ser<sup>4</sup>Thr substitution enhanced potency, either by fine-tuning of the hydrophobic interactions or by influencing the conformation of the three adjacent residues that are essential for activation.

The UCN<sup>4-15</sup> SAR mentioned above is to compare with several single point mutation studies on the full length CRH hormone. In particular, Rivier et al. have performed alanine and D-amino acid scans of the whole CRH sequence (*Kornreich et al.* 1992; *Rivier et al.* 1993). As CRH and UCN share a high degree of homology in the activation segment (e.g., the fragments 4-7 in UCN and the corresponding 5-8 in CRH are only slightly different, the Ser<sup>6</sup> is conserved while Leu residues are exchanged by Ile residues and vice versa; the UCN<sup>8-15</sup> fragment is completely conserved in CRH<sup>9-16</sup>; Table 2), the SAR between N-termini of the two hormones can be correlated. The results are striking: Ala<sup>4</sup>UCN<sup>4-15</sup> and Ala<sup>12</sup>UCN<sup>4-15</sup> were well tolerated, as are Ala<sup>5</sup>CRH and Ala<sup>13</sup>CRH. Alanine substitutions at any other position within the UCN<sup>4-15</sup> or CRH<sup>5-16</sup> N termini produced analogues with decreased potencies. Similarly, D-Phe<sup>11</sup>UCN<sup>4-15</sup> and D-Phe<sup>12</sup>CRH substitutions greatly enhanced potency while the latter was dramatically reduced by D-amino acid substitutions at other positions. To a lesser extent, a single point slight alteration study also identified the potency enhancing Trp<sup>12</sup>CRH substitution (corresponding to Trp<sup>11</sup>UCN<sup>4-15</sup> in our screening) (*Beyermann et al.* 1996). The mentioned SAR studies on the full length CRH required the laborious synthesis of the full length hormone to investigate the role of residues located in the N-terminal portion, thus greatly limiting the number of analogues within a library. In contrast, our conjugation strategy produced rapidly a complete SAR profile at each position within the UCN<sup>4-15</sup> sequence. Overall, the activity profiles for SAR studies of CRH<sup>5-16</sup> match perfectly with the UCN<sup>4-15</sup> screening described herein, thus further validating our conjugation methodology.

### **3.2.2 Purification of exemplary conjugates: validation of the crude biomimetic screening**

The precipitation workup procedure allowed the easy and simple isolation of the peptide conjugates (see Section 3.1.4). However, HPLC analysis of the crude conjugates revealed that in some cases, unreacted propargylated peptide precipitates together with the conjugate. Although copper sulfate is soluble in tert-butanol, residual metal might also contaminate the crude conjugates. It remained unclear whether these impurities have a detrimental effect on the potency of the crude conjugates. To ensure the suitability of the previous screening using crude conjugates, fourteen conjugates were purified by HPLC and their activities were compared in the cellular assay with their crude counterparts at 2 nM (Figure 25 and Table 8). We especially focused on sequences with enhanced activity as well as peptide conjugates with lower purities ( $\leq 65\%$ ).

a)



b)

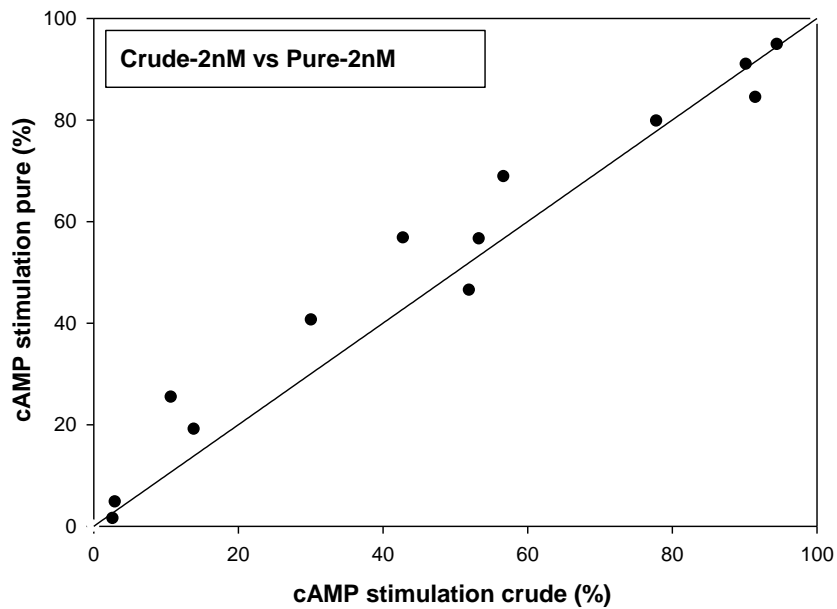


Figure 25. Maximal cAMP stimulation of crude vs. purified single-substituted analogs of human UCN<sup>4-15</sup> at 2 nM.

		Crude		Purified	
		cAMP stimulation (%)	Purity (%)	cAMP stimulation (%)	Purity (%)
2 nM	Thr <sup>4</sup>	90.3±0.6	95	90.9±1.3	100
	Cha <sup>5</sup>	94.5±1.8	82	94.8±0.8	100
	Val <sup>7</sup>	13.9±1.6	42	19.1±6.2	98
	Thr <sup>7</sup>	2.7±2.7	56	1.5±3.0	93
	Chg <sup>7</sup>	77.9±8.9	50	79.8±2.6	90
	D-Asp <sup>8</sup>	3.0±1.2	69	4.8±1.0	98
	tBuAla <sup>9</sup>	42.8±7.8	100	56.7±4.9	100
	D-Phe <sup>11</sup>	91.6±4.5	66	84.4±4.9	92
	Tyr <sup>11</sup>	30.1±4.7	60	40.6±11.8	97
	Chg <sup>11</sup>	-0.7±2.4	51	7.4±0.7	96
	h-Ser <sup>12</sup>	53.3±1.7	67	56.5±6.5	100
	Val <sup>13</sup>	10.7±4.9	61	25.4±2.2	100
	Cha <sup>13</sup>	52.0±10.1	100	46.4±9.5	97
	UCN <sup>4-15</sup>	56.7±8.0	78	68.8±3.5	100

**Table 8. cAMP stimulation of crude vs. purified single-substituted analogs of human UCN<sup>4-15</sup> at 2 nM.**

No differences in potency were observed between crude and purified conjugates of same purities (e.g., Thr<sup>4</sup>, Cha<sup>5</sup>, tBuAla<sup>9</sup> and Cha<sup>13</sup>), thus confirming that residual conjugation components in the precipitate (e.g., copper or unreacted propargylated peptide) do not influence the functional assay. Furthermore, this experiment also validates the stimulation enhancing effects of these amino acid substitutions. For others conjugates, no major differences in activity were found between the crude and the purified conjugates, thus validating the *in situ* screening approach. Importantly, the presence of impurities (unreacted C-terminally propargylated peptide or copper) has only a minimal influence on the potency of the crude peptide conjugates.

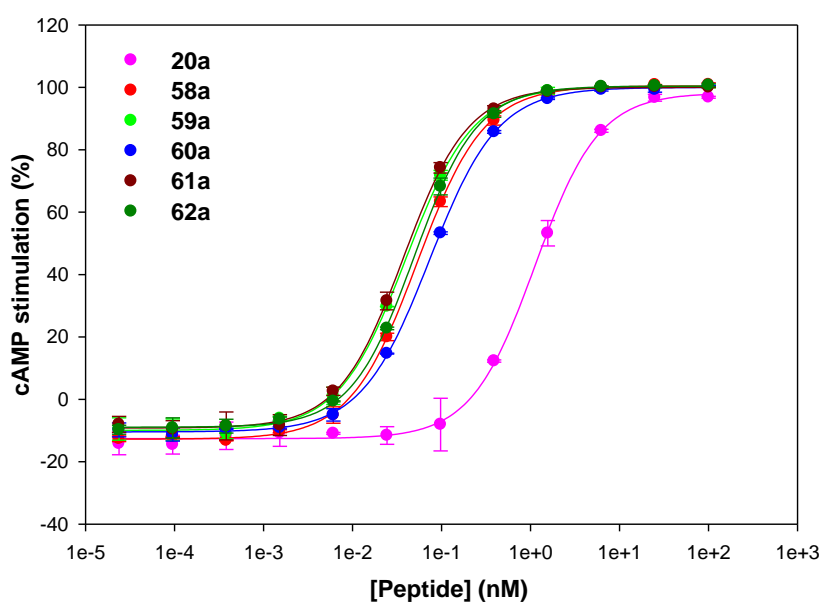
### 3.2.3 Synthesis and evaluation of optimized UCN<sup>4-15</sup> peptide probes

The next step was to investigate whether the enhancing effects of the single substitutions identified in the positional screening were additive. For this purpose, a library of C-terminally propargylated UCN<sup>4-15</sup> peptides bearing multiple substitutions was synthesized. Notably, the substitutions Ser<sup>4</sup>Thr, Leu<sup>5</sup>Cha, and Phe<sup>11</sup>D-Phe provided the greatest individual potency enhancement in the MTS and were chosen as a starting point for the elaboration of more potent conjugates (*Devigny et al.* 2011).

Combination of the first two mutations in conjugate **58a** enhanced potency 24-fold compared to the native UCN<sup>4-15</sup> sequence (Figure 26a and Table 9). The triple mutation in conjugate **59a** further slightly increased potency to provide a 40 pM agonist. These conjugates were so potent that we tested whether they could show any activity, even at a high concentration, without the presence of recruitment segment **2**. An additional library of polysubstituted C-terminally amidated peptides was synthesized. Gratifyingly, untethered peptides **58b** and **59b** showed for the first time a weak but detectable CRHR<sub>1</sub> agonism (Figure 26b and Table 9). These encouraging results led us to incorporate other mutations identified as beneficial in the single substitution screening (Ile<sup>7</sup>Chg, Leu<sup>9</sup>tBuAla, and Leu<sup>13</sup>Cha). This further enhanced the potency of untethered peptides to finally provide the hexasubstituted peptide **62b** as a low nanomolar agonist. Importantly, in both tethered and untethered setups, the incorporation of additional substitutions showed cumulative effects for the potency.

From a structural point of view, it seems that this increase in potency was largely achieved by fine-tuning the hydrophobic interactions through incorporation of the natural and unnatural amino acids side chains (Thr, Cha, Chg and tBuAla). Additionally, these mutations may play an important conformational role by constraining the whole activation segment in a helical conformation. Intriguingly, these additional substitutions did not further increase the potency in the context of the high-affinity carrier. This is in contrast to the cooperative behavior classically expected for conjugated two-site binding fragments (*Murray and Verdonk* 2002). The molecular underpinnings for the apparent lower limit of approximately 50 pM for peptide-carrier **2** conjugates are currently unknown.

a)



b)

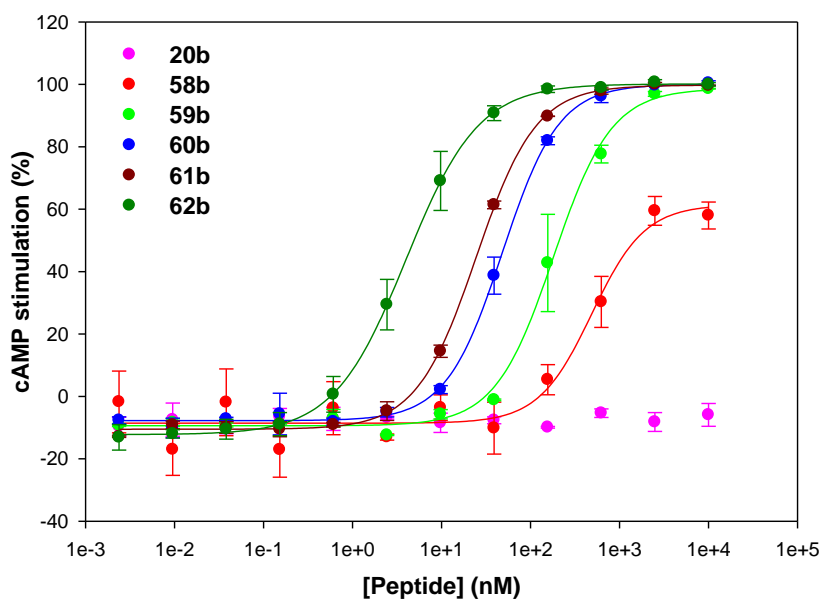
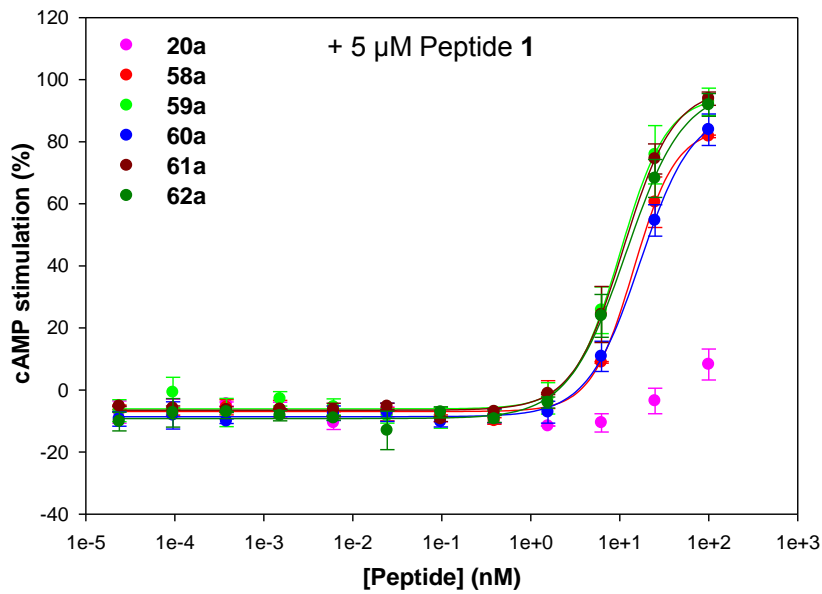


Figure 26. Stimulation of CRHR<sub>1</sub> by multisubstituted peptide conjugates (a) and C-terminally amidated (b) UCN<sup>4-15</sup> peptide fragments.



a)



b)

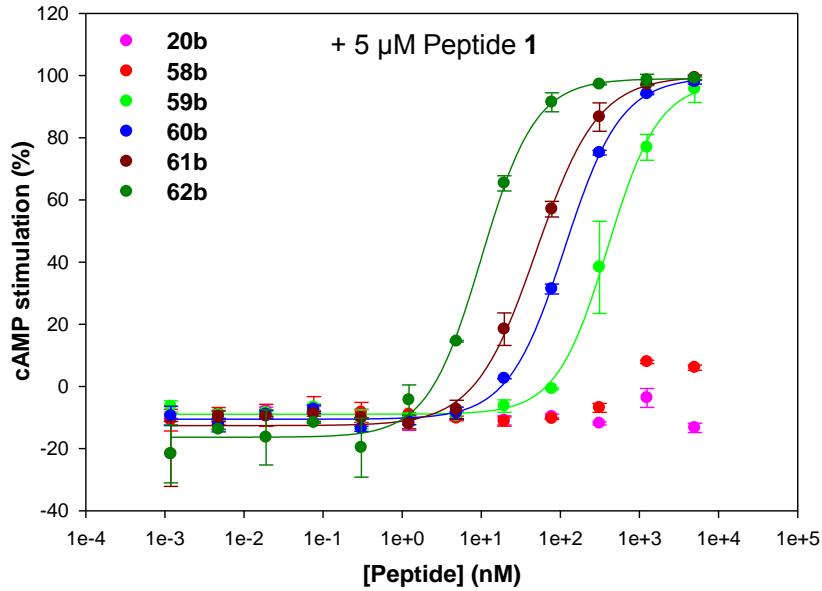


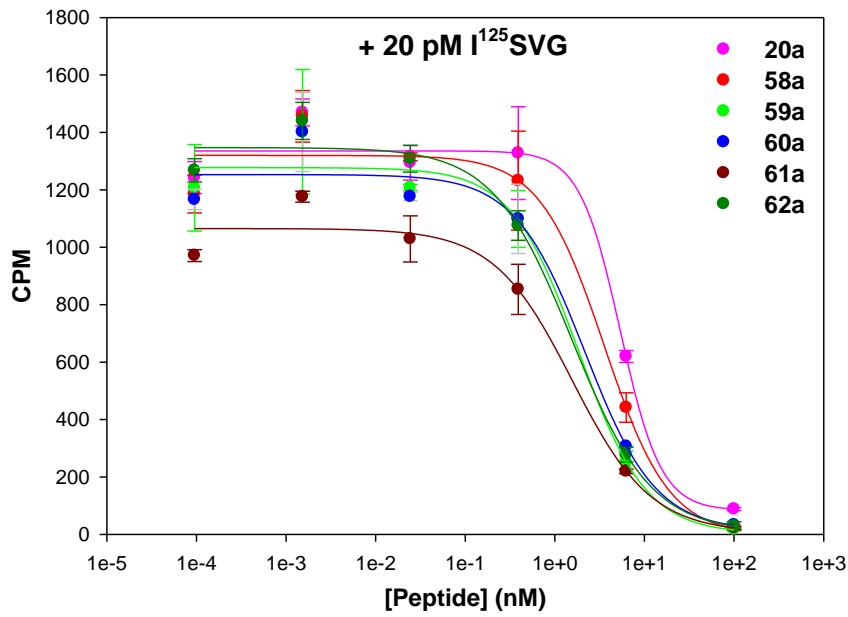
Figure 27. Competitive inhibition of the stimulation of CRHR<sub>1</sub> by multisubstituted peptide conjugates (a) and C-terminally amidated (b) UCN<sup>4-15</sup> peptide fragments in the presence of peptide 1 (5 μM).

The N-terminal part of CRH corresponding to peptide **62b** is believed to primarily interact with the juxtamembrane domain of CRHR<sub>1</sub>. To further characterize the pharmacology of peptide conjugates **58a-62a** and C-terminally amidated peptides **58b-62b**, we decided to investigate the relevance of peptide CRHR<sub>1</sub>-ECD1 recruitment for the ligands potencies. A competition assay between peptides **58-62** and the CRHR<sub>1</sub>-ECD1 specific high-affinity peptide antagonist **1** was performed (Figure 27 and Table 9). The conjugates **20a** and **58a-62a** were very sensitive to the presence of 5 μM of peptide **1**. The native UCN<sup>4-15</sup> sequence of peptide **20a** was rendered completely inactive. The potency of conjugates **58a-62a** was in average 130-fold weaker in the presence of peptide **1**, indicating that the conjugates compete directly for binding the CRHR<sub>1</sub>-ECD1 with peptide **1**. In contrast, this effect was very moderate for untethered peptides **58b-62b**. The weak CRHR<sub>1</sub> agonist **58b** was rendered inactive and the peptides **59b-62b** were in average 2-fold weaker in the presence of 5 μM of peptide **1**.

Obviously, peptide **1** was unable to efficiently inhibit CRHR<sub>1</sub> stimulation by amidated peptides **59b-62b**. The weak inhibitory effect might reside in the mechanism of peptide **59b-62b**. The amino acid sequence of peptides **58b-62b** relies on the native UCN<sup>4-15</sup> sequence and likely interacts with the CRHR<sub>1</sub> transmembrane domain. It is then not surprising that the ECD1 specific antagonist **1** is unable to compete with transmembrane domain agonists.

To further characterize the pharmacology of peptides **58-62**, we performed a radioactive competition assay using hot SVG and membrane preparations overexpressing CRHR<sub>1</sub> (Figure 28). The peptide conjugates **20a** and **58a-62a** fully competed with I<sup>125</sup>-SVG showing affinities in the low nanomolar range (Figure 31a). Interestingly, the binding affinity of the conjugates slightly increased with increasing substitution to reach a lower limit around 2 nM. This non cooperative behavior correlates with the lower limit of potency observed in the CRHR<sub>1</sub> stimulation assay (Figure 26a and Table 9). Consistent with the stimulation assay, peptides **20b** and **58b** were found to be inactive in the binding assay. Likewise, peptides **59b-62b** competed weakly with I<sup>125</sup>(Tyr<sup>0</sup>)-SVG. At higher concentrations, the curves of peptides **59b-62b** converge to approximately 400 CPM. Obviously, a lower SVG displacement limit was reached indicating that peptides **59b-62b** may compete with the N-terminus of SVG, displacing it only partially from binding CRHR<sub>1</sub>.

a)



b)

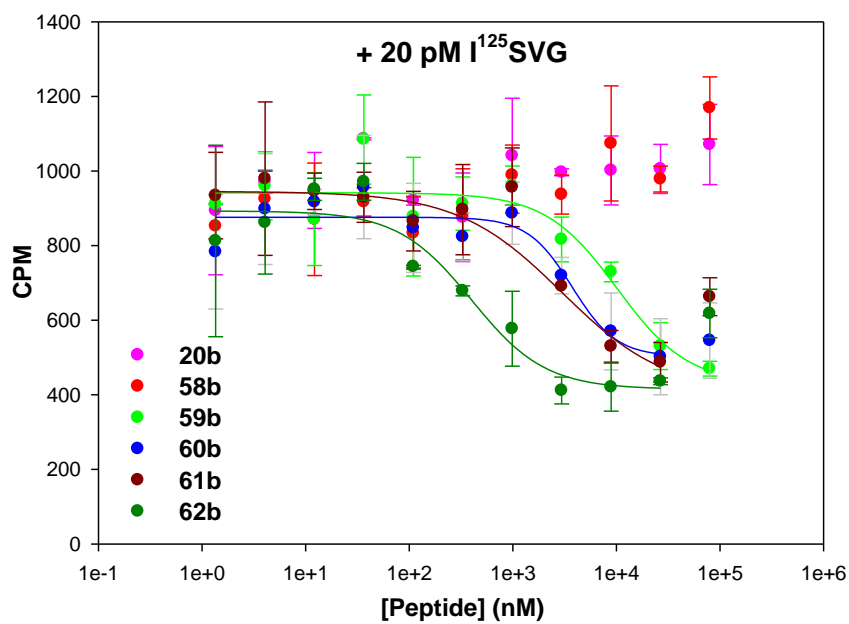


Figure 28. Radioactive competition assay using  $^{125}\text{Tyr}^0\text{-SVG}$  and membrane preparations from HEK293 cells stably overexpressing  $\text{CRHR}_1$ . a) Competition between  $^{125}\text{Tyr}^0\text{-SVG}$  and peptide conjugates. b) Competition between  $^{125}\text{Tyr}^0\text{-SVG}$  and C-terminally amidated peptides.

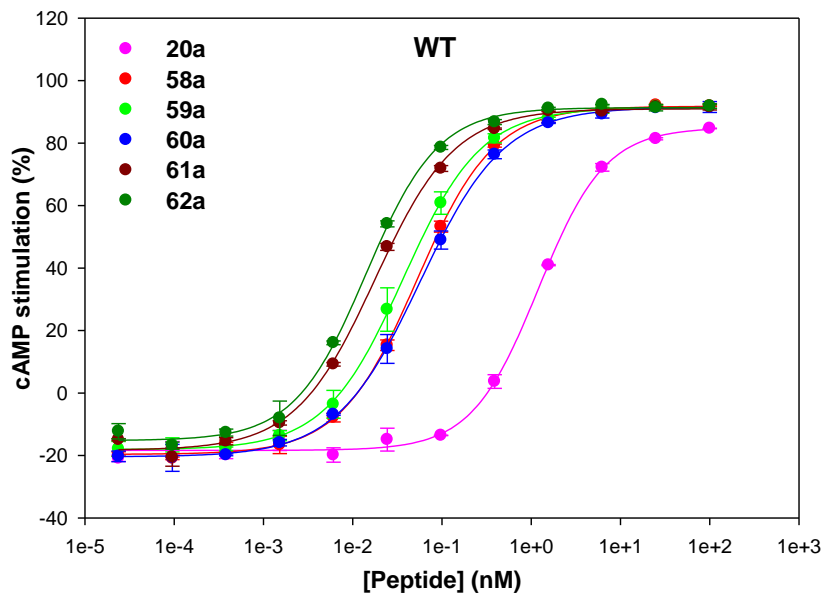
			R = carrier <b>2</b> <sup>(a)</sup>			R = NH <sub>2</sub> <sup>(b)</sup>		
			EC <sub>50</sub> (nM) <sup>(c)</sup>		IC <sub>50</sub> (nM) <sup>(d)</sup>	EC <sub>50</sub> (nM) <sup>(c)</sup>		IC <sub>50</sub> (nM) <sup>(d)</sup>
			-1	+1 (5 μM)	+ <sup>125</sup> I-Svg (20 pM)	-1	+1 (5 μM)	+ <sup>125</sup> I-Svg (20 pM)
●	<b>20</b>	Ac-UCN <sup>4-15</sup>	1.12±0.05	Inact. <sup>(e)</sup>	5.4±2.6	Inact. <sup>(f)</sup>	Inact. <sup>(g)</sup>	Inact. <sup>(h)</sup>
●	<b>58</b>	Ac-[Thr <sup>4</sup> Cha <sup>5</sup> ]UCN <sup>4-15</sup>	0.053±0.001	7.1±0.5	3.6±1.8	487±144 <sup>(l)</sup>	Inact. <sup>(g)</sup>	Inact. <sup>(h)</sup>
●	<b>59</b>	Ac-[Thr <sup>4</sup> Cha <sup>5</sup> D-Phe <sup>11</sup> ]UCN <sup>4-15</sup>	0.040±0.001	5.1±0.5	1.8±0.9	181±15	396±31	10188±6611
●	<b>60</b>	Ac-[Thr <sup>4</sup> Cha <sup>5,13</sup> D-Phe <sup>11</sup> ]UCN <sup>4-15</sup>	0.074±0.001	8.4±0.5	2.2±1.3	48±2	113±7	3738±1604
●	<b>61</b>	Ac-[Thr <sup>4</sup> Cha <sup>5,13</sup> Chg <sup>7</sup> D-Phe <sup>11</sup> ]UCN <sup>4-15</sup>	0.037±0.001	5.5±0.3	1.6±1.0	25±1	50±6	2977±1602
●	<b>62</b>	Ac-[Thr <sup>4</sup> Cha <sup>5,13</sup> Chg <sup>7</sup> tBuAla <sup>9</sup> D-Phe <sup>11</sup> ]UCN <sup>4-15</sup>	0.049±0.001	5.9±0.5	1.6±0.6	4.0±0.1	10.0±1.0	400±190

**Table 9. Binding to or stimulation of CRHR<sub>1</sub> by multisubstituted peptide fragments and conjugates in a stable CRHR<sub>1</sub> overexpressing cell line.** <sup>(a)</sup> Propargylated peptides conjugated to peptide **2**. <sup>(b)</sup> C-terminally amidated. <sup>(c)</sup> cAMP stimulation of a stable CRHR<sub>1</sub> overexpressing cell line in the absence or presence of 5 μM of the extracellular domain-specific antagonist **1**. <sup>(d)</sup> Radioactive binding assay using membrane preparations from CRHR<sub>1</sub>-overexpressing HEK293 cells. <sup>(e)</sup> Inactive up to 50 nM. <sup>(f)</sup> Inactive up to 10 μM. <sup>(g)</sup> Inactive up to 5 μM. <sup>(h)</sup> Inactive up to 80 μM. <sup>(l)</sup> Partial agonist.

The role of the CRHR<sub>1</sub>-ECD1 for the conjugates or peptide amides potencies was further investigated using HEK293 cells transiently overexpressing either the full length wild type CRHR<sub>1</sub> (WT) or a truncated mutant lacking the ECD1 (ΔECD1; Figures 29, 30 and Table 10).

As expected, the peptide conjugates **20a** and **58a-62a** were potent in a cAMP stimulation assay using a cell line transiently overexpressing the WT-CRHR<sub>1</sub> (Figure 29a). Notably, the potency values were similar in assays using cell lines stably or transiently overexpressing CRHR<sub>1</sub> (Tables 9 and 10). The peptide conjugates were inactive in a cAMP stimulation assay using a cell line transiently overexpressing a mutant CRHR<sub>1</sub> that lacks the ECD1 (ΔECD1-CRHR<sub>1</sub>, Figure 29b). For conjugates **58a-62a** incorporating the potency enhancing N-terminal amino acid substitutions, it is thus somewhat surprising that these conjugates are not able to stimulate CRHR<sub>1</sub>. Although conjugates **61a** and **62a** starts to weakly stimulate CRHR<sub>1</sub> at higher concentrations (dark red and dark green plots respectively), their potencies are substantially reduced compared to the untethered analogs (compare to Figure 30b). The ligated C-terminal recruitment fragment **2** therefore seems to hinder the activation segment from binding to the CRHR<sub>1</sub>-TMD.

a)



b)

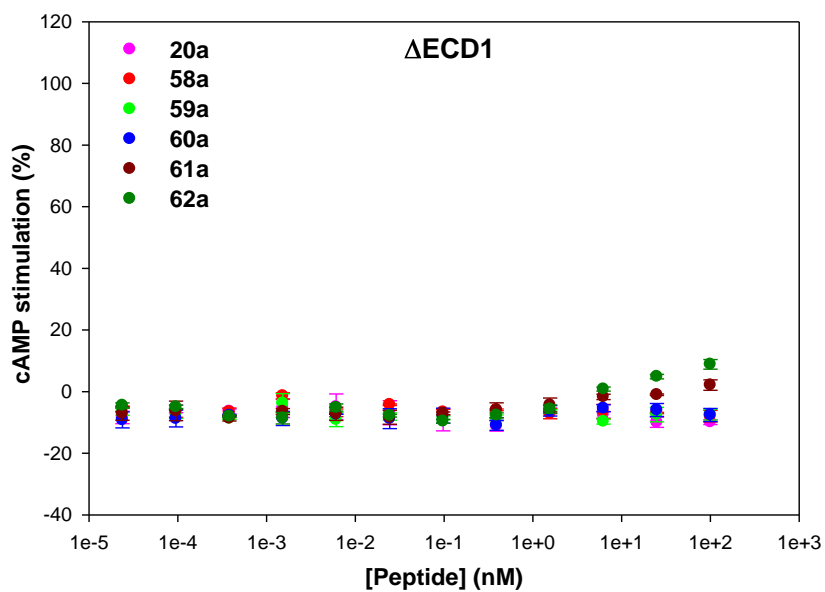
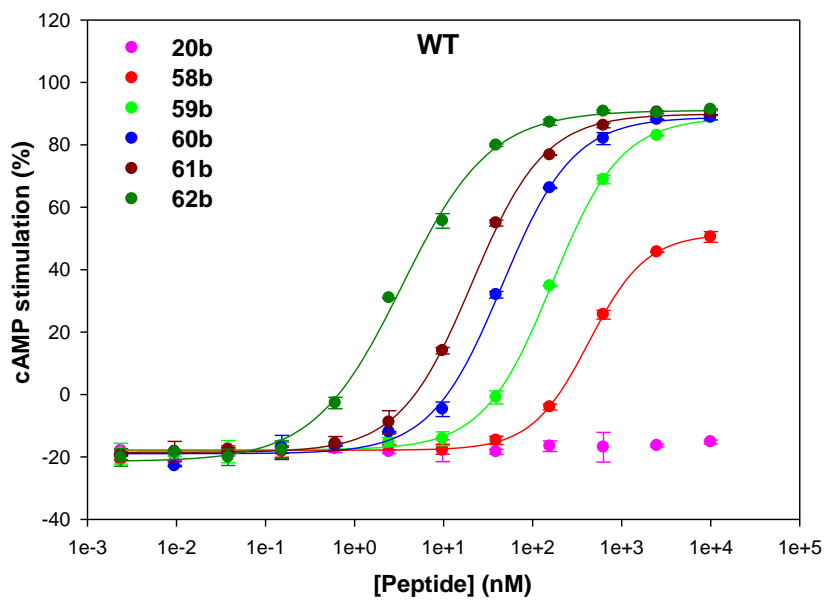


Figure 29. cAMP stimulation curves of multisubstituted peptide conjugates using HEK293 cells transiently overexpressing a) WT-CRHR<sub>1</sub> or b)  $\Delta$ ECD1-CRHR<sub>1</sub>.

a)



b)

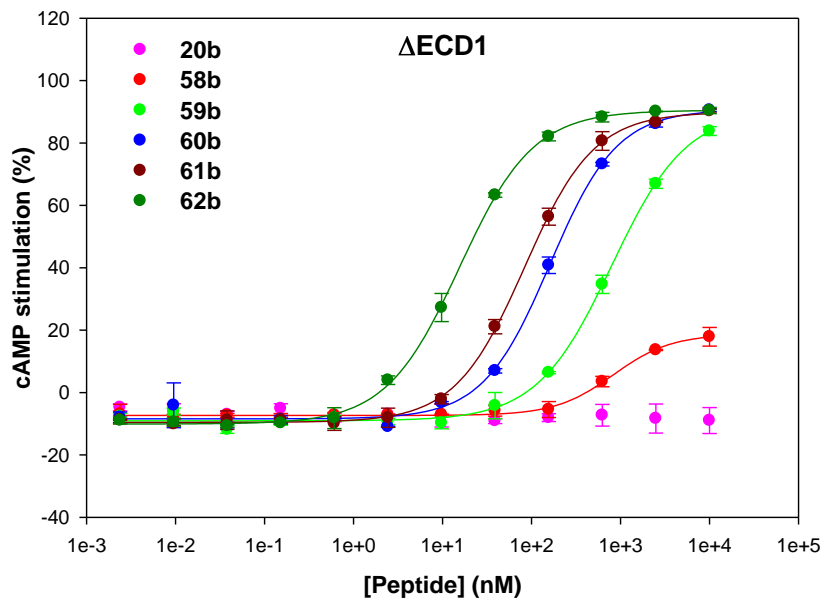


Figure 30. cAMP stimulation curves of C-terminally amidated multisubstituted peptides using HEK293 cells transiently overexpressing a) WT-CRHR1 or b)  $\Delta$ ECD1-CRHR1.

			R = carrier 2 <sup>(a)</sup>		R = NH2 <sup>(b)</sup>	
			EC <sub>50</sub> (nM)		EC <sub>50</sub> (nM)	
			WT	ΔECD	WT	ΔECD
●	20	Ac-UCN <sup>4-15</sup> -R	1.20±0.08	Inact.	Inact.	Inact.
●	58	Ac-[Thr <sup>4</sup> Cha <sup>5</sup> ]UCN <sup>4-15</sup> -R	0.052±0.002	Inact.	429±31	831±86
●	59	Ac-[Thr <sup>4</sup> Cha <sup>5</sup> D-Phe <sup>11</sup> ]UCN <sup>4-15</sup> -R	0.037±0.001	Inact.	165±8	797±79
●	60	Ac-[Thr <sup>4</sup> Cha <sup>5,13</sup> D-Phe <sup>11</sup> ]UCN <sup>4-15</sup> -R	0.057±0.001	Inact.	46±3	161±13
●	61	Ac-[Thr <sup>4</sup> Cha <sup>5,13</sup> Chg <sup>7</sup> D-Phe <sup>11</sup> ]UCN <sup>4-15</sup> -R	0.018±0.001	Inact.	20.9±0.8	84±2
●	62	Ac-[Thr <sup>4</sup> Cha <sup>5,13</sup> Chg <sup>7</sup> tBuAla <sup>9</sup> D-Phe <sup>11</sup> ]UCN <sup>4-15</sup> -R	0.014±0.001	Inact.	3.4±0.3	15.6±0.5

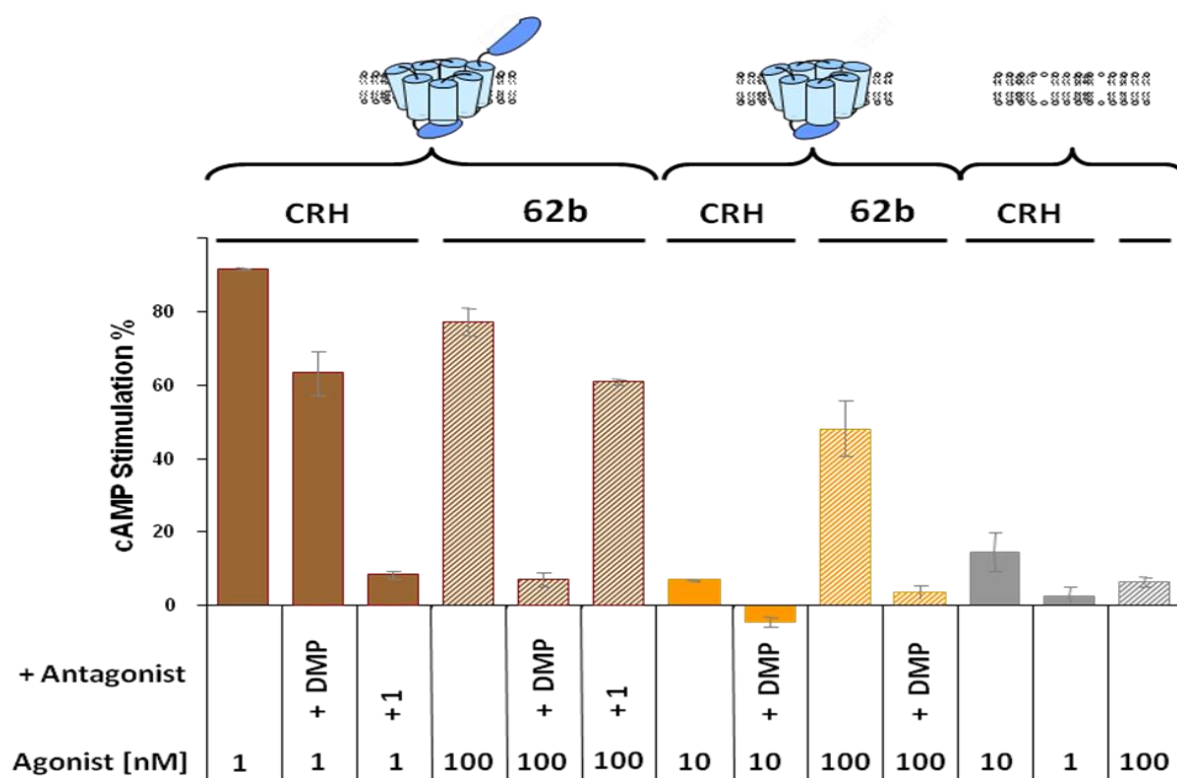
**Table 10. Stimulation of CRHR<sub>1</sub> by multisubstituted peptide fragments and conjugates in a transient CRHR<sub>1</sub> wild type or ΔECD1 overexpressing cell line.** <sup>(a)</sup> Propargylated peptides conjugated to peptide 2. <sup>(b)</sup> C-terminally amidated.

Similarly, the potencies of untethered peptides **58b-62b** correlated perfectly between assays using cell lines stably or transiently overexpressing the WT-CRHR<sub>1</sub> (Tables 9 and 10). The peptides **58b-62b**, however, all activated the ΔECD1-CRHR<sub>1</sub> mutant, albeit with about 4-fold reduced potency (Figure 30b and Table 10) and consistently produced partial agonism (**58b**) or full agonism (**59b-62b**). Notably, the untethered peptides were able to stimulate the ΔECD1-CRHR<sub>1</sub> mutant with good potency (e.g., 15.6 ± 0.5 nM for peptide **62b**), while their conjugated counterparts (e.g., **62a**) were inactive in the same settings. This observation confirms that the carrier peptide **2** can actually negatively affect the conjugation partners when not bound to the ECD1.

This experiment clearly and directly shows that the transmembrane domain (CRHR<sub>1</sub>-TMD) is the primary interaction site for these N-terminally derived CRH analogs, with only minor contributions from the extracellular domain, possibly indirectly by stabilizing the correct conformation of the juxtamembrane domain. Incorporation of six amino acid potency-enhancing substitutions identified in the single point screening led to the optimized untethered peptide **62b**. At this point, we decided to rename the peptide **62b** in **transtressin**; “trans” refers to the “transmembrane domain” of the CRHR<sub>1</sub> and “stressin” refers to the potency of **62b** to stimulate the CRHR<sub>1</sub>.

### 3.2.4 Pharmacological characterization of a CRHR<sub>1</sub>-TMD specific probe

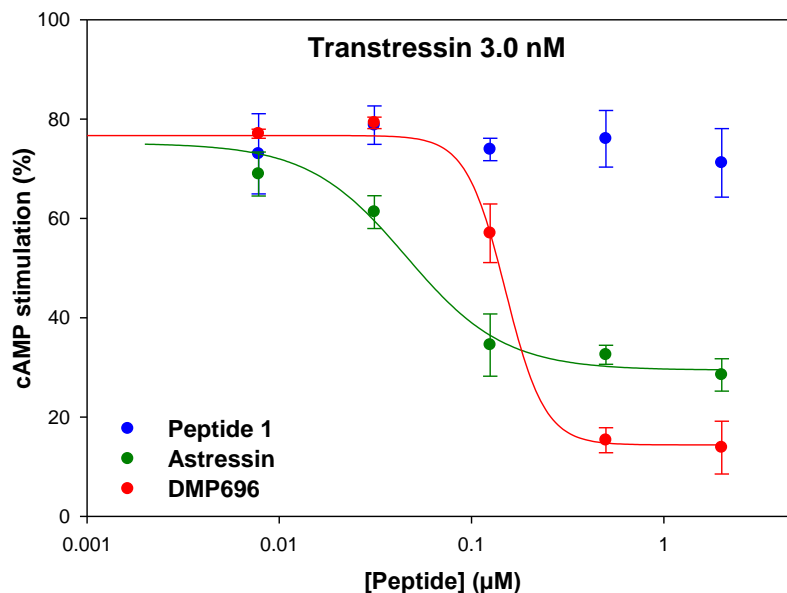
The binding mode of the hexasubstituted untethered peptide transtressin (**62b**) was further characterized in several assays. First, we tested the sensitivity of transtressin toward peptide **1**, an antagonist specific for the CRHR<sub>1</sub> extracellular domain, and DMP696, a nonpeptidic antagonist specific for the CRHR<sub>1</sub> juxtamembrane domain (generous gift of Bristol-Myers-Squibb, see Introduction). In a competition assay using the full length CRHR<sub>1</sub> construct, the endogenous hormone CRH (1 nM) was very sensitive to a saturating concentration of peptide **1** (10 μM), while DMP696 (2 μM) had only a weak inhibitory effect (Figure 31, dark brown bars). In contrast, DMP696 completely abolished CRHR<sub>1</sub> stimulation produced by transtressin (100 nM) while peptide **1** had no effect (Figure 31, light brown bars) in the same settings. In a similar assay using the truncated CRHR<sub>1</sub> mutant (ΔECD1-CRHR<sub>1</sub>), CRH was completely inactive even in the absence of DMP696. In contrast, transtressin was potent and sensitive to the presence of DMP696 (Figure 31, yellow bars).



**Figure 31. Stimulation of CRHR<sub>1</sub> and extracellular domain-truncated CRHR<sub>1</sub> by an optimized peptide agonist.** HEK293 cells transiently overexpressing full length CRHR<sub>1</sub><sup>24-415</sup> (brown bars), a truncated version CRHR<sub>1</sub><sup>112-415</sup> (yellow bars), or an empty vector (gray bars) were stimulated with CRH (filled) or transtressin (**62b**, hatched) at the indicated concentration in the absence or presence of the antagonists DMP696 (2 μM) or peptide **1** (10 μM). After 30 min, cAMP accumulation was determined and normalized.



These preliminary results clearly identify the CRHR<sub>1</sub>-TMD as a primary interaction site for transtressin. Interestingly, CRH binds so tightly to the CRHR<sub>1</sub> that DMP696 has only a weak inhibitory effect. Despite being one of the most potent CRHR<sub>1</sub> nonpeptide antagonists, it seems that this compound is not potent enough to displace the endogenous hormone in this concentration range. Moreover, it seems that DMP696 stabilized an inactive conformation of the mutant CRHR<sub>1</sub> (Figure 31, yellow filled bar). In agreement with our previous experiments, transtressin was slightly less potent in an assay using the  $\Delta$ ECD1-CRHR<sub>1</sub> than the WT-CRHR<sub>1</sub> constructs (Figures 30 and 31). In these cell lines transiently overexpressing the WT-CRHR<sub>1</sub> or  $\Delta$ ECD1-CRHR<sub>1</sub> constructs, the differences in potency observed may rise from different receptor expression level, from different functionality of the mutant receptor, or both.



**Figure 32. cAMP inhibition curves of transtressin by the CRHR<sub>1</sub>-ECD1 specific peptide 1, astressin and the CRHR<sub>1</sub>-TMD specific antagonist DMP696.** HEK293 cells stably overexpressing the full length CRHR<sub>1</sub> were incubated with increasing concentrations of antagonists: peptide 1 (blue), astressin (green) and DMP696 (red). After that the cells were incubated for 30 min, a fixed concentration of transtressin (3 nM) was added and the cells were further incubated for 30 min. Finally, the cells were lysed and the cAMP production was determined.

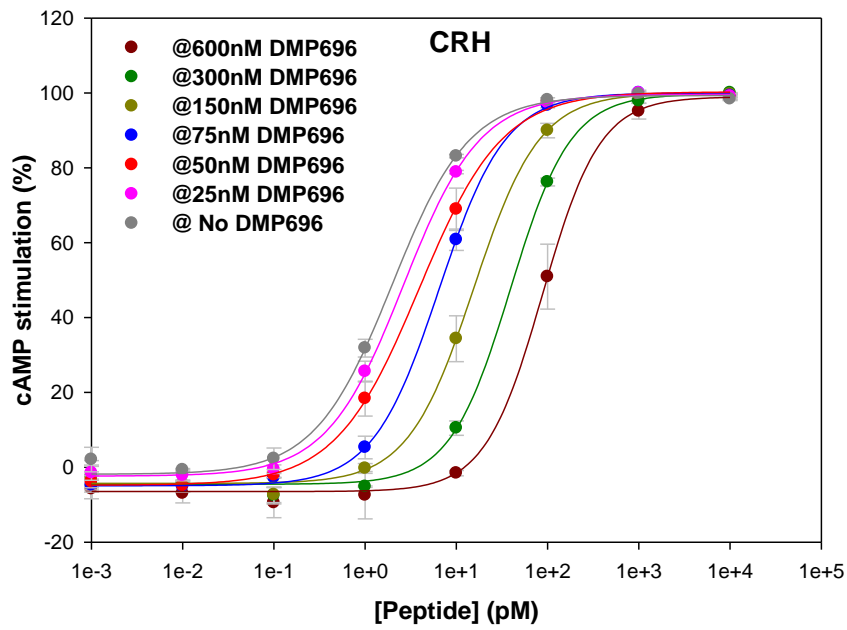
Transtressin was further characterized in a dose-response cAMP competition assay. In this setup, HEK293 stably overexpressing the full length CRHR<sub>1</sub> construct were first incubated with increasing concentrations of each antagonists: peptide 1, astressin (AST) and DMP696 respectively; a fixed EC<sub>50</sub>-corresponding concentration of transtressin was then added (EC<sub>50</sub> = 3 nM, identified in cAMP stimulation assay, Table 10). Consistently, the CRHR<sub>1</sub>-ECD1 specific peptide antagonist 1 was unable

to inhibit the CRHR<sub>1</sub> stimulation produced by transtressin (Figure 32, blue plots). DMP696, however, competed with transtressin and completely abolished CRHR<sub>1</sub> stimulation at higher concentrations (red curve). Interestingly, the peptide antagonist astressin also had an inhibitory effect; however at higher astressin concentrations the cAMP stimulation reached a lower limit around 30 % (green curve). Hence the competition effect of astressin with transtressin suggests that the antagonistic potency of this peptide arises not only from CRHR<sub>1</sub>-ECD1 binding but also from an interaction with the CRHR<sub>1</sub>-TMD.

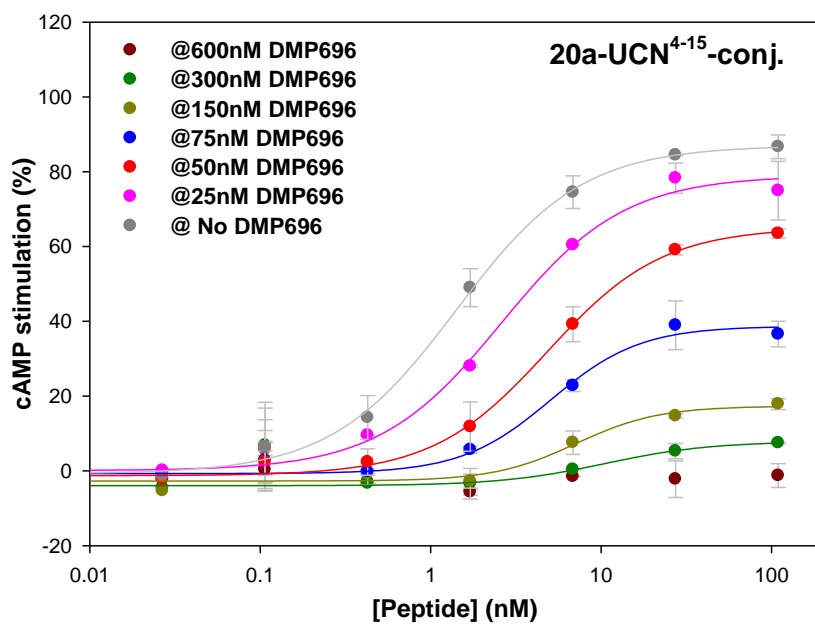
The dose-response cAMP competition assays of transtressin with several CRHR<sub>1</sub>-domains specific antagonists clearly establish the latter as a specific CRHR<sub>1</sub>-TMD peptide agonist. Starting from the 40-amino acid long sequence of the endogenous UCN hormone, the conjugation methodology allowed us to identify and optimize the ligand-CRHR<sub>1</sub>-TMD interactions in order to obtain a specific and highly potent twelve-amino acid CRHR<sub>1</sub> agonist. Gratifyingly, transtressin is the first known CRHR<sub>1</sub> transmembrane domain specific agonist.

The dose sensitivity of the endogenous hormone CRH, the conjugates **20a**, **62a** and transtressin to the CRHR<sub>1</sub>-TMD specific nonpeptide antagonist DMP696 was further investigated (Figure 33 and Table 11) in a cAMP inhibition assay. Nonpeptidic CRHR<sub>1</sub> antagonists such as DMP696 are well known to bind an allosteric site within the J-domain, producing a conformational change that blocks peptide agonists to bind their orthosteric site. Because the peptide can no longer bind the J-domain, it can no longer activate the CRHR<sub>1</sub>. This effect is concentration-dependent; hence a Schild regression analysis may provide crucial details about the molecular activation mechanism of each agonist. In this competition setup, HEK293 cells stably overexpressing the CRHR<sub>1</sub> were first incubated with increasing concentrations of DMP696. Increasing concentrations of the peptide agonists were then added and the subsequent cAMP production was determined.

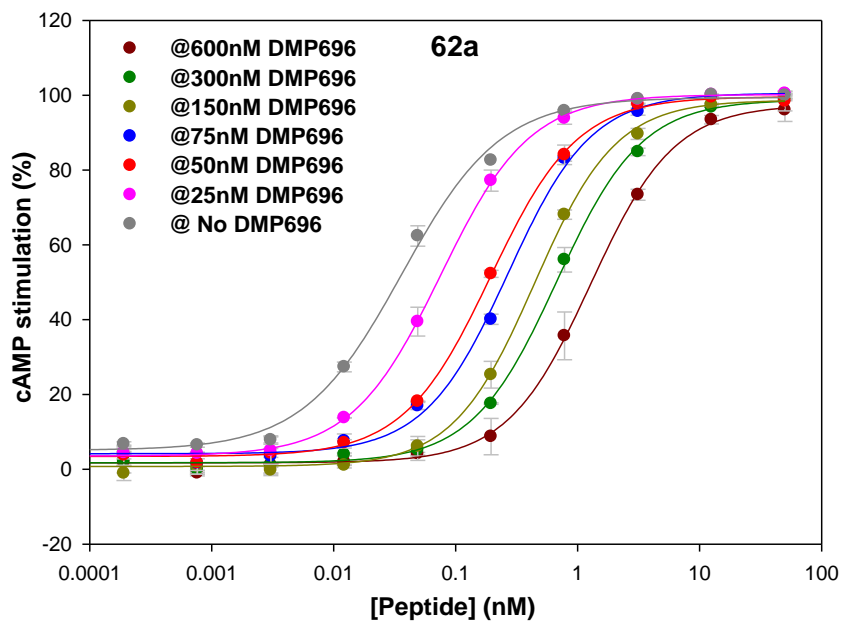
a)



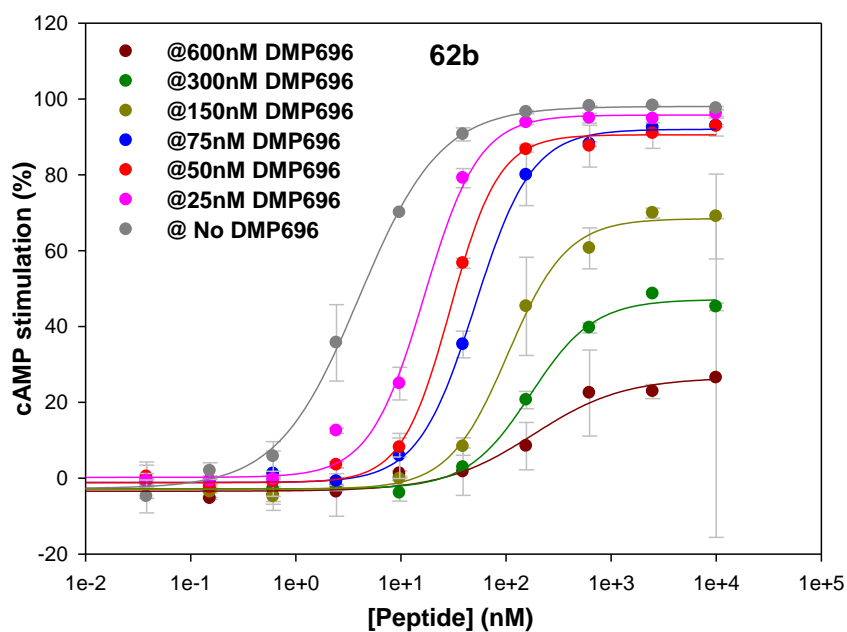
b)



c)



d)



**Figure 33. Mechanistic analysis of DMP696 inhibition vs peptide agonists CRH, 20a, 62a and transtressin.** Full dose-response curves for (a) CRH, (b) conjugate 20a, (c) conjugate 62a and (d) transtressin (62b) stimulated cAMP production in absence or presence of increasing concentrations of DMP696 using HEK293 cells stably overexpressing CRHR<sub>1</sub>.

DMP696 (nM)	CRH		20a		62a		62b	
	EC <sub>50</sub> (pM)	% E <sub>max</sub>	EC <sub>50</sub> (nM)	% E <sub>max</sub>	EC <sub>50</sub> (nM)	% E <sub>max</sub>	EC <sub>50</sub> (nM)	% E <sub>max</sub>
600	88.1±4.0	99	n.a.	n.a.	1.3±0.1	98	183±55	27
300	39.1±2.8	100	n.a.	n.a.	0.68±0.03	99	172±17	47
150	15.5±1.0	100	7.1±3.9	17	0.44±0.03	99	104±9	69
75	6.5±0.2	100	5.1±0.8	39	0.27±0.02	100	51±3	92
50	3.9±0.2	100	4.8±0.5	65	0.19±0.01	100	30±2	91
25	2.6±0.1	100	2.6±0.4	79	0.075±0.002	100	17±2	96
0	2.0±0.2	99	1.4±0.1	87	0.036±0.003	99	4.0±0.3	98

**Table 11. Schild analysis of competitive properties of DMP696 vs. peptide agonists CRH, 20a, 62a and transtresin (62b).**

Increasing concentrations of DMP696 incrementally depressed the maximal stimulation ( $E_{max}$ ) induced by conjugate **20a** while only weakly affecting the potency of the latter, consistently with a noncompetitive mode of inhibition (Figure 33b). This is in line with the two-domain model where the receptor occupancy is largely determined by the extracellular domain and its high-affinity to the carrier peptide (unaffected by DMP696), while efficacy is primarily determined by the interaction of the transmembrane domain with the N-terminal UCN<sup>4-15</sup> segment. Importantly, the two-domain model predicts that concentrations of conjugate **20a** that fully saturate the extracellular domain constitute an upper limit to the effective (“intramolecular”) concentration of the conjugated peptide **20** that can be “perceived” by the transmembrane domain. Further increasing concentrations of free conjugated **20a** unligated to the extracellular domain can be neglected in this context. This maximal effective concentration of **20** is eventually unable to overcome the increasing concentrations of DMP696 thus providing a rationale for the observed noncompetitive mode of inhibition.

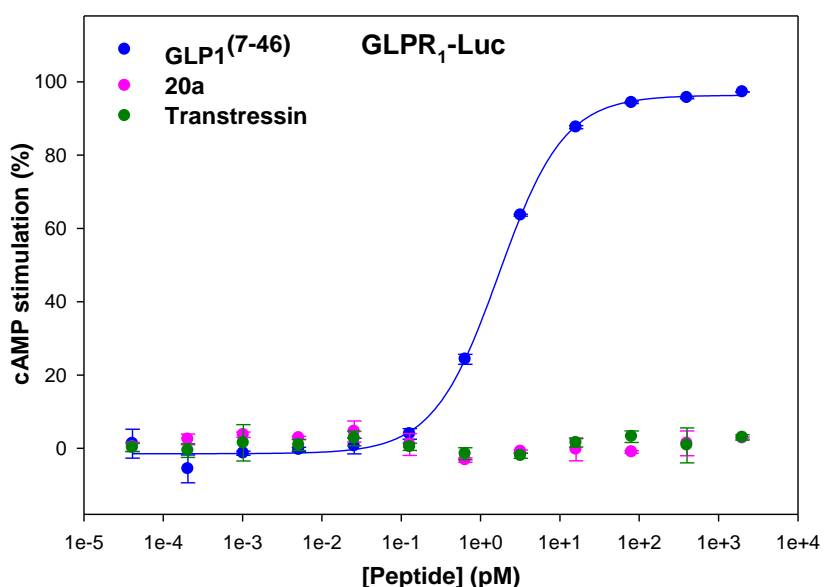
In contrast, increasing concentrations of DMP696 dramatically affected the potency of the endogenous hormone CRH. However, DMP696 had no effect on the maximal stimulation ( $E_{max}$ ) induced by CRH and, at higher concentrations, full CRHR<sub>1</sub> stimulation was observed (Figure 33a). Increasing concentrations of DMP696 had similar effects on the cAMP dose response of conjugate **62a** (Figure 33c). In both cases, the decrease in potency was directly proportional to the concentration of DMP696; however at higher concentrations of the peptide agonists, DMP696 was not able to inhibit the CRHR<sub>1</sub> stimulation. This effect is consistent with a competitive mode of inhibition of DMP696 in which the antagonist competes directly with the peptide N-terminus for

binding the CRHR<sub>1</sub>-TMD. This mode of inhibition is not in line with the two domain model; it seems that the effective concentration of agonist N-terminus “perceived” by the CRHR<sub>1</sub>-TMD does not depend of the binding of the peptides to the CRHR<sub>1</sub>-ECD1. We assume that this mechanism is characteristic of highly potent peptide agonists such as CRH and conjugate **62a**. In this concentration range, the CRHR<sub>1</sub>-ECD1 is not saturated with peptide C-terminus and allows a direct competition at the CRHR<sub>1</sub>-TMD; it is possible that a higher concentration of DMP696 would reveal a noncompetitive mode of inhibition similar to that observed with conjugate **20a**.

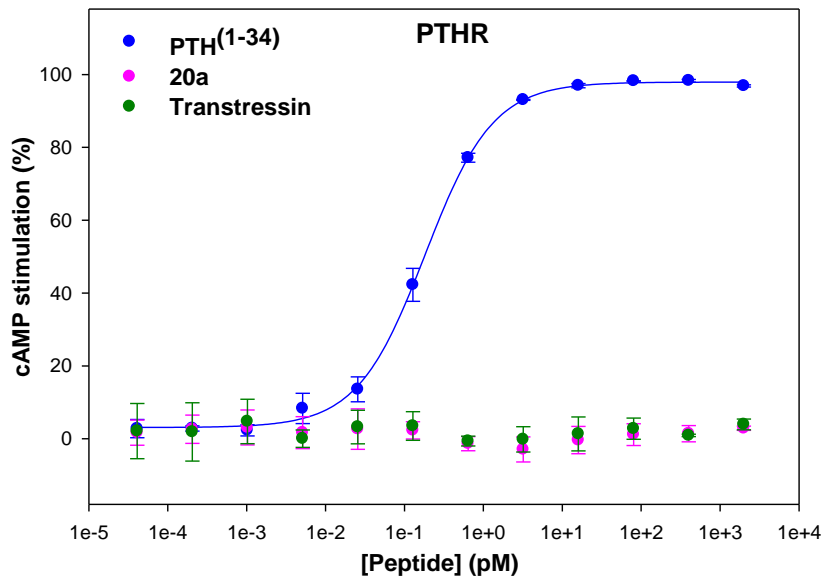
The sensitivity of transtresin toward increasing concentrations of DMP696 revealed an interaction reminiscent of a mixed competitive mode of inhibition. DMP696 strongly affected the EC<sub>50</sub> of transtresin even at low concentrations, while at higher concentrations it also reduced the *E*<sub>max</sub> of the latter (Figure 33d). This is completely in line with a direct competition between DMP696 and transtresin for binding at the CRHR<sub>1</sub>-TMD. Transtresin is able to displace DMP696 from binding the CRHR<sub>1</sub>-TMD up to a concentration of 75 nM of the latter (blue curve). Above this limit, the CRHR<sub>1</sub>-TMD is saturated with DMP696 thus decreasing the transtresin-induced cAMP stimulation (*E*<sub>max</sub> level). This mode of inhibition is characteristic of a CRHR<sub>1</sub>-TMD specific agonist and a unique feature of our new CRHR<sub>1</sub> modulator transtresin.

Finally, the specificity of the conjugate **20a** and transtresin for CRH receptors was tested in collaboration with Serena Cuboni. A cAMP stimulation assay was performed using HEK293 cells transiently overexpressing GLPR<sub>1</sub>, PTHR and CRHR<sub>2</sub> (Figure 34).

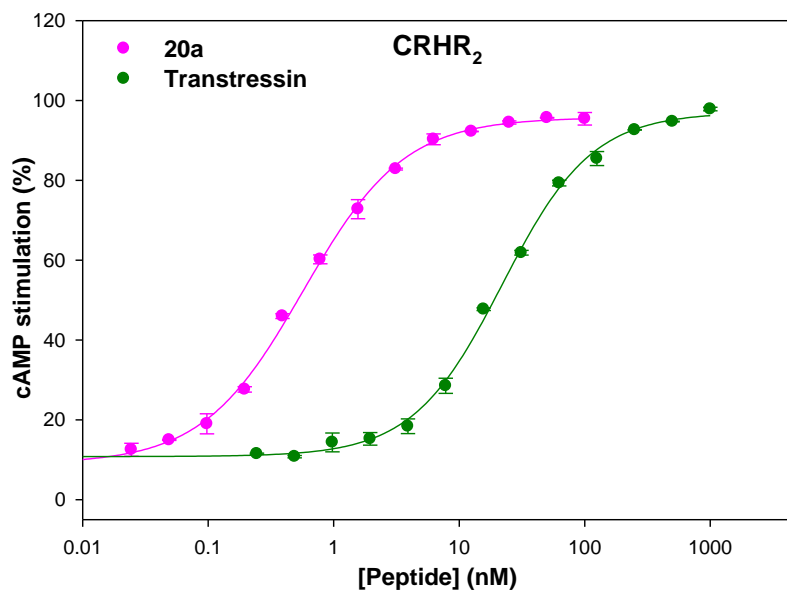
a)



b)



c)



**Figure 34. cAMP stimulation curves of peptide conjugate 20a and transtresin in cell lines transiently overexpressing (a) GLP<sub>1</sub>, (b) PTHR and (c) CRHR<sub>2</sub>.**

Transtresin and conjugate **20a** were unable to stimulate the GLP<sub>1</sub> and the PTH receptors, showing that there is no cross-reactivity for other closely related receptors. However, transtresin and the conjugate **20a** were active at the CRHR<sub>2</sub> ( $22.04 \pm 1.12$  nM and  $0.57 \pm 0.03$  nM respectively, Figure 34c), the closest homologue of CRHR<sub>1</sub> (> 70 % amino acid sequence identity). The low degree

of selectivity between the two CRH receptor subtypes is not surprising as CRHR<sub>2</sub> is also potently stimulated by the endogenous ligand UCN from which transtressin and the conjugate **20a** were derived. The highest degree of sequence homology between CRHR<sub>1</sub> and CRHR<sub>2</sub> is found in the intracellular loops and the seven transmembrane helices (~ 90 % and ~ 85 % identity respectively), while the extracellular domains are conserved to a lesser extent (~ 60 %), thus explaining the slight differences of potencies for transtressin and the conjugate **20a** between the two receptor subtypes. In particular, the ligand selectivity profile of CRHR<sub>1</sub> and CRHR<sub>2</sub> were well investigated. Dautzenberg et al. have shown that the unusual ligand selectivity of the CRHR<sub>1</sub> resided completely in its ECD1 domain; suggesting that the others extracellular loops of CRHRs do not contribute significantly to the selectivity of this receptor (*Dautzenberg et al.* 1999). Hence, transtressin is a nonselective CRHR<sub>1</sub> and CRHR<sub>2</sub> agonist.

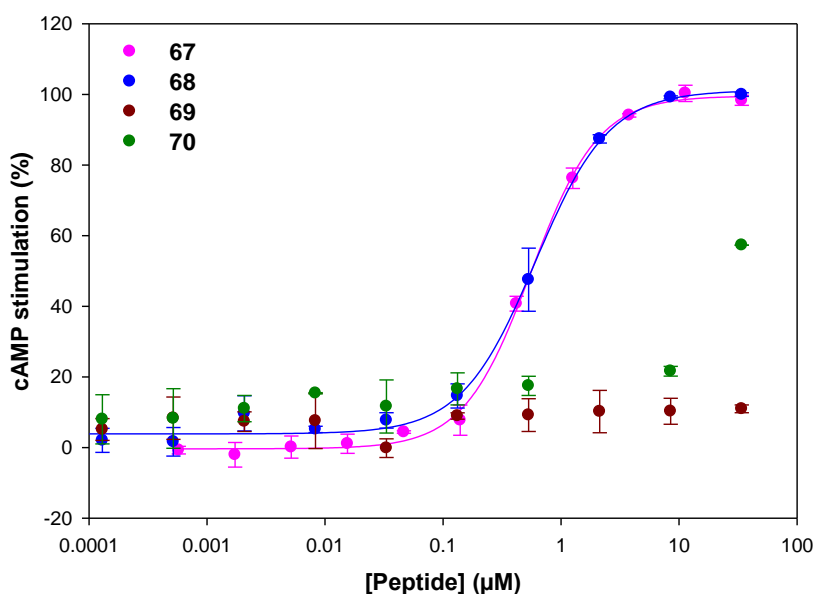
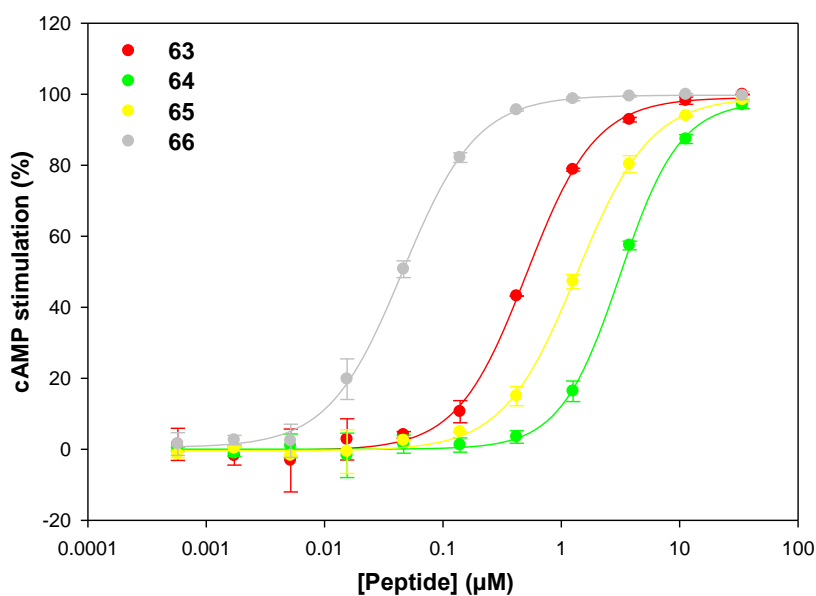
Recently, a transtressin analogue with an N-terminal tyrosine amino acid residue was synthesized. This modification retained the agonistic potency of transtressin (data not shown). This peptide could be used to obtain a radioactive analogue of transtressin that could be used in binding assays; such direct binding experiment would complement the pharmacological characterization of this new modulator of the CRHRs.

Finally, a hallmark of the biomimetic screening is the possibility to target the unmodified native receptors. The peptide-carrier conjugates should therefore also be applicable to the endogenous receptors in their native environment. This was confirmed in a collaboration with the group of Molecular Neurogenetics (Jan Deussing) at the Max-Planck-Institute for Psychiatry in Munich, which allowed us to test the effects of conjugates in a physiologically relevant system. Katherine Webb (AG Deussing) administered the conjugate **20a** and transtressin directly to the brain of wild-type mice via intracerebroventricular injection. The CRHR<sub>1</sub>-mediated modulation of the stress response was then evaluated using the acoustic startle response paradigm (data not shown). Gratifyingly, the sensitizing effects of the peptide conjugate on the startle response were qualitatively similar to exogenously applied CRH controls (*Devigny et al.* 2011).



### 3.2.5 Synthesis and evaluation of a peptide amide library

Based on the potency-enhancing amino acid substitutions identified in the screening, we decided to complete the SAR of the UCN<sup>4-15</sup> sequence by synthesizing a small library of untethered peptides (Figure 35 and Table 12). We included combinations of amino acid substitutions suited for the untethered template (peptides **63**, **64**, **65**, **66**, **67**, **73**, **75**, **76**, **77**, **78** and **79**); in addition we incorporated more “exotic” amino acid substitutions such as  $\alpha$ -methylated amino acids (peptides **68**, **69**, **70** and **75**) and unnatural amino acids (peptides **71** and **72**). As usual, the library of untethered peptides was tested for CRHR<sub>1</sub> stimulation in a cAMP cell-based assay.



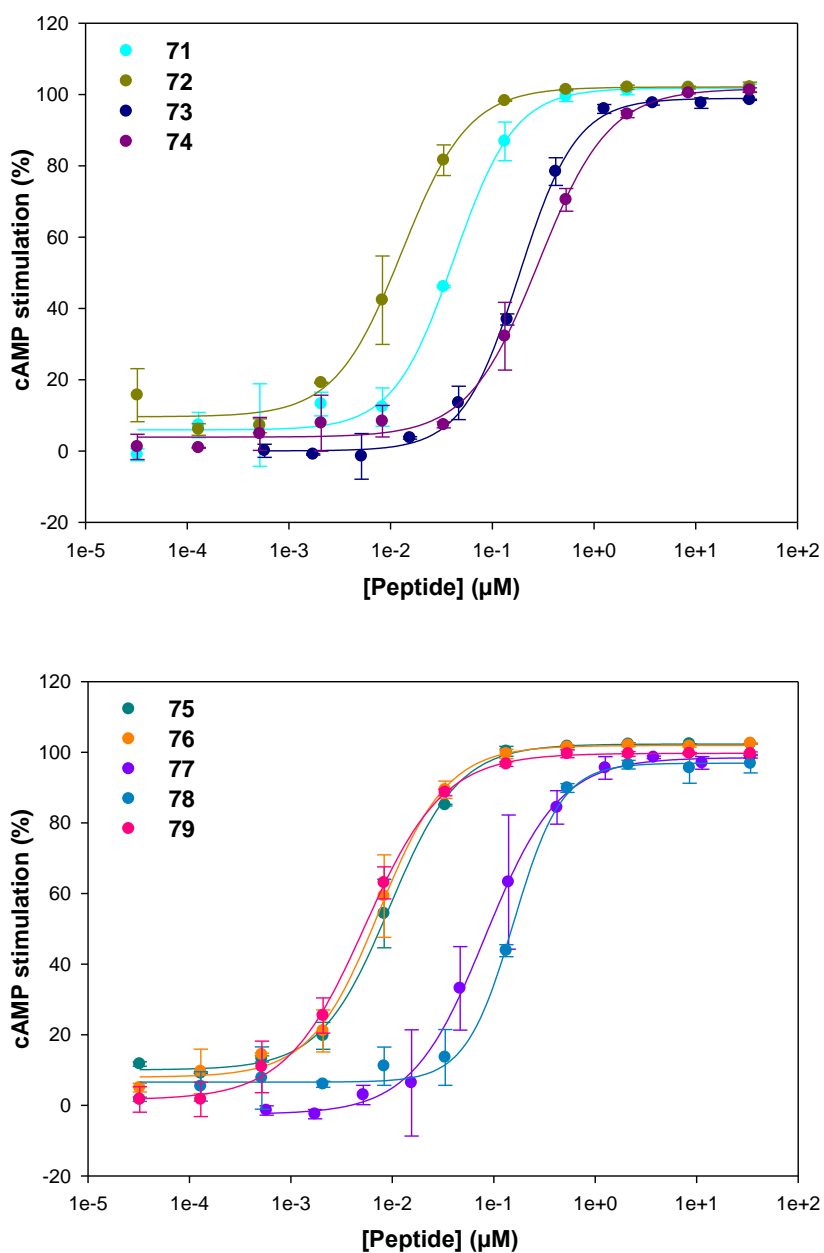


Figure 35. cAMP stimulation curves of an untethered peptide analogs of human UCN<sup>4-15</sup>.

A Phe<sup>11</sup>-D-Phe including double amino acid substituted transressin-analogs **63** and **64** afforded weak yet full CRHR<sub>1</sub> agonists. In contrast, the untethered peptide **58b** was only a partial agonist in the same settings, thus confirming the crucial importance of the Phe<sup>11</sup>-D-Phe substitution for the potency of untethered ligands. The substitution of Leu residues to tBuAla at positions 5 and 13 consistently improved the potency but afforded untethered peptides that were not as potent as their Cha-substituted analogs (peptides **65**, **66** and **67**). Similarly, the Ile<sup>7</sup>tBuGly peptide **74** was dramatically less potent than its Ile<sup>7</sup>Chg analog **61b**. Introduction of a tBuAla residue at position 14 in peptide **76** greatly improved the potency. However, the Cha<sup>14</sup>-substituted analog **77** was found to be

10-fold less potent than **76** and 2-fold less potent than its native Leu<sup>14</sup> analog **60b**. A similar trend was observed at position 9; the Cha<sup>9</sup>-substituted peptide **78** was dramatically less active than its tBuAla<sup>9</sup> analog: transtresin. Finally, the tBuAla heptasubstituted peptide **79** was only slightly less potent than transtresin ( $5.3 \pm 0.2$  nM and  $4.0 \pm 0.1$  nM respectively).

		Sequence	Subst. #	EC <sub>50</sub> (nM)	Rel. Pot./transtresin
●	<b>63</b>	Ac-[Cha <sup>5</sup> D-Phe <sup>11</sup> ]UCN <sup>4-15</sup>	2	509±28	0.006
●	<b>64</b>	Ac-[Thr <sup>4</sup> D-Phe <sup>11</sup> ]UCN <sup>4-15</sup>	2	3135±103	0.001
●	<b>65</b>	Ac-[Thr <sup>4</sup> tBuAla <sup>5</sup> D-Phe <sup>11</sup> ]UCN <sup>4-15</sup>	3	1352±50	0.002
●	<b>66</b>	Ac-[Thr <sup>4</sup> tBuAla <sup>5</sup> D-Phe <sup>11</sup> Cha <sup>13</sup> ]UCN <sup>4-15</sup>	4	46±2	0.07
●	<b>67</b>	Ac-[Thr <sup>4</sup> tBuAla <sup>5,13</sup> D-Phe <sup>11</sup> ]UCN <sup>4-15</sup>	4	556±28	0.005
●	<b>68</b>	Ac-[Thr <sup>4</sup> Cha <sup>5</sup> D-Phe <sup>11</sup> α-MeLeu <sup>13</sup> ]UCN <sup>4-15</sup>	4	605±61	0.005
●	<b>69</b>	Ac-[Thr <sup>4</sup> Cha <sup>5,13</sup> α-MeD-Phe <sup>11</sup> ]UCN <sup>4-15</sup>	4	Inact.	-
●	<b>70</b>	Ac-[Thr <sup>4</sup> α-MeLeu <sup>5</sup> D-Phe <sup>11</sup> Cha <sup>13</sup> ]UCN <sup>4-15</sup>	4	Inact.	-
●	<b>71</b>	Ac-[alloThr <sup>4</sup> Cha <sup>5,13</sup> D-Phe <sup>11</sup> ]UCN <sup>4-15</sup>	4	42±4	0.07
●	<b>72</b>	Ac-[β-PheSer <sup>4</sup> Cha <sup>5,13</sup> D-Phe <sup>11</sup> ]UCN <sup>4-15</sup>	4	13±1	0.23
●	<b>73</b>	Ac-[Thr <sup>4</sup> Cha <sup>5,13,14</sup> D-Phe <sup>11</sup> ]UCN <sup>4-15</sup>	5	184±9	0.02
●	<b>74</b>	Ac-[Thr <sup>4</sup> Cha <sup>5,13</sup> tBuGly <sup>7</sup> D-Phe <sup>11</sup> ]UCN <sup>4-15</sup>	5	284±26	0.01
●	<b>75</b>	Ac-[Thr <sup>4</sup> Cha <sup>5,13</sup> α-MeLeu <sup>9</sup> D-Phe <sup>11</sup> ]UCN <sup>4-15</sup>	5	9.4±0.5	0.11
●	<b>76</b>	Ac-[Thr <sup>4</sup> Cha <sup>5,13</sup> D-Phe <sup>11</sup> tBuAla <sup>14</sup> ]UCN <sup>4-15</sup>	5	7.4±0.5	0.41
●	<b>77</b>	Ac-[Thr <sup>4</sup> Cha <sup>5,13,14</sup> Chg <sup>7</sup> D-Phe <sup>11</sup> ]UCN <sup>4-15</sup>	6	83±5	0.04
●	<b>78</b>	Ac-[Thr <sup>4</sup> Cha <sup>5,9,13</sup> Chg <sup>7</sup> D-Phe <sup>11</sup> ]UCN <sup>4-15</sup>	6	157±11	0.02
●	<b>79</b>	Ac-[Thr <sup>4</sup> tBuAla <sup>5,9,13,14</sup> Chg <sup>7</sup> D-Phe <sup>11</sup> ]UCN <sup>4-15</sup>	7	5.3±0.2	0.57

**Table 12. Stimulation of CRHR<sub>1</sub> by multisubstituted untethered peptides in a stable CRHR<sub>1</sub> overexpressing cell line.**

The incorporation of α-methylated amino acid residues is well known to influence the conformation of peptides by enhancing their ellipticity (*Altmann et al.* 1988). In our template, transtresin analogs **68**, **69** and **70** including α-MeLeu or α-MeD-Phe amino acid substitutions were only poorly active. In contrast, the Leu<sup>9</sup>α-MeLeu substitution in peptide **75** was surprisingly well tolerated and delivered a low nanomolar agonist.

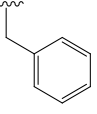
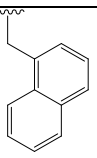
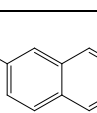
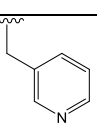
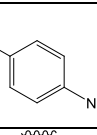
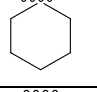
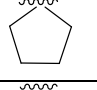

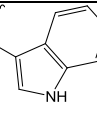
These results clearly reveal that the role of each substituted amino acid residue directly depends on the neighboring context. Generally, the side chain of hydrophobic residues such as Leu and Ile can be positively substituted by another bulkier hydrophobic side chain. However, the size and nature of such substitutions seem to be position-dependent. These side chains can play major roles having an influence on the potency of the peptide ligands: the strength of hydrophobic interactions that naturally occur between ligand and receptor residues may be enhanced; and the bulkiness of the side chain might confer to the peptide a conformation that optimizes ligand-receptor interactions (e.g., by enhancing ellipticity). Although the individual contribution of each amino acid residue to these phenomena remains unclear at the moment, the importance relies in finding the amino acid combinations that confer an optimized potency.

### 3.2.6 Structure-Activity-Relationship at [Phe<sup>11</sup>]UCN<sup>4-15</sup>

By screening the minimized UCN<sup>4-15</sup> activation segment, we identified the Phe<sup>11</sup>D-Phe substitution as one of the most potency enhancing (Table 7 and Figure 24). Our findings in the UCN<sup>4-15</sup> template correlate perfectly with an early single point D-substitution study on the full length CRH endogenous hormone (*Rivier et al.* 1993). It is noteworthy that the D-Phe substitution was systematically used for the synthesis and SAR studies of CRHR<sub>1</sub> peptide agonists and antagonists (*Cervini et al.* 1999; *Gulyas et al.* 1995; *Hernandez et al.* 1993; *Koerber et al.* 1998; *Miranda et al.* 1994; *Miranda et al.* 1997; *Rivier et al.* 1998a; *Rivier et al.* 1998b). To further probe the role of the Phe<sup>11</sup> residue for the potency of ligands, we decided to synthesize a library of UCN<sup>4-15</sup> conjugates bearing Phe<sup>11</sup> substitutions. We especially focused on D-Phe<sup>11</sup>-substituted derivatives depending on the aryl substituents and the commercial availability of the Fmoc-protected amino acid building blocks. The obtained conjugates were tested in a cAMP stimulation assay (curves not shown) and the potencies were compared to the native UCN<sup>4-15</sup> sequence of conjugate **20a** (Table 13).

As previously determined, the Phe<sup>11</sup>D-Phe-substituted UCN<sup>4-15</sup> conjugate **80** was five-fold more potent than the native UCN<sup>4-15</sup> sequence of conjugate **20a**. The close Phe<sup>11</sup>D-Pal (3-pyridyl) analog **83** also enhanced the potency of the UCN<sup>4-15</sup> template. All other Phe<sup>11</sup> substitutions were detrimental for the potency of the conjugates. The Phe<sup>11</sup>D-Trp substitution was well tolerated and the conjugate remained highly potent (conjugate **88**). Similarly, the 1-naphtyl substitution was well-tolerated (conjugate **81**) while its 2-naphtyl related analogue was inactive (conjugate **82**), suggesting that aryl-substitutions at the para-position are detrimental for the potency of the ligands. Consistently, Phe<sup>11</sup>Tyr and Phe<sup>11</sup>PI-Phe analogues were rendered completely inactive in our UCN<sup>4-15</sup> screening (Figure 24). Additional chemical substitutions around the Phe-aryl ring were poorly tolerated (conjugates **81**, **82** and **84**). The inactive Phe<sup>11</sup>Acp and Phe<sup>11</sup>Ach (backbone cyclopentyl and

cyclohexyl amino acids respectively) conjugates **85** and **86** pointed out the importance of the aryl moiety for the potency. Consistently, this effect could be reversed by the introduction of an aryl moiety in the Phe<sup>11</sup>-indane substituted conjugate **87**.

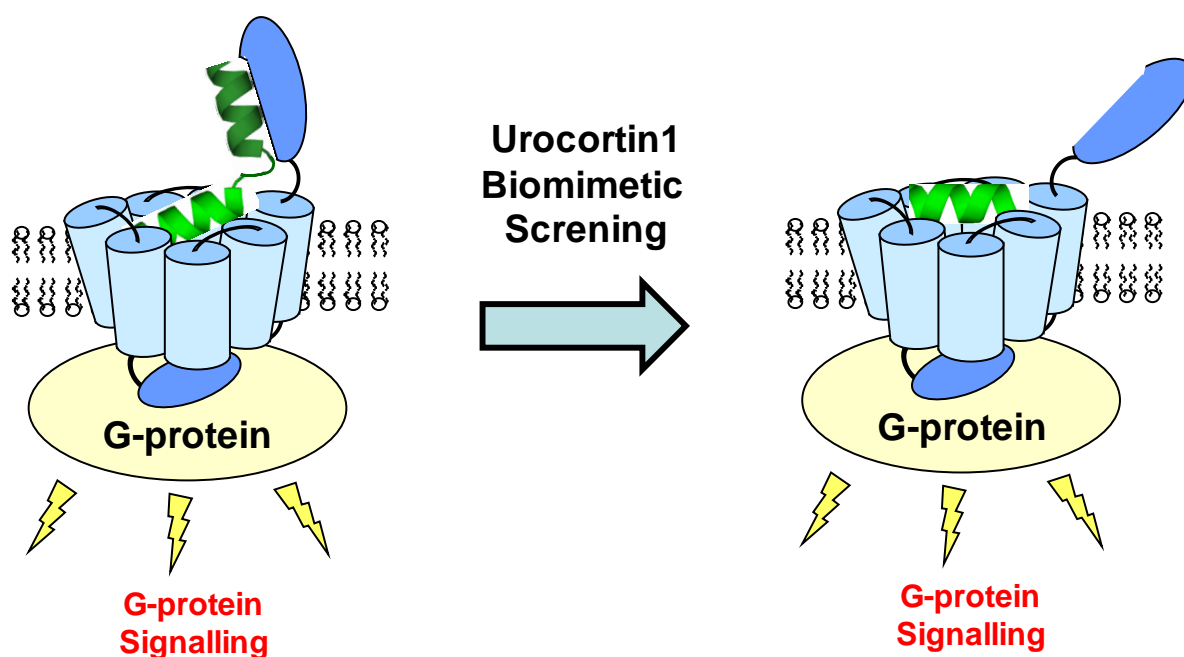
		[Phe <sup>11</sup> ]	Side chain structure	EC <sub>50</sub> (nM)	Rel. Pot./20
●	<b>20a</b>	-	-	3.10±0.57	-
●	<b>80</b>	D-Phe		0.60±0.05	5.2
●	<b>81</b>	D-Nal(1)		12.25±1.69	0.3
●	<b>82</b>	D-Nal(2)		Inactive	-
●	<b>83</b>	D-Pal		1.20±0.13	2.6
●	<b>84</b>	D-pNO <sub>2</sub> -Phe		5.52±0.43	0.6
●	<b>85</b>	Ach		Inactive	-
●	<b>86</b>	Acp		Inactive	-
●	<b>87</b>	Aic		15.75±0.20	0.2
●	<b>88</b>	D-Trp		3.84±0.20	0.8

**Table 13. Stimulation of CRHR<sub>1</sub> by Phe<sup>11</sup>-substituted UCN<sup>4-15</sup> peptide conjugates.**

The SAR profile at the UCN<sup>4-15</sup>Phe<sup>11</sup> gives complementary details about the role of this amino acid residue for ligand-receptor interaction. The aryl moiety of Phe<sup>11</sup> seems to interact directly with the CRHR<sub>1</sub>-TMD. Interestingly, the potency of the UCN<sup>4-15</sup> segment is greatly enhanced by the presence of a Phe<sup>11</sup>D-Phe substitution. This D-amino acid substitution suggests that a helical conformation for this peptide is not favored for an optimized binding.

### 3.2.7 Summary of the UCN biomimetic screening

A rapid approach to chemically probe the interaction domain of class B GPCRs was developed. The conjugation of a high-affinity carrier resulted in a dramatic enhancement in the activity of peptide ligands and allowed the initial testing of peptides whose activity would otherwise have been too weak to be detectable. The synthesis and coupling of short length peptides to reconstitute a fully functional CRHR<sub>1</sub> modulator has several advantages compared to the classical synthesis of whole, full length peptide ligands. For example, it is quicker with higher product purities. Importantly, the fragment conjugation approach obviated the need for HPLC purification of the initial test peptides, thereby enabling a substantially higher screening throughput. Thanks to the exquisite receptor specificity of the conjugates imparted by the carrier segment, the crude peptide conjugates were compatible with functional assays in living cells (*Devigny et al.* 2011).



**Figure 36. Urocortin1 biomimetic screening overview: sequence optimization of a typical class B GPCR peptide hormone.**

By application of this methodology to the class B GPCR CRHR<sub>1</sub> we discovered a low nanomolar agonist, named transtressin (Figure 36). This 12-mer peptide is the first known agonist specific for the activation domain of the receptor. The activation mechanism of transtressin is independent of the extracellular domain and resembles the signaling mechanism of canonical class A GPCRs. We assume that transtressin binds at the endogenous hormone orthosteric site and derives its activity from optimized hydrophobic interactions. Our results are inconsistent with a necessary allosteric

change of the extracellular domain which had been postulated as the initiating step of signal transduction for other class B GPCRs (Dong *et al.* 2006; Dong *et al.* 2008). CRHR<sub>1</sub> therefore resembles more closely the parathyroid hormone receptor 1, the only other class B GPCR for which juxtamembrane-specific agonists have been described (Carter *et al.* 2007; Shimizu *et al.* 2000). Whether transmembrane-specific agonists for other class B GPCRs can be identified by this methodology remains to be determined. The CRHR<sub>1</sub> domain-specificity of transtressin can be advantageously used in competition assays and allows to address the specificity of CRHR<sub>1</sub> ligands (e.g., antagonists) for modulating the CRHR<sub>1</sub> functions. The key principle of this work, testing class B ligands after membrane recruitment, is related in some aspects to a recently published “mammalian class B ligand display” (Fortin *et al.* 2009). However, while potentially superior in the number of tested peptides, the latter approach is inherently limited to genetically encoded amino acids. It is noteworthy that for transtressin, five unnatural amino acids substitutions were necessary to achieve low nanomolar, juxtamembrane-specific ligands. As such the “carrier-conjugate” approach presented in this study might be better suited to produce hits for drug development, as this method can be readily adapted to unnatural or even nonpeptidic substances (Devigny *et al.* 2011).

### 3.3 Biomimetic screening of a synthetic CRHR<sub>1</sub> modulator: **astressin**

The CuCAAC conjugation of peptide fragments is an efficient strategy for the SAR investigation of UCN-like peptide hormones. Ultimately, this powerful approach has led to the discovery of transtressin, the first CRHR<sub>1</sub>-TMD specific peptide agonist. These results encouraged us to apply the conjugation methodology to others CRHR peptide modulators. Beyond endogenous CRHRs peptide agonists such as UCN and CRH, a plethora of synthetic CRHR<sub>1</sub> peptides have been disclosed. All of the non-natural peptide ligands, both agonists and antagonists, have been developed from SAR work and derivatisation of the natural ligands (see Introduction). Chain shortening, residue substitution and cyclization studies have led to the peptide antagonist astressin, a highly potent  $\alpha$ -helical peptide using a lactam bridge constrain. Consistently with the two-domain model, peptide antagonists such as astressin bind the CRHR<sub>1</sub>-ECD1 with high-affinity, the absence of the truncated amino terminus end of the antagonists means inability to initiate the activation of the receptor but effectively blocks the endogenous ligand from binding the receptor (*Grace et al. 2004; Hoare 2005*).

The competition assay between transtressin and astressin revealed that astressin binds not only to the CRHR<sub>1</sub>-ECD1 but unexpectedly seem to interact to some degree also directly with the CRHR<sub>1</sub>-TMD (Figure 32). Indeed, astressin inhibits the CRHR<sub>1</sub> cAMP stimulation induced by transtressin, suggesting that both peptides compete for the same binding site within the CRHR<sub>1</sub>-TMD. Moreover, the inhibition induced by a high dose of astressin reached a minimum ( $E_{min}$ ) and did not completely abrogate the transtressin-induced stimulation, indicating the weak basal agonism of astressin. Thereby, we assume that the C-terminus of astressin binds with high-affinity to the CRHR<sub>1</sub>-ECD1, while the N-terminus weakly interacts with the CRHR<sub>1</sub>-TMD thereby partially inhibiting transtressin. Astressin is particularly well-suited for the biomimetic screening approach: the twelve C-terminal amino acid residues of astressin correspond to the sequence of the peptide carrier **2**, thereby similar CRHR<sub>1</sub>-ECD1 affinities can be expected. Additionally, the five N-terminal amino acid residues of astressin (AST<sup>1-5</sup>) correspond to the fragment (11-15) of UCN; hence similar SARs can be expected for the screening of this fragment. Investigating the interactions between the N-terminus of astressin and the CRHR<sub>1</sub>-TMD may provide important details about the working mechanism of peptide antagonists; also the biomimetic screening approach may lead to the discovery of new CRHR<sub>1</sub> modulators. We thus engaged on a biomimetic screening of astressin analogs; briefly it consists of: 1) reconstitution of an AST biomimetic conjugate → proof of concept; 2) truncation study → characterization of a minimal CRHR<sub>1</sub>-TMD amino acid sequence; 3) positional MTS of a peptide conjugate library → SAR of the AST-minimized template.



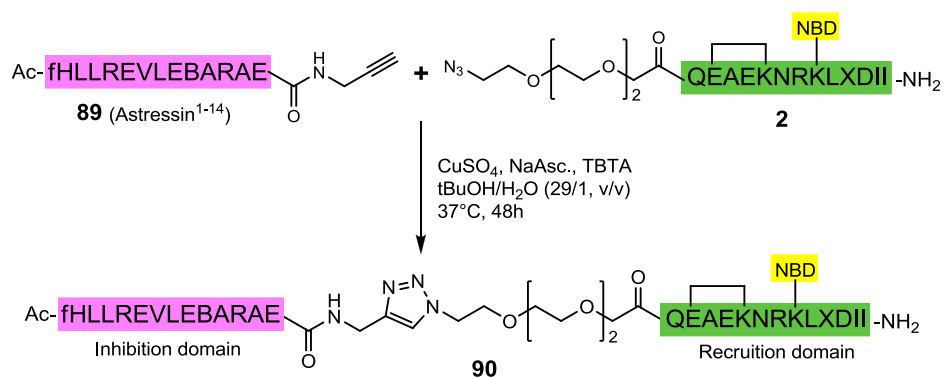
### 3.3.1 Evaluation of astressin conjugates: rationale and proof of concept

We first tested whether a “clicked” astressin analogue inhibit the CRHR<sub>1</sub> stimulation induced by transtressin, and thus reconstitute a peptide antagonist. A focus on the interaction between the peptide antagonist and the CRHR<sub>1</sub>-TMD was chosen. The use of the CRHR<sub>1</sub>-TMD specific peptide agonist transtressin in a competition setup may address efficiently this interaction. As a starting point, the N-terminal (1-14) fragment of astressin was used, assuming that this segment contains the amino acid sequence interacting with the CRHR<sub>1</sub>-TMD and which leads to a potential partial agonism.

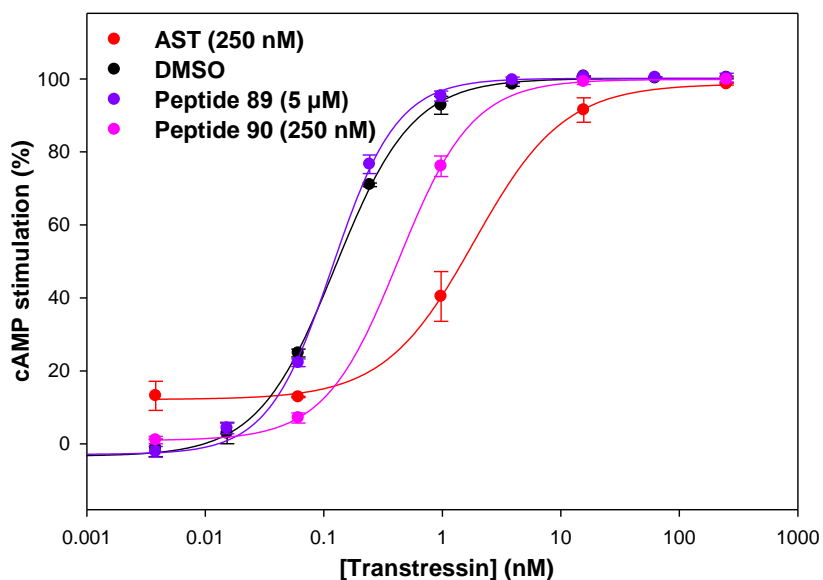
For this purpose, the N-terminal fragment peptide **89** was synthesized using the BAL strategy, and after HPLC purification, it was conjugated to the high-affinity peptide **2** by CuCAAC (Figure 37a). Gratifyingly, the AST<sup>1-14</sup> conjugate **90** precipitated out of solution, thus validating the centrifugation workup which was established for the UCN screening. The conjugate **90** was tested for CRHR<sub>1</sub> inhibition in a transtressin stimulated cell-based cAMP assay (Figure 37b). In this agonist dose-response assay setup, the cells were first incubated with a high concentration of antagonist, astressin itself being used as control; increasing concentrations of transtressin are then added and the resulting cAMP production is determined. Although this assay setup does not allow comparing potencies of antagonists between each other, it uses a “saturating” concentration of the peptide antagonist to determine whether the latter has any inhibitory effect.

The isolated peptide fragment **89** did not show any inhibitory activity at the CRHR<sub>1</sub> by itself in the cellular cAMP inhibition assay. The conjugation of peptide **89** with peptide carrier **2**, however, reconstituted a weak antagonist (Figure 37b and Table 14). Although, the efficacy of conjugate **90** in inhibiting transtressin was much weaker than AST at the same concentration, it produced a significant antagonistic effect thus proving that the fourteen AST N-terminal residues contain a template that interact with the CRHR<sub>1</sub>-TMD and compete with transtressin. The conjugation to the high-affinity carrier **2** consistently enhanced the detection limits for fragments such as peptide **89**. Hence, the CuCAAC conjugation of AST-derived peptide fragments reconstitutes a peptide antagonist, proving that the approach is suitable for investigating the astressin-CRHR<sub>1</sub>-TMD interface.

a)



b)



**Figure 37. Inhibition of transtressin-stimulated CRHR<sub>1</sub> by a peptide conjugate.** a) Synthesis of the inhibition segment **89** (pink) using BAL resin and “click” conjugation with membrane recruitment segment **2** (dark green). B = norleucine; f = D-phenylalanine. b) Inhibition of transtressin-induced cAMP production in HEK293 cells stably over-expressing CRHR<sub>1</sub> by peptide conjugate **90** and AST.

### 3.3.2 Astressin<sup>1-14</sup> truncations: characterization of a minimal inhibition sequence

Having proven that a “clicked” AST conjugate can act as an antagonist, we went on to determine the minimal N-terminal AST-derived peptide sequence necessary to inhibit the transtressin-induced CRHR<sub>1</sub> stimulation. Bidirectionally truncated derivatives of peptide **89** were synthesized using the BAL strategy. The purified truncated peptides were then coupled to peptide **2** by CuCAAC, isolated by centrifugation and further purified by HPLC. After fluorescence quantification, the truncated conjugates were tested for CRHR<sub>1</sub> inhibition in an agonist (transtressin) dose-response setup. The inhibition potencies of the conjugates were normalized to a maximal (astressin, 100 %) and a minimal inhibition (DMSO, 0 %). The C-terminal deletion of amino acid residues led first to a decrease and then to a substantial increase in inhibitory potency (Figure 38 and Table 14). The C-terminal deletion of Arg<sup>12</sup> led to the conjugate **93** for which the relative inhibitory efficacy reached 30% of that of astressin. Truncation beyond Ala<sup>11</sup>, however, completely abrogated the inhibitory potency of the conjugates. The AST<sup>1-5</sup> fragment corresponding to the five C-terminal amino acids of the UCN<sup>4-15</sup> “activation” template were also completely inactive for inhibition of the CRHR<sub>1</sub>, suggesting that additional ligand-receptor contacts are necessary for inhibiting transtressin. To confirm the importance of the N-terminal amino acid residues (and especially D-Phe<sup>1</sup>) for the interaction between astressin and the CRHR<sub>1</sub>-TMD, we also synthesized and tested N-terminally truncated AST<sup>1-11</sup> conjugates.

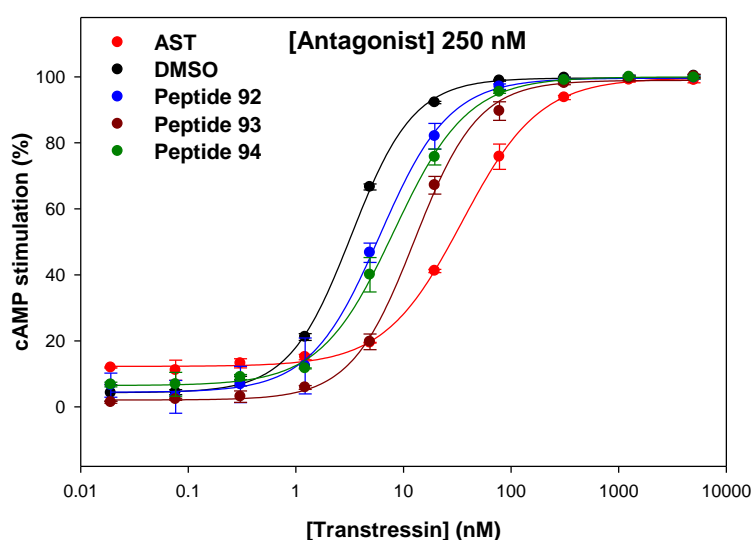
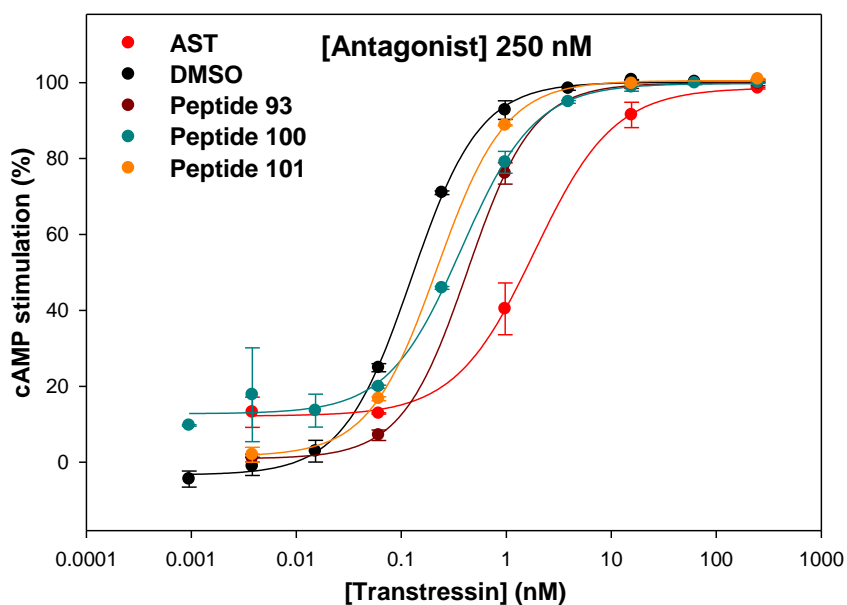


Figure 38. cAMP inhibition curves corresponding to C-terminally truncated AST<sup>1-14</sup> peptide conjugates listed in Table 14.

			Peptide sequence R = carrier	EC <sub>50</sub> [nM] <sup>(a)</sup> (s.e.m.)	Inhib. efficacy <sup>(b)</sup> (%)	
250 nM	●	DMSO	-	-	3.28±0.08	0
	●	AST	-	-	34.9±1.2	100
		90	Ac-AST <sup>(1-14)</sup>	Ac-fHLLREVLEBARAE-R	9.31±0.28	19
		91	Ac-AST <sup>(1-13)</sup>	Ac-fHLLREVLEBARA-R	7.56±0.29	15
	●	92	Ac-AST <sup>(1-12)</sup>	Ac-fHLLREVLEBAR-R	6.04±0.31	9
	●	93	Ac-AST <sup>(1-11)</sup>	Ac-fHLLREVLEBA-R	12.7±0.7	30
	●	94	Ac-AST <sup>(1-10)</sup>	Ac-fHLLREVLEB-R	8.16±0.38	15
		95	Ac-AST <sup>(1-9)</sup>	Ac-fHLLREVLE-R	5.31±0.08	6
		96	Ac-AST <sup>(1-8)</sup>	Ac-fHLLREVL-R	4.57±0.07	4
		97	Ac-AST <sup>(1-7)</sup>	Ac-fHLLREV-R	5.21±0.22	6
		98	Ac-AST <sup>(1-6)</sup>	Ac-fHLLRE-R	4.55±0.19	4
		99	Ac-AST <sup>(1-5)</sup>	Ac-fHLLR-R	5.13±0.11	6

**Table 14. Characterization of C-terminally truncated analogs of the AST<sup>1-14</sup> N-terminal fragment.**

<sup>(a)</sup> EC<sub>50</sub> of transtresin. <sup>(b)</sup> Inhibitory efficacy normalized to astressin (100 %) and DMSO (0 %).



**Figure 39. cAMP inhibition curves corresponding to the N-terminally truncated AST<sup>1-11</sup> peptide conjugates listed in Table 15.**

			Peptide sequence R = carrier	EC <sub>50</sub> [nM] <sup>(a)</sup> (s.e.m.)	Inhib. Efficacy <sup>(b)</sup> (%)	
250 nM	●	DMSO	-	-	0.124±0.004	0
	●	AST	-	-	1.85±0.18	100
	●	93	Ac-AST <sup>(1-11)</sup>	Ac-fHLLREVLEBA-R	0.427±0.001	18
	●	100	H <sub>2</sub> N-AST <sup>(1-11)</sup>	H <sub>2</sub> N-fHLLREVLEBA-R	0.374±0.034	15
	●	101	Ac-AST <sup>(2-11)</sup>	Ac-HLLREVLEBA-R	0.219±0.008	6

**Table 15. Characterization of N-terminally truncated analogs of the AST<sup>1-11</sup> N-terminal fragment.**

<sup>(a)</sup> EC<sub>50</sub> of transtressin. <sup>(b)</sup> Inhibitory efficacy normalized to astressin (100 %) and DMSO (0 %).

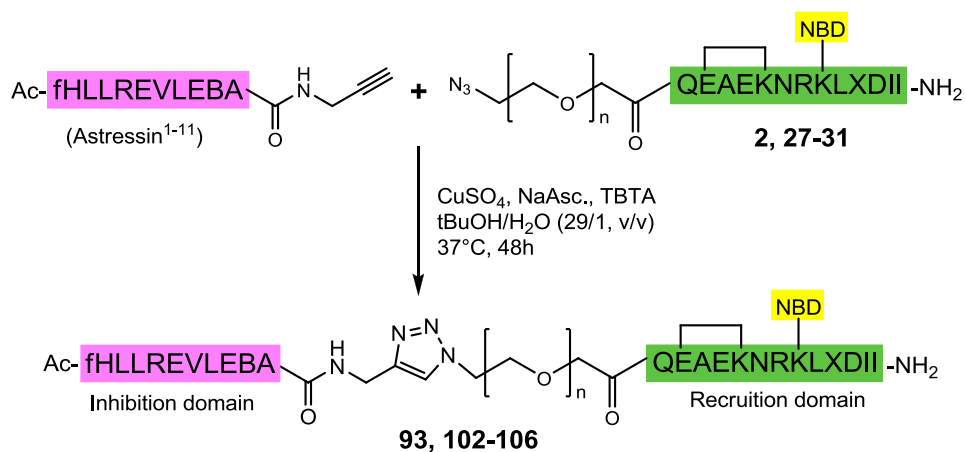
The inhibition efficacies for the conjugates were normalized between DMSO and astressin; however, the EC<sub>50</sub> values for transtressin in the presence of astressin and DMSO in Table 15 are substantially different compared to Table 14 because the reproducibility in inhibition assays is difficult to achieve. Removal of the N-terminal acetyl moiety of the AST<sup>1-11</sup> template resulted in a slight decrease in inhibitory efficacy; however the conjugate **100** retained a good inhibitory efficacy compared to **93**. Further truncation of the D-Phe<sup>1</sup> amino acid residue resulted in a complete loss of efficacy, thus confirming the crucial role of this N-terminal residue for the interaction between the N-terminus of astressin and the CRHR<sub>1</sub>-TMD. Importantly, for both C- and N-terminal truncated conjugates as well as astressin, the CRHR<sub>1</sub>-TMD specific peptide transtressin displaced completely the N-terminus of the antagonists and produced full CRHR<sub>1</sub> stimulation at higher concentrations. These data are fully consistent with a weakly TMD-interacting conjugate. Hereby, the bidirectional truncations established the 11 amino acid AST<sup>1-11</sup> sequence motif as a minimized fragment for the inhibition of the transtressin induced CRHR<sub>1</sub> stimulation.

### 3.3.3 Role of the Astressin<sup>1-11</sup> conjugate middle domain

In the previous UCN<sup>4-15</sup> biomimetic screening study, the TEG (n = 3) ethylene glycol appeared to offer the best compromise between flexibility and distance for the two ligand domains to bind the CRHR<sub>1</sub>. Hence, we decided to investigate if a similar mechanism could be observed using the minimized astressin-derived N-terminal fragment. The C-terminally propargylated AST<sup>1-11</sup> fragment was coupled to the peptide carriers which were N-terminally modified with azide-functionalized ethylene glycol spacers of various lengths (n = 0 to 5). The HPLC purified conjugates **93**, **102-106** were then tested in an inhibition assay. In order to directly compare the potencies of the conjugates

for CRHR<sub>1</sub> inhibition, an antagonist dose-response assay setup was used. HEK293 cells stably over-expressing the CRHR<sub>1</sub> were first incubated with increasing concentrations of the peptide antagonists (AST, **93** and **102-106** respectively). A fixed EC<sub>50</sub>-corresponding concentration of transtresin was then added and the resulting cAMP production was determined.

a)



b)

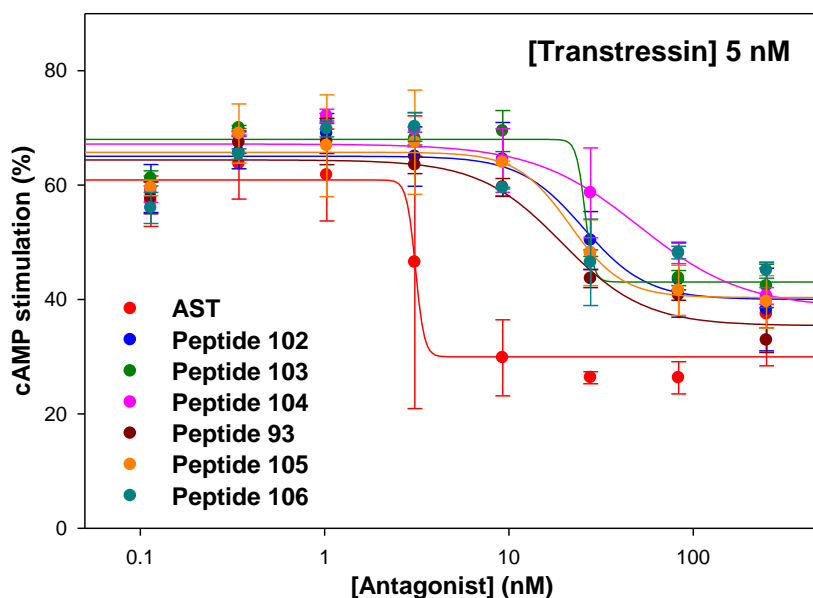


Figure 40. Inhibition of CRHR<sub>1</sub> by “clicked” AST<sup>1-11</sup> peptide conjugates listed in table 16.

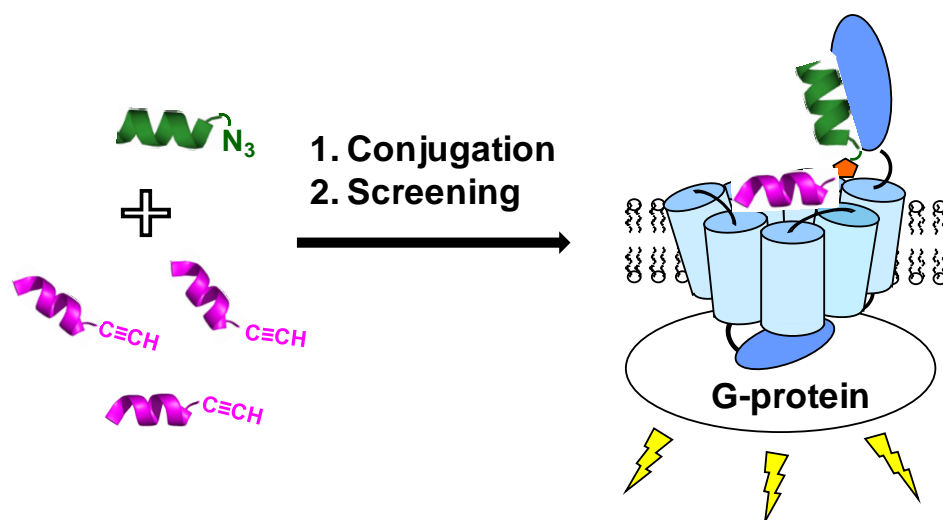
		N-term.	Peptide carrier n =	EC <sub>50</sub> [nM] (s.e.m.)	E <sub>min</sub> (%)
●	AST	-	-	3.11±82887	30
●	102	Ac-AST(1-11)	0	25.3±7.1	40
●	103	Ac-AST(1-11)	1	25.8±394133	43
●	104	Ac-AST(1-11)	2	50.8±39.6	38
●	93	Ac-AST(1-11)	3	19.4±7.6	35
●	105	Ac-AST(1-11)	4	21.4±5.9	40
●	106	Ac-AST(1-11)	5	-	-

**Table 16. Characterization of “clicked” AST<sup>1-11</sup> conjugates.**

The replacement of the middle portion of astressin by ethylene glycol spacers of various lengths reconstituted potent antagonists, thus confirming that the amino acid residues of the middle portion of AST are not important for the ligand-receptor interaction (Table 16). These results are consistent with our similar study on the UCN<sup>4-15</sup> fragment, indentifying the triethylene glycol spacer (n = 3) as offering the best compromise for the N-terminal AST<sup>1-11</sup> fragment to bind the CRHR<sub>1</sub>-TMD. In a lesser extent than for the peptide agonist conjugates, the proposed “three-step” CRHR<sub>1</sub> binding mechanism for peptide conjugates is still relevant: the peptide carrier **2** first binds the CRHR<sub>1</sub>-ECD1 with high-affinity. The AST<sup>1-11</sup> N-terminal portion of the conjugate then freely rotates around the ethylene glycol spacer and takes advantage of both spacer and receptor domains flexibilities to bind the CRHR<sub>1</sub>-TMD in an optimal orientation. Presumably, the AST<sup>1-11</sup> fragment binds to the same orthosteric site than transtressin within J-domain and thus hinders the latter to bind its orthosteric site and trigger G protein signaling. Thereby, the triethylene glycol spacer (n = 3) of conjugate **93** showed the highest inhibitory potency and was used systematically in the following study.

### 3.3.4 Astressin<sup>1-11</sup> stimulation biomimetic screening

The use of CuCAAC “clicked” conjugates allowed us to characterize the 11 amino acid minimal template required for the CRHR<sub>1</sub>-TMD interaction. Since astressin is also a weak partial agonist, we evaluated the AST<sup>1-11</sup> template for CRHR<sub>1</sub> stimulation. We went on to determine the contribution of individual residues to CRHR<sub>1</sub> stimulation in more details using a MTS with AST<sup>1-11</sup> peptide conjugates (Figure 41).



**Figure 41. Biomimetic screening strategy for the investigation of the CRHR<sub>1</sub>-astressin stimulation.**

A library of alkyne-tagged AST<sup>1-11</sup> peptide fragments (pink) is conjugated to a constant peptide fragment (dark green) that has high-affinity for the CRHR<sub>1</sub>-ECD1. These conjugates are probed for modulation of the GPCR transmembrane domain.

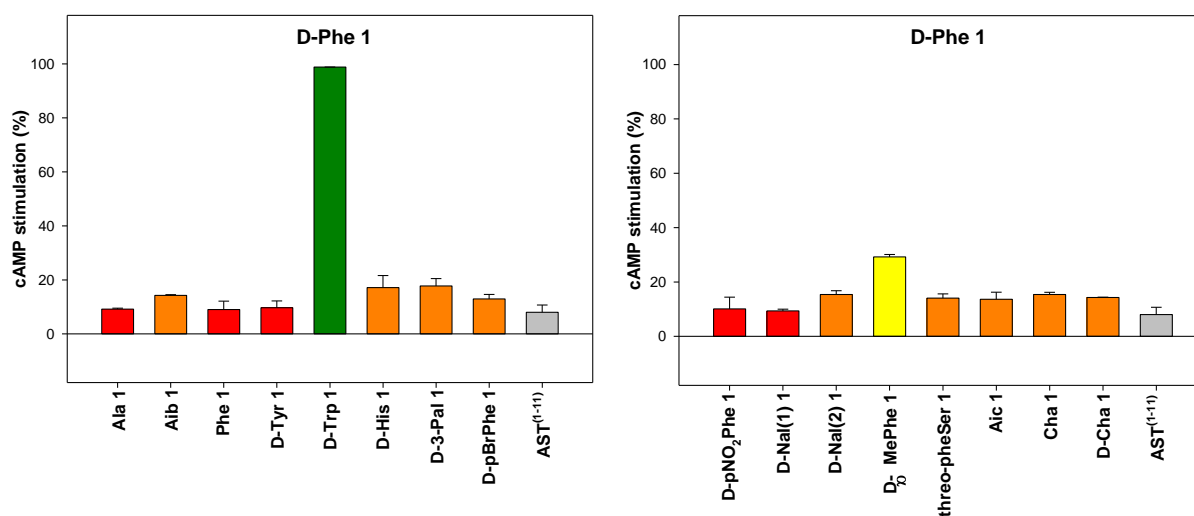
Based on the previously characterized minimal activation template AST<sup>1-11</sup>, a library of 96 C-terminally propargylated peptidic fragments containing a series of single amino acid substitutions was synthesized (Table 17). Each position of the AST<sup>1-11</sup> peptide sequence was systematically changed to alanine, Aib, the corresponding enantiomeric amino acid, as well as structurally related natural and unnatural amino acids. A particular focus was given on the SAR of the N-terminal D-Phe<sup>1</sup> residue. After cleavage from the solid support, the C-terminally propargylated AST<sup>1-11</sup> peptides were analyzed by HPLC and mass spectrometry (data not shown). Gratifyingly, the first estimation of quality revealed that most of the propargylated AST<sup>1-11</sup> peptides presented crude purities above 80%. (89 out of 96, table 28) The purity of the crude propargylated library is the bottleneck of the conjugation approach, because the crude purities are subsequently transferred to the conjugates. The crude C-terminally propargylated AST<sup>1-11</sup> peptides were then coupled to the peptide carrier **2** and isolated by precipitation as previously described. Similarly to the UCN<sup>4-15</sup> screening, the easy isolation of the crude conjugates by simple centrifugation was a crucial feature of the conjugation

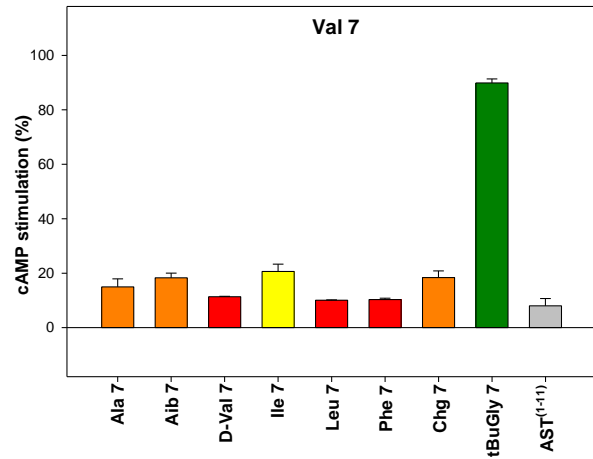
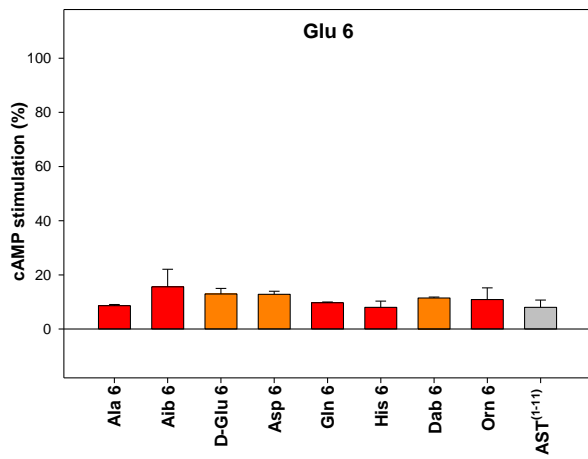
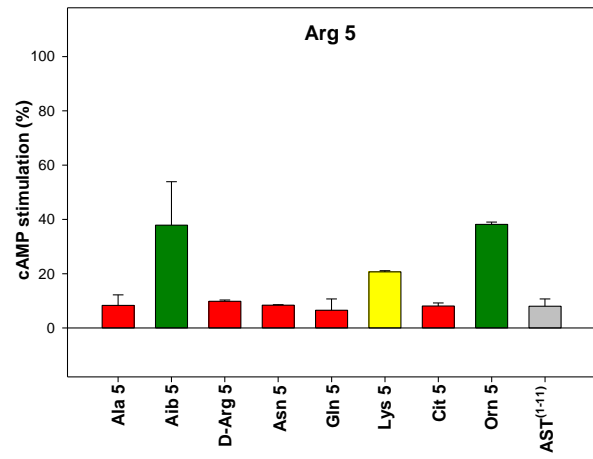
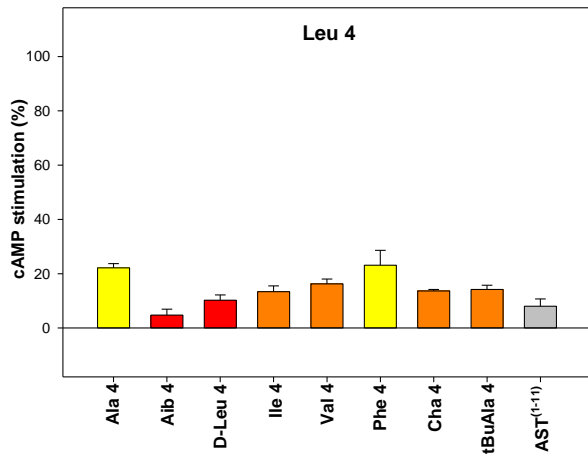
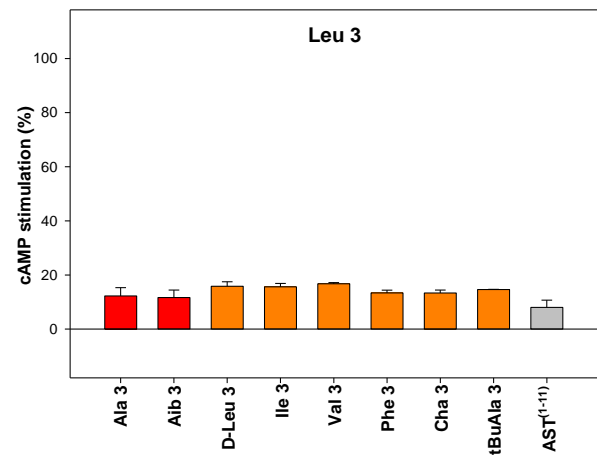
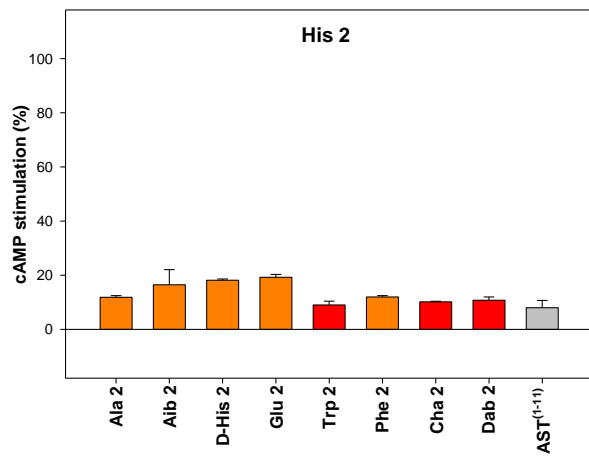


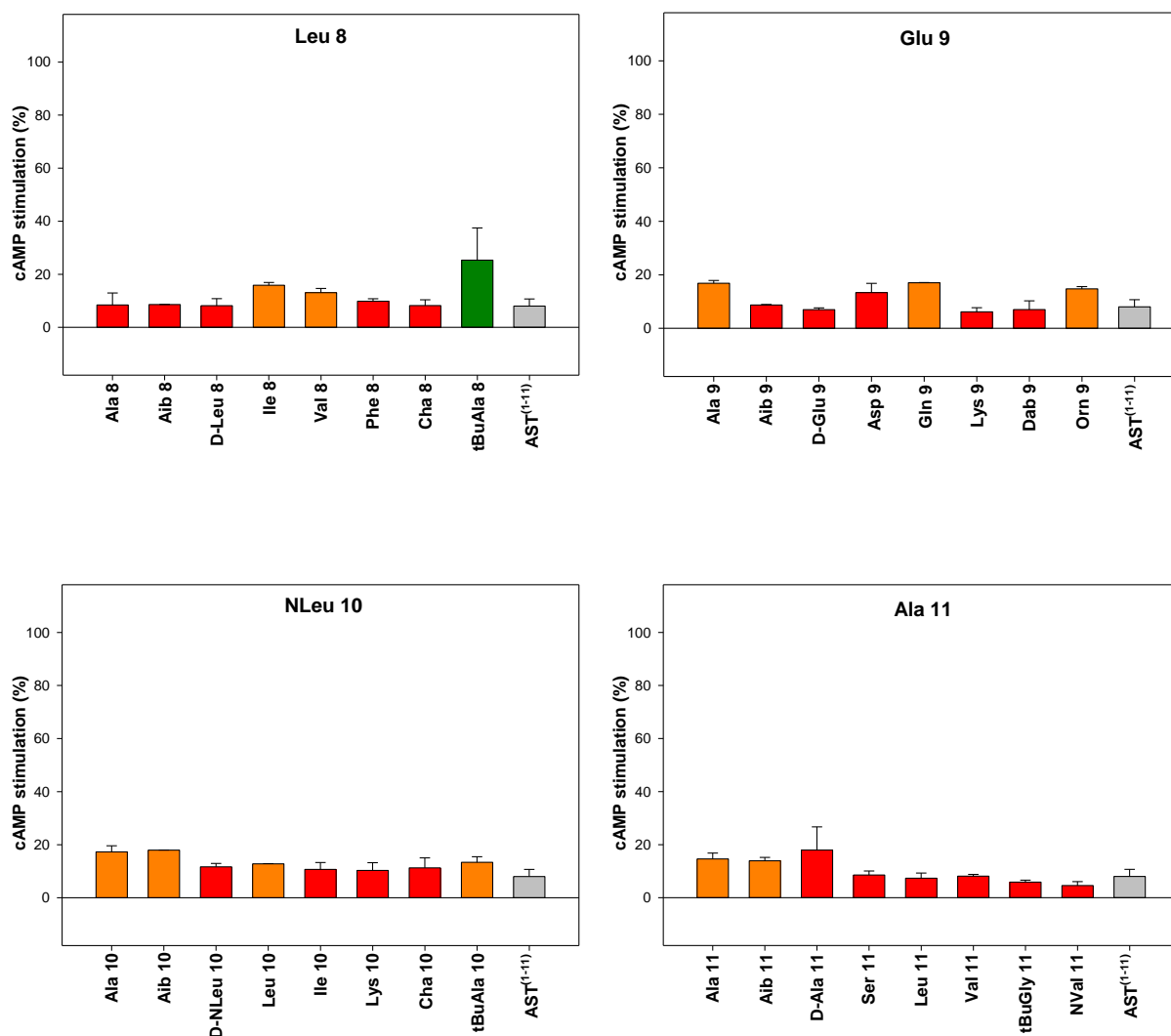
methodology. We decided to first test the activity of the single-substituted AST<sup>1-11</sup> conjugates as such in a cAMP stimulation assay at 250 nM (Figure 42 and Table 17).

D-Phe <sup>1</sup>	D-Phe <sup>1</sup>	His <sup>2</sup>	Leu <sup>3</sup>	Leu <sup>4</sup>	Arg <sup>5</sup>	Glu <sup>6</sup>	Val <sup>7</sup>	Leu <sup>8</sup>	Glu <sup>9</sup>	NLeu <sup>10</sup>	Ala <sup>11</sup>
Ala	D-pNO <sub>2</sub> -Phe	Ala	Ala	Ala	Ala	Ala	Ala	Ala	Ala	Ala	Ala
Aib	D-Nal(1)	Aib	Aib	Aib	Aib	Aib	Aib	Aib	Aib	Aib	Aib
Phe	D-Nal(2)	D-His	D-Leu	D-Leu	D-Arg	D-Glu	D-Val	D-Leu	D-Glu	D-NLeu	D-Ala
D-Tyr	D-αMe-Phe	Glu	Ile	Ile	Asn	Asp	Ile	Ile	Asp	Leu	Ser
D-Trp	Th-pheSer	Trp	Val	Val	Gln	Gln	Leu	Val	Gln	Ile	Leu
D-His	Aic	Phe	Phe	Phe	Lys	His	Phe	Phe	Lys	Lys	Val
D-3-Pal	Cha	Cha	Cha	Cha	Cit	Dab	Chg	Cha	Dab	Cha	tBuGly
D-pBr-Phe	D-Cha	Dab	tBuAla	tBuAla	Orn	Orn	tBuGly	tBuAla	Orn	tBuAla	NVal

**Table 17. Summary of CRHR<sub>1</sub> stimulation by single-point substituted AST<sup>1-11</sup> conjugates.** Crude N-terminally acetylated peptide-peptide conjugates carrying the indicated amino acid modification were assayed at 250 nM for cAMP stimulation of HEK293 cells stably overexpressing CRHR<sub>1</sub>. Sequences with no stimulatory activity are indicated in red, minimal activity is indicated in orange (10 – 20 %), substantial activity is indicated in yellow (20 – 30 %) and significant activity is indicated in green (> 30 %). Aic = 2-aminoindane-2-carboxylic acid; Nal(1) = 1-naphtylalanine; Nal(2) = 2-naphtylalanine; NLeu = norleucine; NVal = norvaline; 3-Pal = 3-pyridylalanine; pBr-Phe = para-bromo phenylalanine; pNO<sub>2</sub>-Phe = para-nitro phenylalanine; Th-pheSer = threo-β-phenylserine.







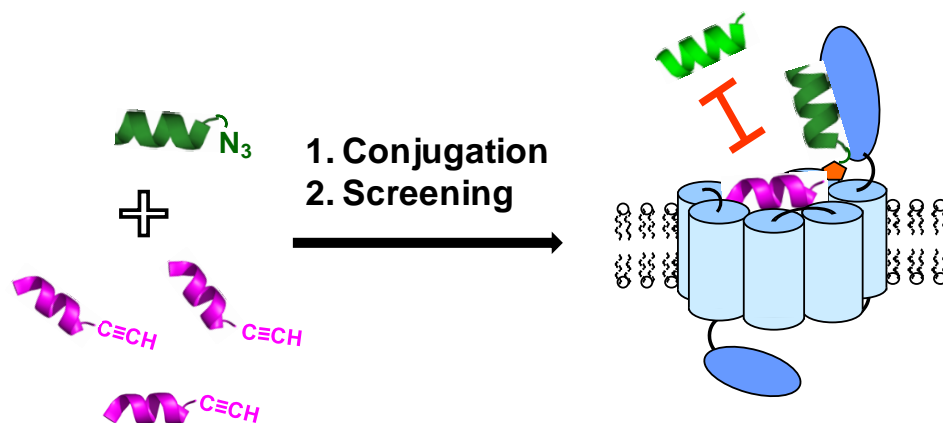
**Figure 42. Positional stimulatory MTS of a crude AST<sup>1-11</sup> peptide conjugate library at 250nM.** Inactive sequences are indicated in red, minimal stimulatory activity is indicated in orange, substantial activity is indicated in yellow and significant activity compared to the original AST<sup>1-11</sup> conjugate **93** is indicated in green.

The biomimetic screening of the AST<sup>1-11</sup> peptide conjugate library resulted in 86 conjugates where the stimulatory activity was very low and not significantly different compared to the AST<sup>1-11</sup> sequence (red and orange, < 20 %). For five of these peptide conjugates, the CRHR<sub>1</sub> stimulatory activity was found to be slightly improved (yellow, 20 – 30 %) and for five others it was greatly enhanced (green, > 30 %). Surprisingly, for two of these conjugates, CRHR<sub>1</sub> full activation was observed (D-Phe<sup>1</sup>D-Trp and Val<sup>7</sup>tBuGly). Several D-Phe<sup>1</sup> amino acid substitutions enhanced weakly the potency of the AST<sup>1-11</sup> conjugate; in particular the D-Phe<sup>1</sup>D-His, D-Phe<sup>1</sup>D-Pal and D-Phe<sup>1</sup>D- $\alpha$ MePhe substitutions showed substantially increased potencies, presumably due to their

close structural resemblance to D-Phe. The D-Phe<sup>1</sup>D-Trp substitution afforded a surprisingly potent conjugate and reconstituted a full agonist at 250 nM. Several other positions were found to be positively sensitive to amino acid substitutions, in particular Leu<sup>4</sup>, Arg<sup>5</sup>, Val<sup>7</sup> and Leu<sup>8</sup>. The Arg<sup>5</sup>Aib and Arg<sup>5</sup>Orn substitutions greatly improved the potency of the conjugates. Consistently with the UCN<sup>4-15</sup> screening, replacement of Val<sup>7</sup> and Leu<sup>8</sup> residues by similar aliphatic residues such tBuGly and tBuAla respectively provided conjugates with improved stimulatory activity. Noteworthy, the latter concentration applied to the cells in this assay being extremely high, these results have to be taken with care and the potency of such ligands should be further assessed with dose-response stimulation curves.

### 3.3.5 Astressin<sup>1-11</sup> inhibition biomimetic screening

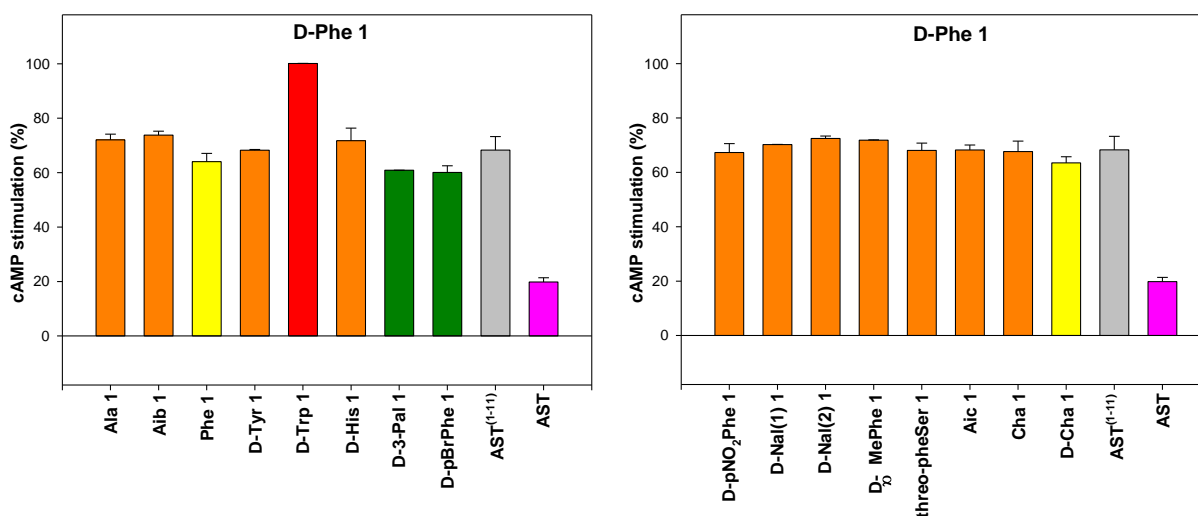
Having investigated the potential CRHR<sub>1</sub> stimulatory activity of the AST<sup>1-11</sup> conjugates, we went on to assess the ability of these conjugates to inhibit the CRHR<sub>1</sub> stimulation induced by the CRHR<sub>1</sub>-TMD specific peptide transtressin (Figure 43). For this single-point inhibition assay, HEK293 cells over-expressing the CRHR<sub>1</sub> were first incubated with 250 nM of the AST<sup>1-11</sup> conjugates; an EC<sub>50</sub>-corresponding concentration of transtressin (5 nM) was then added and the resulting cAMP production was determined.

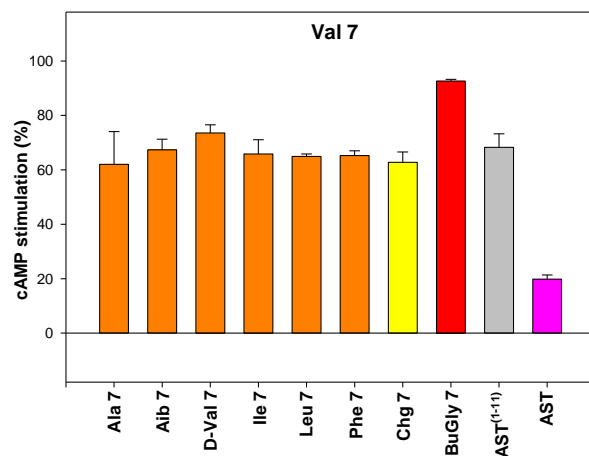
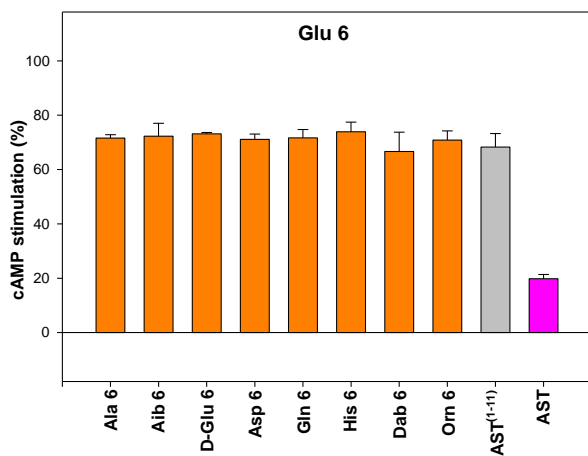
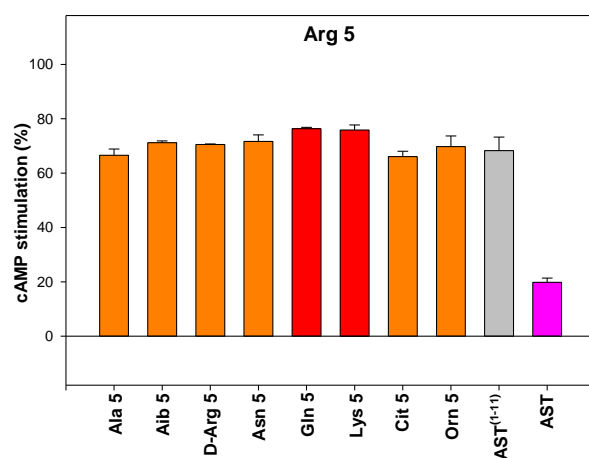
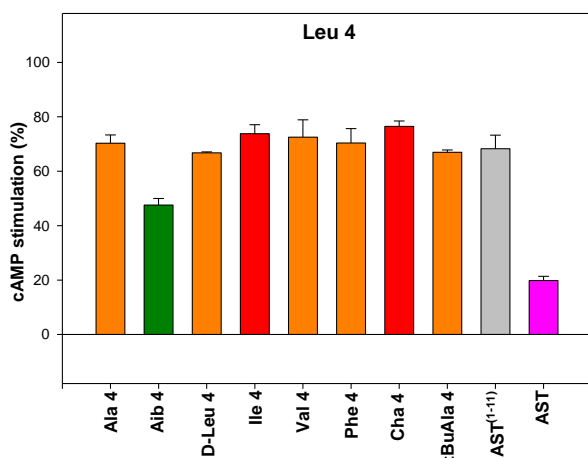
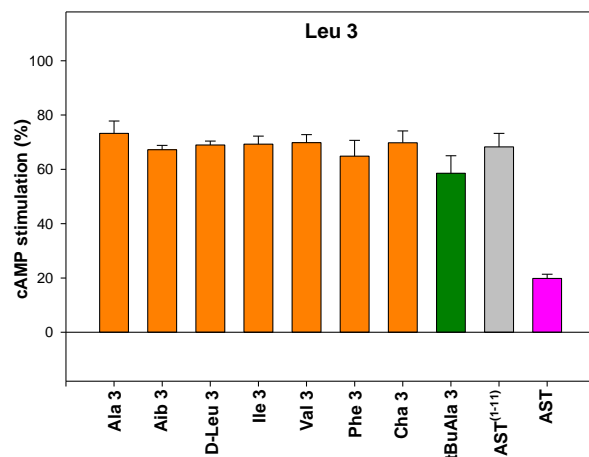
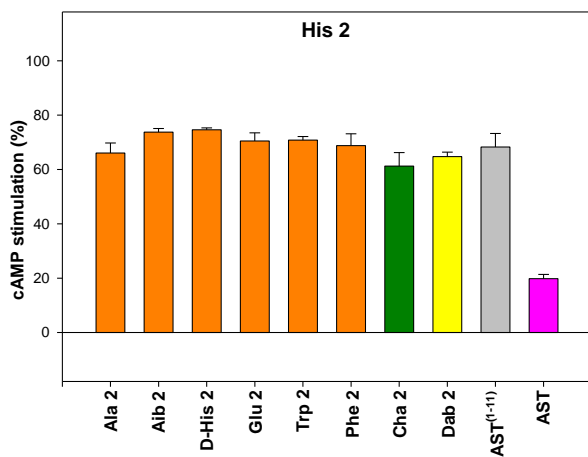


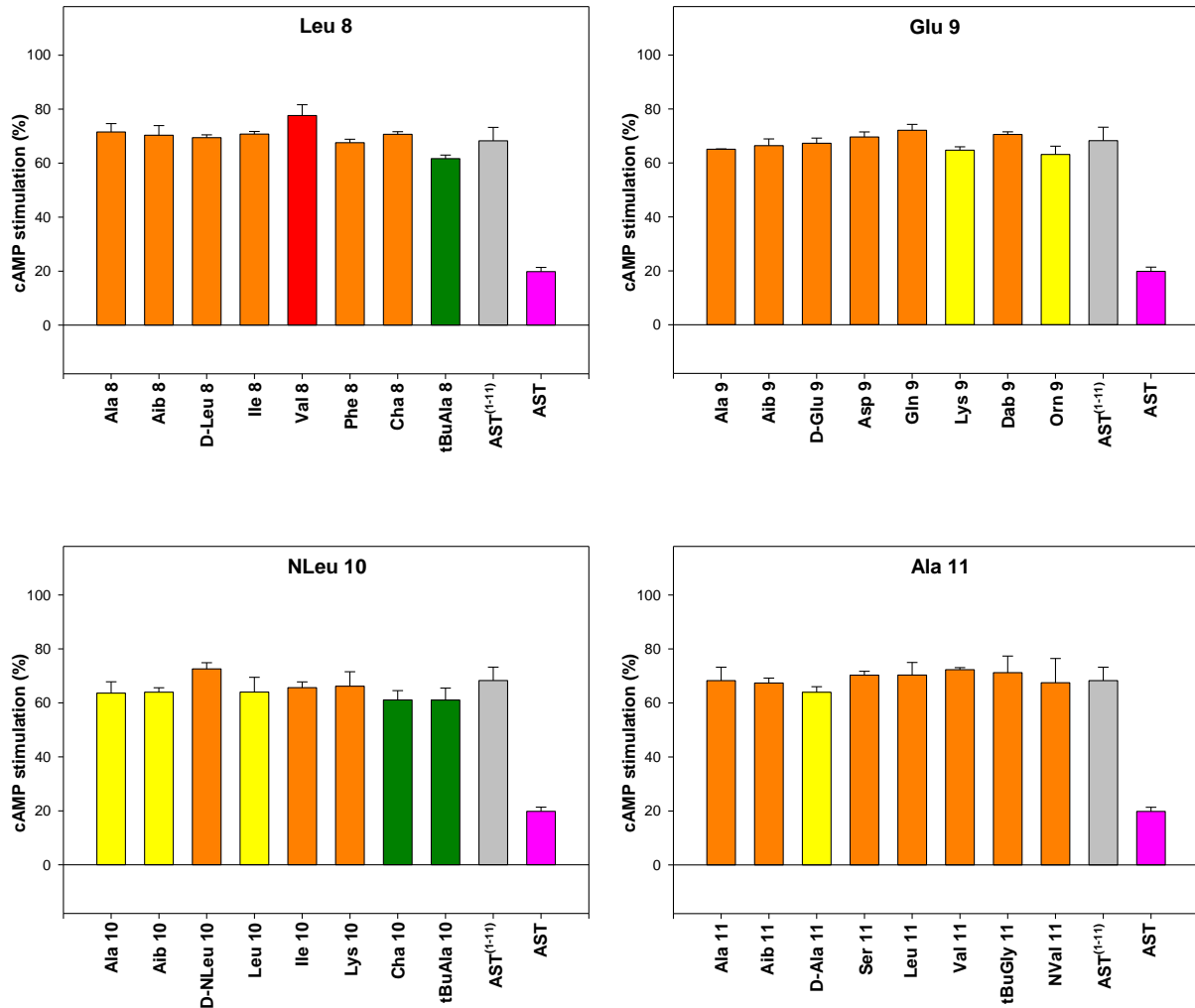
**Figure 43. Biomimetic screening strategy for the investigation of the CRHR<sub>1</sub>-astressin analog inhibition.** A library of alkyne-tagged AST<sup>1-11</sup> peptide fragments (pink) is conjugated to a constant peptide fragment (dark green) that has high-affinity for the CRHR<sub>1</sub>-ECD1. These conjugates are probed for inhibition of the CRHR<sub>1</sub>-TMD specific transtressin-induced CRHR<sub>1</sub> stimulation.

D-Phe <sup>1</sup>	D-Phe <sup>1</sup>	His <sup>2</sup>	Leu <sup>3</sup>	Leu <sup>4</sup>	Arg <sup>5</sup>	Glu <sup>6</sup>	Val <sup>7</sup>	Leu <sup>8</sup>	Glu <sup>9</sup>	NLeu <sup>10</sup>	Ala <sup>11</sup>
Ala	D-pNO <sub>2</sub> -Phe	Ala	Ala	Ala	Ala	Ala	Ala	Ala	Ala	Ala	Ala
Aib	D-Nal(1)	Aib	Aib	Aib	Aib	Aib	Aib	Aib	Aib	Aib	Aib
Phe	D-Nal(2)	D-His	D-Leu	D-Leu	D-Arg	D-Glu	D-Val	D-Leu	D-Glu	D-NLeu	D-Ala
D-Tyr	D-αMe-Phe	Glu	Ile	Ile	Asn	Asp	Ile	Ile	Asp	Leu	Ser
D-Trp	Th-pheSer	Trp	Val	Val	Gln	Gln	Leu	Val	Gln	Ile	Leu
D-His	Aic	Phe	Phe	Phe	Lys	His	Phe	Phe	Lys	Lys	Val
D-3-Pal	Cha	Cha	Cha	Cha	Cit	Dab	Chg	Cha	Dab	Cha	tBuGly
D-pBr-Phe	D-Cha	Dab	tBuAla	tBuAla	Orn	Orn	tBuGly	tBuAla	Orn	tBuAla	NVal

**Table 18. Inhibition summary of transtresstin-stimulated CRHR<sub>1</sub> by single-point substituted AST<sup>1-11</sup> conjugates.** Crude peptide-peptide conjugates carrying the indicated amino acid modification were assayed at 250 nM for cAMP inhibition of HEK293 cells stably overexpressing CRHR<sub>1</sub> stimulated by 5 nM of transtresstin. Sequences with additional stimulatory activity are indicated in red (> 75 %), equal activity compared to the purified AST<sup>1-11</sup> conjugate **93** are indicated in orange (65 – 75 %), substantial enhanced inhibition is indicated in yellow (60 – 65 %) and significant enhanced inhibition is indicated in green (< 60 %).







**Figure 44. Positional inhibitory MTS of a crude AST<sup>1-11</sup> peptide conjugate library.** Sequences with stimulatory activity are indicated in red, equal activity compared to the purified AST<sup>1-11</sup> conjugate **93** are indicated in orange, substantial enhanced inhibition is indicated in yellow and significant enhanced inhibition is indicated in green.

The inhibitory biomimetic screening of the AST<sup>1-11</sup> peptide conjugate library resulted in 71 conjugates where the inhibitory activity for CRHR<sub>1</sub> was not significantly different compared to the native sequence of the purified AST<sup>1-11</sup> conjugate **93** (orange, 65 – 75 %, Figure 44 and Table 18). For ten of the conjugates, the inhibitory efficacy was slightly increased (yellow) and for eight others, the CRHR<sub>1</sub> inhibition was significantly improved (green, < 60 %). Eight of the conjugates showed an additive stimulatory effect to that of transtresin (red, > 75 %). The effects of the conjugates using the inhibition competition assay setup are very low compared to the agonist screening assays performed before; this is mostly due to the limited detection range imposed by the intrinsic low affinity of the AST<sup>1-11</sup> sequence for the CRHR<sub>1</sub>-TMD. The full length astressin itself was used as control and effectively inhibited the transtresin induced CRHR<sub>1</sub> stimulation at 250 nM (pink). The

differences in inhibitory potency observed between full length astressin and the AST<sup>1-11</sup> conjugate **93** suggests that amino acid residues in the middle portion play a significant role for the N-terminus to bind efficiently to the CRHR<sub>1</sub>-TMD. As previously discussed, the middle segment of CRHR<sub>1</sub> peptide ligands might not only define the orientation of the N-terminus segment by conformational constrain, but it might also provide additional ligand-receptor interactions underlining the “low resolution” of the two-domain model. Although the inhibitory effects induced by the AST<sup>1-11</sup> conjugates were weak, the analysis of the activities for the single amino acid substitution AST<sup>1-11</sup> analogs allows several conclusions about the SAR of CRHR<sub>1</sub> peptide antagonists.

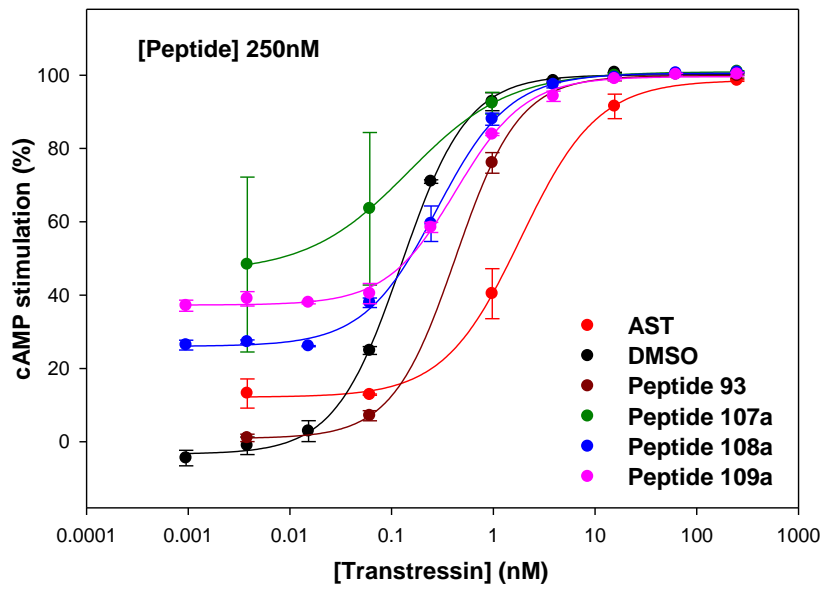
Replacement of the D-Phe<sup>1</sup> residue by several amino acid residues led to enhancement of the inhibitory activity (e.g., D-Phe<sup>1</sup>D-Pal, D-Phe<sup>1</sup>D-pBrPhe and D-Phe<sup>1</sup>D-Cha), suggesting that the side chain of this N-terminal residue interacts directly with the CRHR<sub>1</sub>-TMD. The replacement of Leu<sup>3,8</sup> and NLeu<sup>10</sup> residues by unnatural aliphatic amino acids such as Cha and tBuAla provided conjugates with enhanced inhibition. These results are in line with the SAR screening of the UCN<sup>4-15</sup> “activation” template, indicating that fine-tuning of the hydrophobic interactions in the AST<sup>1-11</sup> motif may also lead to ligands with optimized affinity for the CRHR<sub>1</sub>-TMD. The Leu<sup>4</sup>Aib substitution also afforded a conjugate with enhanced inhibition compared to **93**. Importantly, the conjugates showing the greatest stimulatory activity (e.g., D-Phe<sup>1</sup>D-Trp and Val<sup>7</sup>tBuGly) in the cAMP stimulation screening were also found to potently activate CRHR<sub>1</sub> using the inhibition setup. The biomimetic screening of an antagonistic sequence such as AST<sup>1-11</sup> is more challenging compared to UCN<sup>4-15</sup>. The intrinsic low potency of the native sequence limits the assay output limited. In this case, the results obtained with both setups complement each other quite well and allowed us to identify amino acid substitutions having a modulating effect for the stimulation and for the inhibition of CRHR<sub>1</sub>.

### 3.3.6 Evaluation of multisubstituted Astressin<sup>1-11</sup> biomimetic probes

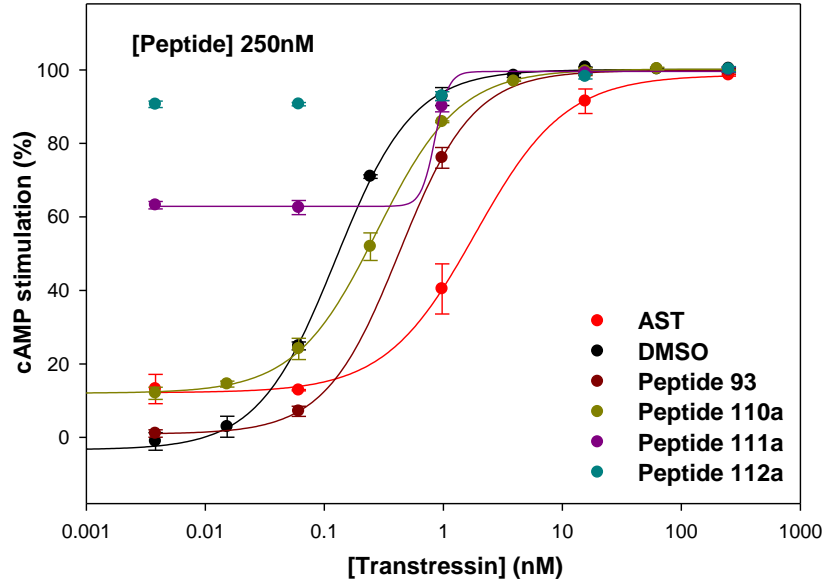
The next step was to investigate whether the effects of the single substitutions identified in the AST<sup>1-11</sup> positional screenings were additive. For this purpose, a library of C-terminally propargylated UCN<sup>4-15</sup> peptides bearing multiple substitutions was synthesized. The focus was given on amino acid substitutions having enhancing inhibitory effects (Table 18; e.g., His<sup>2</sup>Cha, Leu<sup>3</sup>tBuAla, Leu<sup>4</sup>Aib, Leu<sup>8</sup>tBuAla, NLeu<sup>10</sup>Cha and NLeu<sup>10</sup>tBuAla). Although most of these substitutions showed weak effects for inhibiting transtressin, we expected to find optimized antagonistic sequences thanks to the cumulative effects of each substitution. In addition, each multisubstituted AST<sup>1-11</sup> peptide was synthesized either N-terminally acetylated or let as a free amine, thus addressing the role of the N-terminal acetylation for the efficacy. The multisubstituted AST<sup>1-11</sup> conjugates were tested using a transtressin dose-response inhibition assay setup (Figures 45, 46 and Table 19).



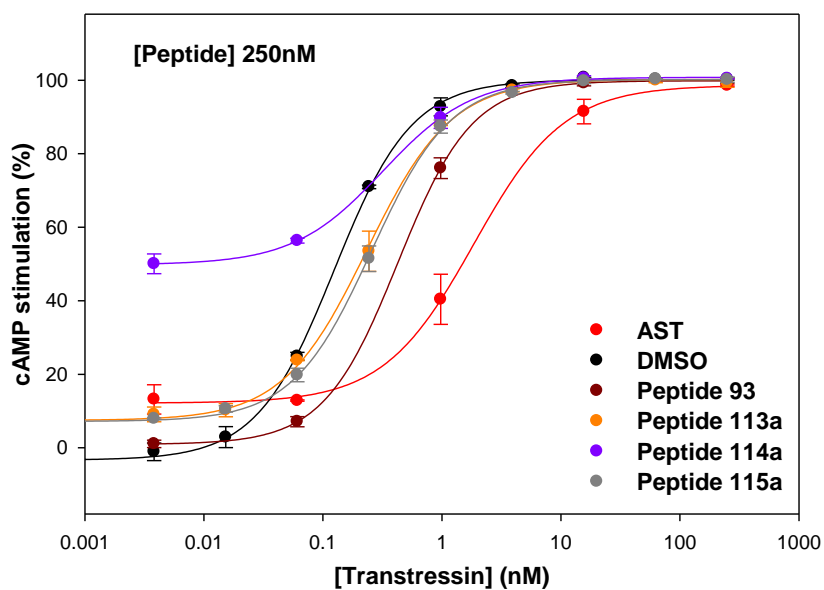
a)



b)

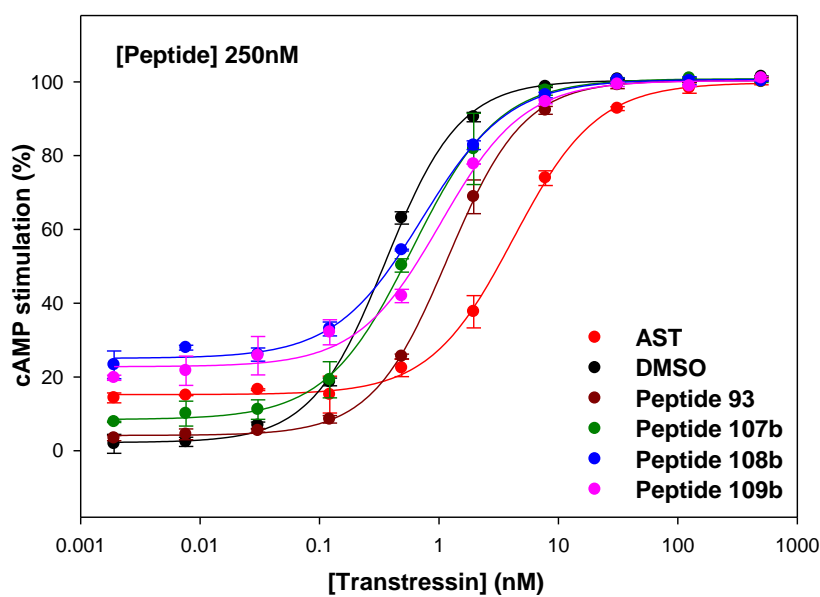


c)

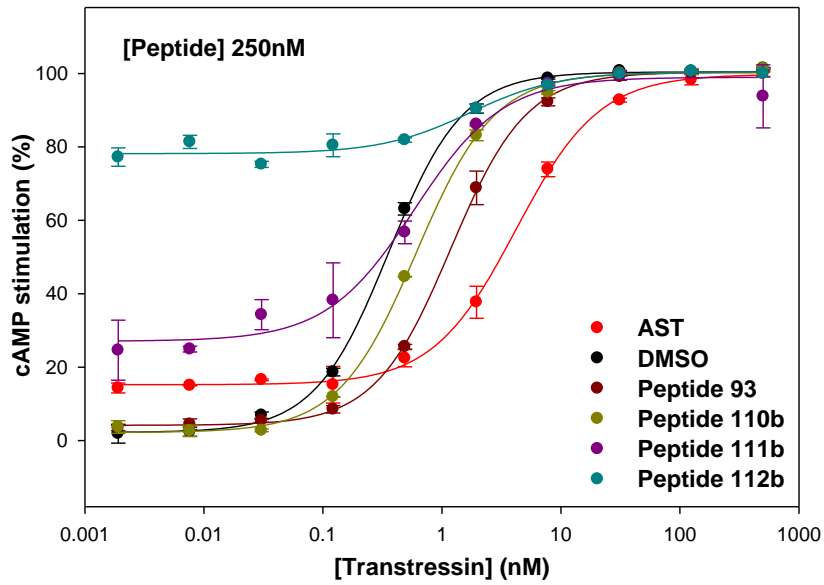


**Figure 45. Inhibition of CRHR<sub>1</sub> by N-terminally free AST<sup>1-11</sup> peptide conjugates listed in table 19.** HEK293 cells over-expressing the CRHR<sub>1</sub> were incubated with 250 nM of the AST<sup>1-11</sup> conjugates bearing multiple amino acids substitutions, increasing concentrations of the CRHR<sub>1</sub>-TMD specific peptide transtresin were then added and the cAMP production determined.

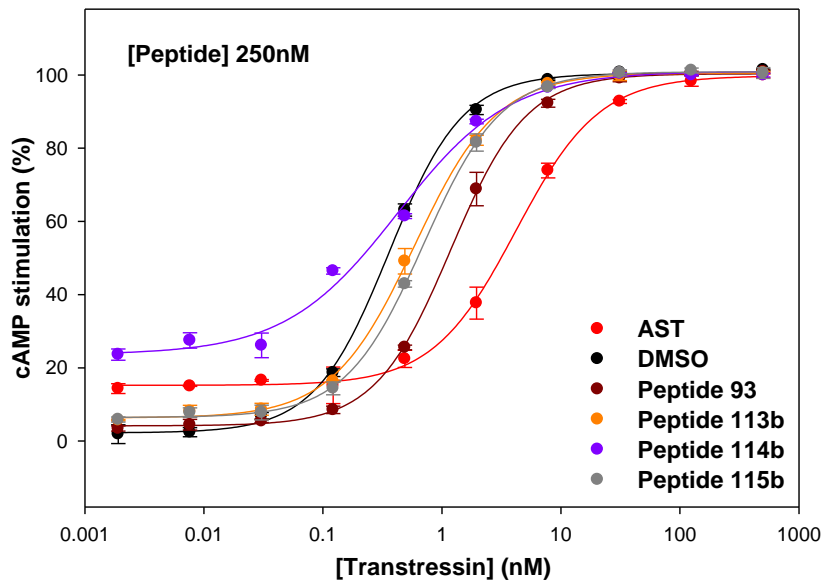
a)



b)



c)



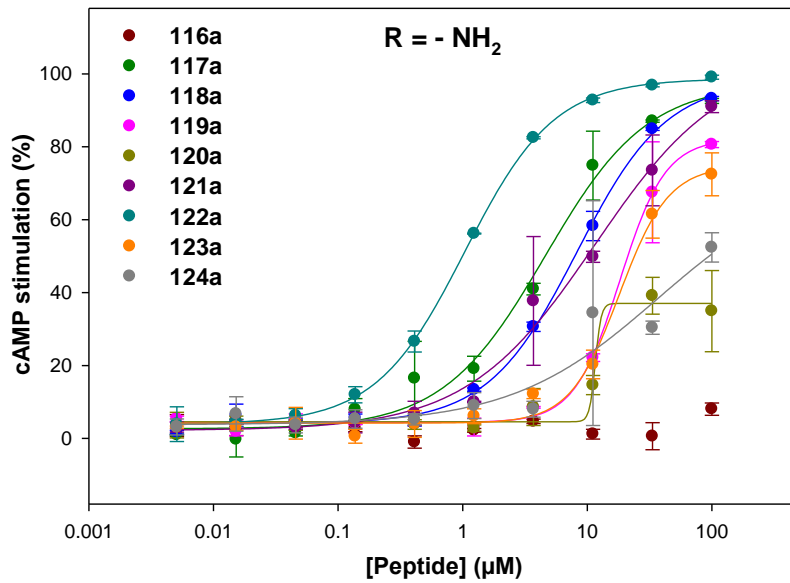
**Figure 46. Inhibition of CRHR<sub>1</sub> by N-terminally acetylated AST<sup>1-11</sup> peptide conjugates listed in table 19.** HEK293 cells over-expressing the CRHR<sub>1</sub> were incubated with 250 nM of the AST<sup>1-11</sup> conjugates bearing multiple amino acids substitutions, increasing concentrations of the CRHR<sub>1</sub>-TMD specific peptide transtresin were then added and the cAMP production determined.

			C-term. = carrier 2					
			R = -NH <sub>2</sub> <sup>(a)</sup>			R = -Ac <sup>(b)</sup>		
			Subst.	EC <sub>50</sub> (nM) <sup>(c)</sup>	E <sub>min</sub> (%)	EC <sub>50</sub> (nM) <sup>(c)</sup>	E <sub>min</sub> (%)	
250nM	●	DMSO	-	-	0.124±0.004	-3.4	0.358±0.014	2.2
	●	AST	-	-	1.85±0.18	12.2	4.19±0.20	15.2
	●	93	AST <sup>1-11</sup>	0	0.427±0.001	0.9	1.19±0.03	4.2
	●	107	R-[Cha <sup>2</sup> tBuAla <sup>3</sup> ]AST <sup>1-11</sup>	2	0.146±0.003	46.2	0.595±0.023	8.5
	●	108	R-[Cha <sup>2</sup> Aib <sup>4</sup> ]AST <sup>1-11</sup>	2	0.277±0.016	26.1	0.721±0.043	25.1
	●	109	R-[tBuAla <sup>3</sup> Aib <sup>4</sup> ]AST <sup>1-11</sup>	2	0.427±0.029	37.3	1.03±0.12	22.8
	●	110	R-[Cha <sup>2</sup> tBuAla <sup>3</sup> Aib <sup>4</sup> ]AST <sup>1-11</sup>	3	0.278±0.005	12.0	0.609±0.025	2.2
	●	111	R-[Cha <sup>2</sup> Aib <sup>4</sup> tBuAla <sup>8</sup> ]AST <sup>1-11</sup>	3	0.180±0.128	62.9	0.589±0.102	27.1
	●	112	R-[D-Pal <sup>1</sup> Cha <sup>2</sup> tBuAla <sup>3</sup> Aib <sup>4</sup> ]AST <sup>1-11</sup>	4	n.d.	>80	1.72±0.51	78.2
	●	113	R-[Cha <sup>2</sup> tBuAla <sup>3,8</sup> Aib <sup>4</sup> ]AST <sup>1-11</sup>	4	0.235±0.011	7.4	0.590±0.023	6.3
	●	114	R-[D-pBrPhe <sup>1</sup> Cha <sup>2,10</sup> Aib <sup>4</sup> tBuAla <sup>8</sup> ]AST <sup>1-11</sup>	5	0.320±0.018	49.8	0.426±0.068	23.6
	●	115	R-[Cha <sup>2,10</sup> tBuAla <sup>3,8</sup> Aib <sup>4</sup> ]AST <sup>1-11</sup>	5	0.257±0.009	7.2	0.700±0.015	6.5

**Table 19. Inhibition of CRHR<sub>1</sub> by purified AST<sup>1-11</sup> multisubstituted peptide conjugates in a stable CRHR<sub>1</sub> overexpressing cell line.** <sup>(a)</sup> N-terminally “free amine” conjugates. <sup>(b)</sup> N-terminally acetylated conjugates. <sup>(c)</sup> EC<sub>50</sub> of transtresstin.

Astressin and the AST<sup>1-11</sup> conjugate **93** inhibited transtresstin; however none of the multisubstituted conjugates showed improved inhibitory efficacies. Surprisingly, several multisubstituted conjugates showed substantial stimulatory effects as indicated by the *E<sub>min</sub>* values obtained in the competition assay (Figure 45, 46 and Table 19). Overall, the N-terminally acetylated conjugates produced weaker stimulations to the N-terminally “free” ones. The conjugates **112a** and **112b** were the most potent at 250 nM, suggesting that the D-Phe<sup>1</sup>D-Pal substitution greatly contribute to CRHR<sub>1</sub> stimulation (compare **112a/b** with **110a/b**). Interestingly, this substitution alone did not further improve the potency of conjugates in the UCN<sup>4-15</sup> context (Table 13). The *E<sub>min</sub>* values for other conjugates suggested partial agonism at 250 nM (e.g., **107a**, **111a**, **114a** and **108b**). Although the expected enhanced CRHR<sub>1</sub> inhibition was not observed, it seems that combining the amino acid substitutions identified in the positional screening greatly improve the stimulatory potency of the AST<sup>1-11</sup> template. Encouraged by these results, we decided to test the multisubstituted C-terminally propargylated AST<sup>1-11</sup> peptides directly for CRHR<sub>1</sub> stimulation (Figure 47 and Table 20).

a)



b)

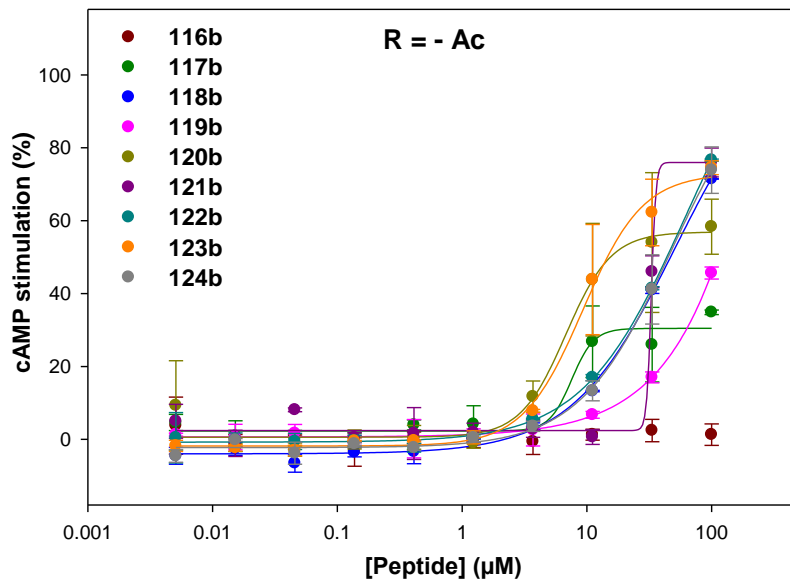


Figure 47. Stimulation of CRHR<sub>1</sub> by multisubstituted C-terminally propargylated AST<sup>1-11</sup> peptides. a) N-terminally free amine peptides. b) N-terminally acetylated peptides.

			C-term. = propargyl				
			R = -NH <sub>2</sub> <sup>(a)</sup>			R = -Ac <sup>(b)</sup>	
			Subst.	EC <sub>50</sub> (μM)	E <sub>max</sub> (%)	EC <sub>50</sub> (μM)	E <sub>max</sub> (%)
●	116	R-AST <sup>1-11</sup>	0	n.a.	n.a.	n.a.	n.a.
●	117	R-[Cha <sup>2</sup> tBuAla <sup>3</sup> ]AST <sup>1-11</sup>	2	4.59±0.90	97±6	7.55±2.59	31±2
●	118	R-[Cha <sup>2</sup> Aib <sup>4</sup> ]AST <sup>1-11</sup>	2	8.27±0.72	98±3	50.45±16.38	108±17
●	119	R-[tBuAla <sup>3</sup> Aib <sup>4</sup> ]AST <sup>1-11</sup>	2	18.24±0.98	82±2	1576±8097	676±2830
●	120	R-[Cha <sup>2</sup> tBuAla <sup>3</sup> Aib <sup>4</sup> ]AST <sup>1-11</sup>	3	11.60±776	37±2	6.78±1.07	57±3
●	121	R-[Cha <sup>2</sup> Aib <sup>4</sup> tBuAla <sup>8</sup> ]AST <sup>1-11</sup>	3	11.56±4.26	104±12	32.81±22034	76±3
●	122	R-[D-Pal <sup>1</sup> Cha <sup>2</sup> tBuAla <sup>3</sup> Aib <sup>4</sup> ]AST <sup>1-11</sup>	4	1.04±0.02	99±1	61.4±14.6	123±14
●	123	R-[Cha <sup>2</sup> tBuAla <sup>3,8</sup> Aib <sup>4</sup> ]AST <sup>1-11</sup>	4	18.08±2.12	75±4	9.31±0.80	73±3
●	125	R-[Cha <sup>2,10</sup> tBuAla <sup>3,8</sup> Aib <sup>4</sup> ]AST <sup>1-11</sup>	5	36.75±84.41	73±54	47.1±11.9	105±14

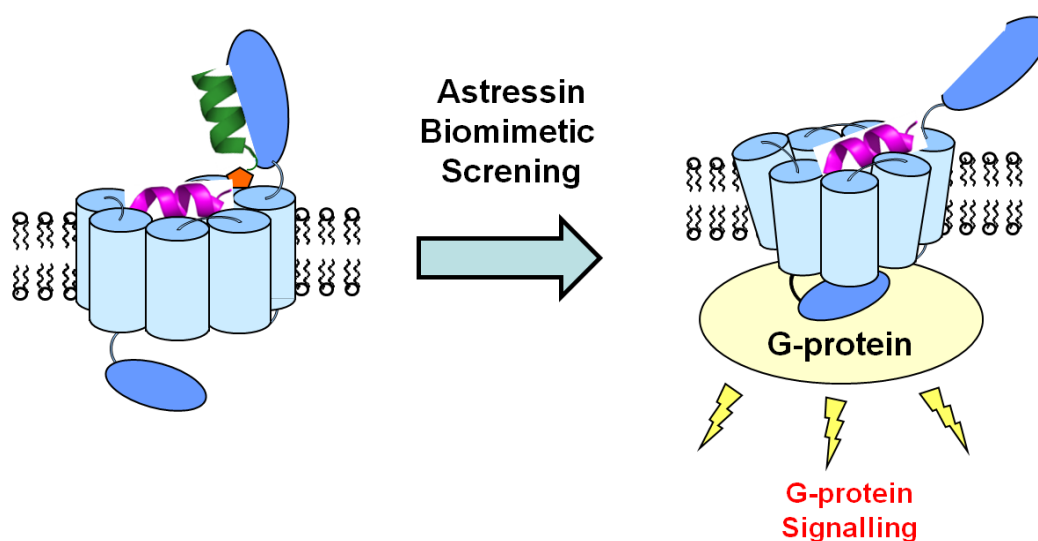
**Table 20. Stimulation of CRHR<sub>1</sub> by multisubstituted C-terminally propargylated AST<sup>1-11</sup> peptides.**

Gratifyingly, the combination of two mutations in conjugates **117**, **118** and **119** turned the inactive AST<sup>1-11</sup> untethered sequence into agonists, potent in the low micromolar range. The N-terminally “free” untethered AST<sup>1-11</sup> peptides were in general more potent than the same N-terminally acetylated sequences, suggesting that the N-terminal primary amine moiety might contribute with its positive charge to the binding to the receptor J-domain. The triple mutation in conjugates **120** and **121** did not further increase potency. The D-Phe<sup>1</sup>D-Pal-including tetrasubstituted peptide **122a**, however, showed a potency of 1.04 ± 0.02 μM, confirming that the pyridyl side chain greatly improve the potency of the AST<sup>1-11</sup> peptide for CRHR<sub>1</sub> stimulation. From a structural point of view, it seems that the CRHR<sub>1</sub> stimulation potency of AST<sup>1-11</sup> untethered peptides was largely achieved by fine-tuning the hydrophobic interactions through incorporation of unnatural amino acid side chains (e.g., Cha, tBuAla). This is in line with the UCN<sup>4-15</sup> sequence optimization; in particular the Leu<sup>3</sup>tBuAla substitution (Leu<sup>13</sup>tBuAla in the UCN<sup>4-15</sup> screening) was already identified as enhancing the stimulation of CRHR<sub>1</sub>. The high potency of the untethered peptide **122a** is surprising because the starting AST<sup>1-11</sup> motif lacks the N-terminal amino acids which were shown as crucial for the CRHR<sub>1</sub> activation. This N-terminally “truncated” peptide agonist may provide new insights into the activation mechanism of CRHR<sub>1</sub> and serve as a starting point for further SAR investigations.

Hereby, we have shown that astressin is in fact a competitive partial agonist and that optimization of the astressin-derived AST<sup>1-11</sup> template leads to potentially new peptide agonists.

Given that the AST<sup>1-11</sup> templates functionally compete with transtressin, we believe that the AST<sup>1-5</sup> motif (corresponding to UCN<sup>11-15</sup>) primarily interact with the juxtamembrane domain of CRHR<sub>1</sub>. The role of the AST<sup>6-11</sup> segment for the potency remains to be determined. In general, the mechanism of action of AST<sup>1-11</sup>-derived peptide agonists requires further pharmacological characterization such as competition assays against known antagonists (e.g., CRHR<sub>1</sub>-ECD1 specific peptide **1** and DMP696) or using cells lines expressing receptor mutants (e.g., ΔECD1-CRHR<sub>1</sub>).

### 3.3.7 Summary of the astressin biomimetic screening



**Figure 48. Astressin biomimetic screening overview: sequence optimization of a class B GPCR synthetic peptide antagonist.**

The conjugation of a high-affinity carrier with peptide fragments derived from a synthetic peptide antagonist results in a dramatic enhancement in activity. This allows the testing of otherwise inactive peptides for modulation of the CRHR<sub>1</sub> activity in various assay setups. By applying the biomimetic screening methodology to the synthetic peptide antagonist astressin, we discovered N-terminally shortened peptide agonists with surprising potencies (Figure 48). Although the approach was first designed to identify the structural features responsible for astressin antagonism, the AST<sup>1-11</sup> amino acid positional screening led to the optimization of single positions for CRHR<sub>1</sub> stimulation and several improved agonists were discovered. This indicates that peptide binding to the TMD seems to be much easier in an activated CRHR<sub>1</sub> conformation. Importantly, the AST<sup>1-11</sup>-derived untethered agonists lack the N-terminal residues which were previously thought as essential for CRHR<sub>1</sub> activation, suggesting a novel mechanism of action for these peptides. Hereby, we also show that the biomimetic screening approach can be easily applied to endogenous and synthetic peptide class B GPCR ligands, agonists and antagonists.

The potencies of the untethered AST<sup>1-11</sup>-derived agonists reach the low micromolar range. These 11-mer ligands have a great potential for further activity optimization. In particular, it is obvious that the synthesis of an extended C-terminally amidated peptide library may lead to new potent ligands; especially by introducing substitutions identified as potency enhancing in the stimulation screening. Interestingly, the AST<sup>1-11</sup>-derived untethered agonists lack the N-terminal amino acid residues previously identified as “crucial” for CRHR<sub>1</sub> stimulation. This suggests that AST<sup>1-11</sup>-derived agonists activate CRHR<sub>1</sub> through a different mechanism of action than transthyrin. The pharmacology of these novel agonists remain to be characterized and may provide a deeper insight into the mechanism of activation of class B GPCRs.



### 3.4 Synthesis and characterization of nonpeptide CRHR<sub>1</sub> antagonists

In recent years, a number of non-peptidergic CRHR<sub>1</sub> antagonists have been identified and characterized. In general, these antagonists exhibit nanomolar affinities for CRHR<sub>1</sub> with > 1000-fold selectivity for CRHR<sub>1</sub> over CRHR<sub>2</sub>. They are also effective in reducing anxiety-like behaviors in several preclinical animal models (*Li et al.* 2005). However, the efficacy of non-peptidergic CRHR<sub>1</sub> antagonists as drugs for the treatment of psychiatric disorders remains to be demonstrated in double-blind clinical trials (see Introduction). Among the reported non-peptidergic CRHR<sub>1</sub> antagonist, DMP696 [4-(1,3-dimethoxyprop-2-ylamine)-2,7-dimethyl-8-(2,4-dichlorophenyl)-pyrazolo-[1,5-a]-1,3,5-triazine] was designed as a drug development candidate for the treatment of anxiety and depression (Figure 8). DMP696 was synthesized following an initial lead compound with 5.7  $\mu\text{M}$  binding affinity at DuPont (*Gilligan et al.* 2009a; *He et al.* 2000; *Li et al.* 2005). Importantly, DMP696 was reported to have reached clinical trials but its status is currently not known. Structurally, the bicyclic pyrazolo-[1,5-a]-triazine core of DMP696 is found in several highly potent CRHR<sub>1</sub> ligands (e.g., pexacerfont); the aliphatic “top” and aryl “bottom” groups follow the well known pharmacophore model of non-peptidergic CRHR<sub>1</sub> antagonists (see Introduction). Being a well described CRHR<sub>1</sub>-TMD specific antagonist, DMP696 was used successfully for the *in vitro* pharmacological characterization of transtressin (see Section 3.2.4).

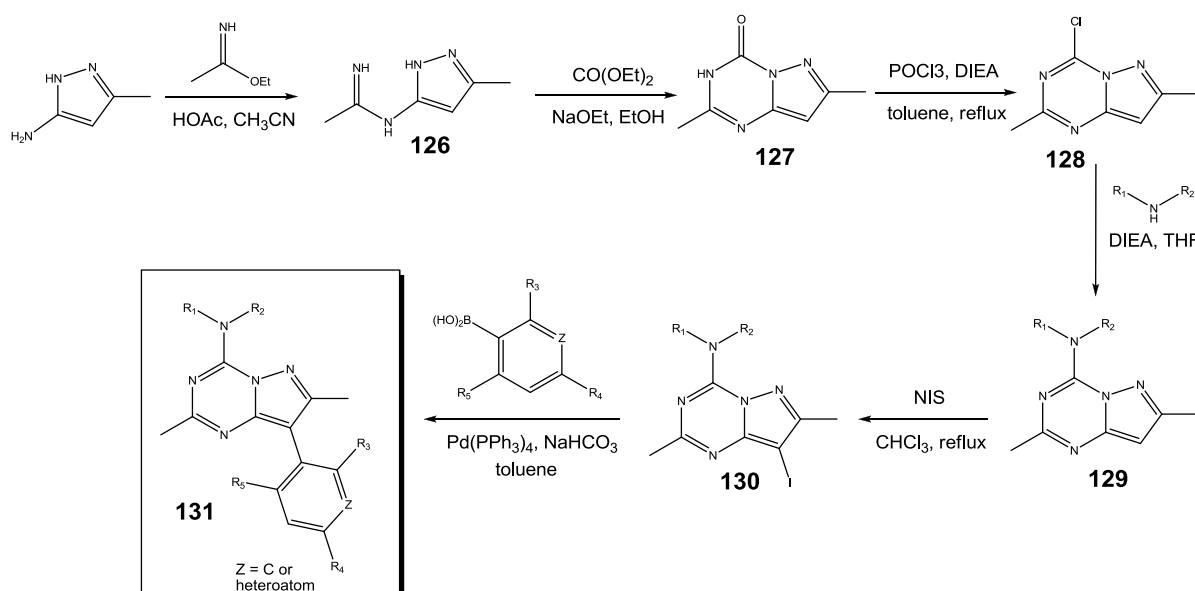
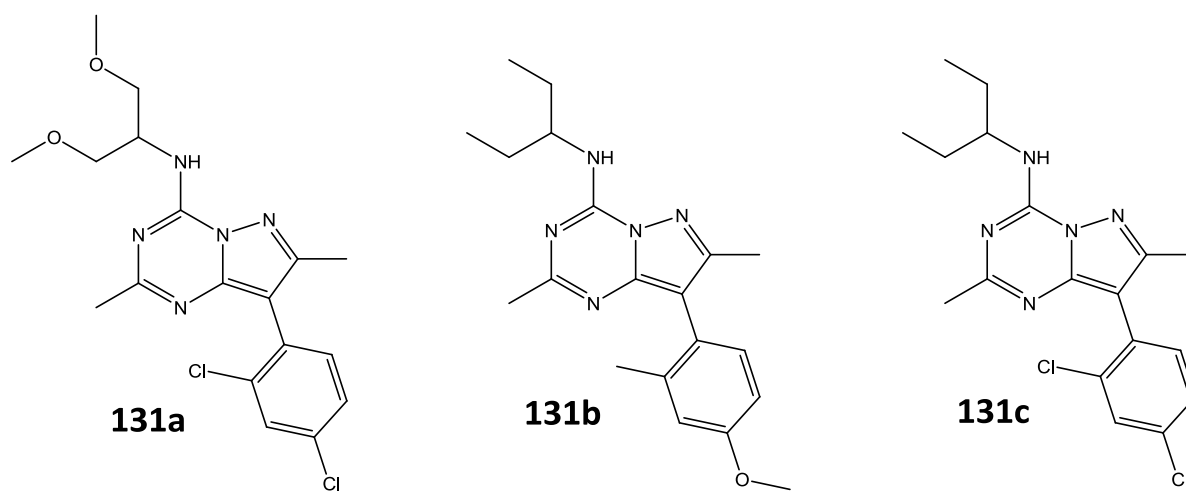


Figure 49. Synthesis of substituted pyrazolo-[1,5-a]-triazines as nonpeptide CRHR<sub>1</sub> antagonists.

DMP696 is not commercially available; and thus had to be synthesized on our own. For this purpose, an efficient and convergent synthetic route for the synthesis of pyrazolo-triazine CRHR<sub>1</sub> antagonists was established (Figure 49). Ethyl acetamidate free base was condensed with 3-amino-methylpyrazole to give **126** as an acetic acid salt. Ring closure to the pyrazolo-[1,5-a]-triazine scaffold of **127** was achieved with diethylcarbonate in strong basic conditions. Finally, the compound **127** was chlorinated with phosphorous oxychloride to give the activated key intermediate **128**.

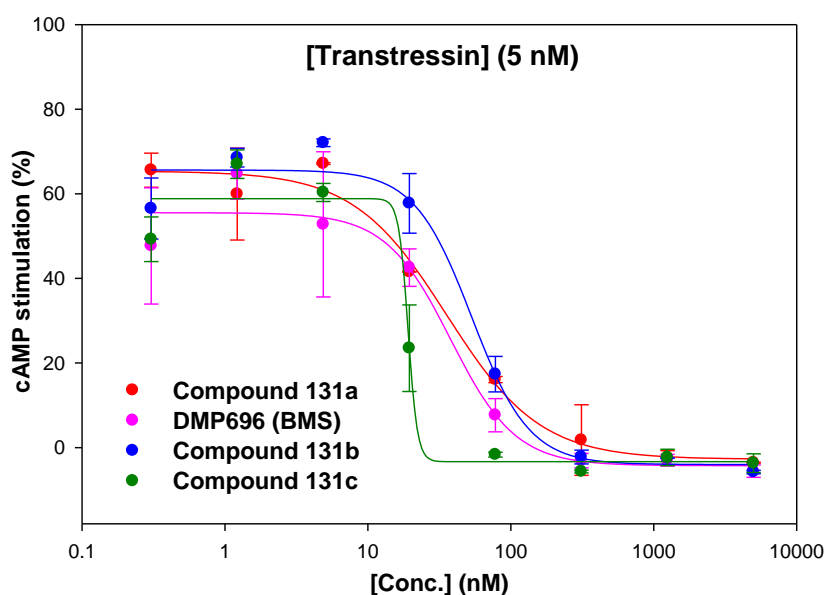
The incorporation of aliphatic top-groups was performed by simple condensation of free amines on the intermediate **128**. After regioselective iodination at position 8 with N-iodosuccinimide (NIS), the bottom aryl group is easily introduced by palladium-catalyzed Suzuki cross-coupling; affording the desired non-peptidergic CRHR<sub>1</sub> antagonist **131**. Our synthetic route is simple, advantageous and convergent compared to the reported synthesis of DMP696: the activated intermediate can be quickly derivatized with a wide choice of commercially available amines and boronic acids. To validate our synthetic route, we synthesized DMP696 (Figure 50, **131a**) as well as several closely related pyrazolo-[1,5-a]-triazines, such as compounds **131b** and **131c** which combine top- and bottom-groups from DMP696 and DMP904 (*Li et al.* 2005).



**Figure 50. Structure of non-peptidergic pyrazolo-[1,5-a]-triazines CRHR<sub>1</sub> antagonists synthesized in this study.** Compound **131a** corresponds to DMP696 itself. Compound **131b** associates the top- and bottom-groups of DMP904 to the core of DMP696. Compound **131c** associates the top-group of DMP904 to DMP696.

The potencies of DMP696 analogs **131a**, **131b** and **131c** were tested in a cAMP competition assay against the CRHR<sub>1</sub>-TMD specific agonist transtressin (Figure 51 and Table 21). In this assay, the CRHR<sub>1</sub> overexpressing HEK293 cells were first incubated with increasing concentrations of the synthesized non-peptidergic CRHR<sub>1</sub> antagonists as well as DMP696 itself (generous gift from Bristol-

Myers Squibb). A fixed concentration of transtresin (5 nM) was then added and the resulting cAMP stimulation determined. Gratifyingly, **131a** (our “in house” synthesized DMP696) and DMP696 similarly inhibited transtresin, thus validating our synthesis of CRHR<sub>1</sub> antagonists. *In vitro*, the analogs **131b** and **131c** were also surprisingly potent. The synthesis of DMP696 (**131a**) by Suzuki cross-coupling was then scaled up and the latter synthesized on a one gram scale.



**Figure 51. cAMP inhibition of CRHR<sub>1</sub> by pyrazolo-[1,5-a]-triazine CRHR<sub>1</sub> antagonists.** HEK293 cells overexpressing the CRHR<sub>1</sub> were first incubated with increasing concentrations of compounds **131a**, **131b**, **131c** and DMP696 (Bristol-Myers Squibb). Transtresin (5 nM) was then added and the cAMP production was determined.

		Transtressin 5 nM		
		EC <sub>50</sub> (nM)	<i>E</i> <sub>min</sub>	<i>E</i> <sub>max</sub>
●	<b>131a</b>	35.7±7.3	-3±3	65±4
●	<b>DMP696 (BMS)</b>	37.9±10.5	-4±4	56±4
●	<b>131b</b>	53.4±11.4	-4±4	66±4
●	<b>131c</b>	19.1±12.0	-3±3	59±4

**Table 21. Characterization of nonpeptide pyrazolo-[1,5-a]-triazine CRHR<sub>1</sub> antagonists.**

Our “in house” synthesized DMP696 was used in cell-based assays, in particular in cAMP competition assays addressing the CRHR<sub>1</sub>-TMD specificity of peptide ligands. In collaboration with the groups of Mathias Schmidt and Mayumi Kimura at the Max-Planck-Institute for Psychiatry (Munich), **131a** was administered to mice for *in vivo* behavioral and physiological experiments. The synthesis of substituted pyrazolo-[1,5-a]-triazines described herein opens the doors for the further synthesis and characterization of CRHR<sub>1</sub> antagonists with improved potencies and pharmacokinetic properties.

## 4 Conclusion

A rapid approach to chemically probe the interaction domain of class B GPCRs was developed. The conjugation of a high-affinity carrier resulted in a dramatic enhancement in the activity of peptide ligands and allowed the initial testing of peptides whose activity would otherwise have been too weak to be detectable. The synthesis and coupling of short length peptides to reconstitute a fully functional CRHR<sub>1</sub> modulator has several advantages compared to the classical synthesis of whole, full length peptide ligands. For example, it is quicker with higher product purities. Importantly, the fragment conjugation approach obviated the need for HPLC purification of the initial test peptides, thereby enabling a substantially higher screening throughput. Thanks to the exquisite receptor specificity of the conjugates imparted by the carrier segment, the crude peptide conjugates were compatible with functional assays in living cells. The method produces peptide conjugates which mimic the two-domain model of activation for class B GPCRs, thus allowing to rapidly address the ligand-receptor interface (*Devigny et al. 2011*).

By applying this methodology to the class B GPCR CRHR<sub>1</sub>, we discovered highly potent agonists that are specific for the activation domain of this receptor. For example, the activation mechanism of transtressin, a low nanomolar agonist, is almost independent of the extracellular domain and resembles the signaling mechanism of canonical class A GPCRs (*Devigny et al. 2011*). Similarly, by applying this methodology to the synthetic antagonist astressin, we discovered N-terminally shortened and surprisingly potent agonists. We assume that small peptide agonists such as transtressin bind at the endogenous hormone orthosteric site and derive their stimulatory activity from optimized hydrophobic interactions and conformation. The structural features which lead to CRHR<sub>1</sub> antagonism, however, remain to be characterized. CRHR<sub>1</sub> domain-specific peptides such as transtressin are crucial for the identification of CRHR<sub>1</sub>-TMD specific inhibitors.

The mechanism of action and specific amino acid interactions between peptide agonists and receptor require to be further characterized (e.g., by CRHR<sub>1</sub> mutagenesis studies). The ability of peptide conjugates to mimic endogenous hormones and their potential for *in vivo* CRHR<sub>1</sub> targeting suggests that fluorescently-tagged conjugates may be successfully used for CRHR<sub>1</sub> *in vitro* and *in vivo* imaging. Given the high mechanistic and structural homology within the class B GPCR family (*Hoare 2005; Parthier et al. 2009*), we expect the biomimetic screening approach to be applicable to many class B GPCRs.



## 5 Material and methods

### 5.1 Chemical methods

#### 5.1.1 Nuclear Magnetic Resonance

If not specified otherwise,  $^1\text{H}$ - and  $^{13}\text{C}$ -NMR spectra were recorded at the Department of Chemistry and Pharmacy at the Ludwig Maximilian University (Munich) on a Bruker AC300, a Bruker XL400 or a Bruker AMX600 at room temperature. Chemicals shifts are reported in parts per million referenced with respect to residual solvent ( $^1\text{H}$ :  $\text{CDCl}_3 = 7.26$  ppm,  $^{13}\text{C}$ :  $\text{CDCl}_3 = 77.16 \pm 0.06$  ppm). The coupling constants ( $J$ ) are given in Hertz (Hz) and the peak multiplicity are abbreviated as such: singlet s, doublet d, triplet t, quartet q and multiplet m.

#### 5.1.2 Mass Spectrometry

ESI mass spectra ( $m/z$ ) were recorded on a Thermo Finnigan LCQ DECA XP Plus mass spectrometer. C-terminal propargylated and amidated peptides were analyzed by MALDI-TOF on Bruker Daltonics Ultraflex I Maldi-TOF/TOF. High resolution mass spectroscopy was carried out at the Max Planck Institute for Biochemistry (Munich), Microchemistry Core Facility.

#### 5.1.3 Liquid chromatography-mass spectrometry

Liquid chromatography-mass spectrometry (LC-MS) was performed using a Beckman System Gold 126 Analytical Solvent Module, a Beckman 166 Detector Module, a Beckman 508 Autosampler Module with a 50  $\mu\text{L}$  sampling loop, a YMC 100 x 4.6mm analytical column (YMC, Germany), and a Thermo Finnigan LCQ DECA XP Plus mass spectrometer. Measurements were performed at a flow rate of 1 mL/min using buffer A: 0.1 % formic acid in water/acetonitrile (95/5, v/v) and buffer B: 0.1 % formic acid in acetonitrile/water (95/5, v/v). HPLC system was interfaced by the 32-Karat software.

#### 5.1.4 High-performance liquid chromatography

##### 5.1.4.1 Analytical and semi-preparative high-performance liquid chromatography

Analytical and semi-preparative reverse phase HPLC spectra were performed using a Beckman System Gold 125S Analytical Solvent Module, a Beckman 168 Diode Array Detector Module, a Hitachi F-1080 Fluorescence Detector Module, a Beckman 508 Autosampler Module with a 50  $\mu\text{L}$  sampling

loop, and a Jupiter 4  $\mu\text{m}$  Proteo 90 Å 250 x 4.6 mm analytical column (Phenomenex, Germany) at a flow rate of 1 mL/min or a Jupiter Proteo semi-preparative column at a flow rate of 5 mL/min using buffer A: 0.1 % TFA in water/acetonitrile (95/5, v/v) and buffer B: 0.1 % TFA in acetonitrile/water (95/5, v/v).

#### **5.1.4.2 Preparative high-performance liquid chromatography**

Reverse phase preparative HPLC was performed with a Beckman System Gold 126NMP Preparative Solvent Module, a Beckman 166 Detector Module, a Beckman SC-100 fraction collector and a Jupiter column (Phenomenex, Germany) at a flow rate of 25 mL/min using buffer A: 0.1 % TFA in water/acetonitrile (95/5, v/v) and buffer B: 0.1 % TFA in acetonitrile/water (95/5, v/v).

HPLC systems were interfaced by the 32-Karat software.

#### **5.1.5 Flash chromatography**

Chromatographic separations were performed either manually or with an Interchim Puriflash 430 automatic flash chromatography system. Silica gel 60 (Merck 70-230 mesh) was used for manual column chromatography. Puriflash columns 50 Silica 50  $\mu\text{M}$  (10 g, 25 g, and 40 g) were used for automated chromatography.

#### **5.1.6 Thin layer chromatography**

Thin layer chromatography (TLC) was performed using Merck-prepared aluminium plates (Silica 60 F254, 0.25 mm). The substances were detected with UV-light ( $\lambda = 254/366$  nm). Thin layers plates were also stained with the following solutions:

- Hanessian's: 5 g  $\text{CeSO}_4$ , 25 g  $\text{NH}_4\text{MO}_7\text{O}_{24}\cdot 4 \text{H}_2\text{O}$ , 450 mL  $\text{H}_2\text{O}$ , 50 mL  $\text{H}_2\text{SO}_4$ .
- Potassium permanganate: 1.5 g  $\text{KMnO}_4$ , 10 g  $\text{K}_2\text{CO}_3$ , 1.25 mL 10 %  $\text{NaOH}$  in 200 mL  $\text{H}_2\text{O}$ .

The TLC plates were shortly dipped in the staining solution and heated until visualization.



### 5.1.7 Chemicals

The chemicals were purchased from the companies *Acros*, *Alfa Aesar*, *Bachem*, *Fluka*, *Iris Biotech*, *Novabiochem*, *PolyPeptide Group*, *Sigma-Aldrich* and *VWR* with the mentioned purities. The following chemicals were used without further purification.

Substance	CAS-Number	Supplier	Purity
Acetic acid	64-19-7	Roth	100%
Acetic anhydride	108-24-7	Roth	> 99.0 %
3-Amino-5-methylpyrazole	31230-17-8	Sigma-Aldrich	97.0 %
(+)-Ascorbic acid sodium salt	134-03-2	Roth	> 99.0 %
Bromoacetic acid	79-08-3	Alfa Aesar	> 98.0 %
tert-Butyl bromoacetate	5292-43-3	Alfa Aesar	> 98.0 %
4-Carboxybenzaldehyde	619-66-9	Sigma-Aldrich	> 99.0 %
p-Chloranil	118-75-2	Merck	> 98.0 %
Chloroform D1	865-49-6	Roth	99.8 %
6-Chloronicotinic acid	5326-23-8	Acros	99.0 %
4-Chloro-7-nitrobenzofurazane	10199-89-0	Fluka	> 99.0 %
Chromium(VI) oxide	1333-82-0	Sigma-Aldrich	> 99.0 %
Copper(II) sulfate pentahydrate	7758-99-8	Sigma-Aldrich	99.999 %
1,8-Diazabicyclo[5.4.0]undec-7-ene	6674-22-2	Fluka	> 99.0 %
2,4-Dichlorobenzeneboronic acid	68716-47-2	Chempur	> 99.0 %
Diethyl carbonate	105-58-8	Sigma-Adrich	> 99.0 %
Diethylene glycol	111-46-6	Merck	> 99.0 %
N,N-Diisopropylethylamine	7087-68-5	Merck	> 98.0 %
Di-tert-butyl dicarbonate	24424-99-5	Fluka	> 98.0 %
Ethyl acetamidate hydrochloride	2208-07-3	Sigma-Aldrich	> 97.0 %

## MATERIAL &amp; METHODS

Ethylene glycol	107-21-1	Sigma-Aldrich	> 99.0 %
Fmoc-chloride	28920-43-6	Bachem	> 98.0 %
FMPB-linker	26628-22-8	Iris Biotech	> 98.0 %
HATU	148893-10-1	Novabiochem	> 98.0 %
HBTU	94790-37-1	Novabiochem	> 98.0 %
1-Hydroxybenzotriazole hydrate	123333-53-9	Fluka	> 99.0 %
Hydrazine monohydrate	7803-57-8	Sigma-Aldrich	98.0 %
2-Hydrazinopyridine	4930-98-7	Sigma-Aldrich	97.0 %
Hydrochloric acid	7647-01-0	Roth	37 %
Iodomethane	74-88-4	Merck	> 99.0 %
N-Iodosuccinimide	516-12-1	Sigma-Aldrich	95.0 %
Magnesium sulfate	7487-88-9	Roth	> 99.0 %
4-Methoxy-2-methylbenzene boronic acid	208399-66-0	Alfa Aesar	98.0 %
4-Methylmorpholine	109-02-4	Sigma-Aldrich	> 99.5 %
Ninhydrin	485-47-2	Roth	> 99.0 %
4-Nitrobenzaldehyde	555-16-8	Fluka	> 99.0 %
Pentaethylene glycol	4792-15-8	Alfa Aesar	> 98.0 %
3-Pentylamine	616-24-0	Sigma-Aldrich	97.0 %
Phenol	108-95-2	Merck	> 99.0 %
Phosphorous oxychloride	10025-87-3	Sigma-Aldrich	> 99.0 %
Potassium carbonate	584-08-7	Roth	> 99.0 %
Potassium hydroxide	1310-58-3	Merck	> 85.0 %
Potassium iodide	7681-11-0	Roth	> 99.0 %
Potassium permanganate	7722-64-7	Merck	> 99.0 %
Potassium tert-butyrate	865-47-4	Merck	> 98.0 %

Propargylamine	2450-71-7	Sigma-Aldrich	98.0 %
PyBOP	128625-52-5	Novabiochem	> 97.0 %
Seesand		Roth	
Serinol	534-03-2	Sigma-Aldrich	> 98.0 %
Silver(I) oxide	7758-99-8	Merck	> 98.0 %
Sodium	7440-23-5	Sigma-Aldrich	> 99.0 %
Sodium azide	26628-22-8	Merck	> 99.0 %
Sodium chloride	7647-14-5	Merck	> 99.5 %
Sodium cyanoborohydride	25895-60-7	Fluka	> 95.0 %
Sodium diethyldithiocarbamate trihydrate	20624-25-3	Fluka	> 99.0 %
Sodium hydride	7646-69-7	Sigma-Aldrich	95.0 %
Sodium hydrogen carbonate	144-55-8	Roth	> 99.0 %
Sodium hydroxide	1310-73-2	VWR	> 99.0 %
Sulfuric acid	7664-93-9	Roth	> 99.5 %
Tetraethylene glycol	112-60-7	Alfa Aesar	> 99.0 %
Tetrakis(triphenylphosphine)palladium(0)	14221-01-3	Acros	99.0 %
Toluene sulfonyl chloride	98-59-9	Fluka	> 99.0 %
Triethylene glycol	112-27-6	Merck	> 99.0 %
Trifluoroacetic acid	76-05-1	Roth	> 99.9 %
2,2,2-Trifluoroethanol	75-89-8	Fluka	> 99.0 %
Triisopropyl silane	6485-79-6	Sigma-Aldrich	99.0 %
Tris[(1-benzyl-1H-1,2,3-triazol-4-yl)methyl]amine	510758-28-8	Sigma-Aldrich	> 97.0 %

Table 22. Chemicals.

Substance	CAS-Number	Supplier	Purity
Fmoc-Aib-OH	94744-50-0	Novabiochem	> 98.0 %
Fmoc-Aic-OH	135944-07-9	NeoMPS	> 98.0 %
Fmoc-Ala-OH	35661-39-3	Novabiochem	> 98.0 %
Fmoc-D-Ala-OH	79990-15-1	Novabiochem	> 98.0 %
Fmoc-tBu-Ala-OH	139551-74-9	NeoMPS	> 98.0 %
Fmoc-1-amino-cyclohexane carboxylic acid	162648-54-6	NeoMPS	> 98.0 %
Fmoc-1-amino-cyclopentane carboxylic acid	117322-30-2	NeoMPS	> 98.0 %
Fmoc-Arg(Pbf)-OH	154445-77-9	Novabiochem	> 98.0 %
Fmoc-D-Arg(Pbf)-OH	187618-60-6	Novabiochem	> 98.0 %
Fmoc-Asn(Trt)-OH	132388-59-1	Novabiochem	> 98.0 %
Fmoc-Asp(OtBu)-OH	71989-14-5	Novabiochem	> 98.0 %
Fmoc-D-Asp(OtBu)-OH	112883-39-3	Bachem	> 98.0 %
Fmoc-Cha-OH	135673-97-1	Novabiochem	> 98.0 %
Fmoc-D-Cha-OH	144701-25-7	NeoMPS	>99.0 %
Fmoc-Chg-OH	161321-36-4	Bachem	> 98.0 %
Fmoc-Cit-OH	133174-15-9	Fluka	> 98.0 %
Fmoc-Dab(Boc)-OH	125238-99-5	NeoMPS	> 98.0 %
Fmoc-Dap(Boc)-OH	162558-25-0	NeoMPS	> 98.0 %
Fmoc-Gln(Trt)-OH	132327-8-1	Novabiochem	> 98.0 %
Fmoc-Glu(OAll)-OH	133464-46-7	Bachem	> 98.0 %
Fmoc-Glu(OtBu)-OH	71989-18-9	Novabiochem	> 98.0 %
Fmoc-Gly-OH	29022-11-5	Novabiochem	> 98.0 %
Fmoc-tBu-Gly-OH	132684-60-7	NeoMPS	> 98.0 %

Fmoc-His(Trt)-OH	109425-51-6	Novabiochem	> 98.0 %
Fmoc-D-His(Trt)-OH	135610-90-1	Bachem	> 98.0 %
Fmoc-Ile-OH	71989-23-6	Novabiochem	> 98.0 %
Fmoc-D-Ile-OH	143688-83-9	Fluka	> 98.0 %
Fmoc-Leu-OH	35661-60-0	Novabiochem	> 98.0 %
Fmoc-D-Leu-OH	114360-54-2	Fluka	> 98.0 %
Fmoc- $\alpha$ -Me-Leu-OH	312624-65-0	Bachem	> 98.0 %
Fmoc-Lys(Aloc)-OH	146982-27-6	Bachem	> 98.0 %
Fmoc-Lys(Boc)-OH	71989-26-9	Novabiochem	> 98.0 %
Fmoc-Lys(ivDde)-OH	204777-78-6	Novabiochem	> 96.0 %
Fmoc-D-Nal(1)-OH	138774-93-3	NeoMPS	> 98.0 %
Fmoc-D-Nal(2)-OH	138774-94-4	NeoMPS	> 98.0 %
Fmoc-Nle-OH	77284-32-3	Novabiochem	> 98.0 %
Fmoc-Nva-OH	135112-28-6	NeoMPS	> 98.0 %
Fmoc-Orn(Boc)-OH	109425-55-0	Fluka	> 98.0 %
Fmoc-D-3-Pal-OH	142994-45-4	NeoMPS	> 98.0 %
Fmoc-Phe-OH	35661-40-6	Novabiochem	> 98.0 %
Fmoc-4-bromo-D-Phe-OH	198545-76-5	Bachem	> 98.0 %
Fmoc-4-nitro-D-Phe-OH	177966-63-1	NeoMPS	> 98.0 %
Fmoc-Phg-OH	102410-65-1	Fluka	> 98.0 %
Fmoc-D-Phe-OH	86123-10-6	Novabiochem	> 98.0 %
Fmoc- $\alpha$ -Me-D-Phe-OH	152436-04-9	Bachem	> 98.0 %
Fmoc-Pro-OH	71989-31-6	Novabiochem	> 98.0 %
Fmoc-Ser(tBu)-OH	71989-33-8	Novabiochem	> 98.0 %
Fmoc-D-Ser(tBu)-OH	128107-47-1	Novabiochem	> 98.0 %

Fmoc-homoSer(Trt)-OH	111061-55-3	Fluka	> 98.0 %
Fmoc-Thr(tBu)-OH	71989-35-0	Novabiochem	> 98.0 %
Fmoc-D-Thr(tBu)-OH	138797-71-4	Fluka	> 98.0 %
Fmoc-allo-Thr(tBu)-OH	201481-37-0	Bachem	> 98.0 %
Fmoc-threo- $\beta$ -phenylserine	487060-72-0	NeoMPS	> 97.0 %
Fmoc-Trp(Boc)-OH	143824-78-6	Novabiochem	> 98.0 %
Fmoc-D-Trp(Boc)-OH	163619-04-3	NeoMPS	> 98.0 %
Fmoc-Tyr(tBu)-OH	71989-38-3	Novabiochem	> 98.0 %
Fmoc-D-Tyr(tBu)-OH	118488-18-9	Novabiochem	> 98.0 %
Fmoc-Val-OH	68858-20-8	NeoMPS	> 98.0 %
Fmoc-D-Val-OH	84624-17-9	NeoMPS	> 98.0 %
Rink amide MBHA resin	431041-83-7	Novabiochem	
Tentagel™ S-NH <sub>2</sub>		Sigma-Aldrich	

**Table 23. Resins and building blocks used for the solid phase synthesis of peptides.**

### 5.1.8 Solvents

Solvents were purchased from the companies *Roth* and *Sigma-Aldrich* in ROTISOLV®, ROTIPURAN®, ROTIDRY® or HPLC Gradient Grade quality. The solvents were used without further purification.

Solvent	CAS number	Supplier	Quality
Acetone	67-64-1	Roth	ROTIPURAN® > 99.8 %
Acetonitrile	75-05-8	Roth	ROTISOLV® > 99.9 %
Acetonitrile	75-05-8	Roth	ROTIPURAN® > 99.5 %
tert-Butanol	75-65-0	Roth	> 99.5 %
Cyclohexane	110-82-7	Roth	ROTIPURAN > 99.9 %
Chloroform	67-66-3	Roth	ROTIPURAN > 99 %

Chloroform	67-66-3	Sigma-Aldrich	Anhydrous > 99 %
Dichloromethane	75-09-2	Roth	ROTIDRY > 99.8%
Diethyl ether	60-29-7	Roth	ROTISOLV® > 99.8 %
1,4-Dioxane	123-91-1	Sigma-Aldrich	Anhydrous 99.8 %
N,N-Dimethylformamide	68-12-2	Roth	Peptide synthesis grade > 99.8 %
N,N-Dimethylformamide	68-12-2	Roth	Synthesis grade > 99.5 %
Ethanol	64-17-5	Roth	ROTIPURAN® > 99.8 %
Ethyl acetate	141-78-6	Roth	ROTISOLV® > 99.9 %
n-Hexane	110-54-3	Roth	ROTIPURAN® > 99 %
Methanol	67-56-1	Roth	ROTISOLV® > 99.9 %
Methanol	67-56-1	Roth	ROTIPURAN® > 99.9 %
N-methyl-2-pyrrolidone	872-50-4	Roth	Peptide synthesis grade > 99.8 %
Tetrahydrofuran	109-99-9	Roth	ROTIDRY® > 99.5 %
Toluene	108-88-3	Roth	ROTIDRY® > 99.5 %
Water	7732-18-5	On tap	

**Table 24. Solvents.**

### 5.1.9 Others materials

Polypropylene syringe reactors for Solid Phase Peptide Synthesis were purchased from Multisynth GmbH (Germany). The Flexchem® Synthesis System for combinatorial peptide synthesis was purchased from SciGene (CA, USA).

## 5.2 Synthetic methods

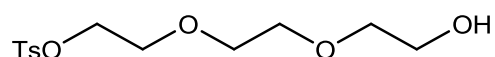
### 5.2.1 Synthesis of azide-functionalized spacers

#### General procedure for the synthesis of 2-hydroxyethyl tosylates **4**, **39** and **40**:

The compounds were synthesized as published (*Bouzide and Sauve 2002*).

To a stirred solution of ethylene glycol (10 mmol) in methylene chloride (50 mL) were added silver oxide (1.5 eq., 3.48 g, 15 mmol), potassium iodide (0.2 eq., 332 mg, 2 mmol) and toluene sulfonyl chloride (1.1 eq., 2.1 g, 11 mmol). The mixture was stirred at room temperature for 1 hr and then filtered over a celite pad. The filtrate was concentrated and purified by flash chromatography using ethyl acetate/hexane (50/50, v/v).

- **2-[2-(2-hydroxyethoxy)ethoxy]ethyl tosylate **4**:**



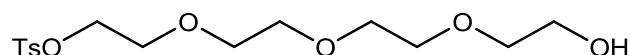
A colorless oil was obtained (2.4 g, 77 %).

$^1\text{H-NMR}$  (300 MHz,  $\text{CDCl}_3$ ):  $\delta$  = 7.80 (d,  $J$  = 8 Hz, 2H), 7.34 (d,  $J$  = 8 Hz, 2H), 4.17 (m, 2H), 3.71 (m, 4H), 3.61 (s, 4H), 3.57 (m, 2H), 2.63 (s, 1H), 2.44 (s, 3H) ppm.  $^{13}\text{C-NMR}$  (75 MHz,  $\text{CDCl}_3$ ):  $\delta$  = 145.19, 133.33, 130.17, 128.31, 72.74, 71.14, 70.66, 69.49, 69.07, 62.11, 21.98 ppm.

MS (ESI) calc. for  $[\text{C}_{13}\text{H}_{20}\text{O}_6\text{S} + \text{H}]^+$ : 305.10; found: 305.31.

TLC (AcOEt/Hexane, 1/1, v/v):  $R_f$  = 0.10.

- **2-[2-[2-(2-Hydroxyethoxy)ethoxy]ethoxy]ethyl tosylate **39**:**



A colorless oil was obtained (1.9 g, 53 %).

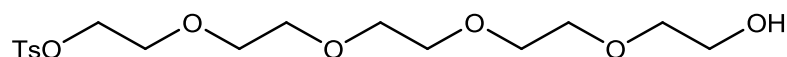
$^1\text{H-NMR}$  (300 MHz,  $\text{CDCl}_3$ ):  $\delta$  = 7.79 (d,  $J$  = 8 Hz, 2H), 7.34 (d,  $J$  = 8 Hz, 2H), 4.16 (m, 2H), 3.57 - 3.72 (m, 15H), 2.44 (s, 3H) ppm.  $^{13}\text{C-NMR}$  (75 MHz,  $\text{CDCl}_3$ ):  $\delta$  = 145.12, 133.34, 130.14, 128.29, 72.79, 71.07, 70.98, 70.80, 70.66, 69.56, 69.04, 62.06, 21.96 ppm.

MS (ESI) calc. for  $[\text{C}_{15}\text{H}_{24}\text{O}_7\text{S} + \text{Na}]^+$ : 371.11; found: 370.79.

TLC (AcOEt):  $R_f$  = 0.30.



- **Pentaethylene glycol monotosylate 40:**



A colorless oil was obtained (2.1 g, 54 %).

$^1\text{H-NMR}$  (300 MHz,  $\text{CDCl}_3$ ):  $\delta$  = 7.79 (d,  $J$  = 8 Hz, 2H), 7.33 (d,  $J$  = 8 Hz, 2H), 4.15 (m, 2H), 3.58 - 3.72 (m, 19H), 2.44 (s, 3H) ppm.  $^{13}\text{C-NMR}$  (75MHz,  $\text{CDCl}_3$ ):  $\delta$  = 145.10, 135.37, 130.14, 128.30, 72.82, 71.07, 70.93, 70.91, 70.87, 70.84, 70.66, 69.57, 69.01, 62.06, 21.96 ppm.

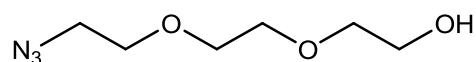
MS (ESI) calc. for  $[\text{C}_{17}\text{H}_{28}\text{O}_8\text{S} + \text{Na}]^+$ : 415.14; found: 415.63.

TLC (AcOEt):  $R_f$  = 0.20.

**General procedure for the synthesis of azides 5, 41 and 42:**

To a stirred solution of the tosylates **4,39** or **40** (5 mmol) in dimethylformamide (20 mL) sodium azide (2 eq., 10 mmol) was added. The mixture was stirred for 16 hrs at room temperature. Dichloromethane (50 mL) was added and the mixture was washed with brine (4 x 100 mL). The organic phase was dried over magnesium sulfate, filtered, and concentrated under reduced pressure. The residue was purified by flash chromatography using ethyl acetate/hexane (50/50, v/v).

- **2-[2-(2-azidoethoxy)ethoxy]ethanol 5:**



A colorless oil was obtained (0.73 g, 83 %).

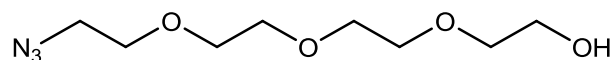
$^1\text{H-NMR}$  (300 MHz,  $\text{CDCl}_3$ ):  $\delta$  = 3.46 - 3.78 (m, 11 H), 3.27 - 3.46 (m, 2 H), 2.74 (br. s, 1 H) ppm.

$^{13}\text{C-NMR}$  (75 MHz,  $\text{CDCl}_3$ ):  $\delta$  = 72.4, 70.5, 70.2, 69.8, 61.5, 50.5 ppm.

MS (ESI) calc. for  $[\text{C}_6\text{H}_{13}\text{N}_3\text{O}_3 + \text{Na}]^+$ : 198.09; found: 198.13.

TLC (AcOEt/Hexane, 1/1, v/v):  $R_f$  = 0.37.

- **2-[2-[2-(2-Azidoethoxy)ethoxy]ethoxy]ethanol 41:**



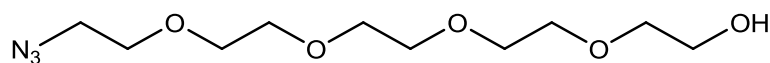
A colorless oil was obtained (0.69 g, 63 %).

$^1\text{H-NMR}$  (300 MHz,  $\text{CDCl}_3$ ):  $\delta$  = 3.68 - 3.72 (m, 2H), 3.64 - 3.67 (m, 10H), 3.58 - 3.61 (m, 2H), 3.38 (t,  $J$  = 5 Hz, 2H), 2.59 (br. s, 1H) ppm.  $^{13}\text{C-NMR}$  (75 MHz,  $\text{CDCl}_3$ ):  $\delta$  = 72.58, 70.80, 70.76, 70.69, 70.45, 70.14, 61.82, 50.77 ppm.

MS (ESI) calc. for  $[\text{C}_8\text{H}_{17}\text{N}_3\text{O}_4 + \text{Na}]^+$ : 242.11; found: 242.64.

TLC (AcOEt):  $R_f = 0.25$ .

- **14-Azido-3,6,9,12-tetraoxatetradecan-1-ol 42:**



A colorless oil was obtained (0.93 g, 71 %).

$^1\text{H-NMR}$  (300 MHz,  $\text{CDCl}_3$ ):  $\delta = 3.67 - 3.75$  (br. m, 3H), 3.65 – 3.67 (m, 13H), 3.59 – 3.62 (m, 2H), 3.38 (t,  $J = 10$  Hz, 2H), 2.61 (br. s, 1H) ppm.  $^{13}\text{C-NMR}$  (75 MHz,  $\text{CDCl}_3$ ):  $\delta = 72.65, 70.83, 70.78, 70.76, 70.74, 70.71, 70.48, 70.15, 61.89, 50.82$  ppm.

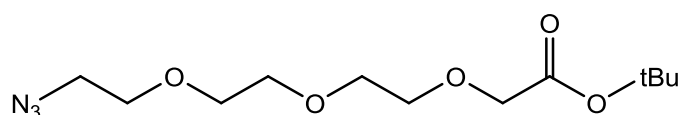
MS (ESI) calc. for  $[\text{C}_{10}\text{H}_{21}\text{N}_3\text{O}_5 + \text{Na}]^+$ : 286.14; found: 286.18.

TLC (AcOEt):  $R_f = 0.20$ .

### General procedure for the synthesis of tert-butyl acetates 6, 36, 43 and 44:

To a stirred solution of the azides **5**, **41** or **42** (4 mmol) in tert-butanol (30 mL), potassium tert-butoxide (1.5 eq., 6 mmol) was added. The mixture was stirred at 30 °C for 15 min and tert-butyl bromoacetate (2 eq., 8 mmol) was added. The mixture was stirred at 30 °C for 16 hrs and then the solvent was evaporated under reduced pressure. The crude product was dissolved in dichloromethane (30 mL) and washed with brine (3 x 30 mL). The organic phase was dried over magnesium sulfate, filtered, and evaporated under reduced pressure. The crude product was purified by flash chromatography using ethyl acetate/hexane (50/50, v/v).

- **Tert-butyl-2-[2-(2-(2-azidoethoxy)ethoxy)ethoxy]acetate 6:**



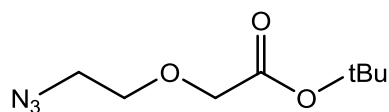
A colorless oil was obtained (0.76 g, 2.6 mmol, 66 %).

$^1\text{H-NMR}$  (300 MHz,  $\text{CDCl}_3$ ):  $\delta = 4.02$  (s, 2 H), 3.62 – 3.72 (m, 10H), 3.38 (t,  $J = 5$  Hz, 2H), 1.47 (s, 9H) ppm.  $^{13}\text{C-NMR}$  (75 MHz,  $\text{CDCl}_3$ ):  $\delta = 169.64, 81.55, 70.74, 70.69, 70.66, 70.03, 69.06, 50.70, 28.11$  ppm.

MS (ESI) calc. for  $[\text{C}_{12}\text{H}_{23}\text{N}_3\text{O}_5 + \text{Na}]^+$ : 312.15; found: 312.07.

TLC (AcOEt/Hexane, 1/2, v/v):  $R_f = 0.39$ .

- **Tert-butyl-2-(2-azidoethoxy)acetate 36:**



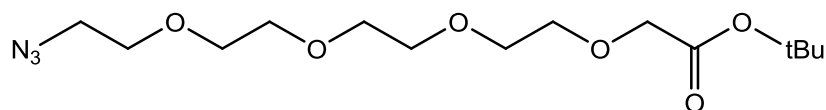
A colorless oil was obtained (0.40 g, 2.0 mmol, 49 %).

$^1\text{H-NMR}$  (300 MHz,  $\text{CDCl}_3$ ):  $\delta$  = 4.02 (s, 2H), 3.72 (t,  $J$  = 5 Hz, 2H), 3.44 (t,  $J$  = 5 Hz, 2H), 1.48 (s, 9H) ppm.  $^{13}\text{C-NMR}$  (75 MHz,  $\text{CDCl}_3$ ):  $\delta$  = 169.43, 81.99, 70.29, 69.12, 50.97, 28.24 ppm.

MS (ESI) calc. for  $[\text{C}_8\text{H}_{15}\text{N}_3\text{O}_3 + \text{Na}]^+$ : 224.10; found: 224.10.

TLC (AcOEt/Hexane, 1/9, v/v):  $R_f$  = 0.25.

- **Tert-butyl-2-[2-[2-[2-(2-azidoethoxy)ethoxy]ethoxy]ethoxy]acetate 43:**



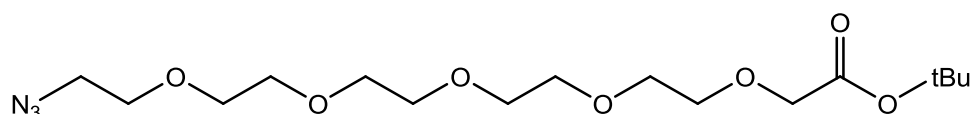
A colorless oil was obtained (1.31 g, 3.9 mmol, 98 %).

$^1\text{H-NMR}$  (300 MHz,  $\text{CDCl}_3$ ):  $\delta$  = 4.01 (s, 2H), 3.68 – 3.72 (m, 4H), 3.65 – 3.67 (m, 10H), 3.38 (t,  $J$  = 5 Hz, 2H), 1.47 (s, 9H) ppm.  $^{13}\text{C-NMR}$  (75 MHz,  $\text{CDCl}_3$ ):  $\delta$  = 169.79, 81.65, 70.87, 70.84, 70.80, 70.79, 70.77, 70.74, 70.17, 69.20, 50.85, 28.26 ppm.

MS (ESI) calc. for  $[\text{C}_{14}\text{H}_{27}\text{N}_3\text{O}_6 + \text{Na}]^+$ : 356.18; found: 356.14.

TLC (AcOEt/Hexane, 1/1, v/v):  $R_f$  = 0.31.

- **Tert-butyl-2-[2-[2-[2-[2-(2-azidoethoxy)ethoxy]ethoxy]ethoxy]ethoxy]acetate 44:**



A colorless oil was obtained (0.64 g, 1.7 mmol, 43 %).

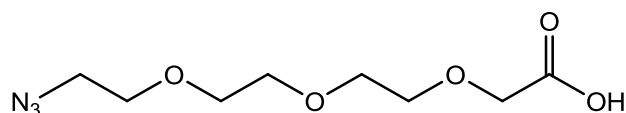
$^1\text{H-NMR}$  (300 MHz,  $\text{CDCl}_3$ ):  $\delta$  = 4.01 (s, 2H), 3.65 – 3.71 (m, 17H), 3.38 (t,  $J$  = 5 Hz, 2H), 1.47 (s, 9H) ppm.  $^{13}\text{C-NMR}$  (75 MHz,  $\text{CDCl}_3$ ):  $\delta$  = 169.79, 81.65, 70.87, 70.84, 70.80, 70.79, 70.77, 70.74, 70.17, 69.20, 50.85, 28.26 ppm.

MS (ESI) calc. for  $[\text{C}_{16}\text{H}_{31}\text{N}_3\text{O}_7 + \text{Na}]^+$ : 400.21; found: 400.18.

TLC (AcOEt/Hexane, 1/1, v/v):  $R_f$  = 0.27.

**General procedure for the synthesis of azidoacetic acids 7, 37, 45 and 46:**

The tert-butyl acetates **6**, **36**, **43** or **44** (2.4 mmol) were dissolved in dichloromethane/trifluoroacetic acid (50/50, v/v) and the mixture was stirred at room temperature for 30 min. The solvent was evaporated under reduced pressure and the residue was dissolved in water (40 mL). The pH was adjusted to pH = 10 by addition of an aqueous sodium hydroxide solution (1 M). The solution was washed with diethylether (3 x 40 mL) and the pH was adjusted to 2 by addition of an aqueous hydrochloric acid solution (3 M). The aqueous layer was extracted with ethyl acetate (5 x 50 mL). The combined extracts were dried over magnesium sulfate, filtered, and evaporated under reduced pressure. The obtained products were used without further purification. Eventually, the crude was purified by flash chromatography using dichloromethane/methanol/acetic acid (90/8/2, v/v/v).

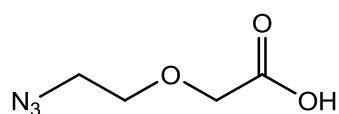
**• 2-[2-(2-(2-azidoethoxy)ethoxy)ethoxy]acetic acid 7:**

A yellowish oil was obtained (g, mmol, %).

$^1\text{H-NMR}$  (300 MHz,  $\text{CDCl}_3$ ):  $\delta$  = 6.33 (br. s, 1H), 4.16 (s, 2H), 3.79-3.74 (m, 2H), 3.73-3.66 (m, 8H), 3.40 (t,  $J$  = 4.8 Hz, 2H) ppm.  $^{13}\text{C-NMR}$  (75 MHz,  $\text{CDCl}_3$ ):  $\delta$  = 172.35, 71.62, 70.84, 70.58, 70.32, 70.21, 68.96, 50.83 ppm.

MS (ESI) calc. for  $\text{C}_8\text{H}_{15}\text{N}_3\text{O}_5$  neg.: 232.21; found: 232.20.

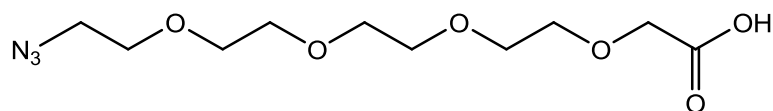
TLC (Dichloromethane/Methanol/Acetic acid, 90/8/2, v/v/v):  $R_f$  = 0.25.

**• 2-(2-azidoethoxy)acetic acid 37:**

A yellowish oil was obtained (g, mmol, %).

$^1\text{H-NMR}$  (300 MHz,  $\text{CDCl}_3$ ):  $\delta$  = 9.31 (br. s, 1H), 4.20 (s, 2H), 3.75 (t,  $J$  = 5 Hz, 2H), 3.46 (t,  $J$  = 5 Hz, 2H) ppm.  $^{13}\text{C-NMR}$  (75 MHz,  $\text{CDCl}_3$ ):  $\delta$  = 175.26, 70.55, 68.11, 50.80 ppm.

• **2-[2-[2-[2-(2-azidoethoxy)ethoxy]ethoxy]ethoxy]-acetic acid 45:**

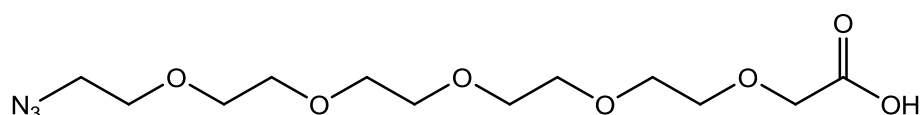


A yellowish oil was obtained (g, mmol, %).

$^1\text{H-NMR}$  (400 MHz,  $\text{CDCl}_3$ ):  $\delta$  = 10.08 (br. s, 1H), 4.11 (s, 2H), 3.68 – 3.71 (m, 2H), 3.60 – 3.65 (m, 12H), 3.33 (t,  $J$  = 5 Hz, 2H) ppm.  $^{13}\text{C-NMR}$  (100 MHz,  $\text{CDCl}_3$ ):  $\delta$  = 173.39, 71.13, 70.58, 70.53, 70.48, 70.41, 70.30, 69.94, 68.51, 50.57 ppm.

MS (ESI) calc. for  $[\text{C}_{10}\text{H}_{19}\text{N}_3\text{O}_6 + \text{Na}]^+$ : 300.12; found: 300.31.

• **2-[2-[2-[2-[2-(2-azidoethoxy)ethoxy]ethoxy]ethoxy]ethoxy]-acetic acid 46:**

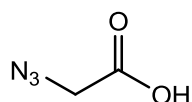


A yellowish oil was obtained (g, mmol, %).

$^1\text{H-NMR}$  (400 MHz,  $\text{CDCl}_3$ ):  $\delta$  = 8.91 (br. s, 1H), 4.11 (s, 2H), 3.67 – 3.70 (m, 2H), 3.60 – 3.65 (m, 16H), 3.35 (t,  $J$  = 5 Hz, 2H) ppm.  $^{13}\text{C-NMR}$  (100 MHz,  $\text{CDCl}_3$ ):  $\delta$  = 173.04, 78.89, 70.53, 70.46, 70.44, 70.43, 70.30, 70.26, 70.21, 69.93, 68.66, 50.58 ppm.

MS (ESI) calc. for  $[\text{C}_{12}\text{H}_{23}\text{N}_3\text{O}_7 + \text{Na}]^+$ : 344.14; found: 344.34.

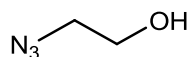
**Synthesis of 2-azidoacetic acid 34:**



The compound was synthesized as published (*Parkhouse et al.* 2008).

Sodium azide (2 eq., 0.98 g, 15 mmol) was dissolved in water (10 mL) and cooled on an ice bath. Bromoacetic acid (1.04 g, 7.5 mmol) was added to the mixture and was stirred at 5 °C for 2 hrs. The mixture was allowed to warm to room temperature and further stirred for 24 hrs. The mixture was acidified to pH = 5 with an aqueous hydrochloric acid solution (1 M), and extracted with diethylether (3 x 30 mL). The ethereal extract was dried and evaporated to dryness to give 2-azidoacetic acid as pale yellow oil (0.26 g, 32 %).

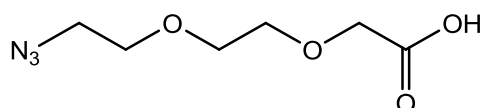
$^1\text{H-NMR}$  (300 MHz,  $\text{CDCl}_3$ ):  $\delta$  = 11.28 (br. s, 1H), 3.97 (s, 2H) ppm.  $^{13}\text{C-NMR}$  (75 MHz,  $\text{CDCl}_3$ ):  $\delta$  = 174.56, 50.08 ppm.

**Synthesis of 2-azidoethanol 35:**

The compound was synthesized as published (*Cheng et al.* 2005).

2-Chloroethanol (16.1 mL, 200 mmol) was added to a solution of sodium azide (1.23 eq., 16.0 g, 246 mmol) and sodium hydroxide (0.1 eq., 0.8 g, 20 mmol) in water (60 mL). The mixture was stirred at room temperature for 3 days, and sodium sulfate was added (19 g). After 10 min, the mixture was extracted with dichloromethane (3 x 37 mL). The combined organic phases were dried over magnesium sulfate, filtered and evaporated. The residue was distilled to give 2-azidoethanol as colourless oil (16.4 g, 94 %).

$^1\text{H-NMR}$  (300 MHz,  $\text{CDCl}_3$ ):  $\delta$  = 3.75 (t,  $J$  = 10 Hz, 2H), 3.41 (t,  $J$  = 10 Hz, 2H), 2.52 (s, 1H) ppm.  $^{13}\text{C-NMR}$  (75 MHz,  $\text{CDCl}_3$ ):  $\delta$  = 61.48, 53.58 ppm.

**Synthesis of 2-[2-(2-azidoethoxy)ethoxy]-acetic acid 38:**

To a stirred solution of 2-[2-(2-azidoethoxy)ethoxy]ethanol **5** (6 mmol) in acetone (6 mL), cooled to 5 °C, an aqueous solution of chromium oxide (3 eq., 1.8 g, 18 mmol) in hydrochloric acid (10 N, 22.5 mL) was added slowly at such a rate that the internal temperature was maintained between 5 and 15 °C. After the addition was complete, the reaction mixture was stirred at 5 °C for 1.5 hr and then at room temperature for 1 hr. After concentration under reduced pressure, the residue was dissolved in water (10 mL) and extracted with diethylether (6 x 20 mL). The combined extracts were washed with water (3 x 20 mL), dried over magnesium sulfate and concentrated. The crude was purified by flash chromatography using dichloromethane/methanol/acetic acid (90/8/2, v/v/v).

A yellowish oil was obtained (g, mmol, %).

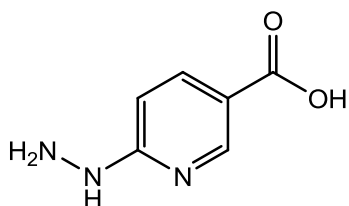
$^1\text{H-NMR}$  (300 MHz,  $\text{CDCl}_3$ ):  $\delta$  = 10.24 (br. s, 1H), 4.17 (s, 2H), 3.63 – 3.74 (m, 6H), 3.41 (t,  $J$  = 5 Hz, 2H) ppm.  $^{13}\text{C-NMR}$  (75 MHz,  $\text{CDCl}_3$ ):  $\delta$  = 174.80, 71.03, 70.47, 70.33, 69.99, 68.29, 67.96, 50.57 ppm.

MS (ESI) calc. for  $[\text{C}_6\text{H}_{11}\text{N}_3\text{O}_4 + \text{Na}]^+$ : 212.06; found: 212.31.

TLC (Dichloromethane/Methanol/Acetic acid, 90/8/2, v/v/v):  $R_f$  = 0.32.

## 5.2.2 Synthesis of HNA and SFB modification reagents

### Synthesis of 6-hydrazinopyridine-3-carboxylic acid **132**:



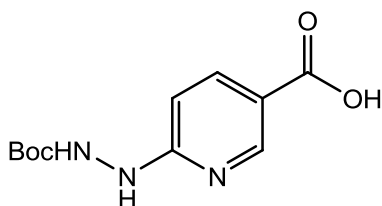
The compound was synthesized as published (*Abrams et al.* 1990).

6-Chloronicotinic acid (1.70 g, 10.8 mmol) was added to 80 % hydrazine monohydrate (large excess) and stirred at 100 °C in an oil bath for 4 hrs. The mixture was cooled to room temperature and concentrated to dryness to give a brown solid. The solid was dissolved in water (30 mL) and the pH was adjusted to 5.5 by addition of an aqueous hydrochloric acid solution (2 M). A yellow precipitate was formed and isolated by filtration. The precipitate was washed with a cold mixture of ethanol and diethylether (95/5, v/v). The precipitate was dried under vacuum and used without further purification (1.33 g, 81 %).

<sup>1</sup>H-NMR (300 MHz, DMSO-d<sub>6</sub>): δ = 8.52 (s, 1H), 8.30 (br. s, 1H), 7.86 (d, *J* = 9 Hz, 1H), 6.71 (s, 1H) ppm. <sup>13</sup>C-NMR (75 MHz, DMSO-d<sub>6</sub>): δ = 166.74, 163.47, 150.60, 137.62, 114.48, 104.91 ppm.

MS (ESI) calc. for [C<sub>6</sub>H<sub>7</sub>N<sub>3</sub>O<sub>2</sub> + H]<sup>+</sup>: 154.05; found: 153.23.

### Synthesis of 6-Boc-hydrazinopyridine-3-carboxylic acid **9** (HNA):



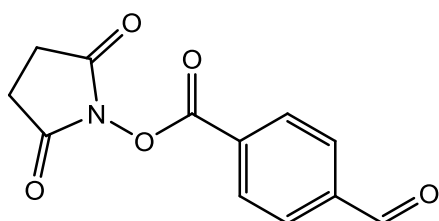
The compound was synthesized as published (*Abrams et al.* 1990).

To a solution of 6-hydrazinopyridine-3-carboxylic acid **132** (0.35 g, 2.5 mmol) and triethylamine (1.2 eq., 3.0 mmol) in dimethylformamide (3 mL) was added di-tert-butyl dicarbonate (1 eq., 0.53 g). The reaction mixture was stirred for 16 hrs. The reaction mixture was concentrated to dryness under reduced pressure to give a brown solid. The residue was triturated in cold ethyl acetate (10 mL), and then filtered to give the desired product as a light yellow solid, which was used without further purification (0.31 g, 53 %).

$^1\text{H-NMR}$  (300 MHz,  $\text{DMSO-d}_6$ ):  $\delta$  = 12.57 (br. s, 1H), 8.97 (br. s, 1H), 8.89 (s, 1H), 8.58 (s, 1H), 7.97 (d,  $J$  = 9 Hz, 1H), 6.54 (d,  $J$  = 9 Hz, 1H), 1.42 (s, 9H) ppm.  $^{13}\text{C-NMR}$  (75 MHz,  $\text{DMSO-d}_6$ ):  $\delta$  = 166.48, 155.67, 150.43, 138.38, 116.62, 79.26, 28.07 ppm.

MS (ESI) calc. for  $[\text{C}_{11}\text{H}_{15}\text{N}_3\text{O}_4 + \text{H}]^+$ : 254.11; found: 254.14.

### Synthesis of p-formylbenzoic acid N-hydroxysuccinimide ester 24 (SFB):

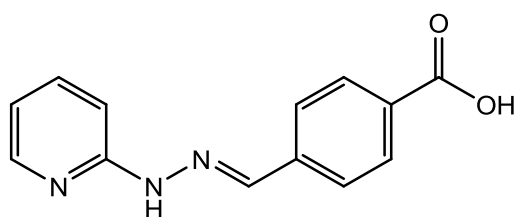


A stirred solution of carboxybenzaldehyde (0.40 g, 2.7 mmol), N-hydroxysuccinimide (1.5 eq., 0.46 g, 4.0 mmol) and diisopropylethylamine (2.2 eq., 6.0 mmol) in dry tetrahydrofuran (50 mL) was cooled to 0°C. N-(3-dimethylaminopropyl)-N'-ethylcarbodiimide (1.1 eq., 3. mmol) was added. The solution was stirred at 0 °C for 30 min and then allowed to warm at room temperature. The reaction was further stirred for 2 hrs, then concentrated under reduced pressure, and finally purified by flash chromatography.

$^1\text{H-NMR}$  (300 MHz,  $\text{CDCl}_3$ ):  $\delta$  = 9.74 (s, 1H), 8.16 (d,  $J$  = 7 Hz, 2H), 7.92 (d,  $J$  = 7 Hz, 2H), 3.53 (s, 4H) ppm.  $^{13}\text{C-NMR}$  (75 MHz,  $\text{CDCl}_3$ ):  $\delta$  = 191.27, 169.05, 161.20, 141.51, 131.34, 129.87, 25.84 ppm.

TLC (AcOEt)  $R_f$  = 0.54.

### Synthesis of 4-[[2-(2-pyridinyl)hydrazinylidene]methyl]-benzoic acid 133:



Carboxybenzaldehyde (3 mmol) was dissolved in a mixture of "conjugation buffer" (100 mM acetate, pH 5.0) and DMF (50/50, v/v) (5 mL). 2-Hydrazinopyridine (1 eq., 3 mmol) was added portionwise under vigorous stirring. The mixture was stirred for 16 hrs and the mixture was filtered. The precipitate was washed with cold diethylether (3 x 20 mL) and dried under vacuum to afford compound **133** as a light brown solid (0.72 g, 100 %).

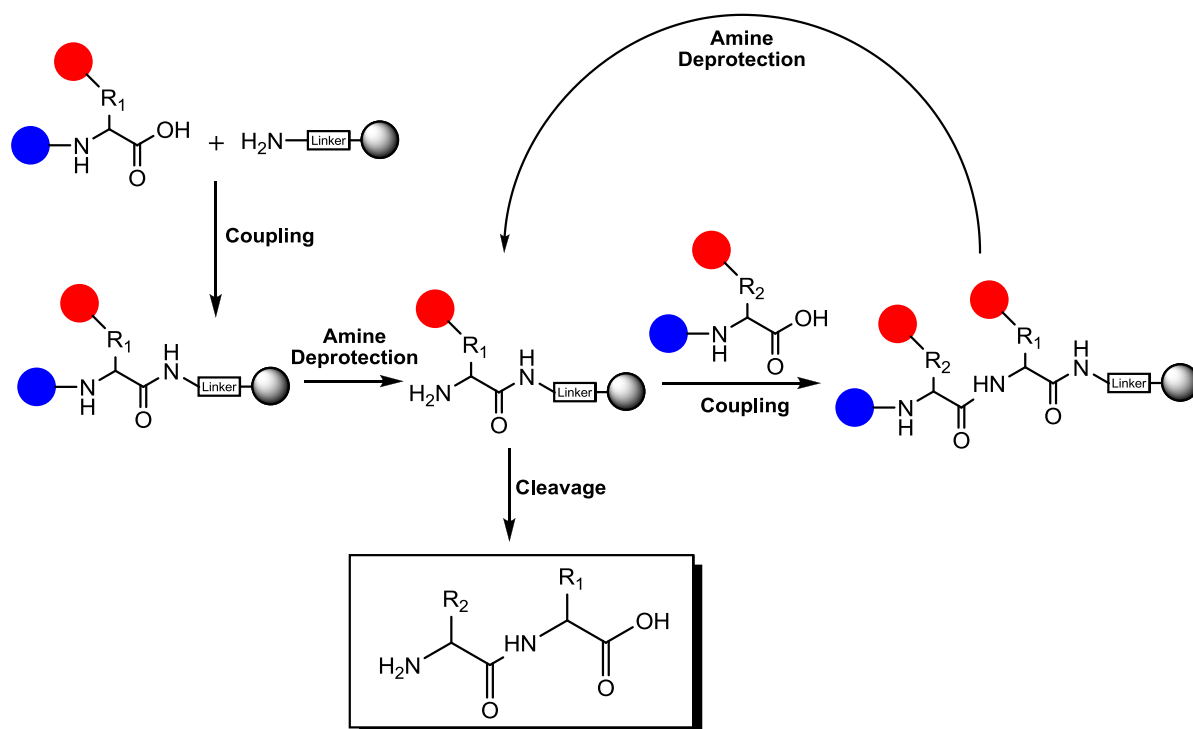


$^1\text{H-NMR}$  (300 MHz,  $\text{DMSO-d}_6$ ):  $\delta = 8.20$  (s, 1H), 8.17 (d,  $J = 6$  Hz, 1H), 8.01 (br. s, 1H), 7.98 (br. s, 1H), 7.94 (br. s, 1H), 7.91, (br. s, 1H), 7.28 (d,  $J = 9$  Hz, 1H), 6.99 (t,  $J = 6$  Hz, 1H) ppm.  $^{13}\text{C-NMR}$  (75 MHz,  $\text{DMSO-d}_6$ ):  $\delta = 166.95, 158.79, 158.46, 158.14, 157.81, 138.39, 131.28, 129.68, 126.95, 118.22, 115.33$  ppm.

MS (ESI) calc. for  $[\text{C}_{13}\text{H}_{11}\text{N}_3\text{O}_2 + \text{H}]^+$ : 242.09; found: 242.10.

## 5.2.3 Solid phase synthesis of peptides

### 5.2.3.1 Standard SPPS procedure



**Figure 52: The coupling-wash-deprotection-wash cycle in SPPS.** N-protected amino acid residues are coupled sequentially on a functionalized resin. Cleavage from the solid support releases the fully unprotected peptide.

A functionalized resin was weighted in a polypropylene syringe reactor. It was swelled for 1 hr in dried DCM (1 mL/100 mg resin), then filtered and washed with DMF (4 x 1 mL/100 mg resin). The resin was treated with 20 % 4-methylpiperidine in DMF (1 mL/100 mg resin) for 20 min, then filtered and washed with DMF (4 x 1 mL/100 mg resin). To the resin was added a solution of Fmoc-AA-OH (4 eq.), HATU (3.8 eq.) or HBTU (3.8 eq.)/HOBt (3.8 eq.) and DIEA (8 eq.) in DMF (1 mL/100 mg resin) or DMF/NMP (50/50, v/v) (1 mL/100 mg resin) respectively. HATU was used for N-Fmoc amino acid residue coupling to secondary amino acid residues. Unless otherwise mentioned, HBTU/HOBt was systematically used as coupling reagent. After the mixture was shaken for 2 hrs, the resin was

filtered and washed with DMF (1 mL/100 mg resin). The resin was treated with acetic anhydride (8 eq.) and DIEA (8 eq.) in DMF (1 mL/100 mg resin) for 15 min. The resin was filtered and washed with DMF (1 mL/100 mg resin). The above operation cycle was repeated with the desired N-Fmoc protected amino acid residues. After coupling of the final amino acid, the resin was treated with 20 % 4-methylpiperidine in DMF (1 mL/100 mg resin) for 20 min. The resin was filtered and washed with DMF (4 x 1 mL/100 mg resin). The resin was then either left as a free terminal amine or treated with acetic anhydride (8 eq.) and DIEA (8 eq.) in DMF (1 mL/100 mg resin) for 15 min. The resin was filtered and washed with DMF (4 x 1 mL/100 mg resin), methanol (4 x 1 mL/100 mg resin), chloroform (1 mL/100 mg resin) and diethylether (4 x 1 mL/100 mg resin), and then dried under vacuum. The resin was transferred into a round bottom flask and TFA/water/TIS (95/2.5/2.5, v/v/v) (1 mL/100 mg resin) was added. After the mixture was shaken for 2 hrs, the resin was filtered and washed with TFA/water/TIS (95/2.5/2.5) (0.5 mL/100 mg resin). The filtrate and washings were combined, and then concentrated to approximately 1 mL with a light air stream. To the solution was added cold diethylether (20 mL/100 mg resin), the mixture was then shaken and centrifugated. After removal of supernatant by decantation, the precipitate was washed again with diethylether, and then dried. Typically, the dried precipitate was dissolved in acetonitrile/water/trifluoroacetic acid (1/1/1, v/v/v) and analyzed by reverse phase HPLC. The peptides were purified by preparative HPLC where indicated.

#### **5.2.3.2 Synthesis of CRHR<sub>1</sub>-ECD1 specific high-affinity peptide probes**

Rink amide resin (0.45 mmol/g, 100-200 mesh) (0.25 g, 0.113 mmol) was treated with 20 % 4-methylpiperidine in DMF (2.5 mL) for 20 min. The resin was filtered and washed with DMF (4 x 2.5 mL). To the resin was added a solution of Fmoc-Ile-OH (4 eq., 0.45 mmol), HBTU (3.8 eq., 0.43 mmol), HOBt (3.8 eq., 0.43 mmol) and DIEA (8 eq., 0.9 mmol) in DMF/NMP (50/50, v/v) (2.5 mL). The mixture was shaken for 2 hrs, then the resin was filtered and washed with DMF (4 x 2.5 mL). The resin was treated with acetic anhydride (8 eq., 0.9 mmol) and DIEA (8 eq., 0.9 mmol) in DMF/NMP (50/50, v/v) (2.5 mL). The above operation cycle was repeated with the following N-Fmoc protected amino acid residues: Fmoc-Ile-OH, Fmoc-Asp(OtBu)-OH, Fmoc-Cha-OH, Fmoc-Leu-OH, Fmoc-Lys(Boc)-OH or Fmoc-Lys(ivDde)-OH (for the synthesis of fluorescently tagged peptides), Fmoc-Arg(Pbf)-OH, Fmoc-Lys(alloc)-OH, Fmoc-Glu(OtBu)-OH, Fmoc-Ala-OH, Fmoc-Glu(OAll)-OH and Fmoc-Gln(Trt)-OH. After the final amino acid coupling, the resin was filtered and washed with DMF (4 x 2.5 mL), methanol (2 x 2.5 mL), chloroform (4 x 2.5 mL) and diethylether (2.5 mL), then dried under vacuum. The resin was transferred into a round bottom flask (25 mL) and swelled in a solution of chloroform (9.5 mL), acetic acid (0.5 mL) and NMM (0.25 mL). After argon gas was bubbled through the mixture for 15 min, (Ph<sub>3</sub>P)<sub>4</sub>Pd (3 eq., 0.34 mmol) was added. After the mixture was shaken for 16

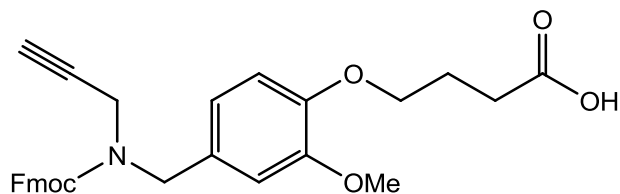
hrs, the resin was filtered and washed with chloroform (3 x 2.5 mL), DMF (3 x 2.5 mL), 0.5% DIEA in DMF (3 x 2.5 mL), 0.02M EtNCS<sub>2</sub>Na in DMF (3 x 2.5 mL) and DMF (5 x 2.5 mL). To the resin was added a solution of PyBop (3 eq., 0.34 mmol), HOBt (3 eq., 0.34 mmol) and DIEA (9 eq., 0.45 mmol) in DMF/NMP (50/50, v/v) (7.5 mL). After the mixture was shaken for 16 hrs, the resin was filtered and washed with DMF (4 x 2.5 mL). The resin was treated with 20 % 4-methylpiperidine in DMF (2.5 mL) for 20 min. The resin was filtered and washed with DMF (4 x 2.5 mL). To the resin was added a solution of azide-functionalized ethylene glycol spacer **7**, **34**, **37**, **38**, **45**, **46** or HNA **9** (4 eq., 0.45 mmol), HBTU (3.8 eq., 0.43 mmol), HOBt (3.8 eq., 0.43 mmol) and DIEA (8 eq., 0.9 mmol) in DMF/NMP (50/50, v/v) (2.5 mL). Thereafter, the mixture was shaken for 2 hrs, and the resin was filtered and washed with DMF (4 x 2.5 mL). For the synthesis of fluorescently tagged peptides **2**, **27**, **28**, **29**, **30** and **31**, the resin was treated with 3 % hydrazine in DMF (10 x 2.5 mL) for 5 min. The resin was filtered and washed with DMF (5 x 2.5 mL). To the resin was added a solution of 4-chloro-7-nitrobenzofurazan (4 eq., 0.45 mmol) and DIEA (8 eq., 0.9 mmol) in DMF/NMP (50/50, v/v) (2.5 mL). After the mixture was shaken for 16 hrs, the 4-chloro-7-nitrobenzofurazan coupling was repeated. The mixture was shaken for 2 hrs, the resin was filtered and washed with DMF (4 x 2.5 mL), methanol (2 x 2.5 mL), chloroform (4 x 2.5 mL) and diethylether (2.5 mL), then dried under vacuum. The resin was transferred into a round bottom flask (10 mL) and TFA/water/TIS (95/2.5/2.5, v/v/v) (4 mL) was added. After the mixture was shaken for 1 hr, the resin was filtered and washed with TFA/water/TIS (95/2.5/2.5, v/v/v) (2 x 1 mL). The filtrate and washings were combined and concentrated down to 2 mL using a light air stream. To the solution was added cold diethylether (35 mL), and the mixture was shaken and centrifugated. After removal of supernatant by decantation, the precipitate was washed with cold diethylether, and then dried under vacuum. The precipitate was dissolved in acetonitrile/water (50/50, v/v), then purified by preparative HPLC according to the following procedure: a solution of the crude peptidic carrier in acetonitrile/water (50/50, v/v) (1.5 mL) was loaded onto the column (Jupiter 10µm Proteo 90Å 250 x 21.2 mm) at a flow of 25 mL/min. The mobile phase was held at 60 % in buffer A (buffer A: 0.1 % TFA in water/acetonitrile, 95/5, v/v; buffer B: 0.1 % TFA in acetonitrile/water, 95/5, v/v) for 3 min, then the gradient was started at 40 % B in A to 60 % B in A in 15 min. The peptide containing fractions were combined and lyophilized to give pure the desired peptide carrier.

	Peptide sequence	R =	Mass calc. [M+H] <sup>+</sup>	Mass calc. [M+2H] <sup>2+</sup>	Mass found [M+2H] <sup>2+</sup>	Purity (%)	Yield (%)
1	R-EAEK <sup>K</sup> NRK <sup>K</sup> LXDII-NH <sub>2</sub>	Ac-	1504.88	752.94	753.53	97	17
2	R-QEAEK <sup>K</sup> NRK <sup>K</sup> LXDII-NH <sub>2</sub>	N <sub>3</sub> -TEG	1969.02	985.01	996.33	99	8
3	R-QEAEK <sup>K</sup> NRK <sup>K</sup> LXDII-NH <sub>2</sub>	HNA	1725.97	863.49	864.00	95	12
27	R-QEAEK <sup>K</sup> NRK <sup>K</sup> LXDII-NH <sub>2</sub>	N <sub>3</sub> -	1836.94	918.97	930.31 <sup>(a)</sup>	92	10
28	R-QEAEK <sup>K</sup> NRK <sup>K</sup> LXDII-NH <sub>2</sub>	N <sub>3</sub> -MEG	1880.97	940.99	952.36	96	5
29	R-QEAEK <sup>K</sup> NRK <sup>K</sup> LXDII-NH <sub>2</sub>	N <sub>3</sub> -DEG	1924.99	963.00	974.47	96	5
30	R-QEAEK <sup>K</sup> NRK <sup>K</sup> LXDII-NH <sub>2</sub>	N <sub>3</sub> -PEG <sup>4</sup>	2013.04	1007.02	1018.40	95	8
31	R-QEAEK <sup>K</sup> NRK <sup>K</sup> LXDII-NH <sub>2</sub>	N <sub>3</sub> -PEG <sup>5</sup>	2057.07	1029.04	1040.39	99	11

**Table 25. Characterization of purified CRHR<sub>1</sub>-ECD1 high-affinity peptide probes.** <sup>(a)</sup> Mass found corresponds to [M + H + Na]<sup>2+</sup>. EAEK = lactam bridge; K = NBD-tagged lysine.

### 5.2.3.3 Synthesis of BAL solid support

#### Synthesis of 4-(3-methoxy-4-((9H-fluoren-9-ylmethoxycarbonyl)(prop-2-ynyl)-amino)methyl)(1)phenoxy) butanoic Acid 21:



To a stirred solution of 4-(4'-formyl-3'-methoxyphenoxy) butanoic acid (Iris Biotech, Germany) (1.2 g, 5 mmol) in anhydrous methanol (75 mL) and under argon atmosphere were added propargylamine (1.5 eq., 7.5 mmol), acetic acid (1.5 eq., 7.5 mmol) and sodium cyanoborohydride (1.2 eq., 6 mmol). The mixture was stirred for 90 min followed by evaporation of the solvents under reduced pressure. The crude product was dissolved in 1,4-dioxane/acetonitrile/water (1/1/1, v/v/v) (15 mL), and then cooled down to 0 °C in an ice bath. Sodium hydrogen carbonate (3 eq., 15 mmol) was added and the mixture was stirred for 5 min. To the mixture was added dropwise a solution of 9-fluorenylmethyl chloroformate (2 eq., 10 mmol) in 1,4-dioxane (10 mL). The mixture was stirred for 16 hrs at room temperature. The organic phase was evaporated under reduced pressure and the aqueous phase was acidified to pH = 2 using an aqueous hydrochloric acid solution (5 %). The aqueous phase was extracted with ethyl acetate (4 x 100 mL). The combined organic phases were dried over magnesium sulfate, filtered and concentrated under reduced pressure. The crude product was purified by flash chromatography using ethyl acetate/hexanes (50/50, v/v). A white solid was obtained (1.9 g, 3.9 mmol, 77 %).

$^1\text{H-NMR}$  (400 MHz,  $\text{CDCl}_3$ ):  $\delta$  = 7.75 (d,  $J$  = 8 Hz, 2H), 7.58 (br. s., 2H), 7.38 (t,  $J$  = 7 Hz, 2H), 7.28 (t,  $J$  = 7 Hz, 2H), 6.46 (d,  $J$  = 2 Hz, 1H), 6.40 (br. s., 1H), 4.54 (br. s., 2H), 4.49 (d,  $J$  = 6 Hz, 2H), 4.27 (br. s., 1H), 4.08 (br. s., 2H), 4.03 (t,  $J$  = 6 Hz, 2H), 3.80 (s, 3H), 2.59 (t,  $J$  = 7 Hz, 2H), 2.19 (m, 1H), 2.13 (m, 2H) ppm.  $^{13}\text{C-NMR}$  (100 MHz,  $\text{CDCl}_3$ ):  $\delta$  = 178.0, 159.9, 144.3, 141.6, 127.8, 127.2, 125.3, 125.3, 120.1, 118.0, 105.3, 99.3, 79.8, 71.5, 68.0, 67.0, 55.6, 47.6, 44.9, 36.3, 30.5, 24.7 ppm.

MS (ESI) calc. for  $[\text{C}_{30}\text{H}_{29}\text{NO}_6 + \text{Na}]^+$ : 522.19; found: 522.13.

TLC (AcOEt):  $R_f$  = 0.22.

**Synthesis of solid support 22:**

Tentagel™ S-NH<sub>2</sub> resin (0.45 mmol/g, 150-200 μm, Sigma-Aldrich, Germany) (1.0 g, 0.45 mmol) was swollen in dichloromethane (10 mL) for 1 hr. The resin was filtered and washed with DMF (4 x 10 mL). To the resin was added a solution of modified FMPB linker **21** (4 eq., 1.8 mmol), HATU (4 eq., 1.8 mmol) and DIEA (8 eq., 3.6 mmol) in DMF (10 mL). After that the mixture was shaken for 4 hrs, the resin was filtered and washed with DMF (4 x 10 mL), methanol (2 x 10 mL), chloroform (4 x 10 mL) and diethylether (10 mL), then dried under vacuum. Final loading (0.38 mmol/g) of the resin was calculated according to the UV-Fmoc test.

**5.2.3.4 Synthesis of C-terminally propargylated peptides**

BAL resin **22** (0.38 mmol/g) (100 mg, 38 μmol) was swollen in dichloromethane (1 mL) for 1 hr. The resin was filtered and washed with DMF (4 x 1 mL). The resin was treated with 20 % 4-methylpiperidine in DMF (1 mL) for 20 min. The resin was filtered and the previous treatment was repeated. The resin was filtered and washed with DMF (5 x 1 mL). To the resin was added a solution of Fmoc-AA-OH (4 eq., 152 μmol), HATU (3.8 eq., 144 μmol) and DIEA (8 eq., 304 μmol) in DMF (1 mL). After the mixture was shaken for 4 hrs, the resin was filtered and the coupling step was repeated. After the mixture was shaken for 2 hrs, the resin was filtered and washed with DMF (4 x 1 mL). The resin was treated with acetic anhydride (8 eq., 304 μmol) and DIEA (8 eq., 304 μmol) in DMF/NMP (50/50, v/v) (1 mL) for 15 min. The resin was filtered and washed with DMF (4 x 1 mL). The resin was treated with 20 % 4-methylpiperidine in DMF (1 mL) for 20 min. The resin was filtered and washed with DMF (5 x 1 mL). To the resin was added a solution of Fmoc-AA-OH (4 eq., 152 μmol), HBTU (3.8 eq., 144 μmol), HOBT (3.8 eq., 144 μmol) and DIEA (8 eq., 304 μmol). After the mixture was shaken for 2 hrs, the resin was filtered and washed with DMF (4 x 1 mL). The resin was treated with acetic anhydride (8 eq., 304 μmol) and DIEA (8 eq., 304 μmol) in DMF/NMP (50/50, v/v) (1 mL) for 15 min. The resin was filtered and washed with DMF (4 x 1 mL). The above operation cycle was repeated with the desired N-Fmoc protected amino acid residues. After coupling of the final amino acid, the resin was treated with 20 % 4-methylpiperidine in DMF (1 mL) for 20 min. The resin was filtered and washed with DMF (5 x 1 mL). The resin was treated with acetic anhydride (8 eq., 304 μmol) and DIEA (8 eq., 304 μmol) in DMF/NMP (50/50, v/v) (1 mL) for 15 min. The resin was filtered and washed with DMF (4 x 1 mL), methanol (2 x 1 mL), chloroform (4 x 1 mL) and ether (1 mL), then dried under vacuum. The resin was transferred into a round bottom flask (5 mL) and TFA/water/TIS (95/2.5/2.5, v/v/v) (1.5 mL) was added. After the mixture was shaken for 1 hr, the resin was filtered and washed with TFA/water/TIS (95/2.5/2.5, v/v/v) (0.5 mL). The filtrate and washings were combined, and then concentrated to approximately 1 mL with a light air stream. To the solution was

added cold ether (20 mL), and the mixture was shaken and centrifugated. After removal of the supernatant by decantation, the precipitate was washed with diethylether, and then dried. The precipitate was dissolved in acetonitrile/water (1/1, v/v) and used directly for conjugation.

R = propargyl		Mass calc. [M+H] <sup>+</sup>	Mass found [M+H] <sup>+</sup>	Purity (%)	Yield (%)	
Peptide sequence						
15	Ac-UCN <sup>1-15</sup> -R	Ac-DNPSLSIDLTFHLLR-R	1819.96	1819.93	92	12
	Ac-UCN <sup>1-14</sup> -R	Ac-DNPSLSIDLTFHLL-R	1663.86	1663.91	96	34
	Ac-UCN <sup>2-15</sup> -R	Ac-NPSLSIDLTFHLLR-R	1704.94	1704.90	92	45
	Ac-UCN <sup>3-15</sup> -R	Ac-PSLSIDLTFHLLR-R	1590.89	1590.94	97	9
	Ac-UCN <sup>4-15</sup> -R	Ac-SLSIDLTFHLLR-R	1493.84	1493.77	94	71
	Ac-UCN <sup>5-15</sup> -R	Ac-LSIDLTFHLLR-R	1406.81	1406.75	96	71
	Ac-UCN <sup>6-15</sup> -R	Ac-SIDLTFHLLR-R	1293.72	1293.72	95	80
	Ac-[Thr <sup>4</sup> Cha <sup>5</sup> ]UCN <sup>4-15</sup> -R		1547.89	1548.04	97	65
	Ac-[Thr <sup>4</sup> Cha <sup>5</sup> D-Phe <sup>11</sup> ]UCN <sup>4-15</sup> -R		1547.89	1548.10	97	68
	Ac-[Thr <sup>4</sup> Cha <sup>5,13</sup> D-Phe <sup>11</sup> ]UCN <sup>4-15</sup> -R		1587.92	1588.07	98	67
	Ac-[Thr <sup>4</sup> Cha <sup>5,13</sup> Chg <sup>7</sup> D-Phe <sup>11</sup> ]UCN <sup>4-15</sup> -R		1613.93	1614.07	100	42
	Ac-[Thr <sup>4</sup> Cha <sup>5,13</sup> Chg <sup>7</sup> tBuAla <sup>9</sup> D-Phe <sup>11</sup> ]UCN <sup>4-15</sup> -R		1627.95	1628.11	98	46
	Ac-[D-Phe <sup>11</sup> ]UCN <sup>4-15</sup> -R		1493.84	1493.90	92	43
	Ac-[D-Nal(1) <sup>11</sup> ]UCN <sup>4-15</sup> -R		1543.86	1543.93	71	45
	Ac-[D-Nal(2) <sup>11</sup> ]UCN <sup>4-15</sup> -R		1543.86	1543.91	70	53
	Ac-[D-Pal <sup>11</sup> ]UCN <sup>4-15</sup> -R		1494.84	1494.89	88	75
	Ac-[D-pNO <sub>2</sub> -Phe <sup>11</sup> ]UCN <sup>4-15</sup> -R		1538.83	1538.86	92	25
	Ac-[Ach <sup>11</sup> ]UCN <sup>4-15</sup> -R		1471.86	1472.00	69	27
	Ac-[Acp <sup>11</sup> ]UCN <sup>4-15</sup> -R		1457.84	1457.88	88	32
	Ac-[Aic <sup>11</sup> ]UCN <sup>4-15</sup> -R		1505.84	1527.81	54	44
Ac-[D-Trp <sup>11</sup> ]UCN <sup>4-15</sup> -R		1532.85	1532.75	92	14	
90	Ac-AST <sup>1-14</sup> -R	Ac-fHLLREVLEBARAE-R	1774.99	887.47 <sup>(a)</sup>	95	10
	Ac-AST <sup>1-13</sup> -R	Ac-fHLLREVLEBARA-R	1645.95	823.90 <sup>(a)</sup>	94	77
	Ac-AST <sup>1-12</sup> -R	Ac-fHLLREVLEBAR-R	1574.91	1547.94	98	48
	Ac-AST <sup>1-11</sup> -R	Ac-fHLLREVLEBA-R	1418.81	1418.80	98	35

MATERIAL & METHODS

	Ac-AST <sup>1-10</sup> -R	Ac-fHLLREVLEB-R	1347.77	1347.75	98	65
	Ac-AST <sup>1-9</sup> -R	Ac-fHLLREVLE-R	1234.69	624.41 <sup>(a)</sup>	92	79
	Ac-AST <sup>1-8</sup> -R	Ac-fHLLREVL-R	1105.64	1104.71	98	76
	Ac-AST <sup>1-7</sup> -R	Ac-fHLLREV-R	992.56	992.63	99	86
	Ac-AST <sup>1-6</sup> -R	Ac-fHLLRE-R	893.49	893.56	98	91
	Ac-AST <sup>1-5</sup> -R	Ac-fHLLR-R	764.45	764.54	98	90
	H <sub>2</sub> N-AST <sup>1-11</sup> -R	H <sub>2</sub> N-fHLLREVLEBA-R	1376.80	1376.93	97	42
	Ac-AST <sup>2-11</sup> -R	Ac-HLLREVLEBA-R	1271.74	1271.82	88	64
	Ac-[Cha <sup>2</sup> tBuAla <sup>3</sup> ]AST <sup>1-11</sup> -R		1448.88	1449.00	75	72
	Ac-[Cha <sup>2</sup> Aib <sup>4</sup> ]AST <sup>1-11</sup> -R		1406.83	1406.85	72	61
	Ac-[tBuAla <sup>3</sup> Aib <sup>4</sup> ]AST <sup>1-11</sup> -R		1404.79	1404.85	65	70
	Ac-[Cha <sup>2</sup> tBuAla <sup>3</sup> Aib <sup>4</sup> ]AST <sup>1-11</sup> -R		1420.85	1420.91	82	70
	Ac-[Cha <sup>2</sup> Aib <sup>4</sup> tBuAla <sup>8</sup> ]AST <sup>1-11</sup> -R		1420.85	1420.85	88	55
	Ac-[D-Pal <sup>1</sup> Cha <sup>2</sup> tBuAla <sup>3</sup> Aib <sup>4</sup> ]AST <sup>1-11</sup> -R		1421.84	1421.90	94	79
	Ac-[Cha <sup>2</sup> tBuAla <sup>3,8</sup> Aib <sup>4</sup> ]AST <sup>1-11</sup> -R		1434.86	1435.01	92	9
	Ac-[D-pBrPhe <sup>1</sup> Cha <sup>2,10</sup> Aib <sup>4</sup> tBuAla <sup>8</sup> ]AST <sup>1-11</sup> -R		1538.79	1540.78	72	64
	Ac-[Cha <sup>2,10</sup> tBuAla <sup>3,8</sup> Aib <sup>4</sup> ]AST <sup>1-11</sup> -R		1474.90	1475.06	84	62
	H <sub>2</sub> N-[Cha <sup>2</sup> tBuAla <sup>3</sup> ]AST <sup>1-11</sup> -R		1406.87	1406.93	96	79
	H <sub>2</sub> N-[Cha <sup>2</sup> Aib <sup>4</sup> ]AST <sup>1-11</sup> -R		1364.82	1364.91	94	73
	H <sub>2</sub> N-[tBuAla <sup>3</sup> Aib <sup>4</sup> ]AST <sup>1-11</sup> -R		1362.78	1362.86	97	89
	H <sub>2</sub> N-[Cha <sup>2</sup> tBuAla <sup>3</sup> Aib <sup>4</sup> ]AST <sup>1-11</sup> -R		1378.84	1378.89	91	80
	H <sub>2</sub> N-[Cha <sup>2</sup> Aib <sup>4</sup> tBuAla <sup>8</sup> ]AST <sup>1-11</sup> -R		1378.84	1378.89	98	91
	H <sub>2</sub> N-[D-Pal <sup>1</sup> Cha <sup>2</sup> tBuAla <sup>3</sup> Aib <sup>4</sup> ]AST <sup>1-11</sup> -R		1379.83	1379.91	98	72
	H <sub>2</sub> N-[Cha <sup>2</sup> tBuAla <sup>3,8</sup> Aib <sup>4</sup> ]AST <sup>1-11</sup> -R		1392.85	1392.96	97	90
	H <sub>2</sub> N-[D-pBrPhe <sup>1</sup> Cha <sup>2,10</sup> Aib <sup>4</sup> tBuAla <sup>8</sup> ]AST <sup>1-11</sup> -R		1496.78	1498.80	92	79
	H <sub>2</sub> N-[Cha <sup>2,10</sup> tBuAla <sup>3,8</sup> Aib <sup>4</sup> ]AST <sup>1-11</sup> -R		1432.89	1433.00	94	80

**Table 26. Characterization of truncated and substituted analogs of the N-terminally propargylated fragments of human urocortin1 and astressin.** <sup>(a)</sup> Mass found corresponds to  $[M + 2H]^{2+}$ .



### 5.2.3.5 Flexchem synthesis of the propargylated peptide libraries

In each vial of a FlexChem® 96 well reactor block (SciGene, CA, USA) was introduced BAL resin **22** (0.38 mmol/g) (10 mg x 96). The resins were swollen in dichloromethane for 1 hr, then filtered and washed with DMF (4 x 1 mL). The resins were treated with 20 % 4-methylpiperidine for 20 min. The resins were filtered and washed with DMF (5 x 1 mL). In each well was added a solution of Fmoc-AA-OH (5 eq., 19 µmol), HATU (4.8 eq., 18 µmol) and DIEA (10 eq., 38 µmol) in DMF (0.5 mL). After that the reactor block was shaken for 4 hrs, the resins were filtered and washed with DMF (1 mL x 4). The resins were treated with acetic anhydride (10 eq., 38 µmol) and DIEA (10 eq., 38 µmol) in DMF/NMP (50/50, v/v) (0.5 mL) for 15 min. The resins were filtered and washed with DMF (4 x 1 mL). The resins were treated with 20 % 4-methylpiperidine in DMF (1 mL) for 20 min. The resins were filtered and washed with DMF (5 x 1 mL). In each well was added a solution of Fmoc-AA-OH (5 eq., 19 µmol), HBTU (4.8 eq., 18 µmol), HOBt (4.8 eq., 18 µmol) and DIEA (10 eq., 38 µmol) in DMF/NMP (50/50, v/v) (0.5 mL). After that the reactor block was shaken for 2 hrs, the resins were filtered and washed with DMF (4 x 1 mL). The above operation cycle was repeated with the desired N-Fmoc protected amino acid residues. After that the final amino acid was coupled, the resins were treated with 20 % 4-methylpiperidine in DMF (1 mL) for 20 min. The resins were filtered and washed with DMF (5 x 1 mL). The resins were treated with acetic anhydride (10 eq., 38 µmol) and DIEA (10 eq., 38 µmol) in DMF/NMP (50/50, v/v) (0.5 mL) for 15 min. The resins were filtered and washed with DMF (4 x 1 mL), methanol (2 x 1 mL), chloroform (4 x 1 mL) and diethylether (1 mL), then dried under vacuum. In each well was added TFA/water/TIS (95/2.5/2.5, v/v/v) (0.5 mL) and the reactor block was shaken for 1 hr. The resins were filtered and filtrates were collected into a 96 x 2 mL well plate. The resins were washed with TFA/water/TIS (95/2.5/2.5, v/v/v) (2 x 0.2 mL). The filtrate and washings were combined and reduced down to 0.1 mL with a light air stream. In each well was added cold ether (2 mL), and the mixture was shaken and centrifugated. After removal of supernatant by decantation, the precipitates were washed with ether (0.5 mL), and then dried under vacuum. The precipitate were dissolved in acetonitrile/water (1/1, v/v) and transferred into reaction tubes (1.5 mL). The solvents were evaporated under reduced pressure and the crude residues were dissolved in buffer A/B (1/1, v/v) to a final concentration of 1 mM.

		R = propargyl			Mass calc. [M+H] <sup>+</sup>	Mass found [M+H] <sup>+</sup>	Purity (%)	Yield (%)
Peptide	Subst.	N-terminal Sequence						
Ser <sup>4</sup>	A1	Ala	Ac-ALSIDLTFHLLR-		1477.85	1478.03	53	23
	B1	Aib	Ac-(Aib)LSIDLTFHLLR-		1491.86	1492.04	41	10
	C1	D-Ser	Ac-(D-Ser)LSIDLTFHLLR-		1493.84	1494.03	30	36
	D1	Thr	Ac-TLSIDLTFHLLR-		1507.86	1508.09	38	20
	E1	Glu	Ac-ELSIDLTFHLLR-		1535.85	1535.00	61	13
	F1	Lys	Ac-KLSIDLTFHLLR-		1534.90	1535.08	61	22
	G1	Dap	Ac-(Dap)LSIDLTFHLLR-		1492.86	1493.21	51	32
	H1	h-Ser	Ac-(h-Ser)LSIDLTFHLLR-		1507.86	1507.98	32	8
Leu <sup>5</sup>	A2	Ala	Ac-SASIDLTFHLLR-		1451.79	1451.99	83	31
	B2	Aib	Ac-S(Aib)SIDLTFHLLR-		1465.81	1465.98	80	8
	C2	D-Leu	Ac-S(D-Leu)SIDLTFHLLR-		1493.84	1494.02	41	24
	D2	Ile	Ac-SISIDLTFHLLR-		1493.84	1493.94	37	26
	E2	Glu	Ac-SESIDLTFHLLR-		1509.80	1509.98	79	24
	F2	Lys	Ac-SKSIDLTFHLLR-		1508.85	1508.99	51	21
	G2	Cha	Ac-S(Cha)SIDLTFHLLR-		1533.87	1534.05	59	18
	H2	Nleu	Ac-S(Nleu)SIDLTFHLLR-		1493.84	1494.03	38	24
Ser <sup>6</sup>	A3	Ala	Ac-SLAIDLTFHLLR-		1477.85	1478.02	72	25
	B3	Aib	Ac-SL(Aib)IDLTFHLLR-		1491.86	1492.04	55	9
	C3	D-Ser	Ac-SL(D-Ser)IDLTFHLLR-		1493.84	1493.96	78	21
	D3	Thr	Ac-SLTIDLTFHLLR-		1507.86	1508.09	61	21
	E3	Glu	Ac-SLEIDLTFHLLR-		1535.85	1536.04	72	27
	F3	Lys	Ac-SLKIDLTFHLLR-		1534.90	1535.07	47	22
	G3	Dap	Ac-SL(Dap)IDLTFHLLR-		1492.86	1493.02	39	34
	H3	h-Ser	Ac-SL(h-Ser)IDLTFHLLR-		1507.86	1508.03	41	14
Ile <sup>7</sup>	A4	Ala	Ac-SLSADLTFHLLR-		1451.79	1451.93	53	21
	B4	Aib	Ac-SLS(Aib)DLTFHLLR-		1465.81	1465.99	67	13
	C4	D-Ile	Ac-SLS(D-Ile)DLTFHLLR-		1493.84	1494.10	28	34
	D4	Leu	Ac-SLSLDLTFHLLR-		1493.84	1494.01	29	20
	E4	Val	Ac-SLSVDLTFHLLR-		1479.82	1480.00	65	25

	<b>F4</b>	Thr	Ac-SLSTDLTFHLLR-	1481.80	1481.94	74	25
	<b>G4</b>	Chg	Ac-SLS(Chg)DLTFHLLR-	1519.86	1520.03	70	23
	<b>H4</b>	tBuGly	Ac-SLS(tBuGly)DLTFHLLR-	1493.84	1494.03	51	30
<b>Asp<sup>8</sup></b>	<b>A5</b>	Ala	Ac-SLSIALTFHLLR-	1449.85	1450.15	59	32
	<b>B5</b>	Aib	Ac-SLSI(Aib)LTFHLLR-	1463.87	1464.06	84	8
	<b>C5</b>	D-Asp	Ac-SLSI(D-Asp)LTFHLLR-	1493.84	1494.01	24	23
	<b>D5</b>	Asn	Ac-SLSINLTFHLLR-	1492.86	1493.02	28	24
	<b>E5</b>	Glu	Ac-SLSIELTFHLLR-	1507.86	1508.00	31	17
	<b>F5</b>	Thr	Ac-SLSITLTFHLLR-	1479.86	1480.19	19	21
	<b>G5</b>	Dab	Ac-SLSI(Dab)LTFHLLR-	1478.88	1478.05	39	26
	<b>H5</b>	h-Ser	Ac-SLSI(h-Ser)LTFHLLR-	1479.86	1480.00	41	21
<b>Leu<sup>9</sup></b>	<b>A6</b>	Ala	Ac-SLSIDATFHLLR-	1451.79	1452.05	72	30
	<b>B6</b>	Aib	Ac-SLSID(Aib)TFHLLR-	1465.81	1465.99	58	16
	<b>C6</b>	D-Leu	Ac-SLSID(D-Leu)TFHLLR-	1493.84	1494.05	42	21
	<b>D6</b>	Ile	Ac-SLSIDITFHLLR-	1493.84	1494.16	66	20
	<b>E6</b>	Val	Ac-SLSIDVTFHLLR-	1479.82	1480.21	100	21
	<b>F6</b>	Phe	Ac-SLSIDFTFHLLR-	1527.82	1527.99	61	38
	<b>G6</b>	Cha	Ac-SLSID(Cha)TFHLLR-	1533.87	1534.02	51	24
	<b>H6</b>	tBuAla	Ac-SLSID(tBuAla)TFHLLR-	1507.86	1508.03	27	19
<b>Thr<sup>10</sup></b>	<b>A7</b>	Ala	Ac-SLSIDLAFHLLR-	1463.83	1464.25	71	27
	<b>B7</b>	Aib	Ac-SLSIDL(Aib)FHLLR-	1477.85	740.10	50	15
	<b>C7</b>	D-Thr	Ac-SLSIDL(D-Thr)FHLLR-	1493.84	1493.98	33	23
	<b>D7</b>	Ser	Ac-SLSIDLSFHLLR-	1479.82	1479.99	85	22
	<b>E7</b>	Glu	Ac-SLSIDLEFHLLR-	1521.84	1522.00	22	35
	<b>F7</b>	Lys	Ac-SLSIDLKFHLLR-	1520.89	1521.06	56	18
	<b>G7</b>	Dap	Ac-SLSIDL(Dap)FHLLR-	1478.84	1479.12	79	25
	<b>H7</b>	h-Ser	Ac-SLSIDL(h-Ser)FHLLR-	1493.84	1494.05	59	24
<b>Phe<sup>11</sup></b>	<b>A8</b>	Ala	Ac-SLSIDLTAHLLR-	1417.81	1418.21	81	28
	<b>B8</b>	Aib	Ac-SLSIDLT(Aib)HLLR-	1431.82	1432.00	75	10
	<b>C8</b>	D-Phe	Ac-SLSIDLT(D-Phe)HLLR-	1493.84	1494.00	50	21
	<b>D8</b>	Tyr	Ac-SLSIDLTYHLLR-	1509.84	1510.02	43	37

MATERIAL & METHODS

	<b>E8</b>	Trp	Ac-SLSIDLTWHLR-	1532.85	1533.01	30	24
	<b>F8</b>	Lys	Ac-SLSIDLTKHLR-	1474.87	1475.06	85	22
	<b>G8</b>	pI-Phe	Ac-SLSIDLT(pI-Phe)HLR-	1619.74	1619.92	46	26
	<b>H8</b>	Phg	Ac-SLSIDLT(Phg)HLR-	1479.82	1480.00	26	22
<b>His<sup>12</sup></b>	<b>A9</b>	Ala	Ac-SLSIDLTFALLR-	1427.82	1427.94	63	26
	<b>B9</b>	Aib	Ac-SLSIDLTF(Aib)LLR-	1441.83	1442.03	76	20
	<b>C9</b>	D-His	Ac-SLSIDLTF(D-His)LLR-	1493.84	1494.03	31	22
	<b>D9</b>	Arg	Ac-SLSIDLTFRLLR-	1512.88	1513.04	67	27
	<b>E9</b>	Glu	Ac-SLSIDLTFELLR-	1485.82	1486.00	44	25
	<b>F9</b>	Lys	Ac-SLSIDLTFKLLR-	1484.88	1485.03	34	25
	<b>G9</b>	Cha	Ac-SLSIDLTF(Cha)LLR-	1509.90	1510.02	43	20
	<b>H9</b>	h-Ser	Ac-SLSIDLTF(h-Ser)LLR-	1457.83	1458.00	50	12
<b>Leu<sup>13</sup></b>	<b>A10</b>	Ala	Ac-SLSIDLTFHALR-	1451.79	1452.12	62	27
	<b>B10</b>	Aib	Ac-SLSIDLTFH(Aib)LR-	1465.81	1466.06	95	19
	<b>C10</b>	D-Leu	Ac-SLSIDLTFH(D-Leu)LR-	1493.84	1494.14	36	23
	<b>D10</b>	Ile	Ac-SLSIDLTFHILR-	1493.84	1494.01	38	24
	<b>E10</b>	Val	Ac-SLSIDLTFHVLRL-	1479.82	1480.00	82	24
	<b>F10</b>	Phe	Ac-SLSIDLTFHFRLR-	1527.82	1527.97	32	18
	<b>G10</b>	Cha	Ac-SLSIDLTFH(Cha)LR-	1533.87	1533.02	38	23
	<b>H10</b>	tBuAla	Ac-SLSIDLTFH(tBuAla)LR-	1507.86	1508.06	46	20
<b>Leu<sup>14</sup></b>	<b>A11</b>	Ala	Ac-SLSIDLTFHLAR-	1451.79	1452.12	61	30
	<b>B11</b>	Aib	Ac-SLSIDLTFHL(Aib)R-	1465.81	1466.13	46	13
	<b>C11</b>	D-Leu	Ac-SLSIDLTFHL(D-Leu)R-	1493.84	1494.16	36	20
	<b>D11</b>	Ile	Ac-SLSIDLTFHLIR-	1493.84	1494.13	33	22
	<b>E11</b>	Val	Ac-SLSIDLTFHLVRL-	1479.82	1480.05	42	20
	<b>F11</b>	Phe	Ac-SLSIDLTFHLFR-	1527.82	1528.11	37	35
	<b>G11</b>	Cha	Ac-SLSIDLTFHL(Cha)R-	1533.87	1534.02	26	28
	<b>H11</b>	tBuAla	Ac-SLSIDLTFHL(tBuAla)R-	1507.86	1508.01	60	23
<b>Arg<sup>15</sup></b>	<b>A12</b>	Ala	Ac-SLSIDLTFHLLA-	1408.78	1409.24	75	25
	<b>B12</b>	Aib	Ac-SLSIDLTFHLL(Aib)-	1422.79	1422.93	34	20
	<b>C12</b>	D-Arg	Ac-SLSIDLTFHLL(D-Arg)-	1493.84	1494.12	44	17

	<b>D12</b>	Gln	Ac-SLSIDLTFHLLQ-	1465.80	1465.97	67	26
	<b>E12</b>	Glu	Ac-SLSIDLTFHLLLE-	1466.78	1466.97	42	22
	<b>F12</b>	Lys	Ac-SLSIDLTFHLLK-	1465.83	1465.98	30	22
	<b>G12</b>	Cit	Ac-SLSIDLTFHLL(Cit)-	1494.82	1494.97	69	10
	<b>H12</b>	Orn	Ac-SLSIDLTFHLL(Orn)-	1451.82	1451.99	33	12

**Table 27. Characterization of crude single-substituted analogs of the C-terminally propargylated fragment of human urocortin1<sup>4-15</sup>.**

		R = propargyl			Mass calc. [M+H] <sup>+</sup>	Mass found [M+H] <sup>+</sup>	Purity (%) <sup>(a)</sup>	Yield (%)
Peptide	Subst.	N-terminal Sequence						
D-Phe <sup>1</sup>	<b>A1</b>	Ala	Ac-AHLLREVLEBA-R		1342.78	1343.91	100	71
	<b>B1</b>	Aib	Ac-(Aib)HLLREVLEBA-R		1356.79	1357.24	100	82
	<b>C1</b>	Phe	Ac-FHLLREVLEBA-R		1418.81	710.73 <sup>(a)</sup>	100	84
	<b>D1</b>	D-Tyr	Ac-(D-Tyr)HLLREVLEBA-R		1434.80	1435.10	97	76
	<b>E1</b>	D-Trp	Ac-(D-Trp)HLLREVLEBA-R		1457.82	1458.08	71	75
	<b>F1</b>	D-His	Ac-(D-His)HLLREVLEBA-R		1408.80	1409.29	92	79
	<b>G1</b>	D-3-Pal	Ac-(D-Pal)HLLREVLEBA-R		1419.80	1420.95	100	80
	<b>H1</b>	D-pBrPhe	Ac-(D-pBrPhe)HLLREVLEBA-R		1496.72	1498.91	96	94
D-Phe <sup>1</sup>	<b>A2</b>	D-pNO <sub>2</sub> Phe	Ac-(D-pNO <sub>2</sub> Phe)HLLREVLEBA-R		1463.79	1463.93	92	77
	<b>B2</b>	D-Nal(1)	Ac-(D-Nal1)HLLREVLEBA-R		1468.82	1469.03	88	75
	<b>C2</b>	D-Nal(2)	Ac-(D-Nal2)HLLREVLEBA-R		1468.82	1468.95	87	70
	<b>D2</b>	D-αMePhe	Ac-(D-αMePhe)HLLREVLEBA-R		1432.82	1433.95	92	42
	<b>E2</b>	thr-pheSer	Ac-(thr-pheSer)HLLREVLEBA-R		1434.80	1435.16	27	58
	<b>F2</b>	Aic	Ac-(Aic)HLLREVLEBA-R		1430.81	1431.86	96	64
	<b>G2</b>	Cha	Ac-(Cha)HLLREVLEBA-R		1424.86	713.43 <sup>(a)</sup>	87	79
	<b>H2</b>	D-Cha	Ac-(D-Cha)HLLREVLEBA-R		1424.86	1425.14	92	82
His <sup>2</sup>	<b>A3</b>	Ala	Ac-fALLREVLEBA-R		1352.79	1352.92	100	83
	<b>B3</b>	Aib	Ac-f(Aib)LLREVLEBA-R		1366.80	1366.91	76	51
	<b>C3</b>	D-His	Ac-f(D-His)LLREVLEBA-R		1418.81	701.97 <sup>(a)</sup>	100	67

## MATERIAL &amp; METHODS

	<b>D3</b>	Glu	Ac-fELLREVLEBA-R	1410.79	1410.90	100	49
	<b>E3</b>	Trp	Ac-fWLLREVLEBA-R	1467.83	734.76 <sup>(a)</sup>	94	75
	<b>F3</b>	Phe	Ac-fFLLREVLEBA-R	1428.82	715.35 <sup>(a)</sup>	95	71
	<b>G3</b>	Cha	Ac-f(Cha)LLREVLEBA-R	1434.86	701.96 <sup>(a)</sup>	92	58
	<b>H3</b>	Dab	Ac-f(Dab)LLREVLEBA-R	1381.81	1382.86	100	69
<b>Leu<sup>3</sup></b>	<b>A4</b>	Ala	Ac-fHALREVLEBA-R	1376.76	1377.15	100	79
	<b>B4</b>	Aib	Ac-fH(Aib)LREVLEBA-R	1390.78	1391.05	97	75
	<b>C4</b>	D-Leu	Ac-fH(D-Leu)LREVLEBA-R	1418.81	1418.92	96	81
	<b>D4</b>	Ile	Ac-fHILREVLEBA-R	1418.81	1418.94	100	80
	<b>E4</b>	Val	Ac-fHVLREVLEBA-R	1404.79	1404.96	100	46
	<b>F4</b>	Phe	Ac-fHFLREVLEBA-R	1452.79	1452.98	100	57
	<b>G4</b>	Cha	Ac-fH(Cha)LREVLEBA-R	1458.84	730.44 <sup>(a)</sup>	93	84
	<b>H4</b>	tBuAla	Ac-fH(tBuAla)LREVLEBA-R	1432.82	1433.00	86	72
<b>Leu<sup>4</sup></b>	<b>A5</b>	Ala	Ac-fHLAREVLEBA-R	1376.76	1377.01	100	77
	<b>B5</b>	Aib	Ac-fHL(Aib)REVLEBA-R	1390.78	1390.99	89	75
	<b>C5</b>	D-Leu	Ac-fHL(D-Leu)REVLEBA-R	1418.81	710.46 <sup>(a)</sup>	90	45
	<b>D5</b>	Ile	Ac-fHLIREVLEBA-R	1418.81	1418.98	72	86
	<b>E5</b>	Val	Ac-fHLVREVLEBA-R	1404.79	1405.03	94	71
	<b>F5</b>	Phe	Ac-fHLFREVLEBA-R	1452.79	727.35 <sup>(a)</sup>	77	92
	<b>G5</b>	Cha	Ac-fHL(Cha)REVLEBA-R	1458.84	730.38 <sup>(a)</sup>	93	74
	<b>H5</b>	tBuAla	Ac-fHL(D-Cha)REVLEBA-R	1432.82	1432.93	85	78
<b>Arg<sup>5</sup></b>	<b>A6</b>	Ala	Ac-fHLLAEVLEBA-R	1333.74	1333.78	90	81
	<b>B6</b>	Aib	Ac-fHLL(Aib)EVLEBA-R	1347.76	1347.80	86	57
	<b>C6</b>	D-Arg	Ac-fHLL(D-Arg)EVLEBA-R	1418.81	1418.99	87	69
	<b>D6</b>	Asn	Ac-fHLLNEVLEBA-R	1376.75	1376.84	81	76
	<b>E6</b>	Gln	Ac-fHLLQEVLEBA-R	1390.77	1390.79	86	71
	<b>F6</b>	Lys	Ac-fHLLKEVLEBA-R	1390.80	1390.86	81	71
	<b>G6</b>	Cit	Ac-fHLL(Cit)EVLEBA-R	1419.79	1419.95	85	56
	<b>H6</b>	Orn	Ac-fHLL(Orn)EVLEBA-R	1376.79	1376.94	90	85
<b>Glu<sup>6</sup></b>	<b>A7</b>	Ala	Ac-fHLLRAVLEBA-R	1360.80	1360.93	100	84
	<b>B7</b>	Aib	Ac-fHLLR(Aib)VLEBA-R	1374.82	1374.96	89	75

	<b>C7</b>	D-Glu	Ac-fHLLR(D-Glu)VLEBA-R	1418.81	1418.98	91	74
	<b>D7</b>	Asp	Ac-fHLLRDVLEBA-R	1404.79	1405.00	86	65
	<b>E7</b>	Gln	Ac-fHLLRQVLEBA-R	1417.82	1417.96	77	81
	<b>F7</b>	His	Ac-fHLLRHVLEBA-R	1426.82	1427.04	94	79
	<b>G7</b>	Dab	Ac-fHLLR(Dab)VLEBA-R	1389.83	1390.08	92	71
	<b>H7</b>	Orn	Ac-fHLLR(Orn)VLEBA-R	1403.84	1404.08	93	54
<b>Val<sup>7</sup></b>	<b>A8</b>	Ala	Ac-fHLLREALEBA-R	1390.78	1391.04	98	77
	<b>B8</b>	Aib	Ac-fHLLRE(Aib)LEBA-R	1404.79	1405.07	91	64
	<b>C8</b>	D-Val	Ac-fHLLRE(D-Val)LEBA-R	1418.81	1419.14	100	68
	<b>D8</b>	Ile	Ac-fHLLREILEBA-R	1432.82	1432.94	91	71
	<b>E8</b>	Leu	Ac-fHLLRELEBA-R	1432.82	1432.94	77	78
	<b>F8</b>	Phe	Ac-fHLLREFLEBA-R	1466.81	1466.92	85	62
	<b>G8</b>	Chg	Ac-fHLLRE(Chg)LEBA-R	1458.84	1458.98	88	54
	<b>H8</b>	tBuGly	Ac-fHLLRE(tBuGly)LEBA-R	1432.82	1433.06	100	80
<b>Leu<sup>8</sup></b>	<b>A9</b>	Ala	Ac-fHLLREVAEBA-R	1376.76	1376.91	90	87
	<b>B9</b>	Aib	Ac-fHLLREV(Aib)EBA-R	1390.78	1390.93	88	52
	<b>C9</b>	D-Leu	Ac-fHLLREV(D-Leu)EBA-R	1418.81	1418.98	88	67
	<b>D9</b>	Ile	Ac-fHLLREVIEBA-R	1418.81	1418.94	100	72
	<b>E9</b>	Val	Ac-fHLLREVEBA-R	1404.79	1404.97	84	64
	<b>F9</b>	Phe	Ac-fHLLREVFEBAR	1452.79	1452.90	80	68
	<b>G9</b>	Cha	Ac-fHLLREV(Cha)EBA-R	1458.84	1458.99	100	90
	<b>H9</b>	tBuAla	Ac-fHLLREV(tBuAla)EBA-R	1432.82	1432.96	93	70
<b>Glu<sup>9</sup></b>	<b>A10</b>	Ala	Ac-fHLLREVLABA-R	1360.80	1360.95	100	58
	<b>B10</b>	Aib	Ac-fHLLREVL(Aib)BA-R	1374.82	1375.02	97	79
	<b>C10</b>	D-Glu	Ac-fHLLREVL(D-Glu)BA-R	1418.81	1419.03	87	74
	<b>D10</b>	Asp	Ac-fHLLREVLDBA-R	1404.79	1404.93	94	71
	<b>E10</b>	Gln	Ac-fHLLREVLQBA-R	1417.82	1417.97	90	83
	<b>F10</b>	Lys	Ac-fHLLREVLKBA-R	1417.86	1418.08	83	56
	<b>G10</b>	Dab	Ac-fHLLREVL(Dab)BA-R	1389.83	1458.99	97	69
	<b>H10</b>	Orn	Ac-fHLLREVL(Orn)BA-R	1403.84	1404.04	86	68
<b>Nleu<sup>10</sup></b>	<b>A11</b>	Ala	Ac-fHLLREVLEAA-R	1376.76	1376.96	94	79

	<b>B11</b>	Aib	Ac-fHLLREVLE(Aib)A-R	1390.78	1391.02	92	56
	<b>C11</b>	D-Nleu	Ac-fHLLREVLE(D-Nleu)A-R	1418.81	1418.98	85	58
	<b>D11</b>	Leu	Ac-fHLLREVLELA-R	1418.81	1418.93	89	67
	<b>E11</b>	Ile	Ac-fHLLREVLEIA-R	1418.81	1418.95	89	87
	<b>F11</b>	Lys	Ac-fHLLREVLEKA-R	1433.82	1434.03	100	73
	<b>G11</b>	Cha	Ac-fHLLREVLE(Cha)A-R	1458.84	1459.10	93	71
	<b>H11</b>	tBuAla	Ac-fHLLREVLE(tBuAla)A-R	1432.82	1432.94	83	69
<b>Ala<sup>11</sup></b>	<b>A12</b>	Ala	Ac-fHLLREVLEBA-R	1418.81	1418.94	100	78
	<b>B12</b>	Aib	Ac-fHLLREVLEB(Aib)-R	1432.82	1432.94	80	56
	<b>C12</b>	D-Ala	Ac-fHLLREVLEB(D-Ala)-R	1418.81	1418.99	93	43
	<b>D12</b>	Ser	Ac-fHLLREVLEBS-R	1434.80	1435.00	50	58
	<b>E12</b>	Leu	Ac-fHLLREVLEBL-R	1460.86	1461.01	82	69
	<b>F12</b>	Val	Ac-fHLLREVLEBV-R	1446.84	1446.97	91	75
	<b>G12</b>	tBuGly	Ac-fHLLREVLEB(tBuGly)-R	1460.86	1461.04	88	69
	<b>H12</b>	Nval	Ac-fHLLREVLEB(Nval)-R	1446.84	1446.93	100	75

**Table 28. Characterization of crude single-substituted analogs of the C-terminally propargylated fragment of astressin<sup>1-11</sup>.** (a) Mass found corresponds to  $[M + 2H]^{2+}$  or  $[M + H + Na]^{2+}$ .

### 5.2.3.6 Synthesis of C-terminally amidated peptides

C-terminally amidated peptides were synthesized using a Rink Amide MBHA resin (Novabiochem) and the standard SPPS procedure described above.

<b>R = NH<sub>2</sub></b>		<b>Mass calc. [M+H]<sup>+</sup></b>	<b>Mass found [M+H]<sup>+</sup></b>	<b>Purity (%)</b>	<b>Yield (%)</b>
<b>20b</b>	<b>Peptide sequence</b>				
<b>20b</b>	Ac-UCN <sup>4-15</sup> -R	1455.82	1455.78	95	23
<b>23</b>	Ac-SLSIDLTFHLLR-spacer-K-R	1728.99	1729.12	100	14
<b>58b</b>	Ac-[Thr <sup>4</sup> Cha <sup>5</sup> ]UCN <sup>4-15</sup> -R	1509.87	1509.87	94	35
<b>59b</b>	Ac-[Thr <sup>4</sup> Cha <sup>5</sup> D-Phe <sup>11</sup> ]UCN <sup>4-15</sup> -R	1509.87	1509.83	95	32
<b>60b</b>	Ac-[Thr <sup>4</sup> Cha <sup>5,13</sup> D-Phe <sup>11</sup> ]UCN <sup>4-15</sup> -R	1549.90	1549.80	97	28
<b>61b</b>	Ac-[Thr <sup>4</sup> Cha <sup>5,13</sup> Chg <sup>7</sup> D-Phe <sup>11</sup> ]UCN <sup>4-15</sup> -R	1575.92	1575.91	96	31



<b>62b</b>	Ac-[Thr <sup>4</sup> Cha <sup>5,13</sup> Chg <sup>7</sup> tBuAla <sup>9</sup> D-Phe <sup>11</sup> ]Ucn1 <sup>4-15</sup> -R	1589.93	1589.90	98	22
<b>63</b>	Ac-[Cha <sup>5</sup> D-Phe <sup>11</sup> ]Ucn1 <sup>4-15</sup> -R	1495.86	1495.81	99	16
<b>64</b>	Ac-[Thr <sup>4</sup> D-Phe <sup>11</sup> ]Ucn1 <sup>4-15</sup> -R	1469.84	1469.84	99	28
<b>65</b>	Ac-[Thr <sup>4</sup> tBuAla <sup>5</sup> D-Phe <sup>11</sup> ]Ucn1 <sup>4-15</sup> -R	1483.86	1483.85	98	10
<b>66</b>	Ac-[Thr <sup>4</sup> tBuAla <sup>5</sup> D-Phe <sup>11</sup> Cha <sup>13</sup> ]Ucn1 <sup>4-15</sup> -R	1523.89	1550.10	96	21
<b>67</b>	Ac-[Thr <sup>4</sup> tBuAla <sup>5,13</sup> D-Phe <sup>11</sup> ]Ucn1 <sup>4-15</sup> -R	1497.87	1498.01	96	32
<b>68</b>	Ac-[Thr <sup>4</sup> Cha <sup>5</sup> D-Phe <sup>11</sup> α-MeLeu <sup>13</sup> ]Ucn1 <sup>4-15</sup> -R	1523.89	1524.05	96	20
<b>69</b>	Ac-[Thr <sup>4</sup> Cha <sup>5,13</sup> α-MeD-Phe <sup>11</sup> ]Ucn1 <sup>4-15</sup> -R	1563.92	780.86	99	17
<b>70</b>	Ac-[Thr <sup>4</sup> α-MeLeu <sup>5</sup> D-Phe <sup>11</sup> Cha <sup>13</sup> ]Ucn1 <sup>4-15</sup> -R	1523.89	762.97	94	25
<b>71</b>	Ac-[alloThr <sup>4</sup> Cha <sup>5,13</sup> D-Phe <sup>11</sup> ]Ucn1 <sup>4-15</sup> -R	1549.90	1550.14	96	24
<b>72</b>	Ac-[β-PheSer <sup>4</sup> Cha <sup>5,13</sup> D-Phe <sup>11</sup> ]Ucn1 <sup>4-15</sup> -R	1611.92	1612.10	96	24
<b>73</b>	Ac-[Thr <sup>4</sup> Cha <sup>5,13,14</sup> D-Phe <sup>11</sup> ]Ucn1 <sup>4-15</sup> -R	1589.93	1589.84	97	24
<b>74</b>	Ac-[Thr <sup>4</sup> Cha <sup>5,13</sup> tBuGly <sup>7</sup> D-Phe <sup>11</sup> ]Ucn1 <sup>4-15</sup> -R	1549.90	1550.16	97	18
<b>75</b>	Ac-[Thr <sup>4</sup> Cha <sup>5,13</sup> α-MeLeu <sup>9</sup> D-Phe <sup>11</sup> ]Ucn1 <sup>4-15</sup> -R	1563.92	1564.04	97	11
<b>76</b>	Ac-[Thr <sup>4</sup> Cha <sup>5,13</sup> D-Phe <sup>11</sup> tBuAla <sup>14</sup> ]Ucn1 <sup>4-15</sup> -R	1563.92	1564.09	100	23
<b>77</b>	Ac-[Thr <sup>4</sup> Cha <sup>5,13,14</sup> Chg <sup>7</sup> D-Phe <sup>11</sup> ]Ucn1 <sup>4-15</sup> -R	1615.95	1615.91	93	35
<b>78</b>	Ac-[Thr <sup>4</sup> Cha <sup>5,9,13</sup> Chg <sup>7</sup> D-Phe <sup>11</sup> ]Ucn1 <sup>4-15</sup> -R	1615.95	1616.09	100	24
<b>79</b>	Ac-[Thr <sup>4</sup> tBuAla <sup>5,9,13,14</sup> Chg <sup>7</sup> D-Phe <sup>11</sup> ]Ucn1 <sup>4-15</sup> -R	1551.92	1551.88	95	18

**Table 29. Characterization of purified analogs of the C-terminally amidated fragment of human urocortin1<sup>4-15</sup>.**

## 5.2.4 The bioconjugation of peptide fragments

### 5.2.4.1 Typical procedure for the CuCAAC of peptide fragments

The azide functionalized peptide (1 mM solution in acetonitrile/water 50/50, v/v) (15 nmol) and the desired propargylated peptide (1 mM solution in acetonitrile/water 50/50, v/v) (4 eq., 60 nmol) were transferred to a reaction tube (1.5 mL). The mixture was evaporated under reduced pressure. The residue was dissolved in tert-butanol/water (43/1, v/v, 722  $\mu$ L); sonication was used to help peptide dissolution when necessary. To this solution were added sequentially TBTA (1 mM solution in tert-butanol/water 43/1, v/v, 1.3 eq., 20 nmol, 20  $\mu$ L), sodium ascorbate (71 mM solution in water, 28 eq., 412 nmol, 5.8  $\mu$ L) and copper sulfate (140 mM solution in water, 21 eq., 308 nmol, 2.2  $\mu$ L). The mixture was shaken for 40 hrs at 37 °C. The tube was cooled down to room temperature, and then centrifugated (13000 rpm, 5 min). The supernatant was removed by decantation and the precipitate was washed with tert-butanol/water (43/1, v/v, 100  $\mu$ L). The precipitate was dried under vacuum. Typically, the conjugates were dissolved in DMSO and analyzed by reverse phase HPLC. The NBD-tagged conjugates were systematically quantified by fluorescence spectroscopy using standard dilutions of peptide carrier **2** in DMSO as a reference.

		Peptide sequence	R = carrier	Mass calc. [M+3H] <sup>3+</sup>	Mass found [M+3H] <sup>3+</sup>	Purity (%)	Yield (%)
18	Ac-UCN <sup>1-15</sup> -R	Ac-DNPSLSIDLTFHLLR-R	2	1263.33	1263.95	97	31
19	Ac-UCN <sup>1-14</sup> -R	Ac-DNPSLSIDLTFHLL-R	2	1211.29	1211.91	94	37
20	Ac-UCN <sup>2-15</sup> -R	Ac-NPSLSIDLTFHLLR-R	2	1224.98	1225.61	97	22
21	Ac-UCN <sup>3-15</sup> -R	Ac-PSLSIDLTFHLLR-R	2	1186.97	1187.31	98	14
22	Ac-UCN <sup>4-15</sup> -R	Ac-SLSIDLTFHLLR-R	2	1154.62	1154.91	93	26
23	Ac-UCN <sup>5-15</sup> -R	Ac-LSIDLTFHLLR-R	2	1125.61	1126.24	95	32
24	Ac-UCN <sup>6-15</sup> -R	Ac-SIDLTFHLLR-R	2	1087.91	1088.11	100	44
32	Ac-UCN <sup>4-15</sup> -R	Ac-SLSIDLTFHLLR-R	27	1110.59	1110.91	97	20
33	Ac-UCN <sup>4-15</sup> -R	Ac-SLSIDLTFHLLR-R	28	1125.27	1125.54	97	20
34	Ac-UCN <sup>4-15</sup> -R	Ac-SLSIDLTFHLLR-R	29	1139.94	1140.33	95	18
35	Ac-UCN <sup>4-15</sup> -R	Ac-SLSIDLTFHLLR-R	30	1169.29	1169.70	96	22
36	Ac-UCN <sup>4-15</sup> -R	Ac-SLSIDLTFHLLR-R	31	1183.97	1184.18	97	19

**Table 30. Characterization of purified truncated “clicked” analogs of the N-terminal fragment of human urocortin1<sup>1-15</sup>.**

	Peptide	Subst.	N-terminal Sequence	Mass calc. [M+3H] <sup>3+</sup>	Mass found [M+3H] <sup>3+</sup>	Purity (%)	Yield (%)	Activity (%) <sup>(b)</sup>
Ser <sup>4</sup>	A1	Ala	Ac-ALSIDLTFHLLR-	1149.29	1149.62	97	87	86.5
	B1	Aib	Ac-(Aib)LSIDLTFHLLR-	1153.67	1154.27	100	58	35.7
	C1	D-Ser	Ac-(D-Ser)LSIDLTFHLLR-	1154.64	1154.93	96	79	72.4
	D1	Thr	Ac-TLSIDLTFHLLR-	1159.01	1159.60	95	99	90.3
	E1	Glu	Ac-ELSIDLTFHLLR-	1168.62	1168.97	100	100	90.7
	F1	Lys	Ac-KLSIDLTFHLLR-	1168.31	1168.83	100	69	80.0
	G1	Dap	Ac-(Dap)LSIDLTFHLLR-	1154.01	1154.94	88	100	84.1
	H1	h-Ser	Ac-(h-Ser)LSIDLTFHLLR-	1159.01	1159.93	88	97	85.1
Leu <sup>5</sup>	A2	Ala	Ac-SASIDLTFHLLR-	1140.32	1140.94	100	84	5.2
	B2	Aib	Ac-S(Aib)SIDLTFHLLR-	1144.99	1145.59	79	100	1.3
	C2	D-Leu	Ac-S(D-Leu)SIDLTFHLLR-	1154.33	1155.27	86	87	4.2
	D2	Ile	Ac-SISIDLTFHLLR-	1154.33	1155.14	73	100	56.8
	E2	Glu	Ac-SESIDLTFHLLR-	1159.94	1160.44	91	99	9.7
	F2	Lys	Ac-SKSIDLTFHLLR-	1159.29	1160.20	89	99	21.7
	G2	Cha	Ac-S(Cha)SIDLTFHLLR-	1167.68	1168.20	92	78	94.5
	H2	Nleu	Ac-S(Nleu)SIDLTFHLLR-	1154.62	1154.86	100	94	68.7
Ser <sup>6</sup>	A3	Ala	Ac-SLAIDLTFHLLR-	1149.30	1149.93	92	75	12.8
	B3	Aib	Ac-SL(Aib)IDLTFHLLR-	1153.67	1154.27	100	87	22.3
	C3	D-Ser	Ac-SL(D-Ser)IDLTFHLLR-	1154.64	1154.93	100	93	2.5
	D3	Thr	Ac-SLTIDLTFHLLR-	1159.01	1159.94	95	98	0.6
	E3	Glu	Ac-SLEIDLTFHLLR-	1168.62	1168.87	100	100	0.3
	F3	Lys	Ac-SLKIDLTFHLLR-	1168.31	1168.78	100	87	0.4
	G3	Dap	Ac-SL(Dap)IDLTFHLLR-	1154.01	1154.53	71	94	2.9
	H3	h-Ser	Ac-SL(h-Ser)IDLTFHLLR-	1159.01	1159.52	92	95	4.7
Ile <sup>7</sup>	A4	Ala	Ac-SLSADLTFHLLR-	1140.32	1141.18	63	100	0
	B4	Aib	Ac-SLS(Aib)DLTFHLLR-	1144.99	1145.58	95	99	3.5
	C4	D-Ile	Ac-SLS(D-Ile)DLTFHLLR-	1154.33	1154.96	83	79	0
	D4	Leu	Ac-SLSLDLTFHLLR-	1154.33	1155.20	71	92	50.3
	E4	Val	Ac-SLSVDLTFHLLR-	1149.66	1150.52	51	90	13.9

MATERIAL & METHODS

	<b>F4</b>	Thr	Ac-SLSTDLTFHLLR-	1150.61	1151.28	50	87	2.7
	<b>G4</b>	Chg	Ac-SLS(Chg)DLTFHLLR-	1163.29	1163.63	45	100	77.9
	<b>H4</b>	tBuGly	Ac-SLS(tBuGly)DLTFHLLR-	1154.33	1154.94	66	94	42.7
<b>Asp<sup>8</sup></b>	<b>A5</b>	Ala	Ac-SLSIALTFHLLR-	1139.67	1140.60	83	86	2.9
	<b>B5</b>	Aib	Ac-SLSI(Aib)LTFHLLR-	1144.34	1144.95	87	94	1.0
	<b>C5</b>	D-Asp	Ac-SLSI(D-Asp)LTFHLLR-	1154.33	1155.19	66	71	3.0
	<b>D5</b>	Asn	Ac-SLSINLTFHLLR-	1154.01	1154.53	73	90	12.5
	<b>E5</b>	Glu	Ac-SLSIELTFHLLR-	1159.01	1159.33	69	98	25.8
	<b>F5</b>	Thr	Ac-SLSITLTFHLLR-	1149.67	1150.60	68	93	4.9
	<b>G5</b>	Dab	Ac-SLSI(Dab)LTFHLLR-	1149.35	1150.21	71	56	7.6
	<b>H5</b>	h-Ser	Ac-SLSI(h-Ser)LTFHLLR-	1149.67	1150.63	76	78	3.0
<b>Leu<sup>9</sup></b>	<b>A6</b>	Ala	Ac-SLSIDATFHLLR-	1140.32	1140.91	100	84	0.3
	<b>B6</b>	Aib	Ac-SLSID(Aib)TFHLLR-	1144.99	1145.95	82	97	2.9
	<b>C6</b>	D-Leu	Ac-SLSID(D-Leu)TFHLLR-	1154.33	1154.93	100	100	16.6
	<b>D6</b>	Ile	Ac-SLSIDITFHLLR-	1154.33	1155.30	73	86	33.4
	<b>E6</b>	Val	Ac-SLSIDVTFHLLR-	1149.66	1150.60	79	67	24.3
	<b>F6</b>	Phe	Ac-SLSIDFTFHLLR-	1165.66	1166.29	74	79	1.8
	<b>G6</b>	Cha	Ac-SLSID(Cha)TFHLLR-	1167.68	1168.64	81	69	0.4
	<b>H6</b>	tBuAla	Ac-SLSID(tBuAla)TFHLLR-	1159.01	1155.19	100	80	42.8
<b>Thr<sup>10</sup></b>	<b>A7</b>	Ala	Ac-SLSIDLAFHLLR-	1144.33	1145.26	97	98	28.7
	<b>B7</b>	Aib	Ac-SLSIDL(Aib)FHLLR-	1149.00	1149.93	86	84	23.4
	<b>C7</b>	D-Thr	Ac-SLSIDL(D-Thr)FHLLR-	1154.33	1155.19	80	100	2.9
	<b>D7</b>	Ser	Ac-SLSIDLSFHLLR-	1149.66	1150.52	77	87	11.3
	<b>E7</b>	Glu	Ac-SLSIDLEFHLLR-	1163.95	1163.63	86	67	0
	<b>F7</b>	Lys	Ac-SLSIDLKFHLLR-	1163.64	1163.95	100	52	1.8
	<b>G7</b>	Dap	Ac-SLSIDL(Dap)FHLLR-	1178.01	1178.21	43	91	0
	<b>H7</b>	h-Ser	Ac-SLSIDL(h-Ser)FHLLR-	1154.33	1150.26	76	88	13.7
<b>Phe<sup>11</sup></b>	<b>A8</b>	Ala	Ac-SLSIDLTAHLLR-	1128.99	1129.96	100	100	23.1
	<b>B8</b>	Aib	Ac-SLSIDLT(Aib)HLLR-	1133.66	1134.26	85	85	60.4
	<b>C8</b>	D-Phe	Ac-SLSIDLT(D-Phe)HLLR-	1154.33	1154.96	66	99	91.6
	<b>D8</b>	Tyr	Ac-SLSIDLTYHLLR-	1159.95	1160.29	57	68	30.1

	<b>E8</b>	Trp	Ac-SLSIDLTWHLR-	1167.62	1168.53	82	77	79.0
	<b>F8</b>	Lys	Ac-SLSIDLTKHLR-	1148.29	1148.54	100	97	6.2
	<b>G8</b>	pI-Phe	Ac-SLSIDLT(pI-Phe)HLR-	1196.30	1197.16	70	100	2.0
	<b>H8</b>	Phg	Ac-SLSIDLT(Phg)HLR-	1149.95	1150.19	51	64	0
<b>His<sup>12</sup></b>	<b>A9</b>	Ala	Ac-SLSIDLTFALLR-	1132.33	1132.93	100	95	63.9
	<b>B9</b>	Aib	Ac-SLSIDLTF(Aib)LLR-	1137.28	1138.01	100	99	1.1
	<b>C9</b>	D-His	Ac-SLSIDLTF(D-His)LLR-	1154.33	1155.26	100	86	0.2
	<b>D9</b>	Arg	Ac-SLSIDLTFRLLR-	1160.68	1161.54	100	100	2.1
	<b>E9</b>	Glu	Ac-SLSIDLTFRLLR-	1151.66	1152.62	68	81	0.3
	<b>F9</b>	Lys	Ac-SLSIDLTFKLLR-	1151.63	1151.88	75	79	69.0
	<b>G9</b>	Cha	Ac-SLSIDLTF(Cha)LLR-	1159.97	1160.29	78	98	47.7
	<b>H9</b>	h-Ser	Ac-SLSIDLTF(h-Ser)LLR-	1142.33	1143.19	67	87	53.3
<b>Leu<sup>13</sup></b>	<b>A10</b>	Ala	Ac-SLSIDLTFHALR-	1140.32	1140.92	100	100	0
	<b>B10</b>	Aib	Ac-SLSIDLTFH(Aib)LR-	1144.99	1145.92	100	100	3.3
	<b>C10</b>	D-Leu	Ac-SLSIDLTFH(D-Leu)LR-	1154.33	1154.93	100	97	3.6
	<b>D10</b>	Ile	Ac-SLSIDLTFHILR-	1154.33	1155.29	90	100	59.9
	<b>E10</b>	Val	Ac-SLSIDLTFHVLR-	1149.66	1150.62	100	77	10.7
	<b>F10</b>	Phe	Ac-SLSIDLTFHFLR-	1165.66	1166.19	85	84	6.6
	<b>G10</b>	Cha	Ac-SLSIDLTFH(Cha)LR-	1167.68	1168.53	100	97	52.0
	<b>H10</b>	tBuAla	Ac-SLSIDLTFH(tBuAla)LR-	1159.01	1159.94	77	100	70.6
<b>Leu<sup>14</sup></b>	<b>A11</b>	Ala	Ac-SLSIDLTFHLAR-	1140.32	1140.92	100	74	9.6
	<b>B11</b>	Aib	Ac-SLSIDLTFHL(Aib)R-	1144.99	1145.92	100	89	13.1
	<b>C11</b>	D-Leu	Ac-SLSIDLTFHL(D-Leu)R-	1154.33	1154.96	97	96	17.3
	<b>D11</b>	Ile	Ac-SLSIDLTFHLIR-	1154.33	1155.27	80	100	46.6
	<b>E11</b>	Val	Ac-SLSIDLTFHLVR-	1149.66	1150.60	83	78	18.1
	<b>F11</b>	Phe	Ac-SLSIDLTFHLFR-	1165.66	1166.60	77	86	5.5
	<b>G11</b>	Cha	Ac-SLSIDLTFHL(Cha)R-	1167.68	1168.53	100	100	19.3
	<b>H11</b>	tBuAla	Ac-SLSIDLTFHL(tBuAla)R-	1159.01	1159.87	87	97	31.2
<b>Arg<sup>15</sup></b>	<b>A12</b>	Ala	Ac-SLSIDLTFHLLA-	1125.98	1126.57	93	69	9.9
	<b>B12</b>	Aib	Ac-SLSIDLTFHLL(Aib)-	1130.65	1130.21	100	100	60.3
	<b>C12</b>	D-Arg	Ac-SLSIDLTFHLL(D-Arg)-	1154.33	1154.93	100	87	11.9

	<b>D12</b>	Gln	Ac-SLSIDLTFHLLQ-	1144.99	1145.91	89	74	14.6
	<b>E12</b>	Glu	Ac-SLSIDLTFHLL-	1145.60	1145.85	69	64	9.0
	<b>F12</b>	Lys	Ac-SLSIDLTFHLLK-	1145.00	1145.92	72	52	10.9
	<b>G12</b>	Cit	Ac-SLSIDLTFHLL(Cit)-	1154.66	1155.52	100	97	33.5
	<b>H12</b>	Orn	Ac-SLSIDLTFHLL(Orn)-	1140.33	1141.28	100	100	14.9

**Table 31. Characterization of crude single-substituted “clicked” analogs of the human urocortin1<sup>4-15</sup>.** <sup>(a)</sup> cAMP stimulation activity at 2 nM. The cAMP stimulation activity of conjugate UCN<sup>4-15</sup> (**20a**) was 56.7 % at 2 nM.

Peptide	Subst.	[M+3H] <sup>3+</sup>		Purity (%)	
		Calc.	Found	Crude	Purified
<b>D1</b>	Thr <sup>4</sup>	1159.01	1159.56	95	100
<b>G2</b>	Cha <sup>5</sup>	1167.68	1168.24	82	100
<b>E4</b>	Val <sup>7</sup>	1149.66	1150.19	42	98
<b>F4</b>	Thr <sup>7</sup>	1150.61	1150.21	56	93
<b>G4</b>	Chg <sup>7</sup>	1163.29	1163.56	50	90
<b>C5</b>	D-Asp <sup>8</sup>	1154.33	1155.29	69	98
<b>H6</b>	tBuAla <sup>9</sup>	1159.01	1159.96	100	100
<b>C8</b>	D-Phe <sup>11</sup>	1154.33	1155.22	66	92
<b>D8</b>	Tyr <sup>11</sup>	1159.95	1160.29	60	97
<b>H8</b>	Phg <sup>11</sup>	1149.95	1150.53	51	96
<b>H9</b>	h-Ser <sup>12</sup>	1142.33	1143.19	67	100
<b>E10</b>	Val <sup>13</sup>	1149.66	1150.55	61	100
<b>G10</b>	Cha <sup>13</sup>	1167.68	1168.30	100	97
<b>UCN<sup>4-15</sup></b>	-	1154.52	1154.91	78	100

**Table 32. Characterization of crude and purified single-substituted “clicked” analogs of the human urocortin1<sup>4-15</sup>.**

	R = carrier 2		Mass calc. [M+3H] <sup>3+</sup>	Mass found [M+3H] <sup>3+</sup>	Purity (%)	Yield (%)
	Peptide sequence					
<b>58a</b>	Ac-[Thr <sup>4</sup> Cha <sup>5</sup> ]UCN <sup>4-15</sup> -R		1172.63	1172.72	98	47
<b>59a</b>	Ac-[Thr <sup>4</sup> Cha <sup>5</sup> D-Phe <sup>11</sup> ]UCN <sup>4-15</sup> -R		1172.63	1172.65	100	59
<b>60a</b>	Ac-[Thr <sup>4</sup> Cha <sup>5,13</sup> D-Phe <sup>11</sup> ]UCN <sup>4-15</sup> -R		1185.98	1186.13	94	55
<b>61a</b>	Ac-[Thr <sup>4</sup> Cha <sup>5,13</sup> Chg <sup>7</sup> D-Phe <sup>11</sup> ]UCN <sup>4-15</sup> -R		1194.65	1194.81	97	51
<b>62a</b>	Ac-[Thr <sup>4</sup> Cha <sup>5,13</sup> Chg <sup>7</sup> tBuAla <sup>9</sup> D-Phe <sup>11</sup> ]UCN <sup>4-15</sup> -R		1199.32	1199.39	98	43

**Table 33. Characterization of purified (multi-)substituted “clicked” analogs of the human urocortin1<sup>4-15</sup>.**

		Peptide sequence	R = carrier	Mass calc. [M+3H] <sup>3+</sup>	Mass found [M+3H] <sup>3+</sup>	Purity (%)	Yield (%)
<b>90</b>	Ac-AST <sup>1-14</sup> -R	Ac-fHLLREVLEBARAE-R	<b>2</b>	1249.00	1249.14	94	12
<b>91</b>	Ac-AST <sup>1-13</sup> -R	Ac-fHLLREVLEBARA-R	<b>2</b>	1205.98	1206.13	97	31
<b>92</b>	Ac-AST <sup>1-12</sup> -R	Ac-fHLLREVLEBAR-R	<b>2</b>	1182.30	1182.38	100	47
<b>93</b>	Ac-AST <sup>1-11</sup> -R	Ac-fHLLREVLEBA-R	<b>2</b>	1130.27	1130.36	100	52
<b>94</b>	Ac-AST <sup>1-10</sup> -R	Ac-fHLLREVLEB-R	<b>2</b>	1106.59	1106.71	100	66
<b>95</b>	Ac-AST <sup>1-9</sup> -R	Ac-fHLLREVLE-R	<b>2</b>	1068.89	1069.00	98	50
<b>96</b>	Ac-AST <sup>1-8</sup> -R	Ac-fHLLREVL-R	<b>2</b>	1025.88	1025.93	95	63
<b>97</b>	Ac-AST <sup>1-7</sup> -R	Ac-fHLLREV-R	<b>2</b>	988.19	988.40	100	37
<b>98</b>	Ac-AST <sup>1-6</sup> -R	Ac-fHLLRE-R	<b>2</b>	954.50	955.67	100	45
<b>99</b>	Ac-AST <sup>1-5</sup> -R	Ac-fHLLR-R	<b>2</b>	911.49	912.38	100	79
<b>100</b>	H <sub>2</sub> N-AST <sup>1-11</sup> -R	H <sub>2</sub> N-fHLLREVLEBA-R	<b>2</b>	1116.26	1116.31	100	56
<b>101</b>	Ac-AST <sup>2-11</sup> -R	Ac-HLLREVLEBA-R	<b>2</b>	1081.25	1081.32	99	62
<b>102</b>	Ac-AST <sup>1-11</sup> -R	Ac-fHLLREVLEBA-R	<b>27</b>	1085.91	1086.05	94	34
<b>103</b>	Ac-AST <sup>1-11</sup> -R	Ac-fHLLREVLEBA-R	<b>28</b>	1100.59	1100.65	97	22
<b>104</b>	Ac-AST <sup>1-11</sup> -R	Ac-fHLLREVLEBA-R	<b>29</b>	1115.26	1115.37	98	45
<b>105</b>	Ac-AST <sup>1-11</sup> -R	Ac-fHLLREVLEBA-R	<b>30</b>	1144.61	1144.75	98	38
<b>106</b>	Ac-AST <sup>1-11</sup> -R	Ac-fHLLREVLEBA-R	<b>31</b>	1159.29	1159.44	100	11

**Table 34. Characterization of purified truncated “clicked” analogs of the N-terminal fragment of astressin<sup>1-11</sup>.**

	R = carrier 2	Mass calc. [M+3H] <sup>3+</sup>	Mass found [M+3H] <sup>3+</sup>	Purity (%)	Yield (%)
	Peptide sequence				
<b>107b</b>	Ac-[Cha <sup>2</sup> tBuAla <sup>3</sup> ]AST <sup>1-11</sup> -R	1140.29	1140.38	100	36
<b>108b</b>	Ac-[Cha <sup>2</sup> Aib <sup>4</sup> ]AST <sup>1-11</sup> -R	1126.28	1126.46	97	27
<b>109b</b>	Ac-[tBuAla <sup>3</sup> Aib <sup>4</sup> ]AST <sup>1-11</sup> -R	1125.60	1125.75	95	41
<b>110b</b>	Ac-[Cha <sup>2</sup> tBuAla <sup>3</sup> Aib <sup>4</sup> ]AST <sup>1-11</sup> -R	1130.95	1131.16	98	38
<b>111b</b>	Ac-[Cha <sup>2</sup> Aib <sup>4</sup> tBuAla <sup>8</sup> ]AST <sup>1-11</sup> -R	1130.95	1131.14	100	35
<b>112b</b>	Ac-[D-Pal <sup>1</sup> Cha <sup>2</sup> tBuAla <sup>3</sup> Aib <sup>4</sup> ]AST <sup>1-11</sup> -R	1131.28	1131.39	99	46
<b>113b</b>	Ac-[Cha <sup>2</sup> tBuAla <sup>3,8</sup> Aib <sup>4</sup> ]AST <sup>1-11</sup> -R	1135.62	1135.73	100	39
<b>114b</b>	Ac-[D-pBrPhe <sup>1</sup> Cha <sup>2,10</sup> Aib <sup>4</sup> tBuAla <sup>8</sup> ]AST <sup>1-11</sup> -R	1170.26	1170.44	99	42
<b>115b</b>	Ac-[Cha <sup>2,10</sup> tBuAla <sup>3,8</sup> Aib <sup>4</sup> ]AST <sup>1-11</sup> -R	1148.97	1148.99	99	33
<b>107a</b>	H <sub>2</sub> N-[Cha <sup>2</sup> tBuAla <sup>3</sup> ]AST <sup>1-11</sup> -R	1126.29	1126.46	98	69
<b>108a</b>	H <sub>2</sub> N-[Cha <sup>2</sup> Aib <sup>4</sup> ]AST <sup>1-11</sup> -R	1112.27	1112.35	100	74
<b>109a</b>	H <sub>2</sub> N-[tBuAla <sup>3</sup> Aib <sup>4</sup> ]AST <sup>1-11</sup> -R	1111.59	1111.77	95	68
<b>110a</b>	H <sub>2</sub> N-[Cha <sup>2</sup> tBuAla <sup>3</sup> Aib <sup>4</sup> ]AST <sup>1-11</sup> -R	1116.95	1117.08	100	54
<b>111a</b>	H <sub>2</sub> N-[Cha <sup>2</sup> Aib <sup>4</sup> tBuAla <sup>8</sup> ]AST <sup>1-11</sup> -R	1116.95	1117.12	97	82
<b>112a</b>	H <sub>2</sub> N-[D-Pal <sup>1</sup> Cha <sup>2</sup> tBuAla <sup>3</sup> Aib <sup>4</sup> ]AST <sup>1-11</sup> -R	1117.28	1117.46	100	78
<b>113a</b>	H <sub>2</sub> N-[Cha <sup>2</sup> tBuAla <sup>3,8</sup> Aib <sup>4</sup> ]AST <sup>1-11</sup> -R	1121.62	1121.81	97	73
<b>114a</b>	H <sub>2</sub> N-[D-pBrPhe <sup>1</sup> Cha <sup>2,10</sup> Aib <sup>4</sup> tBuAla <sup>8</sup> ]AST <sup>1-11</sup> -R	1156.26	1156.39	96	83
<b>115a</b>	H <sub>2</sub> N-[Cha <sup>2,10</sup> tBuAla <sup>3,8</sup> Aib <sup>4</sup> ]AST <sup>1-11</sup> -R	1134.96	1135.35	100	68

**Table 35. Characterization of purified (multi-)substituted “clicked” analogs of the N-terminal fragment of astressin<sup>1-11</sup>.**



		R = carrier 2							
Peptide	Subst.	N-terminal Sequence	Mass calc. [M+3H] <sup>3+</sup>	Mass found [M+3H] <sup>3+</sup>	Purity (%)	Yield (%)	Activity (%) <sup>(a)</sup>	Efficacy (%) <sup>(b)</sup>	
D-Phe <sup>1</sup>	A1	Ala	Ac-AHLLREVLEBA-R	1104.93	1105.20	76	39	9.2	72.0
	B1	Aib	Ac-(Aib)HLLREVLEBA-R	1109.60	1110.47	87	27	14.3	73.8
	C1	Phe	Ac-FHLLREVLEBA-R	1130.27	1130.64	76	46	9.0	64.0
	D1	D-Tyr	Ac-(D-Tyr)HLLREVLEBA-R	1135.60	1135.80	88	46	9.7	68.2
	E1	D-Trp	Ac-(D-Trp)HLLREVLEBA-R	1143.27	1143.38	49	51	98.8	100
	F1	D-His	Ac-(D-His)HLLREVLEBA-R	1126.93	1127.00	82	34	17.2	71.7
	G1	D-3-Pal	Ac-(D-Pal)HLLREVLEBA-R	1130.60	1130.88	86	42	17.8	60.9
	H1	D-pBrPhe	Ac-(D-pBrPhe)HLLREVLEBA-R	1156.24	1156.93	84	42	12.9	60.1
D-Phe <sup>1</sup>	A2	D-pNO <sub>2</sub> Phe	Ac-(D-pNO <sub>2</sub> Phe)HLLREVLEBA-R	1145.26	1145.47	82	45	10.1	67.3
	B2	D-Nal(1)	Ac-(D-Nal1)HLLREVLEBA-R	1146.94	1146.97	83	45	9.4	70.2
	C2	D-Nal(2)	Ac-(D-Nal2)HLLREVLEBA-R	1146.94	1147.18	82	44	15.4	72.5
	D2	D-αMePhe	Ac-(D-αMePhe)HLLREVLEBA-R	1134.94	1135.13	90	21	29.2	71.9
	E2	thr-pheSer	Ac-(thr-pheSer)HLLREVLEBA-R	1135.60	1135.94	49	47	14.1	68.1
	F2	Aic	Ac-(Aic)HLLREVLEBA-R	1134.27	1134.63	88	28	13.7	68.3
	G2	Cha	Ac-(Cha)HLLREVLEBA-R	1132.29	1132.46	79	41	15.4	67.7
	H2	D-Cha	Ac-(D-Cha)HLLREVLEBA-R	1132.29	1132.42	90	37	14.3	63.5
His <sup>2</sup>	A3	Ala	Ac-fALLREVLEBA-R	1108.26	1108.86	100	23	11.8	66.1
	B3	Aib	Ac-f(Aib)LLREVLEBA-R	1112.93	1113.30	75	18	16.5	73.8
	C3	D-His	Ac-f(D-His)LLREVLEBA-R	1130.27	1131.00	78	22	18.2	74.6
	D3	Glu	Ac-fELLREVLEBA-R	1127.60	1127.82	73	37	19.2	70.5
	E3	Trp	Ac-fWLLREVLEBA-R	1146.60	1147.37	71	36	9.0	70.8
	F3	Phe	Ac-fFLLREVLEBA-R	1133.61	1133.71	65	19	12.0	68.8
	G3	Cha	Ac-f(Cha)LLREVLEBA-R	1135.62	1135.78	85	20	10.2	61.2
	H3	Dab	Ac-f(Dab)LLREVLEBA-R	1117.94	1118.77	86	42	10.8	64.7
Leu <sup>3</sup>	A4	Ala	Ac-fHALREVLEBA-R	1116.25	1116.51	88	37	12.3	73.2
	B4	Aib	Ac-fH(Aib)LREVLEBA-R	1120.93	1121.12	90	17	11.7	67.2
	C4	D-Leu	Ac-fH(D-Leu)LREVLEBA-R	1130.27	1130.44	82	28	15.8	69.0
	D4	Ile	Ac-fHILREVLEBA-R	1130.27	1130.31	81	33	15.6	69.3
	E4	Val	Ac-fHVLREVLEBA-R	1125.60	1125.79	80	42	16.8	69.8

MATERIAL & METHODS

	<b>F4</b>	Phe	Ac-fHFLREVLEBA-R	1141.60	1141.76	81	39	13.4	64.9
	<b>G4</b>	Cha	Ac-fH(Cha)LREVLEBA-R	1143.61	1144.11	76	46	13.3	69.8
	<b>H4</b>	tBuAla	Ac-fH(tBuAla)LREVLEBA-R	1134.94	1135.83	72	47	14.6	58.6
<b>Leu<sup>4</sup></b>	<b>A5</b>	Ala	Ac-fHLAREVLEBA-R	1116.25	1116.60	76	37	22.2	70.3
	<b>B5</b>	Aib	Ac-fHL(Aib)REVLEBA-R	1120.93	1122.08	100	16	4.8	47.6
	<b>C5</b>	D-Leu	Ac-fHL(D-Leu)REVLEBA-R	1130.27	1130.94	81	23	10.2	66.8
	<b>D5</b>	Ile	Ac-fHLIREVLEBA-R	1130.27	1130.48	65	29	13.4	73.8
	<b>E5</b>	Val	Ac-fHLVREVLEBA-R	1125.60	1125.96	70	48	16.3	72.5
	<b>F5</b>	Phe	Ac-fHLFREVLEBA-R	1141.60	1142.47	76	37	23.1	70.4
	<b>G5</b>	Cha	Ac-fHL(Cha)REVLEBA-R	1143.61	1143.81	74	44	13.7	76.5
	<b>H5</b>	tBuAla	Ac-fHL(D-Cha)REVLEBA-R	1134.94	1135.52	79	41	14.2	67.0
<b>Arg<sup>5</sup></b>	<b>A6</b>	Ala	Ac-fHLLAEVLEBA-R	1101.91	1102.76	89	34	8.3	66.6
	<b>B6</b>	Aib	Ac-fHLL(Aib)EVLEBA-R	1106.59	1106.71	100	12	37.9	71.2
	<b>C6</b>	D-Arg	Ac-fHLL(D-Arg)EVLEBA-R	1130.27	1130.98	100	17	9.8	70.5
	<b>D6</b>	Asn	Ac-fHLLNEVLEBA-R	1116.25	1137.85	78	51	8.4	71.7
	<b>E6</b>	Gln	Ac-fHLLQEVLEBA-R	1120.92	1121.47	76	46	6.5	76.3
	<b>F6</b>	Lys	Ac-fHLLKEVLEBA-R	1120.93	1121.09	86	36	20.7	75.8
	<b>G6</b>	Cit	Ac-fHLL(Cit)EVLEBA-R	1130.60	1131.09	85	37	8.1	66.1
	<b>H6</b>	Orn	Ac-fHLL(Orn)EVLEBA-R	1116.26	1116.78	100	20	38.2	69.8
<b>Glu<sup>6</sup></b>	<b>A7</b>	Ala	Ac-fHLLRAVLEBA-R	1110.93	1111.16	85	20	8.6	71.6
	<b>B7</b>	Aib	Ac-fHLLR(Aib)VLEBA-R	1115.61	1116.49	100	17	15.6	72.3
	<b>C7</b>	D-Glu	Ac-fHLLR(D-Glu)VLEBA-R	1130.27	1130.67	88	20	13.0	73.1
	<b>D7</b>	Asp	Ac-fHLLRDVLEBA-R	1125.60	1126.49	88	23	12.8	71.1
	<b>E7</b>	Gln	Ac-fHLLRQVLEBA-R	1129.94	1130.97	84	23	9.7	71.7
	<b>F7</b>	His	Ac-fHLLRHVLEBA-R	1132.94	1133.28	79	7	8.0	73.9
	<b>G7</b>	Dab	Ac-fHLLR(Dab)VLEBA-R	1120.61	1120.87	100	17	11.5	66.6
	<b>H7</b>	Orn	Ac-fHLLR(Orn)VLEBA-R	1125.28	1125.32	100	17	10.9	70.8
<b>Val<sup>7</sup></b>	<b>A8</b>	Ala	Ac-fHLLREALEBA-R	1120.93	1121.38	100	16	15.0	62.0
	<b>B8</b>	Aib	Ac-fHLLRE(Aib)LEBA-R	1125.60	1126.96	100	8	18.3	67.4
	<b>C8</b>	D-Val	Ac-fHLLRE(D-Val)LEBA-R	1130.27	1130.80	76	27	11.4	73.6
	<b>D8</b>	Ile	Ac-fHLLREILEBA-R	1134.94	1135.74	100	22	20.7	65.8

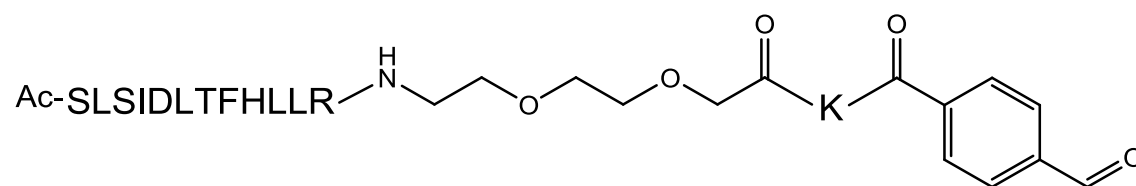
	<b>E8</b>	Leu	Ac-fHLLRELLEBA-R	1134.94	1135.82	100	13	10.1	65.0
	<b>F8</b>	Phe	Ac-fHLLREFLEBA-R	1146.27	1146.41	100	16	10.3	65.2
	<b>G8</b>	Chg	Ac-fHLLRE(Chg)LEBA-R	1143.61	1144.45	100	23	18.4	62.8
	<b>H8</b>	tBuGly	Ac-fHLLRE(tBuGly)LEBA-R	1134.94	1135.64	89	23	89.9	92.6
<b>Leu<sup>8</sup></b>	<b>A9</b>	Ala	Ac-fHLLREVAEBA-R	1116.25	1116.39	100	15	8.4	71.6
	<b>B9</b>	Aib	Ac-fHLLREV(Aib)EBA-R	1120.93	1120.98	100	9	8.6	70.4
	<b>C9</b>	D-Leu	Ac-fHLLREV(D-Leu)EBA-R	1130.27	1130.99	100	13	8.2	69.5
	<b>D9</b>	Ile	Ac-fHLLREVIEBA-R	1130.27	1130.51	90	27	15.8	70.8
	<b>E9</b>	Val	Ac-fHLLREVVEBA-R	1125.60	1126.45	90	38	13.1	77.6
	<b>F9</b>	Phe	Ac-fHLLREVFEBA-R	1141.60	1141.64	75	36	9.8	67.6
	<b>G9</b>	Cha	Ac-fHLLREV(Cha)EBA-R	1143.61	1144.60	88	30	8.2	70.7
	<b>H9</b>	tBuAla	Ac-fHLLREV(tBuAla)EBA-R	1134.94	1135.18	88	35	25.4	61.7
<b>Glu<sup>9</sup></b>	<b>A10</b>	Ala	Ac-fHLLREVLABA-R	1110.67	1111.28	100	14	16.8	65.1
	<b>B10</b>	Aib	Ac-fHLLREVL(Aib)BA-R	1115.61	1115.79	100	9	8.7	66.4
	<b>C10</b>	D-Glu	Ac-fHLLREVL(D-Glu)BA-R	1130.27	1131.06	100	9	7.0	67.3
	<b>D10</b>	Asp	Ac-fHLLREVLDBA-R	1125.60	1125.85	91	22	13.3	69.7
	<b>E10</b>	Gln	Ac-fHLLREVLQBA-R	1129.94	1130.60	100	15	17.0	72.1
	<b>F10</b>	Lys	Ac-fHLLREVLKBA-R	1129.95	1130.05	79	41	6.2	64.8
	<b>G10</b>	Dab	Ac-fHLLREVL(Dab)BA-R	1120.61	1120.79	100	19	7.0	70.6
	<b>H10</b>	Orn	Ac-fHLLREVL(Orn)BA-R	1125.84	1125.56	100	19	14.8	63.2
<b>Nleu<sup>10</sup></b>	<b>A11</b>	Ala	Ac-fHLLREVLEAA-R	1116.25	1116.51	90	24	17.3	63.6
	<b>B11</b>	Aib	Ac-fHLLREVLE(Aib)A-R	1120.93	1121.14	100	10	18.0	64.0
	<b>C11</b>	D-Nleu	Ac-fHLLREVLE(D-Nleu)A-R	1130.27	1130.39	92	23	11.7	72.6
	<b>D11</b>	Leu	Ac-fHLLREVLELA-R	1130.27	1130.54	90	26	12.8	64.0
	<b>E11</b>	Ile	Ac-fHLLREVLEIA-R	1130.27	1130.36	94	27	10.7	65.6
	<b>F11</b>	Lys	Ac-fHLLREVLEKA-R	1135.27	1135.42	81	20	10.3	66.2
	<b>G11</b>	Cha	Ac-fHLLREVLE(Cha)A-R	1143.61	1143.84	100	15	11.3	61.1
	<b>H11</b>	tBuAla	Ac-fHLLREVLE(tBuAla)A-R	1134.94	1135.12	83	31	13.4	61.1
<b>Ala<sup>11</sup></b>	<b>A12</b>	Ala	Ac-fHLLREVLEBA-R	1130.27	1130.45	90	19	14.6	68.3
	<b>B12</b>	Aib	Ac-fHLLREVLEB(Aib)-R	1134.94	1135.26	84	7	13.9	67.4
	<b>C12</b>	D-Ala	Ac-fHLLREVLEB(D-Ala)-R	1130.27	1130.57	95	21	18.0	64.0

	<b>D12</b>	Ser	Ac-fHLLREVLEBS-R	1135.60	1135.78	72	33	8.5	70.3
	<b>E12</b>	Leu	Ac-fHLLREVLEBL-R	1144.29	1144.48	98	11	7.3	70.3
	<b>F12</b>	Val	Ac-fHLLREVLEBV-R	1139.61	1136.77		41	8.1	72.3
	<b>G12</b>	tBuGly	Ac-fHLLREVLEB(tBuGly)-R	1144.29	1144.39		29	5.9	71.3
	<b>H12</b>	Nval	Ac-fHLLREVLEB(Nval)-R	1139.61	1139.78		31	4.6	67.5

**Table 35. Characterization of crude single-substituted analogs of the N-terminal fragment of astressin<sup>1-11</sup>.** <sup>(a)</sup> cAMP stimulatory activity at 250 nM. The cAMP stimulatory activity of conjugate AST<sup>1-11</sup> (**93**) was 8.0 % at 250 nM. <sup>(b)</sup> cAMP inhibitory efficacy at 250 nM. The cAMP inhibitory efficacy of conjugate AST<sup>1-11</sup> (**93**) and astressin were 68.3 % and 19.8 % at 250 nM respectively.

#### 5.2.4.2 Typical procedure for the hydrazone ligation of peptides

##### Procedure for the SFB modification of peptides:



Peptide **23** (1  $\mu$ mol) was dissolved in DMF (100  $\mu$ L) and DIEA (10 eq., 10  $\mu$ mol) was added. The mixture was stirred for 15 min, and p-formylbenzoic acid N-hydroxysuccinimide ester **24** (10 eq., 10  $\mu$ mol) in DMF (50  $\mu$ L) was added. The mixture was stirred for 16 hrs and then concentrated under reduced pressure. The crude was redissolved in acetonitrile/water (50/50, v/v) (100  $\mu$ L) and the modified peptide was purified by preparative reverse phase HPLC to afford pure peptide **27** as a white fluffy solid (1.74 mg, 98 %).

HPLC: B (30 %, 5 min), B (30-40 %, 2 min), B (40-55 %, 16 min), B (55-100 %, 3min), B (100 %, 5 min), B (100-30 %, 3 min), B (30 %, 2 min). Retention time: 19.34 min.

HPLC purity: 100%

MS (ESI) calc. for  $[C_{87}H_{137}N_{21}O_{24} + H]^+$ : 1861.01; found: 1861.64.

##### Typical procedure for the hydrazone ligation of peptides:

The HNA functionalized peptide **3** (1 mM solution in acetonitrile/water 50/50, v/v) (100 nmol) and the SFB-modified peptide **27** (2 mM solution in acetonitrile/water 50/50, v/v) (4 eq., 400 nmol) were transferred to a reaction tube (1.5 mL). The mixture was evaporated under reduced pressure. The

residue was dissolved in "conjugation buffer" (100 mM acetate, pH = 5.0). The mixture was shaken at 40 °C for 24 hrs. The tube was cooled down to room temperature and the solvent was removed under reduced pressure. The crude residue was dissolved in acetonitrile/water (50/50, v/v) (100 µL) and purified by semi-preparative reverse phase HPLC to obtain conjugate **26**.

Typically, the conjugates were dissolved in DMSO and quantified by UV-absorption spectroscopy using standard dilutions of compound **133** as a standard.

HPLC: B (30 %, 5 min), B (30-40 %, 2 min), B (40-55 %, 16 min), B (55-100 %, 3min), B (100 %, 5 min), B (100-30 %, 3 min), B (30 %, 2 min). Retention time: 14.21 min.

HPLC purity: 100%

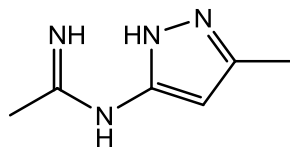
Yield: 94 %

MS (ESI) calc. for  $[C_{164}H_{263}N_{45}O_{44} + 3H]^{3+}$ : 1189.99; found: 1190.05.

## 5.2.5 Synthesis of nonpeptide CRHR<sub>1</sub> antagonists

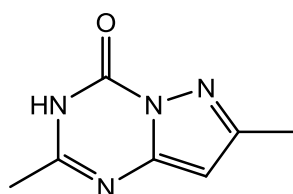
### 5.2.5.1 Synthesis of building block 128

#### Synthesis of 5-acetamido-3-methylpyrazole 126:



Ethyl acetamidate hydrochloride (6.46 g, 52.2 mmol) was added quickly to a rapidly stirred mixture of potassium carbonate (6.95 g, 50.0 mmol), methylene chloride (60 mL), and water (150 mL). The layers were separated and the aqueous layer was extracted with methylene chloride (2 x 60 mL). The combined organic layers were dried over magnesium sulfate and filtered. The solvent was removed under vacuum, and a clear pale-yellow liquid was obtained and used without further purification. Glacial acetic acid (1.0 mL, 17.4 mmol) was added to a stirred mixture of 5-amino-3-methylpyrazole (17.4 mmol), ethyl acetamidate free base, and dichloromethane (100 mL). The resulting reaction mixture was stirred at room temperature for 16hrs. Afterwards, the mixture was concentrated under reduced pressure. The residue was triturated with diethylether, and the product was filtered and washed with copious amounts of cold diethylether. A white solid was obtained and dried in vacuum. It was used without further purification (3.42 g, 100 %).

#### Synthesis of 2,7-dimethyl-[1,5-a]pyrazolo[1,3,5]triazin-4(3H)-one 127:



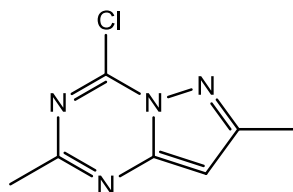
Sodium pellets (3.9 g, 169 mmol) were added portion wise to pure ethanol (200 mL) with vigorous stirring. After all the sodium reacted, 5-acetamido-3-methylpyrazole **126**, acetic acid salt (5.4 g, 16.9 mmol) and diethylcarbonate (16.4 mL, 135.3 mmol) were added. The resulting reaction mixture was heated under reflux and stirred for 18 hrs. The mixture was cooled to room temperature, and the solvent was removed in vacuum. The residue was dissolved in water (50 mL), and the pH was adjusted to 6 with an aqueous hydrochloric acid solution (1M). The aqueous layer was extracted with ethyl acetate (3 x 100 mL). The combined organic layers were dried over magnesium sulfate and filtered. Solvent was removed in vacuum to give a yellowish solid which was purified by flash chromatography. A white solid was obtained (0.81 g, 30 %).

$^1\text{H-NMR}$  (300MHz,  $\text{CDCl}_3$ ):  $\delta$  = 11.05 (br s, 1H), 6.23 (s, 1H), 2.52 (s, 3H), 2.45 (s, 3H) ppm.  $^{13}\text{C-NMR}$  (75MHz,  $\text{CDCl}_3$ ):  $\delta$  = 157.67, 152.67, 149.45, 99.82, 21.59, 14.81 ppm.

MS (ESI) calc. for  $[\text{C}_7\text{H}_8\text{N}_4\text{O} + \text{Na}]^+$ : 187.06; found: 187.13.

TLC (AcOEt):  $R_f$  = 0.51.

### Synthesis of 4-chloro-2,7-dimethyl-[1,5-a]pyrazolo-1,3,5-triazine 128:



A mixture of 2,7-dimethyl-[1,5-a]pyrazolo[1,3,5]triazin-4(3H)-one **127** (2.25 g, 13.7 mmol), diisopropylethylamine (9.5 mL, 54.7 mmol), phosphorous oxychloride (5.1 mL, 54.7 mmol), and toluene (75 mL) were stirred at reflux temperature for 4 hrs. The volatiles were removed in vacuum. The residue was purified by flash chromatography to give a light yellowish solid (1.43 g, 57 %).

$^1\text{H-NMR}$  (300MHz,  $\text{CDCl}_3$ ):  $\delta$  = 6.78 (s, 1H), 6.47 (s, 1H), 2.60 (s, 3H), 2.56 (s, 3H) ppm.  $^{13}\text{C-NMR}$  (75MHz,  $\text{CDCl}_3$ ):  $\delta$  = 158.11, 155.99, 150.07, 107.85, 96.75, 30.91, 24.44, 14.70 ppm.

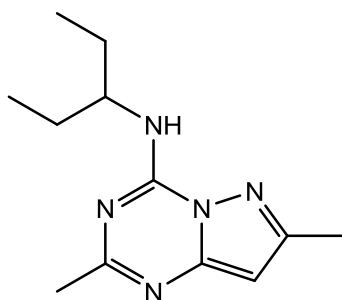
MS (ESI) calc. for  $[\text{C}_7\text{H}_7\text{ClN}_4 + \text{Na}]^+$ : 205.03; found: 205.05.

TLC (AcOEt/Hexane, 1/2, v/v)  $R_f$  = 0.54.

### 5.2.5.2 General procedure for the amine condensation with compound 128

A mixture of 4-chloro-2,7-dimethyl-[1,5-a]pyrazolo-1,3,5-triazine **128** (0.30 g, 1.64 mmol), 2-amino-1,3-dimethoxypropane or 3-pentylamine (1.5 eq.), diisopropylethylamine (4 eq.), and dry THF (2 mL/mmol) was stirred at ambient temperature for 18 hrs. The solvent was removed under vacuum and the residue was purified by flash chromatography.

- **4-(3-aminopentyl)-2,7-dimethyl-[1,5-a]pyrazolo-1,3,5-triazine 129a:**



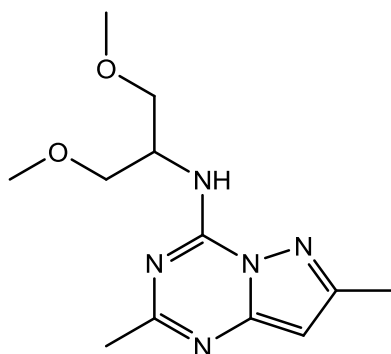
Light yellow oil was obtained (0.29 g, 76 %).

$^1\text{H-NMR}$  (300MHz,  $\text{CDCl}_3$ ):  $\delta$  = 6.12 (br. d,  $J=10$  Hz, 1H), 6.07 (s, 1H), 4.11 – 4.23 (m, 1H), 2.48 (s, 3H), 2.42 (s, 3H), 1.52 – 1.80 (m, 4H), 0.97 (t,  $J=7$  Hz, 6H) ppm.  $^{13}\text{C-NMR}$  (75MHz,  $\text{CDCl}_3$ ):  $\delta$  = 163.81, 155.33, 149.92, 148.44, 94.92, 53.58, 27.52, 26.13, 14.66, 10.29 ppm.

MS (ESI) calc. for  $[\text{C}_{12}\text{H}_{19}\text{N}_5 + \text{H}]^+$ : 234.2; found: 234.4.

TLC (AcOEt/Hexane, 1/4, v/v):  $R_f$  = 0.50.

- **4-(2-amino-1,3-dimethoxypropyl)-2,7-dimethyl-[1,5-a]pyrazolo-1,3,5-triazine 129b:**



A crystalline solid was obtained (0.28 g, 63 %).

$^1\text{H-NMR}$  (300MHz,  $\text{CDCl}_3$ ):  $\delta$  = 6.68 (br. d,  $J=8$  Hz, 1H), 6.08 (s, 1H), 4.58 – 4.63 (m, 1H), 3.57 – 3.66 (m, 4H), 3.41 (s, 6H), 2.49 (s, 3H), 2.43 (s, 3H) ppm.  $^{13}\text{C-NMR}$  (75MHz,  $\text{CDCl}_3$ ):  $\delta$  = 164.79, 156.12, 149.71, 147.13, 93.58, 74.91, 59.34, 55.82, 14.61, 10.27 ppm.

MS (ESI) calc. for  $[\text{C}_{12}\text{H}_{19}\text{N}_5\text{O}_2 + \text{H}]^+$ : 266.2; found: 266.5.

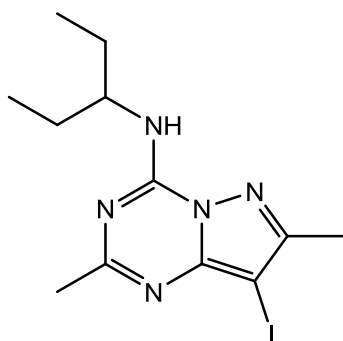
TLC (AcOEt/Hexane, 1/1, v/v):  $R_f$  = 0.78.

### 5.2.5.3 General procedure for the iodination of compounds 129a-b

A solution of 129 (1.25 mmol) and N-iodosuccinimide (1.4 eq.) in anhydrous chloroform (10 mL) was stirred at reflux for 30 min. The solvent was evaporated under reduced pressure. The residue was dissolved in dichloromethane (12 mL) and washed with a saturated solution of sodium thiosulfate (3 x 3 mL). The organic layer was dried over magnesium sulfate and evaporated to dryness under vacuum. The crude product was purified by flash chromatography to afford derivatives **130a-b**.



- **4-(3-aminopentyl)-2,7-dimethyl-8-iodo-[1,5-a]pyrazolo-1,3,5-triazine 130a:**



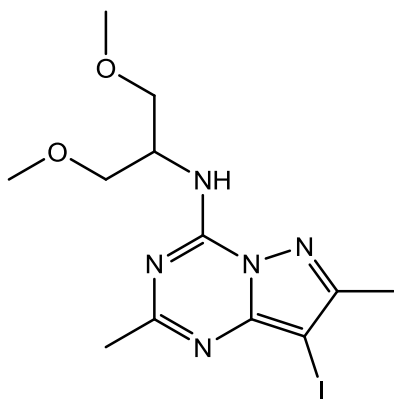
A light yellow solid was obtained (0.37 g, 83 %).

$^1\text{H-NMR}$  (300MHz,  $\text{CDCl}_3$ ):  $\delta$  = 6.12 (br. d,  $J=10$  Hz, 1H), 4.11 – 4.23 (m, 1H), 2.54 (s, 3H), 2.43 (s, 3H), 1.52 – 1.78 (m, 4H), 0.96 (t,  $J=8$  Hz, 6H) ppm.  $^{13}\text{C-NMR}$  (75MHz,  $\text{CDCl}_3$ ):  $\delta$  = 165.43, 156.42, 53.89, 50.58, 27.51, 26.35, 15.00, 10.27 ppm.

MS (ESI) calc. for  $[\text{C}_{12}\text{H}_{18}\text{IN}_5 + \text{H}]^+$ : 360.1; found: 360.3.

TLC (AcOEt/Hexane 1/4):  $R_f$  = 0.67.

- **4-(2-amino-1,3-dimethoxypropyl)-2,7-dimethyl-8-iodo-[1,5-a]pyrazolo-1,3,5-triazine 130b:**



A white solid was obtained (0.35 g, 74 %).

$^1\text{H-NMR}$  (300MHz,  $\text{CDCl}_3$ ):  $\delta$  = 6.67 (d,  $J = 4$  Hz, 1H)), 4.58 - 4.63 (m, 1H), 3.62 (m, 4H), 3.41 (s, 6H), 2.49 (s, 3H), 2.43 (s, 3H) ppm.  $^{13}\text{C-NMR}$  (75MHz,  $\text{CDCl}_3$ ):  $\delta$  = 162.97, 154.30, 147.89, 145.31, 91.76, 73.09, 57.52, 54.00, 14.79, 10.46 ppm.

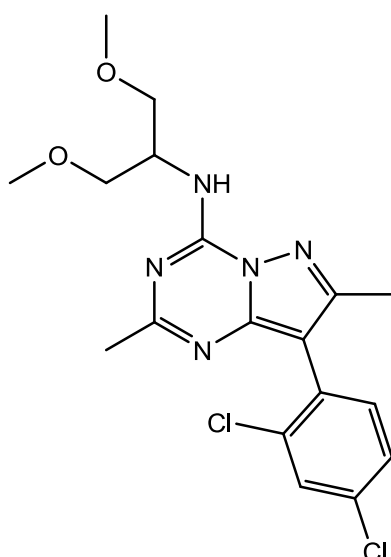
MS (ESI) calc. for  $[\text{C}_{12}\text{H}_{18}\text{IN}_5\text{O}_2 + \text{H}]^+$ : 392.1; found: 392.4.

TLC (AcOEt/Hexane, 1/4, v/v):  $R_f$  = 0.28.

#### 5.2.5.4 General procedure for the Suzuki cross-coupling with compounds 130a-b

To a stirred solution of **129a** or **129b** (0.19 mmol) in anhydrous toluene (1.5 mL) was added tetrakis(triphenylphosphine)palladium (33 mg, 0.028 mmol, 0.15 eq.). The mixture was stirred for 30 min. at room temperature. Phenylboronic acid (0.28 mmol, 1.5 eq.) diluted in ethanol (1 mL) was then added, followed immediately by a saturated aqueous solution of sodium bicarbonate (1 mL). The heterogeneous solution was stirred at reflux for 12hrs. The palladium catalyst was removed by filtration. A saturated aqueous solution of sodium chloride was then added (2 mL), the layers were separated and the aqueous phase was extracted with ethyl acetate (3 x 5 mL). The combined organic extracts were dried over magnesium sulfate and evaporated under reduced pressure. The crude residue was purified by flash chromatography to afford the 8-phenyl derivatives **131**.

- **4-(2-amino-1,3-dimethoxypropyl)-2,7-dimethyl-8-(2,4-dichlorophenyl)[1,5-a]pyrazolo-1,3,5-triazine 131a:**



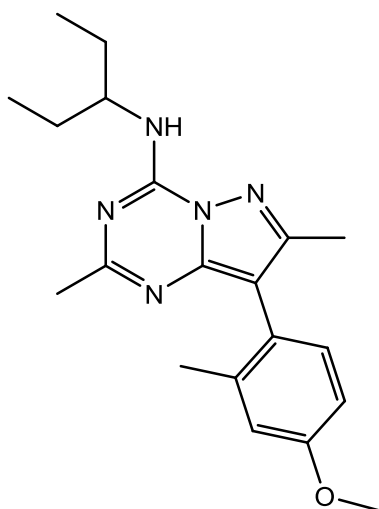
A light brown solid was obtained (0.045 g, 35 %).

$^1\text{H-NMR}$  (300MHz,  $\text{CDCl}_3$ ):  $\delta$  = 7.51 (m, 1H), 7.30 (m, 2H), 6.73 (br. d,  $J=9$  Hz, 1H), 4.59 – 4.69 (m, 1H), 3.58 – 3.70 (m, 4H), 3.43 (s, 6H), 2.48 (s, 3H), 2.34 (s, 3H) ppm.  $^{13}\text{C-NMR}$  (75MHz,  $\text{CDCl}_3$ ):  $\delta$  = 164.42, 154.30, 147.98, 135.76, 134.22, 133.95, 129.84, 129.43, 127.34, 71.14, 59.39, 49.78, 29.86, 26.24, 13.74 ppm.

MS (ESI) calc. for  $[\text{C}_{18}\text{H}_{21}\text{Cl}_2\text{N}_5\text{O}_2 + \text{H}]^+$ : 410.1; found: 410.3.

TLC (AcOEt/Hexane, 1/4, v/v):  $R_f$  = 0.50.

- **4-(3-aminopentyl)-2,7-dimethyl-8-(2-methyl-4-methoxyphenyl)[1,5-a]pyrazolo-1,3,5-triazine 131b:**



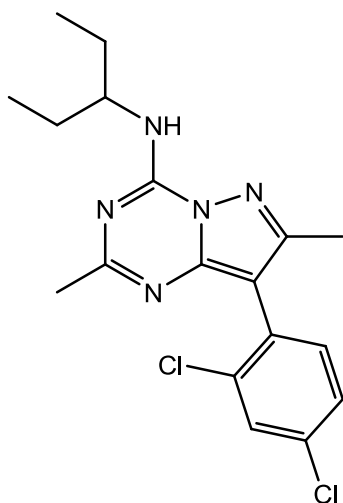
An orange oil was obtained (0.047 g, 70 %).

$^1\text{H-NMR}$  (300MHz,  $\text{CDCl}_3$ ):  $\delta$  = 7.12 (d,  $J=10$  Hz, 1H), 6.86 (d,  $J=2$  Hz, 1H), 6.79 (dd,  $J_1=3$  Hz,  $J_2=8$  Hz, 1H), 6.16 (br. d,  $J=10$  Hz, 1H), 4.14 – 4.26 (m, 1H), 3.82 (s, 3H), 2.47 (s, 3H), 2.30 (s, 3H), 2.19 (s, 3H), 1.57 – 1.83 (m, 4H), 1.00 (t,  $J=8$  Hz, 6H) ppm.  $^{13}\text{C-NMR}$  (75MHz,  $\text{CDCl}_3$ ):  $\delta$  = 163.66, 159.24, 154.02, 139.68, 132.43, 123.34, 115.89, 111.40, 108.43, 55.39, 53.55, 27.54, 26.31, 20.80, 13.34, 10.34 ppm.

MS (ESI) calc. for  $[\text{C}_{20}\text{H}_{27}\text{N}_5\text{O} + \text{H}]^+$ : 354.2; found: 354.5.

TLC (AcOEt/Hexane, 1/4, v/v):  $R_f$  = 0.50.

- **4-(3-aminopentyl)-2,7-dimethyl-8-(2,4-dichlorophenyl)[1,5-a]pyrazolo-1,3,5-triazine 131c:**



A white solid was obtained (0.041g, 57 %).

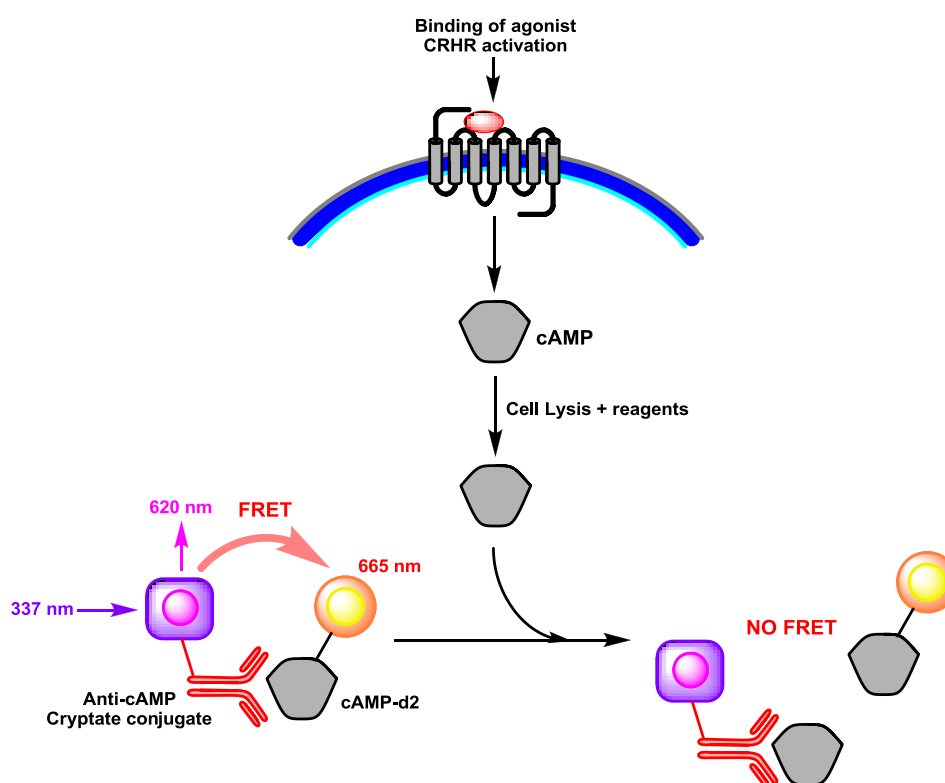
$^1\text{H-NMR}$  (300MHz,  $\text{CDCl}_3$ ):  $\delta$  = 7.52 (t,  $J=1$  Hz, 1H), 7.31 (d,  $J=1$  Hz, 2H), 6.18 (br. d,  $J=10$  Hz, 1H), 4.14 – 4.27 (m, 1H), 2.48 (s, 3H), 2.34 (s, 3H), 1.57 – 1.83 (m, 4H), 1.00 (t,  $J=8$  Hz, 6H) ppm.  $^{13}\text{C-NMR}$  (75MHz,  $\text{CDCl}_3$ ):  $\delta$  = 164.61, 153.94, 148.35, 147.21, 135.73, 134.17, 133.98, 129.84, 129.51, 127.35, 105.83, 53.68, 27.51, 26.35, 13.73, 10.33 ppm.

MS (ESI) calc. for  $[\text{C}_{18}\text{H}_{21}\text{Cl}_2\text{N}_5 + \text{H}]^+$ : 378.1; found: 378.3.

TLC (AcOEt/Hexane, 1/4, v/v):  $R_f$  = 0.50.

### 5.3 cAMP cell-based assays

For the screening of  $\text{CRHR}_1$  ligands, a cell-based assay using the HTRF technology was used. This assay was developed by Cisbio International and allows the screening of GPCR ligands in high-throughput format (Figure 53, <http://www.htrf-assays.com>).



**Figure 53. Description of the HTRF cell-based cAMP stimulation assay and its components.** Assay description: upon agonist binding, native cAMP produced by cells competes with the d2-labeled cAMP for binding a cryptate-labeled cAMP-antibody. The decrease of the FRET specific signal is inversely proportional to the concentration of cAMP in the sample.

### 5.3.1 Stimulation assay typical protocol

For the stimulation assay, HEK293 cells overexpressing CRHR<sub>1</sub> were prepared by Bas Hoogeland (AG Hausch). The cells grown to 50-60 % confluency in DMEM (+ FCS 10%, penicillin/streptomycin) were detached from the culture dish with cell dissociation solution (Sigma, Germany), resuspended in stimulation buffer (SB, 5 mM HEPES, 0,1% BSA, 0,1 mM IBMX in HBSS) and seeded in 5 µl into a Corning 384 well plate (#3572) at a density of 3000 cells/well by Bas Hoogeland. After equilibration for 10 min at room temperature 5 µl of SB containing peptides and/or DMSO, forskolin or DMP696 (generous gift by Bristol-Myers-Squibb) were added. After incubation for 30 min at room temperature, cells were lysed and the cAMP content was measured using the cAMP dynamic HTRF detection kit (CisBio, France) according to the manufactures instructions and using a Tecan Genios Pro equipped with 320/35 nM excitation and 620/10 nM and 665/8 nM emission filters. The ratiometric fluorescence signals obtained were normalized to the positive (forskolin, 100%) and negative controls (DMSO, 0%).

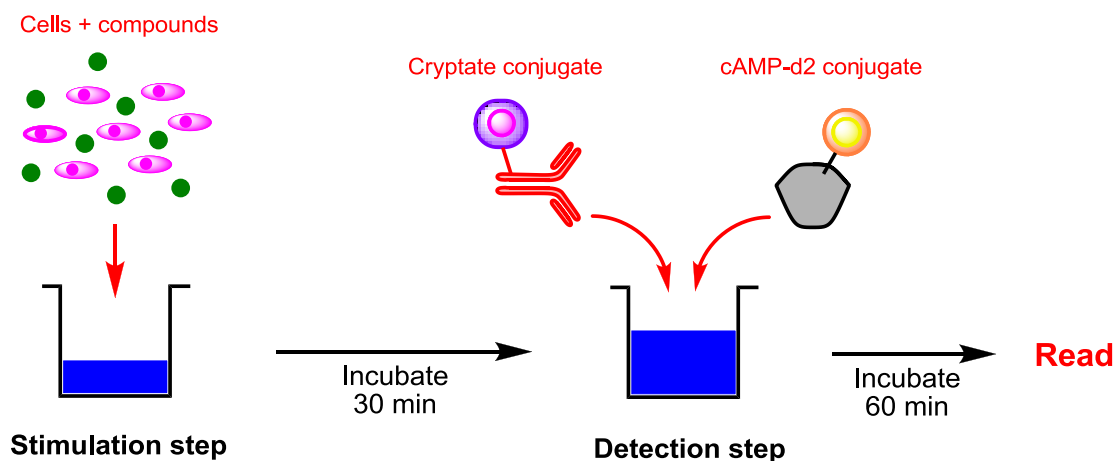


Figure 54. Two-steps protocol for the cAMP stimulation assay.

### 5.3.2 Inhibition assay standard protocol

For the inhibition assay, the same conditions were used. After equilibration for 10 min at room temperature, 2.5 µL of SB containing the antagonist were added. The cells were incubated with the antagonist for 15 min and 2.5 µL of the peptide agonist were then added. After incubation for 30 min, the cAMP content was determined as described previously (Figure 55).

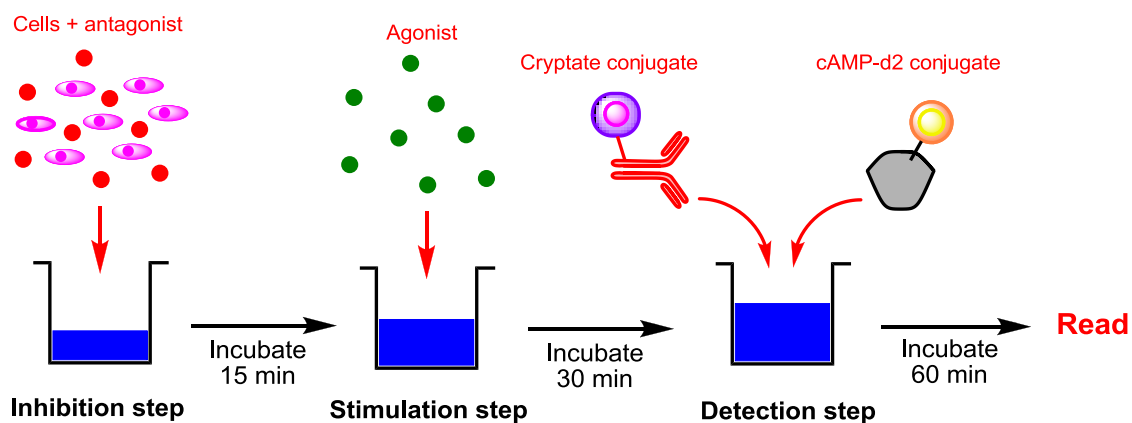


Figure 55. Three-steps protocol for the cAMP inhibition assay.

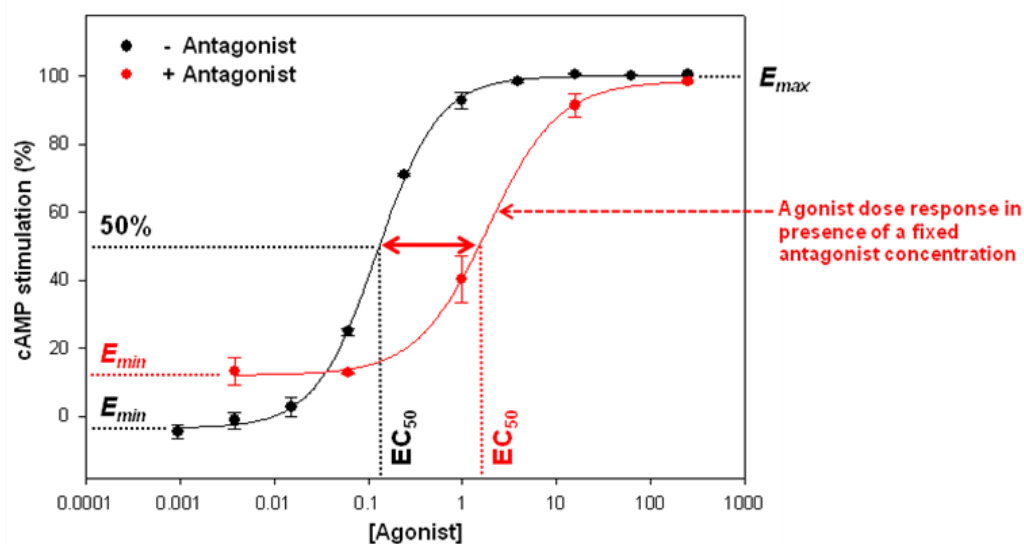
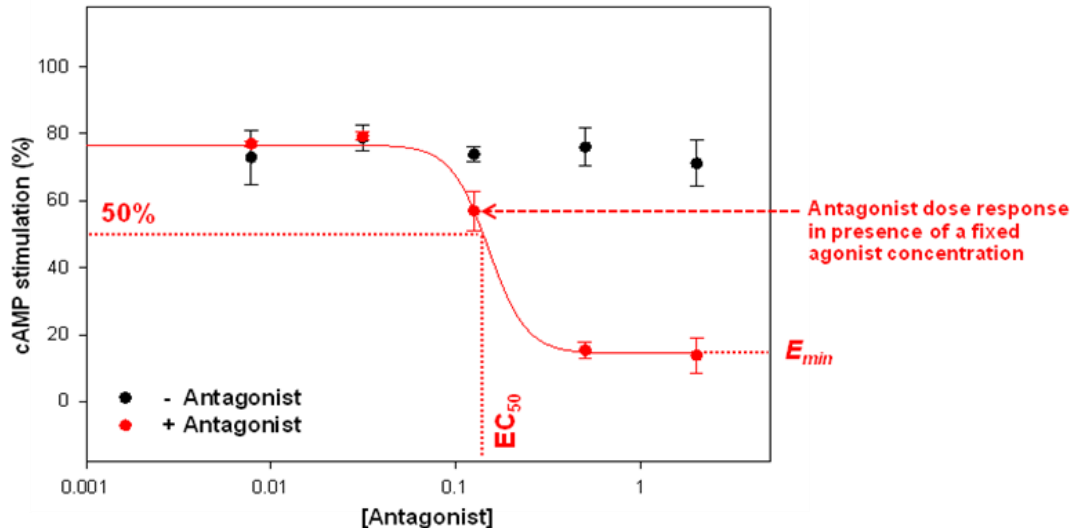


Figure 56. Agonist dose response set-up for the cAMP inhibition assay. Briefly, HEK293 cells overexpressing CRHR<sub>1</sub> are incubated 15 min with a fixed concentration of antagonist. Increasing concentrations of agonist are added and the cells are further incubated for 30 min. The cAMP production level is then determined as described.



**Figure 57. Antagonist dose response set-up for the cAMP inhibition assay.** Briefly, HEK293 cells overexpressing CRHR<sub>1</sub> are incubated 15 min with increasing antagonist concentrations. An EC<sub>50</sub>-corresponding concentration of the agonist is then added and the cells are further incubated for 30 min. After incubation, the cAMP production level is determined as described.

Two setups were commonly used for the determination of the efficacy of antagonists. In a setup which measures the dose-response of the agonist, the cells were first incubated with a fixed concentration of the antagonist, and then increasing concentrations of the agonist were added (Figure 56). Increased EC<sub>50</sub> value and minimal efficacy ( $E_{min}$ ) compared to control indicate the inhibitory efficacy of the antagonist (Figure 57). Another assay setup that measures the dose response of the antagonist was used. Typically, the CRHR<sub>1</sub>-overexpressing cells were first incubated with increasing concentrations of the antagonist, and then a fixed EC<sub>50</sub>-corresponding concentration of the agonist was added. A sigmoidal response and a decreased minimal efficacy ( $E_{min}$ ) compared to control indicate the inhibitory efficacy of the antagonist (Figure 57).

CRHR<sub>1</sub> radioactive ligand binding assays were performed by Bas Hoogeland as described previously (Devigny *et al.* 2011).

## 5.4 Data analysis

SigmaPlot software version 11.0 was used for sigmoidal curve fitting of ligand concentration-response curves and for calculating the EC<sub>50</sub> values as an index of ligand potency. The statistical parameters were generated from a composite nonlinear regression (four parameter logistic curve, SigmaPlot 11.0) of pooled data from two independent samples. In general, the mean and the standard error of the mean (s.e.m.) were expressed for values obtained from duplicate samples. The cAMP production response was normalized to a positive control (Forskolin, 100 %) and a negative control (DMSO, 0 %).



## References

- Abrams, M.J., Juweid, M., tenKate, C.I., Schwartz, D.A., Hauser, M.M., Gaul, F.E., Fuccello, A.J., Rubin, R.H., Strauss, H.W., and Fischman, A.J. Technetium-99m-human polyclonal IgG radiolabeled via the hydrazino nicotinamide derivative for imaging focal sites of infection in rats. *J. Nucl. Med.* (1990) 31,2022-2028.
- Altmann, E., Altmann, K.H., Nebel, K., and Mutter, M. Conformational studies on host-guest peptides containing chiral alpha-methyl-alpha-amino acids. Comparison of the helix-inducing potential of alpha-aminoisobutyric acid, (S)-2-ethylalanine and (S)-2-methylserine. *Int. J. Pept. Protein Res.* (1988) 32,344-351.
- Baghai, T.C., Moller, H.J., and Rupprecht, R. Recent progress in pharmacological and non-pharmacological treatment options of major depression. *Curr. Pharm. Des* (2006) 12,503-515.
- Bale, T.L., Contarino, A., Smith, G.W., Chan, R., Gold, L.H., Sawchenko, P.E., Koob, G.F., Vale, W.W., and Lee, K.F. Mice deficient for corticotropin-releasing hormone receptor-2 display anxiety-like behaviour and are hypersensitive to stress. *Nat. Genet.* (2000) 24,410-414.
- Bale, T.L. and Vale, W.W. CRF and CRF receptors: role in stress responsivity and other behaviors. *Annu. Rev. Pharmacol. Toxicol.* (2004) 44,525-557.
- Beyermann, M., Fechner, K., Furkert, J., Krause, E., and Bienert, M. A single-point slight alteration set as a tool for structure-activity relationship studies of ovine corticotropin releasing factor. *J. Med. Chem.* (1996) 39,3324-3330.
- Beyermann, M., Rothmund, S., Heinrich, N., Fechner, K., Furkert, J., Dathe, M., Winter, R., Krause, E., and Bienert, M. A role for a helical connector between two receptor binding sites of a long-chain peptide hormone. *J. Biol. Chem.* (2000) 275,5702-5709.
- Bhattacharya, S., Subramanian, G., Hall, S., Lin, J., Laoui, A., and Vaidehi, N. Allosteric antagonist binding sites in class B GPCRs: corticotropin receptor 1. *J. Comput. Aided Mol. Des* (2010) 24,659-674.
- Binneman, B., Feltner, D., Kolluri, S., Shi, Y., Qiu, R., and Stiger, T. A 6-week randomized, placebo-controlled trial of CP-316,311 (a selective CRH1 antagonist) in the treatment of major depression. *Am. J. Psychiatry* (2008) 165,617-620.
- Bouzide, A. and Sauve, G. Silver(I) oxide mediated highly selective monotosylation of symmetrical diols. Application to the synthesis of polysubstituted cyclic ethers. *Org. Lett.* (2002) 4,2329-2332.
- Carpenter, L.L., Tyrka, A.R., McDougle, C.J., Malison, R.T., Owens, M.J., Nemeroff, C.B., and Price, L.H. Cerebrospinal fluid corticotropin-releasing factor and perceived early-life stress in depressed patients and healthy control subjects. *Neuropsychopharmacology* (2004) 29,777-784.
- Carter, P.H., Liu, R.Q., Foster, W.R., Tamasi, J.A., Tebben, A.J., Favata, M., Staal, A., Cvijic, M.E., French, M.H., Dell, V., Apanovitch, D., Lei, M., Zhao, Q., Cunningham, M., Decicco, C.P., Trzaskos,

- J.M., and Feyen, J.H. Discovery of a small molecule antagonist of the parathyroid hormone receptor by using an N-terminal parathyroid hormone peptide probe. *Proc. Natl. Acad. Sci. U. S. A* (2007) 104,6846-6851.
- Cervini, L., Theobald, P., Corrigan, A., Craig, A.G., Rivier, C., Vale, W., and Rivier, J. Corticotropin releasing factor (CRF) agonists with reduced amide bonds and Ser7 substitutions. *J. Med. Chem.* (1999) 42,761-768.
- Chalmers, D.T., Lovenberg, T.W., and De Souza, E.B. Localization of novel corticotropin-releasing factor receptor (CRF2) mRNA expression to specific subcortical nuclei in rat brain: comparison with CRF1 receptor mRNA expression. *J. Neurosci.* (1995) 15,6340-6350.
- Chen, C. Recent advances in small molecule antagonists of the corticotropin-releasing factor type-1 receptor-focus on pharmacology and pharmacokinetics. *Curr. Med. Chem.* (2006) 13,1261-1282.
- Chen, Y.L., Braselton, J., Forman, J., Gallaschun, R.J., Mansbach, R., Schmidt, A.W., Seeger, T.F., Sprouse, J.S., Tingley, F.D., III, Winston, E., and Schulz, D.W. Synthesis and SAR of 2-aryloxy-4-alkoxy-pyridines as potent orally active corticotropin-releasing factor 1 receptor antagonists. *J. Med. Chem.* (2008a) 51,1377-1384.
- Chen, Y.L., Mansbach, R.S., Winter, S.M., Brooks, E., Collins, J., Corman, M.L., Dunaiskis, A.R., Faraci, W.S., Gallaschun, R.J., Schmidt, A., and Schulz, D.W. Synthesis and oral efficacy of a 4-(butylethylamino)pyrrolo[2,3-d]pyrimidine: a centrally active corticotropin-releasing factor1 receptor antagonist. *J. Med. Chem.* (1997b) 40,1749-1754.
- Chen, Y.L., Mansbach, R.S., Winter, S.M., Brooks, E., Collins, J., Corman, M.L., Dunaiskis, A.R., Faraci, W.S., Gallaschun, R.J., Schmidt, A., and Schulz, D.W. Synthesis and oral efficacy of a 4-(butylethylamino)pyrrolo[2,3-d]pyrimidine: a centrally active corticotropin-releasing factor1 receptor antagonist. *J. Med. Chem.* (1997a) 40,1749-1754.
- Chen, Y.L., Obach, R.S., Braselton, J., Corman, M.L., Forman, J., Freeman, J., Gallaschun, R.J., Mansbach, R., Schmidt, A.W., Sprouse, J.S., Tingley Iii, F.D., Winston, E., and Schulz, D.W. 2-aryloxy-4-alkylaminopyridines: discovery of novel corticotropin-releasing factor 1 antagonists. *J. Med. Chem.* (2008b) 51,1385-1392.
- Cheng, H., Cao, X., Xian, M., Fang, L., Cai, T.B., Ji, J.J., Tunac, J.B., Sun, D., and Wang, P.G. Synthesis and enzyme-specific activation of carbohydrate-geldanamycin conjugates with potent anticancer activity. *J. Med. Chem.* (2005) 48,645-652.
- Chrousos, G.P. Stressors, stress, and neuroendocrine integration of the adaptive response. The 1997 Hans Selye Memorial Lecture. *Ann. N. Y. Acad. Sci.* (1998) 851,311-335.
- Civelli, O. GPCR deorphanizations: the novel, the known and the unexpected transmitters. *Trends Pharmacol. Sci.* (2005) 26,15-19.
- Coric, V., Feldman, H.H., Oren, D.A., Shekhar, A., Pultz, J., Dockens, R.C., Wu, X., Gentile, K.A., Huang, S.P., Emison, E., Delmonte, T., D'Souza, B.B., Zimbroff, D.L., Grebb, J.A., Goddard, A.W., and Stock, E.G. Multicenter, randomized, double-blind, active comparator and placebo-controlled trial of a

- corticotropin-releasing factor receptor-1 antagonist in generalized anxiety disorder. *Depress. Anxiety.* (2010) 27,417-425.
- Dallman, M.F., Akana, S.F., Cascio, C.S., Darlington, D.N., Jacobson, L., and Levin, N. Regulation of ACTH secretion: variations on a theme of B. *Recent Prog. Horm. Res.* (1987) 43,113-173.
- Dautzenberg, F.M. and Hauger, R.L. The CRF peptide family and their receptors: yet more partners discovered. *Trends Pharmacol. Sci.* (2002) 23,71-77.
- Dautzenberg, F.M., Kilpatrick, G.J., Hauger, R.L., and Moreau, J. Molecular biology of the CRH receptors-- in the mood. *Peptides* (2001) 22,753-760.
- Dautzenberg, F.M., Kilpatrick, G.J., Wille, S., and Hauger, R.L. The ligand-selective domains of corticotropin-releasing factor type 1 and type 2 receptor reside in different extracellular domains: generation of chimeric receptors with a novel ligand-selective profile. *J. Neurochem.* (1999) 73,821-829.
- de, G.C., Rein, C., Piwnica, D., Giordanetto, F., and Rognan, D. Structure-based discovery of allosteric modulators of two related class B G-protein-coupled receptors. *ChemMedChem.* (2011) 6,2159-2169.
- DeBold, C.R., Sheldon, W.R., DeCherney, G.S., Jackson, R.V., Alexander, A.N., Vale, W., Rivier, J., and Orth, D.N. Arginine vasopressin potentiates adrenocorticotropin release induced by ovine corticotropin-releasing factor. *J. Clin. Invest* (1984) 73,533-538.
- Demyttenaere, K., Bruffaerts, R., Posada-Villa, J., Gasquet, I., Kovess, V., Lepine, J.P., Angermeyer, M.C., Bernert, S., de, G.G., Morosini, P., Polidori, G., Kikkawa, T., Kawakami, N., Ono, Y., Takeshima, T., Uda, H., Karam, E.G., Fayyad, J.A., Karam, A.N., Mneimneh, Z.N., Medina-Mora, M.E., Borges, G., Lara, C., de, G.R., Ormel, J., Gureje, O., Shen, Y., Huang, Y., Zhang, M., Alonso, J., Haro, J.M., Vilagut, G., Bromet, E.J., Gluzman, S., Webb, C., Kessler, R.C., Merikangas, K.R., Anthony, J.C., Von Korff, M.R., Wang, P.S., Brugha, T.S., Guilar-Gaxiola, S., Lee, S., Heeringa, S., Pennell, B.E., Zaslavsky, A.M., Ustun, T.B., and Chatterji, S. Prevalence, severity, and unmet need for treatment of mental disorders in the World Health Organization World Mental Health Surveys. *JAMA* (2004) 291,2581-2590.
- DeSouza, E.B. Conspectus. Corticotropin-releasing factor. *Compr. Ther.* (1985) 11,3-5.
- Deussing, J.M. and Wurst, W. Dissecting the genetic effect of the CRH system on anxiety and stress-related behaviour. *C. R. Biol.* (2005) 328,199-212.
- Devigny, C., Perez-Balderas, F., Hoogeland, B., Cuboni, S., Wachtel, R., Mauch, C.P., Webb, K.J., Deussing, J.M., and Hausch, F. Biomimetic screening of class-B G protein-coupled receptors. *J. Am. Chem. Soc.* (2011) 133,8927-8933.
- Dong, M., Gao, F., Pinon, D.I., and Miller, L.J. Insights into the structural basis of endogenous agonist activation of family B G protein-coupled receptors. *Mol. Endocrinol.* (2008) 22,1489-1499.

- Dong, M., Pinon, D.I., Asmann, Y.W., and Miller, L.J. Possible endogenous agonist mechanism for the activation of secretin family G protein-coupled receptors. *Mol. Pharmacol.* (2006) 70,206-213.
- Dubs, P., Bourel-Bonnet, L., Subra, G., Blanpain, A., Melnyk, O., Pinel, A.M., Gras-Masse, H., and Martinez, J. Parallel synthesis of a lipopeptide library by hydrazone-based chemical ligation. *J. Comb. Chem.* (2007) 9,973-981.
- Essex, M.J., Klein, M.H., Cho, E., and Kalin, N.H. Maternal stress beginning in infancy may sensitize children to later stress exposure: effects on cortisol and behavior. *Biol. Psychiatry* (2002) 52,776-784.
- Fortin, J.P., Zhu, Y., Choi, C., Beinborn, M., Nitabach, M.N., and Kopin, A.S. Membrane-tethered ligands are effective probes for exploring class B1 G protein-coupled receptor function. *Proc. Natl. Acad. Sci. U. S. A* (2009) 106,8049-8054.
- Gilligan, P.J., He, L., Clarke, T., Tivitmahaisoon, P., Lelas, S., Li, Y.W., Heman, K., Fitzgerald, L., Miller, K., Zhang, G., Marshall, A., Krause, C., McElroy, J., Ward, K., Shen, H., Wong, H., Grossman, S., Nemeth, G., Zaczek, R., Arneric, S.P., Hartig, P., Robertson, D.W., and Trainor, G. 8-(4-Methoxyphenyl)pyrazolo[1,5-a]-1,3,5-triazines: selective and centrally active corticotropin-releasing factor receptor-1 (CRF1) antagonists. *J. Med. Chem.* (2009b) 52,3073-3083.
- Gilligan, P.J., He, L., Clarke, T., Tivitmahaisoon, P., Lelas, S., Li, Y.W., Heman, K., Fitzgerald, L., Miller, K., Zhang, G., Marshall, A., Krause, C., McElroy, J., Ward, K., Shen, H., Wong, H., Grossman, S., Nemeth, G., Zaczek, R., Arneric, S.P., Hartig, P., Robertson, D.W., and Trainor, G. 8-(4-Methoxyphenyl)pyrazolo[1,5-a]-1,3,5-triazines: selective and centrally active corticotropin-releasing factor receptor-1 (CRF1) antagonists. *J. Med. Chem.* (2009a) 52,3073-3083.
- Gold, P.W., Goodwin, F.K., and Chrousos, G.P. Clinical and biochemical manifestations of depression. Relation to the neurobiology of stress (2). *N. Engl. J. Med.* (1988) 319,413-420.
- Gordon, J.C., Edwards, P., Elmore, C.S., Lazor, L.A., Paschetto, K., Bostwick, R., Sylvester, M., Mauger, R., Scott, C., and Aharony, D. [(1)(2)I]YP20: a novel radioligand specific for the extracellular domain of the CRF receptor. *Eur. J. Pharmacol.* (2010) 649,59-63.
- Grace, C.R., Perrin, M.H., DiGruccio, M.R., Miller, C.L., Rivier, J.E., Vale, W.W., and Riek, R. NMR structure and peptide hormone binding site of the first extracellular domain of a type B1 G protein-coupled receptor. *Proc. Natl. Acad. Sci. U. S. A* (2004) 101,12836-12841.
- Grace, C.R., Perrin, M.H., Gulyas, J., DiGruccio, M.R., Cattle, J.P., Rivier, J.E., Vale, W.W., and Riek, R. Structure of the N-terminal domain of a type B1 G protein-coupled receptor in complex with a peptide ligand. *Proc. Natl. Acad. Sci. U. S. A* (2007) 104,4858-4863.
- Grace, C.R., Perrin, M.H., Gulyas, J., Rivier, J.E., Vale, W.W., and Riek, R. NMR structure of the first extracellular domain of corticotropin-releasing factor receptor 1 (ECD1-CRF-R1) complexed with a high affinity agonist. *J. Biol. Chem.* (2010) 285,38580-38589.
- Grammatopoulos, D.K. and Chrousos, G.P. Functional characteristics of CRH receptors and potential clinical applications of CRH-receptor antagonists. *Trends Endocrinol. Metab* (2002) 13,436-444.

- Grigoriadis, D.E. The corticotropin-releasing factor receptor: a novel target for the treatment of depression and anxiety-related disorders. *Expert. Opin. Ther. Targets.* (2005) 9,651-684.
- Gulyas, J., Rivier, C., Perrin, M., Koerber, S.C., Sutton, S., Corrigan, A., Lahrachi, S.L., Craig, A.G., Vale, W., and Rivier, J. Potent, structurally constrained agonists and competitive antagonists of corticotropin-releasing factor. *Proc. Natl. Acad. Sci. U. S. A* (1995) 92,10575-10579.
- Hauger, R.L., Risbrough, V., Brauns, O., and Dautzenberg, F.M. Corticotropin releasing factor (CRF) receptor signaling in the central nervous system: new molecular targets. *CNS. Neurol. Disord. Drug Targets.* (2006) 5,453-479.
- He, L., Gilligan, P.J., Zaczek, R., Fitzgerald, L.W., McElroy, J., Shen, H.S., Saye, J.A., Kalin, N.H., Shelton, S., Christ, D., Trainor, G., and Hartig, P. 4-(1,3-Dimethoxyprop-2-ylamino)-2,7-dimethyl-8-(2, 4-dichlorophenyl)pyrazolo[1,5-a]-1,3,5-triazine: a potent, orally bioavailable CRF(1) receptor antagonist. *J. Med. Chem.* (2000) 43,449-456.
- Hernandez, J.F., Kornreich, W., Rivier, C., Miranda, A., Yamamoto, G., Andrews, J., Tache, Y., Vale, W., and Rivier, J. Synthesis and relative potencies of new constrained CRF antagonists. *J. Med. Chem.* (1993) 36,2860-2867.
- Hoare, S.R. Mechanisms of peptide and nonpeptide ligand binding to Class B G-protein-coupled receptors. *Drug Discov. Today* (2005) 10,417-427.
- Hoare, S.R., Brown, B.T., Santos, M.A., Malany, S., Betz, S.F., and Grigoriadis, D.E. Single amino acid residue determinants of non-peptide antagonist binding to the corticotropin-releasing factor1 (CRF1) receptor. *Biochem. Pharmacol.* (2006) 72,244-255.
- Hoare, S.R., Fleck, B.A., Gross, R.S., Crowe, P.D., Williams, J.P., and Grigoriadis, D.E. Allosteric ligands for the corticotropin releasing factor type 1 receptor modulate conformational states involved in receptor activation. *Mol. Pharmacol.* (2008) 73,1371-1380.
- Hoare, S.R., Sullivan, S.K., Ling, N., Crowe, P.D., and Grigoriadis, D.E. Mechanism of corticotropin-releasing factor type I receptor regulation by nonpeptide antagonists. *Mol. Pharmacol.* (2003) 63,751-765.
- Holsboer, F. The rationale for corticotropin-releasing hormone receptor (CRH-R) antagonists to treat depression and anxiety. *J. Psychiatr. Res.* (1999) 33,181-214.
- Holsboer, F. The corticosteroid receptor hypothesis of depression. *Neuropsychopharmacology* (2000) 23,477-501.
- Holsboer, F. and Ising, M. Central CRH system in depression and anxiety--evidence from clinical studies with CRH1 receptor antagonists. *Eur. J. Pharmacol.* (2008) 583,350-357.
- Hsu, S.Y. and Hsueh, A.J. Human stresscopin and stresscopin-related peptide are selective ligands for the type 2 corticotropin-releasing hormone receptor. *Nat. Med.* (2001) 7,605-611.

- Ising, M. and Holsboer, F. CRH-sub-1 receptor antagonists for the treatment of depression and anxiety. *Exp. Clin. Psychopharmacol.* (2007) 15,519-528.
- Ising, M., Zimmermann, U.S., Kunzel, H.E., Uhr, M., Foster, A.C., Learned-Coughlin, S.M., Holsboer, F., and Grigoriadis, D.E. High-affinity CRF1 receptor antagonist NBI-34041: preclinical and clinical data suggest safety and efficacy in attenuating elevated stress response. *Neuropsychopharmacology* (2007) 32,1941-1949.
- Juruena, M.F., Cleare, A.J., and Pariante, C.M. [The hypothalamic pituitary adrenal axis, glucocorticoid receptor function and relevance to depression]. *Rev. Bras. Psiquiatr.* (2004) 26,189-201.
- Kehne, J. and De, L.S. Non-peptidic CRF1 receptor antagonists for the treatment of anxiety, depression and stress disorders. *Curr. Drug Targets. CNS. Neurol. Disord.* (2002) 1,467-493.
- Kehne, J.H. and Cain, C.K. Therapeutic utility of non-peptidic CRF1 receptor antagonists in anxiety, depression, and stress-related disorders: evidence from animal models. *Pharmacol. Ther.* (2010) 128,460-487.
- Kirsch, I. Antidepressants and the placebo response. *Epidemiol. Psychiatr. Soc.* (2009) 18,318-322.
- Kirsch, I. Review: benefits of antidepressants over placebo limited except in very severe depression. *Evid. Based. Ment. Health* (2010) 13,49-
- Koerber, S.C., Gulyas, J., Lahrichi, S.L., Corrigan, A., Craig, A.G., Rivier, C., Vale, W., and Rivier, J. Constrained corticotropin-releasing factor (CRF) agonists and antagonists with i-(i+3) Glu-Xaa-DXbb-Lys bridges. *J. Med. Chem.* (1998) 41,5002-5011.
- Kolb, H.C., Finn, M.G., and Sharpless, K.B. Click Chemistry: Diverse Chemical Function from a Few Good Reactions. *Angew. Chem. Int. Ed Engl.* (2001) 40,2004-2021.
- Koob, G.F. Corticotropin-releasing factor, norepinephrine, and stress. *Biol. Psychiatry* (1999) 46,1167-1180.
- Koolhaas, J.M., Bartolomucci, A., Buwalda, B., de Boer, S.F., Flugge, G., Korte, S.M., Meerlo, P., Murison, R., Olivier, B., Palanza, P., Richter-Levin, G., Sgoifo, A., Steimer, T., Stiedl, O., van, D.G., Wohr, M., and Fuchs, E. Stress revisited: a critical evaluation of the stress concept. *Neurosci. Biobehav. Rev.* (2011) 35,1291-1301.
- Kornreich, W.D., Galyean, R., Hernandez, J.F., Craig, A.G., Donaldson, C.J., Yamamoto, G., Rivier, C., Vale, W., and Rivier, J. Alanine series of ovine corticotropin releasing factor (oCRF): a structure-activity relationship study. *J. Med. Chem.* (1992) 35,1870-1876.
- Kunzel, H.E., Zobel, A.W., Nickel, T., Ackl, N., Uhr, M., Sonntag, A., Ising, M., and Holsboer, F. Treatment of depression with the CRH-1-receptor antagonist R121919: endocrine changes and side effects. *J. Psychiatr. Res.* (2003) 37,525-533.

- Li, Y.W., Fitzgerald, L., Wong, H., Lelas, S., Zhang, G., Lindner, M.D., Wallace, T., McElroy, J., Lodge, N.J., Gilligan, P., and Zaczek, R. The pharmacology of DMP696 and DMP904, non-peptidergic CRF1 receptor antagonists. *CNS. Drug Rev.* (2005) 11,21-52.
- Liaw, C.W., Grigoriadis, D.E., Lovenberg, T.W., De Souza, E.B., and Maki, R.A. Localization of ligand-binding domains of human corticotropin-releasing factor receptor: a chimeric receptor approach. *Mol. Endocrinol.* (1997) 11,980-985.
- Mazur, A.W., Wang, F., Tscheiner, M., Donnelly, E., and Isfort, R.J. Determinants of corticotropin releasing factor. Receptor selectivity of corticotropin releasing factor related peptides. *J. Med. Chem.* (2004) 47,3450-3454.
- Miranda, A., Koerber, S.C., Gulyas, J., Lahrichi, S.L., Craig, A.G., Corrigan, A., Hagler, A., Rivier, C., Vale, W., and Rivier, J. Conformationally restricted competitive antagonists of human/rat corticotropin-releasing factor. *J. Med. Chem.* (1994) 37,1450-1459.
- Miranda, A., Lahrichi, S.L., Gulyas, J., Koerber, S.C., Craig, A.G., Corrigan, A., Rivier, C., Vale, W., and Rivier, J. Constrained corticotropin-releasing factor antagonists with i-(i + 3) Glu-Lys bridges. *J. Med. Chem.* (1997) 40,3651-3658.
- Moro, S., Spalluto, G., and Jacobson, K.A. Techniques: Recent developments in computer-aided engineering of GPCR ligands using the human adenosine A3 receptor as an example. *Trends Pharmacol. Sci.* (2005) 26,44-51.
- Murray, C.W. and Verdonk, M.L. The consequences of translational and rotational entropy lost by small molecules on binding to proteins. *J. Comput. Aided Mol. Des* (2002) 16,741-753.
- Nemeroff, C.B. The corticotropin-releasing factor (CRF) hypothesis of depression: new findings and new directions. *Mol. Psychiatry* (1996) 1,336-342.
- Nemeroff, C.B., Widerlov, E., Bissette, G., Walleus, H., Karlsson, I., Eklund, K., Kilts, C.D., Loosen, P.T., and Vale, W. Elevated concentrations of CSF corticotropin-releasing factor-like immunoreactivity in depressed patients. *Science* (1984) 226,1342-1344.
- Parkhouse, S.M., Garnett, M.C., and Chan, W.C. Targeting of polyamidoamine-DNA nanoparticles using the Staudinger ligation: attachment of an RGD motif either before or after complexation. *Bioorg. Med. Chem.* (2008) 16,6641-6650.
- Parthier, C., Reedtz-Runge, S., Rudolph, R., and Stubbs, M.T. Passing the baton in class B GPCRs: peptide hormone activation via helix induction? *Trends Biochem. Sci.* (2009) 34,303-310.
- Perrin, M., Donaldson, C., Chen, R., Blount, A., Berggren, T., Bilezikjian, L., Sawchenko, P., and Vale, W. Identification of a second corticotropin-releasing factor receptor gene and characterization of a cDNA expressed in heart. *Proc. Natl. Acad. Sci. U. S. A* (1995) 92,2969-2973.
- Pioszak, A.A., Parker, N.R., Suino-Powell, K., and Xu, H.E. Molecular recognition of corticotropin-releasing factor by its G-protein-coupled receptor CRFR1. *J. Biol. Chem.* (2008) 283,32900-32912.

- Raadsheer, F.C., Hoogendijk, W.J., Stam, F.C., Tilders, F.J., and Swaab, D.F. Increased numbers of corticotropin-releasing hormone expressing neurons in the hypothalamic paraventricular nucleus of depressed patients. *Neuroendocrinology* (1994) 60,436-444.
- Radulovic, J., Ruhmann, A., Liepold, T., and Spiess, J. Modulation of learning and anxiety by corticotropin-releasing factor (CRF) and stress: differential roles of CRF receptors 1 and 2. *J. Neurosci.* (1999) 19,5016-5025.
- Refojo, D., Schweizer, M., Kuehne, C., Ehrenberg, S., Thoeringer, C., Vogl, A.M., Dedic, N., Schumacher, M., von, W.G., Avrabos, C., Touma, C., Engblom, D., Schutz, G., Nave, K.A., Eder, M., Wotjak, C.T., Sillaber, I., Holsboer, F., Wurst, W., and Deussing, J.M. Glutamatergic and dopaminergic neurons mediate anxiogenic and anxiolytic effects of CRHR1. *Science* (2011) 333,1903-1907.
- Rivier, J., Gulyas, J., Corrigan, A., Martinez, V., Craig, A.G., Tache, Y., Vale, W., and Rivier, C. A stressin analogues (corticotropin-releasing factor antagonists) with extended duration of action in the rat. *J. Med. Chem.* (1998a) 41,5012-5019.
- Rivier, J., Gulyas, J., Kirby, D., Low, W., Perrin, M.H., Kunitake, K., DiGruccio, M., Vaughan, J., Reubi, J.C., Waser, B., Koerber, S.C., Martinez, V., Wang, L., Tache, Y., and Vale, W. Potent and long-acting corticotropin releasing factor (CRF) receptor 2 selective peptide competitive antagonists. *J. Med. Chem.* (2002) 45,4737-4747.
- Rivier, J., Lahrichi, S.L., Gulyas, J., Erchegyi, J., Koerber, S.C., Craig, A.G., Corrigan, A., Rivier, C., and Vale, W. Minimal-size, constrained corticotropin-releasing factor agonists with i-(i+3) Glu-Lys and Lys-Glu bridges. *J. Med. Chem.* (1998b) 41,2614-2620.
- Rivier, J., Rivier, C., Galyean, R., Miranda, A., Miller, C., Craig, A.G., Yamamoto, G., Brown, M., and Vale, W. Single point D-substituted corticotropin-releasing factor analogues: effects on potency and physicochemical characteristics. *J. Med. Chem.* (1993) 36,2851-2859.
- Ruhe, H.G., Huyser, J., Swinkels, J.A., and Schene, A.H. Switching antidepressants after a first selective serotonin reuptake inhibitor in major depressive disorder: a systematic review. *J. Clin. Psychiatry* (2006) 67,1836-1855.
- Sakmar, T.P. Receptors: clicking class B GPCR ligands. *Nat. Chem. Biol.* (2011) 7,500-501.
- Schulz, D.W., Mansbach, R.S., Sprouse, J., Braselton, J.P., Collins, J., Corman, M., Dunaiskis, A., Faraci, S., Schmidt, A.W., Seeger, T., Seymour, P., Tingley, F.D., III, Winston, E.N., Chen, Y.L., and Heym, J. CP-154,526: a potent and selective nonpeptide antagonist of corticotropin releasing factor receptors. *Proc. Natl. Acad. Sci. U. S. A* (1996b) 93,10477-10482.
- Schulz, D.W., Mansbach, R.S., Sprouse, J., Braselton, J.P., Collins, J., Corman, M., Dunaiskis, A., Faraci, S., Schmidt, A.W., Seeger, T., Seymour, P., Tingley, F.D., III, Winston, E.N., Chen, Y.L., and Heym, J. CP-154,526: a potent and selective nonpeptide antagonist of corticotropin releasing factor receptors. *Proc. Natl. Acad. Sci. U. S. A* (1996a) 93,10477-10482.



- SELYE, H. The general-adaptation-syndrom and the gastrointestinal diseases of adaptation. *Am. J. Proctol.* (1951) 2,167-184.
- Shimizu, M., Potts, J.T., Jr., and Gardella, T.J. Minimization of parathyroid hormone. Novel amino-terminal parathyroid hormone fragments with enhanced potency in activating the type-1 parathyroid hormone receptor. *J. Biol. Chem.* (2000) 275,21836-21843.
- Stahl, S.M. and Wise, D.D. The potential role of a corticotropin-releasing factor receptor-1 antagonist in psychiatric disorders. *CNS. Spectr.* (2008) 13,467-483.
- Swanson, L.W., Sawchenko, P.E., Rivier, J., and Vale, W.W. Organization of ovine corticotropin-releasing factor immunoreactive cells and fibers in the rat brain: an immunohistochemical study. *Neuroendocrinology* (1983) 36,165-186.
- Tellew, J.E., Lanier, M., Moorjani, M., Lin, E., Luo, Z., Slee, D.H., Zhang, X., Hoare, S.R., Grigoriadis, D.E., St, D.Y., Di, F.R., Di, M.E., Saunders, J., and Williams, J.P. Discovery of NBI-77860/GSK561679, a potent corticotropin-releasing factor (CRF1) receptor antagonist with improved pharmacokinetic properties. *Bioorg. Med. Chem. Lett.* (2010) 20,7259-7264.
- Tellew, J.E. and Luo, Z. Small molecule antagonists of the corticotropin releasing factor (CRF) receptor: recent medicinal chemistry developments. *Curr. Top. Med. Chem.* (2008) 8,506-520.
- Tornøe, C.W., Christensen, C., and Meldal, M. Peptidotriazoles on solid phase: [1,2,3]-triazoles by regioselective copper(i)-catalyzed 1,3-dipolar cycloadditions of terminal alkynes to azides. *J. Org. Chem.* (2002) 67,3057-3064.
- Tsigos, C. and Chrousos, G.P. Hypothalamic-pituitary-adrenal axis, neuroendocrine factors and stress. *J. Psychosom. Res.* (2002) 53,865-871.
- Vale, W., Rivier, C., Brown, M.R., Spiess, J., Koob, G., Swanson, L., Bilezikjian, L., Bloom, F., and Rivier, J. Chemical and biological characterization of corticotropin releasing factor. *Recent Prog. Horm. Res.* (1983) 39,245-270.
- Vale, W., Spiess, J., Rivier, C., and Rivier, J. Characterization of a 41-residue ovine hypothalamic peptide that stimulates secretion of corticotropin and beta-endorphin. *Science* (1981) 213,1394-1397.
- Van, P.K., Viau, V., Bittencourt, J.C., Chan, R.K., Li, H.Y., Arias, C., Prins, G.S., Perrin, M., Vale, W., and Sawchenko, P.E. Distribution of mRNAs encoding CRF receptors in brain and pituitary of rat and mouse. *J. Comp Neurol.* (2000) 428,191-212.
- Vaughan, J., Donaldson, C., Bittencourt, J., Perrin, M.H., Lewis, K., Sutton, S., Chan, R., Turnbull, A.V., Lovejoy, D., Rivier, C., and . Urocortin, a mammalian neuropeptide related to fish urotensin I and to corticotropin-releasing factor. *Nature* (1995) 378,287-292.
- Yamada, Y., Mizutani, K., Mizusawa, Y., Hantani, Y., Tanaka, M., Tanaka, Y., Tomimoto, M., Sugawara, M., Imai, N., Yamada, H., Okajima, N., and Haruta, J. New class of corticotropin-releasing factor

## REFERENCES

---

- (CRF) antagonists: small peptides having high binding affinity for CRF receptor. *J. Med. Chem.* (2004) 47,1075-1078.
- Young, S.F., Griffante, C., and Aguilera, G. Dimerization between vasopressin V1b and corticotropin releasing hormone type 1 receptors. *Cell Mol. Neurobiol.* (2007) 27,439-461.
- Zobel, A.W., Nickel, T., Kunzel, H.E., Ackl, N., Sonntag, A., Ising, M., and Holsboer, F. Effects of the high-affinity corticotropin-releasing hormone receptor 1 antagonist R121919 in major depression: the first 20 patients treated. *J. Psychiatr. Res.* (2000) 34,171-181.
- Zorrilla, E.P. and Koob, G.F. Progress in corticotropin-releasing factor-1 antagonist development. *Drug Discov. Today* (2010) 15,371-383.

## Acknowledgments

First of all, I would like to express my gratitude to my supervisor, Dr. Felix Hausch for giving me the opportunity to accomplish this doctoral work in his research group. His expertise, helpful guidance, steady support and patience added considerably to my graduate experience. I also thank Felix for proofreading of this PhD thesis.

I also would like to thank Prof. Dr. Chris Turck for representing my PhD thesis at the Ludwig-Maximilian University, and Prof. Dr. Holsboer for giving me the opportunity to work on this fascinating topic at the Max-Planck-Institute of Psychiatry.

I gratefully thank Bas Hoogeland, the heart and soul of this work, for his help and patience at performing assays. I also acknowledge Serena Cuboni for her help, pleasant mood, current and future collaborations. I thank Stefanie Finsterbusch, Evi Stahl and Rudolf Wachtel for the laborious and repetitive synthesis of peptides. Furthermore, I am indebted to Giuseppina Maccarrone and Christiane Rewerts for their help in measuring mass spectrometry.

Altogether, I am grateful to all members of the group for their permanent support in practical and scientific questions, for the relaxed and inspiring working atmosphere. For enduring encouragement, scientific and non-scientific discussions, diverting and unforgettable moments, I gratefully thank the “chemistry team”: Steffen Gaali, Ranganath Gopalakrishnan and Yansong Wang.

I finally thank my family and friends for the support they provided me through my entire life, and in particular I must acknowledge my parents and Helena, without whose love, encouragement and assistance, I would not have finished this thesis.



## Curriculum Vitae

Last name: Devigny

Name: Christian Serge Marie

Date and place of birth: 7<sup>th</sup> march 1982 in Chevreuse (France)

Citizenship: French

### Education

**09/2007 - present:** Graduate studies in the group of Chemical Genomics (AG Hausch) at the Max-Planck-Institute of Psychiatry, Munich, Germany

**09/2006:** Graduation at "CPE-Lyon", master and engineer degree in Chemistry, Lyon, France

**08/2005 – 08/2006:** Diploma and exchange student at the University of Notre Dame, Indiana, USA  
Diploma thesis: "Synthetic studies on the asymmetric hydroformylation of acylnitroso-cycloadducts"  
in the group of Bioorganic Chemistry (AG Miller)

**07/2004 – 07/2005:** Practical studies, Priaton GmbH, Munich, Germany

**09/2000 – 07/2004:** Studies in Chemistry, CPE-Lyon (School of Chemistry Physics Electronics), France

### Posters and oral presentations

**07/2011:** Max-Planck-Institute for Psychiatry Symposium, Munich, Germany (Talk)

**06/2011:** Gordon Research Seminar and Conference "High Throughput Screening and Chemical Biology", Colby-Sawyer College, NH, USA (Poster)

**11/2010:** Max-Planck-Institute for Psychiatry, PhD seminar series, Munich, Germany (Talk)

**10/2010-2011:** 26. And 27. Symposium der AGNP, Munich, Germany (Posters)

**04/2009:** Chemical Genomics Center Symposium, Dortmund, Germany (Poster)

**03/2009:** Synthesefest, Ludwig-Maximilian-University, Munich, Germany (Poster)

**09/2008:** Summer School in Medicinal Chemistry, Regensburg, Germany (Poster)

**07/2008:** Max-Planck-Institute for Psychiatry Symposium, Munich, Germany (Talk)

**03/2008:** Frontiers in Medicinal Chemistry, Regensburg, Germany (Poster)

### Publication

Devigny ,C. , Perez-Balderas, F., Hoogeland, B., Cuboni, S., Wachtel, R., Mauch, C.P., Webb, K., Deussing, J.M., and Hausch, F. Biomimetic Screening of Class-B G Protein-Coupled Receptors *J. Am. Chem. Soc.* (2011) 133,8927-8933.